

Histone Deacetylase-6 ZnF UBP as a regulator of Tau stability and neuronal functions

by

Abhishek Balmik
10BB15J26039

A thesis submitted to the
Academy of Scientific & Innovative Research
for the award of the degree of
DOCTOR OF PHILOSOPHY
in
SCIENCE

Under the supervision of
Dr. Subashchandrabose Chinnathambi



CSIR- National Chemical Laboratory, Pune



Academy of Scientific and Innovative Research
AcSIR Headquarters, CSIR-HRDC campus
Sector 19, Kamla Nehru Nagar,
Ghaziabad, U.P. –201 002, India

November - 2020

Certificate

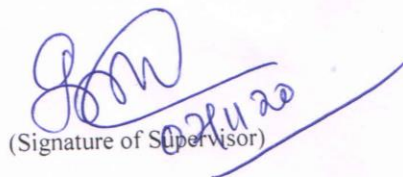
This is to certify that the work incorporated in this Ph.D. thesis entitled "Histone Deacetylase-6 ZnF UBP as a regulator of Tau stability and neuronal functions" submitted by Mr. Abhishek Balmik to Academy of Scientific and Innovative Research (AcSIR) in fulfillment of the requirements for the award of the Degree of Doctor of Philosophy in Science, embodies original research work carried-out by the student. We, further certify that this work has not been submitted to any other University or Institution in part or full for the award of any degree or diploma. Research material(s) obtained from other source(s) and used in this research work has/have been duly acknowledged in the thesis. Image(s), illustration(s), figure(s), table(s) etc., used in the thesis from other source(s), have also been duly cited and acknowledged.



(Signature of Student)

Abhishek Balmik

Date : 02/11/2020



(Signature of Supervisor)

Dr. Subashchandrabose Chinnathambi

Date : 02/11/2020

STATEMENTS OF ACADEMIC INTEGRITY

I, Abhishek Balmik, a Ph.D. student of the Academy of Scientific and Innovative Research (AcSIR) with Registration No. 10BB15J26039 hereby undertake that, the thesis entitled "Histone Deacetylase-6 ZnF UBP as a regulator of Tau stability and neuronal functions" has been prepared by me and that the document reports original work carried out by me and is free of any plagiarism in compliance with the UGC Regulations on "*Promotion of Academic Integrity and Prevention of Plagiarism in Higher Educational Institutions (2018)*" and the CSIR Guidelines for "*Ethics in Research and in Governance (2020)*".

Signature of the Student

Date : 02/11/2020

Place : Pune

It is hereby certified that the work done by the student, under my/our supervision, is plagiarism-free in accordance with the UGC Regulations on "*Promotion of Academic Integrity and Prevention of Plagiarism in Higher Educational Institutions (2018)*" and the CSIR Guidelines for "*Ethics in Research and in Governance (2020)*".

Signature of the Co-supervisor

Name:

Date:

Place:

Signature of the Supervisor

Name: **Dr. Subashchandrabose Chinnathambi**

Date: **02/11/2020**

Place: **Pune**

Acknowledgment

I would like to take the privilege to express my heartfelt gratitude to the people who helped me directly or indirectly during the course of my Ph.D. journey. First and foremost, I would like to extend my sincere thanks to my research advisor **Dr. Subashchandrabose Chinnathambi** for giving me an opportunity to work under his guidance and to help me explore the possibilities in my research by providing constant support, posing challenging questions and making critical suggestions. I appreciate his patience and healthy criticism which greatly helped me to develop scientific temperament and made my Ph.D. journey a great learning experience. It was his valuable comments and suggestions which helped me to ascertain the direction of my research work and to obtain fruitful results.

I am highly thankful to **Director, CSIR-NCL** for providing me with the opportunity to work in this prestigious laboratory and providing the necessary infrastructure for carrying out my research work. I express my gratitude to **CSIR- Shyamaprasad Mukherjee fellowship (CSIR-SPMF)** for the fellowship award which provided financial support in the course of my Ph.D.in terms of my stipend and contingency. I am extremely thankful to **Academy of Scientific and Innovative research (AcSIR)** for their academic support to finish my Ph.D.

I express my sincere obligation to **Chair, Biochemical Science Division**, for extending support and providing institutional facilities.

I owe special thanks to my Doctoral Advisory Committee (DAC) members – **Dr. Dhiman Sarkar, Dr. Dhanasekaran Shanmugam** and **Dr. Mahesh Kulkarni** for their critical comments and valuable suggestions which helped a lot in my research.

I would like to thank **Dr. HV Thulasiram** for permitting me to use his lab facilities and providing valuable suggestions for my research work.

I would also like to thank **Dr. Udaya Kiran Marelli**, Central NMR Facility, Organic Chemistry Division, CSIR-NCL, for his collaboration and conducting the NMR studies which provided useful insights for the interaction analysis work. I would also like to express my gratitude to **Dr. Moneesha Fernandes**, Organic Chemistry Division, CSIR-NCL, for giving me the permission to utilize central facility of Circular Dichroism Spectroscopy.

I am immensely thankful to the Central facilities for electron microscopy, CSIR-NCL, which greatly by providing with timely processing of my samples which aided in my research work. In this regard, I am sincerely grateful to **Mr. Ramakrishna Gholap**, Principal Technical officer, Centre for Material Characterization for providing the facility. I am also greatly thankful to **Pankaj** and **Venkatesh** for their help in processing of my electron microscopy samples.

I am highly indebted to **Dr. Dhanasekaran Shanmugam, Dr. Mahesh Kulkarni, Dr. Suresh Kumar Ramasamy, Dr. Sushma Gaikwad, Dr. Ramchandra Gadre**, for allowing me to use some of their lab facilities.

I would like to extend my sincere thanks to the administrative facilities at CSIR-NCL – Office (Biochemical Sciences Division), Student Academic Office, AcSIR Office at CSIR-NCL, Digital Information Resource Centre (DIRC), Library, Stores and Purchase, Finance, Dispatch, housekeeping and Engineering sections for their help in processing of official works.

I take this opportunity to express my sincere gratitude to my labmates – **Nalini, Shweta, Tushar, Rashmi, Smita and Hariharakrishnan** for their constant support and providing a positive work environment in lab. I especially thank **Nalini and Shweta** for extending their support and help during the course of my research work. I am highly thankful my trainees and interns – **Gokul, Nivethitha, Uma and Rutuja** who worked with me and provided me an opportunity to learn from them. I express my gratitude and admiration for the project assistants - **Lisni and Tanuja**, who helped a lot in my Ph.D. through their perspective towards work and important suggestions. For my collaborative work, I would like to thank **Shweta** for Cell biology work, **Rashmi** for the Melatonin work, **Hariharakrishnan and Debjyoti** for their *in silico* studies and analysis and **Abha** for NMR studies and analysis.

Apart from my labmates, I would like to extend my sincere gratitude to the friends and colleagues in Biochemical Sciences Division CSIR-NCL who helped me directly or indirectly during the course of my Ph.D. I am immensely thankful to the members of Dr. Suresh Kumar's Lab – **Manu, Deepak, Deepanjan, Vijay, Ameya, Yashpal, Shiva and Debjyoti**, members of Dr. Mahesh Kulkarni's Lab – **Rajeshwari, Shakuntala, Prachi, Yugendra, Shabda, Arvind and Babasaheb**, members of Dr. Dhanasekaran's Lab – **Anurag, Meenakshi, Rupali, Sindhuri, Rahul, Parag and Ajinkya**, members of Dr. Kiran Kulkarni's Lab – **Zenia, Anand, Sneha, Debopriya and Aishwarya**, members of Dr. Thulasiram's Lab – **Avinash, Ashish, Sharvani, Pooja and Shrikant**, members of Dr. Koteswara Rao Lab – **Amol and Vishwambhar** and members of Plant Molecular Biology Lab – **Monika and Santosh**. I would like to offer my sincere thanks to all other friends in the division and apologize if I failed to mention their names. I highly appreciate and express my thankfulness to my friends at NCL – **Pratiksh, Rajan, Rashid, Arun, Amarnath, Praveen, Vikash and Shahebaz**. I would also like to mention my friends back at Indore – **Amal, Nikhil, Mayur, Deepak, Arun, Suresh, Ajay, Neeraj, Rahul Sir, Gajendra, Rajkumar, Madhu, Deepanti, Bhagyashree and Jyoti**, who extended their kind support and were always there in times of need.

I would like to extend my special thanks to **Dr. Vinita Kothari, MD (Pathology), Lt. Col. Dr. Nina Dutta Roy, MD (Microbiology) and Dr. Rajeev Lohokare, MD (Biochemistry)** for their support and encouragement.

I owe my deepest sense of gratitude to my parents without whom constant love, support and encouragement, it would not have been possible. I extend my gratitude towards my family and relatives for always been there to provide me support in times of need. I dedicate my work to my late mother who was always there for me and always encouraged me to realize my dreams.

Lastly, I thank almighty god for showing me the path and always giving me strength and courage in all endeavors of my life.

Dedicated to...

My Beloved Mother



Contents

Certificate	ii
STATEMENTS OF ACADEMIC INTEGRITY	iii
Acknowledgement	iv
Dedication	vi
Contents	vii
List of Abbreviations	xi
List of Tables	xiii
List of Figures	xiv
Chapter 1 Introduction	1
1.1 Protein-misfolding and associated diseases	2
1.2 Tau and Amyloid cascades in AD	4
1.3 Alzheimer`s disease and related Tauopathies	4
1.4 Tau structure and function	5
1.5 Tau aggregation induced by poly-anionic agents and underlying mechanism	5
1.6 Post-translational modifications and interacting partners of Tau	6
1.7 Proteolytic and non-proteolytic degradation of Tau	9
1.8 Major protein aggregate clearance pathways in cell	11
1.9 Altered neuronal functions in Alzheimer`s disease	12
1.10 Histone deacetylases – Origin and Classification	13
1.11 Role of HDACs in neurodegenerative diseases	14
1.12 Structure and function of Histone deacetylase 6	15
1.13 Role of HDAC6 in cytoskeletal organization	17
1.14 Inter-relationship between Tau and HDAC6	18
1.15 Therapeutic approaches against Alzheimer`s disease	18
1.16 Melatonin as a multi-faceted drug against AD	20

1.17	Small molecule Baicalein functions as a potent drug against neurodegeneration	22
	Outline and Objectives of the study	24
	Material and Methods	25
Chapter 2	Tau aggregation inhibition and disaggregation of preformed aggregates by HDAC6 ZnF UBP	56
2.1	Background	57
2.2	Aggregation propensity of Tau	58
2.3	Inhibition of Tau aggregation and conformational changes by HDAC6 ZnF UBP	59
2.4	Disaggregation of preformed Tau fibrils by HDAC6 ZnF UBP	62
2.5	Summary	63
Chapter 3	Interaction of HDAC6 ZnF UBP with Tau affects its stability	65
3.1	Background	66
3.2	Interaction analysis of Tau (Full-length and Repeat) with HDAC6 ZnF UBP	67
3.3	¹ H- ¹⁵ N HSQC NMR Spectroscopy for Tau-HDAC6 ZnF UBP interaction	69
3.4	Molecular modelling and docking of HDAC6 ZnF UBP and repeat-Tau	70
3.5	Interaction study of HDAC6 ZnF UBP and repeat-Tau complex by md-simulations	71
3.6	Degradation of monomeric Tau in the presence of HDAC6 ZnF UBP	74
3.7	Summary	77
Chapter 4	Modulation of neuronal functions by HDAC6 ZnF UBP	78
4.1	Background	79
4.2	HDAC6 ZnF UBP is non-toxic and non-apoptotic	81
4.3	HDAC6 ZnF UBP enhances levels of pGSK-3 β	82
4.4	HDAC6 ZnF UBP reduces Tau phosphorylation in neuronal cells	83
4.5	HDAC6 ZnF UBP modulates actin dynamics	85
4.6	Enhancement of podosome-like structures by HDAC6 ZnF UBP	87

4.7	HDAC6 ZnF UBP enhances ApoE nuclear localization	89
4.8	Enhanced Tubulin localization to MTOC with HDAC6 ZnF UBP treatment	90
4.9	Summary	91
Chapter 5	Screening of small molecules against Tau aggregation	93
5.1	Background	94
5.2	Melatonin in higher concentrations inhibits repeat Tau aggregation	96
5.3	Effect of Melatonin on structural conformation of Tau	96
5.4	Melatonin disaggregates pre-formed Repeat Tau aggregates	96
5.5	Melatonin interacts weakly with the Repeat Tau	97
5.6	Characterization of residue specific interaction of Melatonin and Repeat Tau using NMR spectroscopy	100
5.7	Effect of Melatonin on repeat Tau aggregates-mediated toxicity	101
5.8	Baicalein binds to Tau <i>in vitro</i>	102
5.9	Disaggregation and sequestration of repeat Tau oligomers by Baicalein	103
5.10	Baicalein disaggregate mature fibrils of repeat Tau	105
5.11	Characterizing Baicalein-stabilized oligomers by Size-exclusion chromatography	106
5.12	Summary	107
Chapter 6	Discussion	108
6.1	Tau protein in health and disease	109
6.2	Targeting Tau aggregation – importance as a therapeutic approach	110
6.3	HDAC6 ZnF UBP as modulator of Tau aggregation and stability	110
6.4	HDAC6 ZnF UBP plays an important role in diverse neuronal functions	114
6.5	Current status of therapeutic approaches against AD	118
6.6	Therapeutic approaches against AD based on action of small molecules	119

Conclusion and Future directions	123
Conclusion	124
Future directions	125
Bibliography	127
ABSTRACT	144
Details of the publications emanating from the thesis work	145

List of Abbreviations

AD	Alzheimer's disease
ALS	Amyotrophic lateral sclerosis
APP /βAPP	Amyloid precursor protein/ β -amyloid precursor protein
BBB	Blood brain barrier
BUZ	Binder of ubiquitin zinc finger
CBD	Corticobasal degeneration
CDK5	Cyclin-dependent kinase-5
DD1	Deacetylase domain 1
DD2	Deacetylase domain 2
EB1	End-binding protein 1
FTDP-17	Fronto-temporal dementia with Parkinsonism-linked to Chromosome-17
GABA	γ -amino butyric acid
GSK-3β	Glycogen synthase kinase-3 β
HD	Huntington disease
HATs	Histone acetyl transferases
HDACs	Histone deacetylases
HSF1	Heat shock factor 1
HSP90	Heat shock protein 90
MARK	Microtubule affinity regulating kinase
MTOC	Microtubule organizing center
MTs	Microtubules
NFTs	Neurofibrillary tangles
Ni-NTA	Nickel-nitrilo triacetic acid

NMDA	N-methyl –D-Aspartic acid
PD	Parkinson’s disease
PHFs	Paired helical filaments
PNS	Peripheral nervous system
PP1	Protein phosphatase 1
PP-2A	Protein phosphatase-2A
PSP	Progressive supranuclear palsy
PTMs	Post-translational modifications
ROS	Reactive oxygen species
RNS	Reactive nitrogen species
TEM	Transmission electron microscopy
UPS	Ubiquitin proteasomal system
ZnF UBP	Zinc finger ubiquitin binding protein

List of Tables

Table	Title	Page No.
Table 2.1	Wavelength maxima for hTau40wt-HDAC6 ZnF UBP aggregation assay samples.	62
Table 3.1	Wavelength maxima for hTau40wt-HDAC6 ZnF UBP samples for degradation analysis.	76

List of Figures

Figure	Title	Page No.
Figure 1.1	Protein misfolding diseases and afflicted proteins	2
Figure 1.2	Physiological and pathological aspects of MAPT	3
Figure 1.3	Post-translational modifications of Tau	6
Figure 1.4	Tau and its interacting proteins	7
Figure 1.5	A) Enzyme-mediated cleavage of Tau B) Tau auto-proteolysis	10
Figure 1.6	Protein aggregates clearance mechanism in cell	11
Figure 1.7	Neuronal dysfunctions and other pathological aspects of Alzheimer's disease	12
Figure 1.8	Cytoskeletal organization in physiological and pathological conditions	13
Figure 1.9	Classification of Histone Deacetylases	14
Figure 1.10	Regulatory role of HDAC6 in diverse neuronal functions	17
Figure 1.11	Domain organization and functions of HDAC6	18
Figure 1.12	Current therapeutic strategies against Alzheimer's disease	20
Figure 1.13	Multi-faceted role of Melatonin against AD	22
Figure 1.14	Role of Baicalein against neurodegeneration	24

Figure	Title	Page No.
Figure 2.1	Aggregation propensity of Tau	59
Figure 2.2	Effect of HDAC6 ZnF UBP on full-length Tau aggregation and conformation	61
Figure 2.3	Repeat Tau (K18wt) aggregation inhibition by HDAC6 ZnF UBP	62
Figure 2.4	Disaggregation assay for full-length Tau fibrils in presence of HDAC6 ZnF UBP	63
Figure 3.1	Interaction analysis of Tau and HDAC6 ZnF UBP	68
Figure 3.2	Size-exclusion chromatography for detecting Tau-HDAC6 ZnF UBP association	69
Figure 3.3	¹ H- ¹⁵ N HSQC NMR for Tau and HDAC6 ZnF UBP	70
Figure 3.4	Molecular docking and molecular dynamics simulation of HDAC6 ZnF UBP and repeat-Tau (244-373)	71
Figure 3.5	Intermolecular interaction studies of HDAC6 ZnF UBP with repeat-Tau (244-373)	73
Figure 3.6	Hydrogen bond analysis for Tau and HDAC6 ZnF UBP residues	74
Figure 3.7	HDAC6 ZnF UBP induced Tau degradation	75
Figure 3.8	Tau and HDAC6 interaction is not associated with any conformational changes	75
Figure 3.9	Degradation analysis of hTau40 Cysteine double mutant by HDAC6 ZnF UBP	76
Figure 4.1	HDAC6 ZnF UBP treatment to neuro2a cells is non-toxic	80

Figure	Title	Page No.
Figure 4.2	Internalization of HDAC6 ZnF UBP in neuro2a	82
Figure 4.3	Downregulation of GSK-3 β activity by HDAC6	83
Figure 4.4	Inhibition of Tau phosphorylation (pT181) by HDAC6	84
Figure 4.5	Inhibition of Tau phosphorylation (AT8) by HDAC6	85
Figure 4.6	HDAC6 ZnF UBP as a modulator of actin dynamics	86
Figure 4.7	Enhancement of podosome formation by HDAC6	88
Figure 4.8	Podosome, lamellipodia and podonut-like structure-induced by HDAC6 ZnF UBP	89
Figure 4.9	Modulation of ApoE and Tubulin localization by HDAC6	90
Figure 4.10	Modulation of Tubulin localization by HDAC6	91
Figure 5.1	Small molecules Melatonin and Baicalein against Tau aggregates	95
Figure 5.2	Effect of Melatonin on repeat Tau aggregation	97
Figure 5.3	Disaggregation of repeat Tau fibrils by Melatonin	98
Figure 5.4	ITC for repeat Tau and Melatonin interaction at low concentrations of protein and ligand	98
Figure 5.5	Repeat Tau-Melatonin interaction by ITC.	99
Figure 5.6	^1H - ^{15}N HSQC NMR for repeat Tau and Melatonin.	101

Figure	Title	Page No.
Figure 5.7	Cytotoxicity of repeat Tau aggregates on neuro2a and effect of melatonin on Tau aggregates-mediated toxicity	102
Figure 5.8	The interaction of Tau with Baicalein by UV–Visible absorption spectroscopy	103
Figure 5.9	Disaggregation of repeat Tau oligomers by Baicalein	104
Figure 5.10	Disaggregation of repeat Tau fibrils by Baicalein	105
Figure 5.11	Size-exclusion chromatography for repeat Tau aggregates	106
Figure 6.1	HDAC6 ZnF UBP-mediated Tau aggregation inhibition and disaggregation	112
Figure 6.2	HDAC6 ZnF UBP interacts transiently with Tau enhancing its degradation	113
Figure 6.3	HDAC6 ZnF UBP modulates stability and aggregation of Tau	114
Figure 6.4	Effect of HDAC6 ZnF UBP on Tau phosphorylation and ApoE localization	116
Figure 6.5	Effect of HDAC6 ZnF UBP on cytoskeletal organization	117
Figure 6.6	Disaggregation of Tau aggregates by Melatonin	119
Figure 6.7	Tau aggregation inhibition and disaggregation by Baicalein	122
Figure I	Proposed effects of HDAC6 ZnF UBP on Tau stability and neuronal health.	126

Chapter 1

Introduction

1.1 Protein-misfolding and associated diseases

Proteins acquire specific conformation in order to perform their biological functions. The process of protein translation from RNA is coupled with highly regulated protein folding mechanism assisted by molecular chaperones in order to derive the biologically active conformation [1]. The information for folding of protein is contained in its amino acid sequence and theoretically, a protein can acquire multiple possible conformations [2]. The process of protein folding occurs through a series of events comprising the formation of partially folded intermediate conformations. The energy state of a particular conformation of protein decides its lifetime in physiological condition. The phenomenon of protein folding and misfolding amidst its various intermediate states has been elucidated by funneled energy landscape theory of protein folding [3]. Proteins tend to attain the conformation with a lower energy state, which reached by formation of a large number of intermediates. Thus, there could be large number of pathways through which protein attain its final native conformation [4]. There is limited stability of proteins under physiological conditions without attaining proper conformation. Although, well regulated by molecular forces and chaperones assistance, protein folding mechanism is quite error prone [4]. The partially folded intermediates may undergo aberrant folding pathway such that proteins self-associates to form aggregates, which are thermodynamically stable [5]. The regulated rate of protein synthesis, folding and degradation tends to maintain proteostasis in physiological conditions. However, the decline in proteostasis system under certain conditions-like aging and oxidative stress may lead to loss of native conformation resulting in aberrant protein folding and protein aggregation.

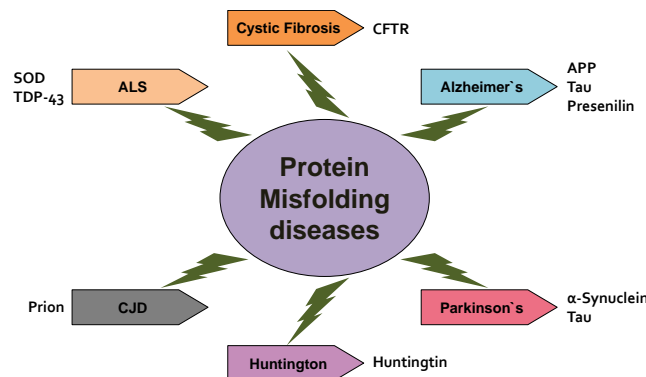


Fig. 1.1. Protein misfolding diseases and afflicted proteins. Protein misfolding may lead to structural aberrations, which could result in pathological conditions. The diseases-associated with protein misfolding are distinguished into gain of function or loss of function diseases. The protein may be rendered dysfunctional due to mutations-like in cystic fibrosis. Most of the neurodegenerative diseases are associated with gain of function due to protein misfolding leading to the formation of ordered insoluble protein aggregates which are toxic to cells. For example, Alzheimer's disease is marked by the defective gain of function of three proteins- amyloid precursor protein (APP), microtubule-associated protein Tau and Presenilin. Amyloid- β peptides form extracellular aggregates in the form of amyloid- β plaques after γ -secretase-mediated cleavage of APP while Tau self-associates under pathological conditions to form intracellular aggregates comprising neurofibrillary tangles (NFTs). Presenilin undergoes point mutations and promotes the γ -secretase-mediated cleavage of APP. Other major diseases associated with protein misfolding include Parkinson's, Huntington, Creutzfeldt Jakob disease (CJD) and amyotrophic lateral sclerosis (ALS).

The formation and accumulation of off-pathway protein aggregates is associated with a variety of protein misfolding diseases. There are a large number of protein misfolding diseases affecting

different cell types and involving different causative proteins (**Fig.1.1**). Protein aggregation is apparent in neurodegenerative diseases like Alzheimer's disease (AD), Progressive supranuclear palsy (PSP), Corticobasal degeneration (CBD), Amyotrophic lateral sclerosis (ALS), Parkinson's disease (PD) and Huntington disease (HD) [6]. The failure of proteostasis results in the deposition of protein aggregates in neuronal cells. The protein aggregates are toxic in nature and hinders the normal physiological functions causing neuronal loss. Neurodegenerative diseases involve the misfolding and aggregation of different proteins specific to the disease. However, the mode of protein aggregation in all neurodegenerative diseases follows similar mechanism in terms of their kinetics. For example, Alzheimer's disease involves the aggregation and accumulation of microtubule-associated protein Tau and amyloid- β peptide obtained after the proteolytic cleavage of amyloid precursor protein (APP) originating in the hippocampal neurons [7]. Parkinson's disease is associated with aggregation of a membrane bound protein α -synuclein as structures called Lewy's bodies in dopaminergic neurons of substantia nigra [8]. It is notable that there are occurrences of cross-reaction in these diseases. For example, Tau is also found to be present in Lewy's bodies along with α -synuclein in case of PD [9]. The process of aggregation takes place in a multi-step manner. The aberrant proteins self-associate to form β -sheet rich species, which includes oligomers with 2-10 protein monomer units and large fibrillar aggregates made up from the ordered arrangement of large number of monomers (**Fig.1.2**). There are various intermediate species composed of few to several hundred monomeric protein units called protofibrils [10]. Earlier, the mature fibrillar aggregates were considered to be the most toxic species and major cause of neurodegeneration. But, later studies suggested evidences, which indicate that oligomers are more hazardous and responsible for neurotoxicity [11].

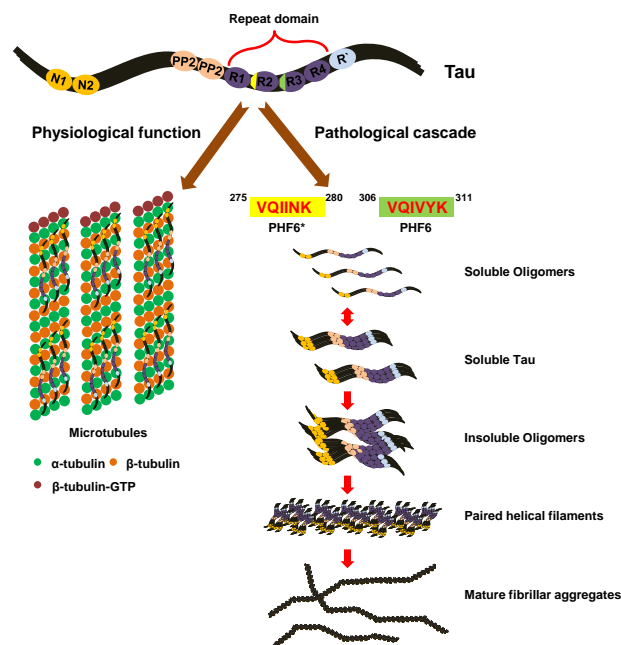


Fig. 1.2. Physiological and pathological aspects of MAPT. Tau associates with microtubules in neuronal cells and promotes their stabilization. The four repeat regions along with PP1 form the microtubule-binding region of Tau whereas the N-terminal directs outward and is known as projection domain. Under pathological conditions, Tau loses its ability to bind microtubules and instead associates with each other through same repeat region to form Tau

aggregates. Two hexa-peptide motifs, namely PHF* (VQIVYK) and PHF (VQIINK) forms β -sheet structure and facilitates self-association. The pathological cascade of Tau aggregation involves formation of several intermediate species. Initially, soluble oligomers are formed which can be reverted back to its constituent free Tau species. Later stages of aggregation are marked with the formation of insoluble oligomeric species, which are considered highly toxic and ultimately lead to the formation of paired helical filaments (PHFs) and neurofibrillary tangles (NFTs).

1.2 Tau and Amyloid cascades in AD

Tau is a microtubule-associated protein in neuronal cells, which functions in binding and stabilizing microtubule structures [12, 13]. The role of Tau is crucial especially in the axonal region where microtubule stabilization is important for transport of cargo towards synapses i.e. retrograde transport [14]. Structurally, Tau is a natively unfolded protein and stays in highly soluble state in neurons. It does not possess a defined conformation but can acquire transient local conformations when associated with other interacting partners. In human, Tau is encoded by chromosome 17q21 and expressed as six isoforms generated by the alternative splicing of exons 2, 3 and 10 [12]. The most prominent isoform of Tau called hTau40 (441 aa) comprise of two N-terminal inserts and four imperfect repeats in the C-terminal. The four repeat regions are flanked by proline-rich region designated as PP1 and PP2 on the N-terminal and a region often addressed as pseudo-repeat region (R[`]) [15]. The alternative splicing gives rise to isoforms consisting of 0, 1 or 2 inserts in combination of 3 or 4 repeat domains. Apart from six major isoforms of Tau, there is one isoform present in peripheral nervous system (PNS) made up of two inserts and four repeats along with 242 amino acids derived from exon 4a [12]. Functionally, hTau40 is composed of two domains- the C-terminal region of Tau which interacts with microtubules named as assembly domain and the N-terminal region that projects away from the microtubules has been termed as projection domain [12]. The assembly domain of Tau mainly consists of four repeat regions and part of poly-proline domain.

1.3 Alzheimer`s disease and related Tauopathies

Alzheimer`s disease is a neurodegenerative ailment arising due to the accumulation of two kinds of toxic species- neurofibrillary tangles (NFTs) in the neuronal cells and amyloid- β plaques in the extracellular regions. Both Tau and amyloid- β aggregates are implicated in other neurodegenerative conditions [16]. Tau aggregates are known to be found in Pick`s disease, Fronto-temporal dementia with Parkinsonism-linked to chr17 (FTDP-17), Guam Parkinson dementia complex etc [17]. The disorders involving the neurotoxicity resulting from the aggregation of Tau are collectively termed as Tauopathies. Similarly, apart from AD, amyloid- β has also been associated with hereditary cerebral hemorrhage with amyloidosis [17, 18]. However, both these aggregates are most prevalent in case of Alzheimer`s disease. The events, which direct these proteins to take up pathological form ranges from genetic predisposition to environmental risk factors. The exact etiology of AD is not clearly understood till date but its risk factors have been assessed. Amyloid- β plaques are formed by the self-aggregation of 42 amino acid residue peptide fragment denoted A β 42. A β 42 is derived from the cleavage of β -amyloid precursor protein (β APP or APP) by the enzymes β -secretase and γ -secretase. Cleavage of β APP by α -secretase generates non-amyloidogenic peptides and is considered a pre-dominant mechanism involved in cell signaling. However, certain mutations within or near the cleavage site in β APP increases the specificity of β -secretase and γ -secretase resulting in higher production of A β 42 peptides. A β 42 peptides released in extracellular region are highly amyloidogenic in nature and can self-associate to form Amyloid- β plaques [19, 20].

1.4 Tau structure and function

Conversion of highly soluble Tau protein into insoluble aggregates structure is an intriguing process. It is noteworthy that there are regions in Tau protein, which have a high propensity to acquire β -structure which lead to the formation of cross β -sheets and ultimately Tau aggregates [21]. The repeat region of Tau is important in this aspect as it forms the basis of its physiological function as well as pathological tendency [21]. There are short hexapeptides motifs- VQIINK and VQIVYK at the beginning of second and third repeats respectively, which have a high tendency to form β -structure. In the process of aggregates formation, these hexapeptides are the regions involved in self-association and forms the core of the fibrillar aggregates [22]. Another factor responsible for driving Tau protein towards aggregation pathway is its charge compensation. The natively unfolded and soluble form of Tau protein is maintained by the unique charge distribution in Tau [23]. Anionic factors such as DNA and heparin have been studied *in vitro* to disturb this charge distribution and initiate the nucleation of Tau proteins to form dimers, oligomers and ultimately aggregates [24]. The determining factor for Tau aggregation *in vivo* is not clearly understood and is probably implicated by myriad of factors instead of a single specific event. Tau hyperphosphorylation is one of the pathological hallmarks in AD, but the underlying mechanism of triggering the events leading to this effect is not clearly understood. Tau is essentially a phospho-protein and requires minimal phosphorylation at specific sites for its function in microtubule stabilization [25]. Several kinases-like cyclin-dependent kinase 5 (CDK5), Glycogen synthase kinase-3 β (GSK-3 β), Microtubule affinity regulating kinase (MARK) etc. are known to phosphorylate Tau at various sites [26]. Most of these are proline directed kinase having Src homology 3 (SH3) domain and employs poly-proline region to act on sites in repeat region [26]. In AD, there is an imbalance between the kinase and its counter-acting phosphatase levels and activity [27]. Thus, one of the therapeutic strategies involves the inhibition or suppression of kinase hyperactivity in order to control the phosphorylation state of Tau.

1.5 Tau aggregation induced by poly-anionic agents and underlying mechanism

Tau exists in a highly soluble form under physiological conditions [12]. The conversion of soluble Tau into pathogenic aggregating form is a multi-factorial event involving re-inclination of various molecular forces. Due to the flexible and highly dynamic nature of Tau molecule, the crystallographic study on Tau has not been able to provide any structural information. However, the crystal structure of aggregated form of Tau has been deduced, which revealed the presence of cross- β structure in the repeat region [28]. *In vitro* studies on the aggregation propensity of Tau has been carried out by using poly-anionic agents such as heparin, heparin sulphate, arachidonic acid and RNA as inducer of aggregation. The poly-anionic inducers affect the stability of intrinsically disordered form of Tau and promote secondary structure formation [24]. Previous studies have revealed that the inducer can bind to Tau in the regions both upstream and downstream of microtubule-binding region as well as in the 2nd and 3rd repeat domains. These inducers interacts with the positively charged amino acid residues, which reduces the overall net charge on Tau and neutralizes the repulsive forces responsible for keeping Tau in natively unfolded form. Apart from this, there is some inherent propensity for β -sheet formation present in the small stretch of repeat regions R2, R3 and R4, notably which involves PHF6 and PHF6* regions [22]. Poly-anionic agents can bind to these regions promoting and stabilizing β -sheet conformation.

1.6 Post-translational modifications and interacting partners of Tau

Another factor that decides the fate of Tau in neurons is the set of post-translational modifications (PTMs). Tau undergoes a large number of PTMs owing to its natively unfolded state which ensures availability of sites for modification (**Fig.1.3**). PTMs determine the structure

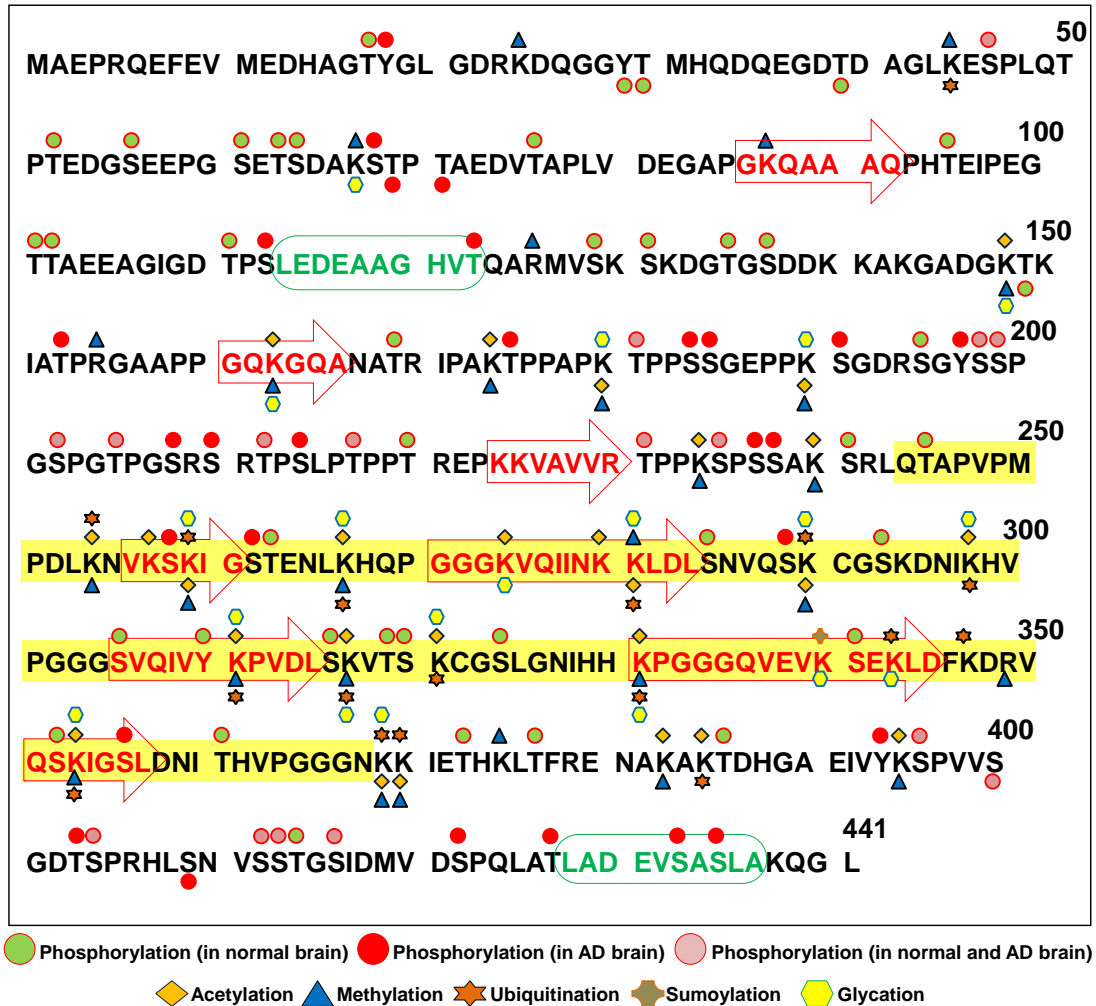


Fig. 1.3. Post-translational modifications of Tau. Tau protein can be subjected to many post-translational modifications owing to its unfolded structure. Tau undergoes post-translational modifications-like phosphorylation, acetylation, methylation, *etc.* which determines its functional state in neurons. Tau is basically a phospho-protein and requires basal level of phosphorylation at specific sites to perform its function. However, in pathological state, phosphorylation signature of Tau differs from that in normal condition. Other post-translational modifications-like acetylation, methylation, ubiquitination and sumoylation also reflects the functional state of Tau as these modifications may compete for a specific lysine residue in Tau with each modification having different effect. For example, ubiquitination marks the protein to direct toward its degradation while other modifications at the same lysine residue may increase its stability. Most of the modifications of Tau are enzyme-mediated and specific in nature while Glycation of Tau occurs non-enzymatically depending on the physiological conditions in neurons.

and function of Tau by regulating the local conformations as well as charge distribution in Tau protein [29]. It is notable that there is a diverse array of interacting proteins which interacts with various domains or regions of Tau to modulate its structure and function (**Fig. 1.4**). There can be as many as 85 possible phosphorylation sites in Tau constituting of 45 serine, 35 threonine and 5

tyrosine residues [30]. Tau phosphorylation serves as the mode of regulation for Tau function. However, increase in the level of Tau phosphorylation hampers its MT binding and

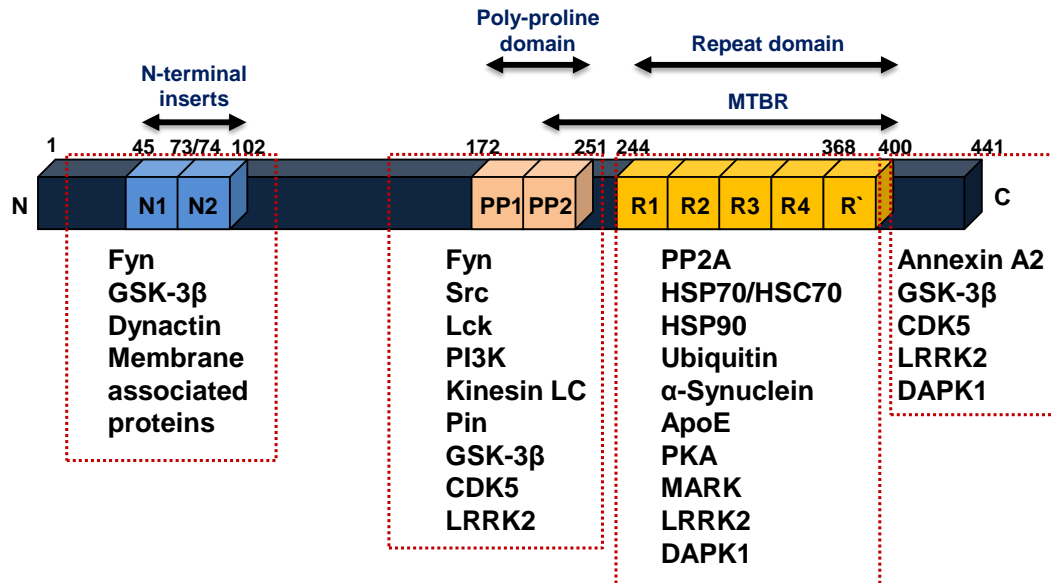


Fig. 1.4. Tau and its interacting proteins. Full-length human Tau consists of two N-terminal inserts (N1 and N2) and four C-terminal domains comprising of imperfect repeat of ~30 amino acids each (R1, R2, R3 and R4). The four repeat regions are flanked on N-terminal by poly-proline domains- PP1 and PP2 while on the C-terminal by pseudo-repeat region - R'. Tau is a natively unfolded protein, which can interact with a wide array of proteins that modulates its function through modifications such as phosphorylation, acetylation *etc.* or modifying its local conformation through transient interactions. The figure shows the major proteins that interact with different regions of Tau protein.

result in its detachment from MT. Mapping of PTMs in Tau protein obtained from AD patient's brain has revealed phosphorylation sites, which are not present in normal conditions. Some of the major pathological sites include AT8 (pS202/pT205), AT100 (pT212/pS214), AT 180 (pT231/pS235) and PHF1 (pS396/pS404) [31]. Most of these sites lie within the repeat region of Tau and are likely to induce Tau aggregation by disturbing the charge distribution and altering intramolecular interactions. Different families of kinases carry out phosphorylation of Tau. These include proline-directed protein kinases-like GSK-3 β , CDK5 and MAP kinases (mitogen-activated protein kinases); non-proline directed protein kinases-like CK (casein kinase), MARKs (microtubule-affinity regulating kinases), PKA (protein kinase A) and tyrosine specific kinases-like SFKs (Src family kinases) [25]. The level and activity of these kinases are elevated in case of AD and most of these are found to be co-localized with NFTs. Tau hyperphosphorylation occurs when there is a net increase in the phosphorylation *i.e.* there is an imbalance between phosphorylation and dephosphorylation. This condition arises generally due to increase in kinase activity along with inhibition of protein phosphatases. PP-2A (Protein phosphatase-2A) is the major phosphatase of the cell with nearly 70% of overall cellular phosphatase activity [32, 33]. PP-2A is regulated by two modes - methylation and action of endogenous cellular inhibitors called I₁ and I₂. PP-2A activity may get reduced up to 50% in AD due to hypomethylation or increase in the levels of its inhibitors [34].

The lysine residues in Tau are subjected to various modifications-like glycation, ubiquitination, SUMOylation, methylation and acetylation [35]. Some of the sites for these modifications may

coincide and it depends on the cellular conditions and functional requirements as which modification would be preferred. Glycation is a PTM of Tau associated with the pathological condition. Glycation is a non-enzymatic addition of sugar moieties like glucose or fructose to the lysine residues on a protein. Once a protein is glycated it becomes less assessable to be degraded by the proteasomal machinery and therefore, leads to its accumulation [36]. The accumulated glycated species are toxic in nature as they eventually form advanced glycation end products (AGEs) and triggers the formation of free radicals [36, 37]. There are twelve lysine residues known to get glycated in Tau out of which seven lies in the microtubule-binding region [38, 39]. Glycated Tau is found to be present in NFTs and hinders Tau degradation and clearance [37].

Ubiquitination is the enzymatic addition of a single or more molecules of ubiquitin to the lysine residue of another protein to be targeted for proteasomal degradation [35]. Addition of ubiquitin involves isopeptide bond formation between the ϵ -amino group of lysine in the target protein and C-terminal carboxyl group of ubiquitin [35]. Tau ubiquitination occurs mostly in the C-terminal region directing Tau for its degradation. Some of the sites present in the microtubule-binding region e.g. K254, K311 and K353 [40]. Ubiquitination requires a series of family of enzymes namely; E1 (for activation), E2 (for conjugation) and E3 (for ligation) [41]. CHIP (C-terminus of the Hsc70-interacting protein) is the major E3 ligase known to ubiquitinate Tau and mediating its degradation [42]. SUMOylation is another modification involving addition of a small protein called small ubiquitin-like modifier (SUMO) to the lysine in the target protein. SUMOylation also involves a cascade of reaction similar to ubiquitination. Out of three SUMO proteins – SUMO1, SUMO2 and SUMO3, Tau is mostly modified by SUMO1 [43]. The exact function of Tau SUMOylation is not clear but it has been associated with pathological condition as it has a direct relationship with hyperphosphorylation of Tau [44]. Tau SUMOylation is known to enhance phosphorylation at AD associated sites-like T231 and S262. Conversely, Tau hyperphosphorylation promotes SUMOylation at K340 inhibiting ubiquitination at this site and thus hindering Tau degradation [45].

Methylation occurs at either lysine or arginine residues of protein and is known to be associated with AD. Methylation is carried out by lysine methyl transferases with S-adenosyl methionine as methyl group donor while its removal is carried out by lysine demethylases [46]. Tau methylation is found in both physiological and pathological conditions. In aggregated Tau, methylation occurs in poly-proline region along with repeats R1 and R2 [47]. There are seven methylation sites in aggregated Tau, which includes K180, K254, K267 and to a lesser extent, K290. In contrast there are eleven methylation sites in normal Tau, which may be mono-methylated or di-methylated. R126, R155 and R349 are the major methylated sites in normal Tau [48]. Tau methylation possibly affects the stability of Tau by enhancing intermolecular interaction while weakening Tau association with MT. Methylation has cross-talks with other modifications like phosphorylation, acetylation and ubiquitination. Methylation at K254 competes with ubiquitination at the same site and hampers Tau degradation. Similarly, pathological phosphorylation at S262 gets enhanced when the site K267 is methylated [47]. There are common methylation and acetylation sites like K163, K174 and K180 but the effect of one preferential modification over other is not yet clear [47]. Acetylation is a PTM at lysine residue mediated by acetyltransferases and play an important regulatory role for many proteins. Tau can be acetylated by two acetyltransferases - p300 or CBP acetyltransferase [49]. Apart from enzymatic acetylation, Tau can also undergo auto-acetylation by a cysteine-catalyzed mechanism *via* C291 and C322 [50]. There are many acetylation sites in the poly-proline region and repeat

region of Tau, which primarily inhibit binding of Tau to MTs. K174, K274, K280 and K281 are important acetylation sites as they co-localizes with hyperphosphorylated Tau in PHFs [49]. Studies on pseudo-acetylated (K280Q) Tau shows that it enhances phosphorylation at S262 and T212/S214 which are considered as pathological phosphorylation sites of Tau [51]. However, acetylation at KXGS motifs in repeat region has a protective role as it diminishes Tau hyperphosphorylation and these sites are found to be hypo-acetylated in AD [52]. The levels of enzymes associated with removal of acetyl group i.e. deacetylases, are reduced in AD. SIRT1 is a cytoplasmic deacetylase of class IV whose level goes down as disease progresses. Histone deacetylase 6 (HDAC6) is another potential deacetylase present in cytoplasm, which is known to be associated with Tau, and has a protective role by mediating aggregates clearance [53, 54].

1.7 Proteolytic and non-proteolytic degradation of Tau

Apart from the various PTMs, which determine the functional state of Tau protein, proteolytic and non-proteolytic cleavage of Tau is another factor determining its physiological role in neurons (**Fig.1.5A and B**). There are cleavage sites in the repeat domain of Tau, which tend to generate Tau fragments of amyloidogenic nature. Cleavage at N-terminus after Lys257 generates fragment named as F1, at C-terminus after Val363 generates fragment named as F2 and at C-terminus after Ile360 generates fragment named as F3 [55]. It is notable that the F2 and F3 fragments are generated only after initial proteolytic cleavage at Lys257 by a thrombin-like protease to give F1 fragment. Both F2 and F3 fragments are more reactive compared to F1 in terms of amyloidogenicity [55]. Tau can be a substrate to many endogenous proteases-like caspases and calpain, which are believed to play an important role in Tauopathies. Caspases 1, 3, 6, 7 and 8 can cleave Tau at Asp421 to generate a fragment 5 KDa smaller than Tau [56]. The removal of this C-terminal part of Tau makes it susceptible to aggregation indicating its protective role against Tau aggregation. Tau truncated at Asp25 (caspase 3-mediated), at Asp402 (caspase 6-mediated) and at Asp421 are found in the AD brain [57]. Apart from caspases, Ca²⁺ dependent enzyme calpain is also known to be involved in Tau cleavage. There are nine putative calpain-mediated cleavage sites in Tau (M11, K44, R230, K254, K257, K267, Y310, K340 and Y394) and studies show that the level of calpain activity is inversely proportional to the phosphorylation state of Tau [58]. Calpain is regulated by an endogenous inhibitor calpastatin whose levels get reduced in AD [59]. Tau cleavage by calpain generates a 17 KDa fragment, which is toxic to neurons and induces apoptosis [55]. Previous studies have shown that Amyloid- β treatment of neurons can cause Tau fragmentation mediated by caspases and calpain possibly by triggering the process of apoptosis [56]. Cathepsins are lysosomal enzymes, which may be released in the cytoplasm under pathological conditions. Cathepsin L is an important enzyme in terms of its role in generating the two amyloidogenic fragment F2 and F3 [55]. There are other enzymes viz. trypsin, chymotrypsin and thrombin which have been studied for Tau cleavage in vitro [60]. Non-enzymatic cleavage of Tau also occurs which shows that Tau possibly has auto-proteolytic activity. Under prolonged incubation conditions, Tau can undergo degradation showing cleavage at the C-terminus of asparagine residues followed by bulky hydrophobic residues viz. Val, Leu and Ile. Tau also has an intrinsic auto-acetylation activity, which has shown to induce auto-proteolysis of Tau possibly through a cysteine-mediated mechanism [50, 61].

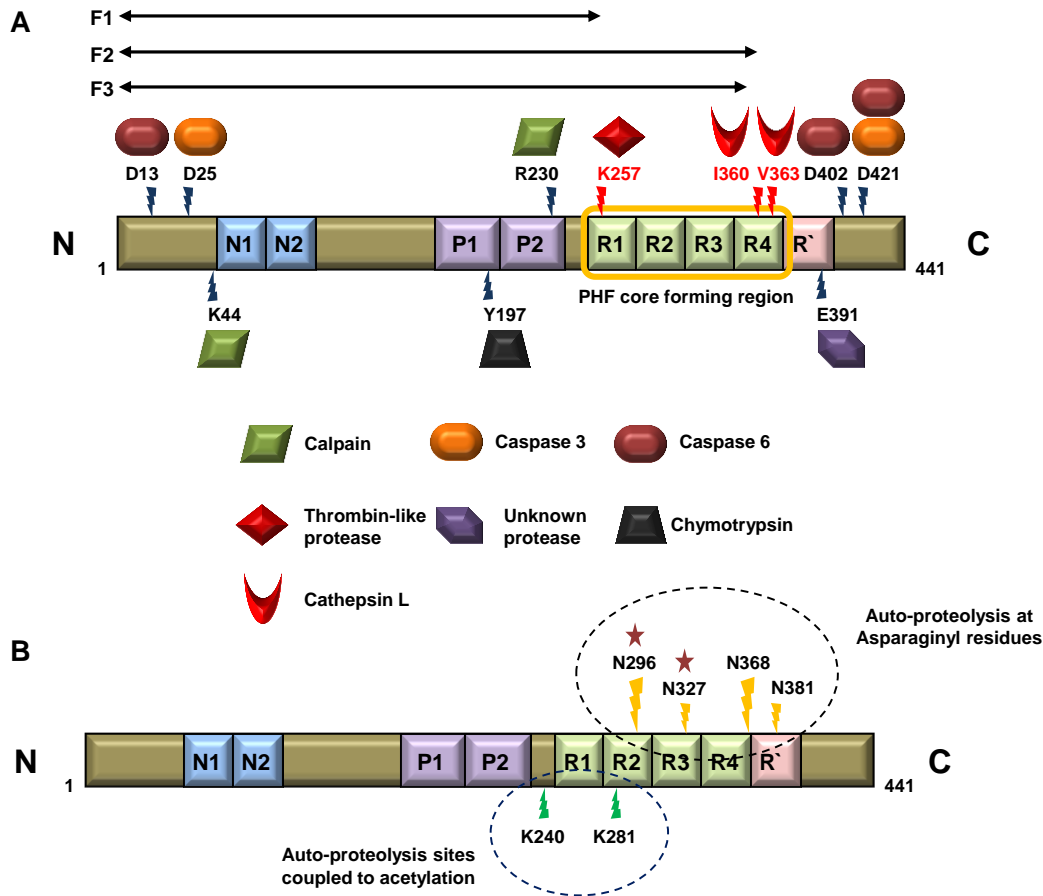


Fig. 1.5. A) Enzyme-mediated cleavage of Tau. Tau can be subjected to enzymatic cleavage under various conditions generating Tau fragments and smaller peptides having diverse role in Tauopathies. Proteolytic enzymes like calpain and caspases targets Tau cleavage at specific sites to generate peptides varying in length from 17-24 KDa. Similarly, Tau cleavage at K257 by a thrombin-like protease generates Tau fragment F1, followed by cleavage by Cathepsin L at V363 or I360 to generate F2 and F3 fragments respectively. These fragments are found to be amyloidogenic in nature and known to be present in neurofibrillary tangles. **B) Tau auto-proteolysis.** Apart from proteolytic enzymes-mediated cleavage of Tau, there are evidences for auto-proteolytic degradation of Tau. The mechanism of Tau auto-proteolysis may involve cysteine-mediated catalysis at asparaginyl residues located in the repeat region of Tau or can be coupled to Tau modification such as acetylation. However, the conditions in which Tau auto-proteolysis is initiated and the underlying mechanism need to be further elucidated.

Human high-temperature serine protease A1 (HTRA1) is an ATP-independent serine protease of HtrA family involved in protein quality control. HTRA1 is known to act on Tau fibrils in Tauopathy conditions [62]. HTRA1 acts on Tau within the repeat region between residues A239 and V399 as they have multiple HTRA1 cleavage sites in between. Tau cleavage by HTRA1 generates fragments having 8 to 22 amino acid residues. The mechanism of action for Tau cleavage by HTRA1 involves initial destabilization of Tau fibrillar structure to expose cleavage sites followed by Tau degradation [62]. The protective role of HTRA1 in Tauopathies can also be attributed to its action on apolipoprotein E, which is considered as a genetic risk factor in AD [63]. ApoE cleavage occurs in an allele-dependent manner, where ApoE4 is preferably cleaved than ApoE3 since it interferes with Tau degradation and clearance in Tauopathies [63].

1.8 Major protein aggregates clearance pathways in cell

In AD, the neurotoxicity arises due to the formation of insoluble aggregate species. Under normal conditions, the protein aggregates formed in the cell are reverted back to its native functional state or cleared from the cell by various mechanisms (**Fig.1.6**). The proteins upon misfolding are either refolded by chaperones or targeted for degradation via ubiquitin proteasomal system (UPS) and these poly-ubiquitinated protein aggregates are degraded and recycled in proteasome [64]. Aggregation and subsequent accumulation of Tau protein aggregates are primarily tackled by chaperones and ubiquitin proteasomal system [65].

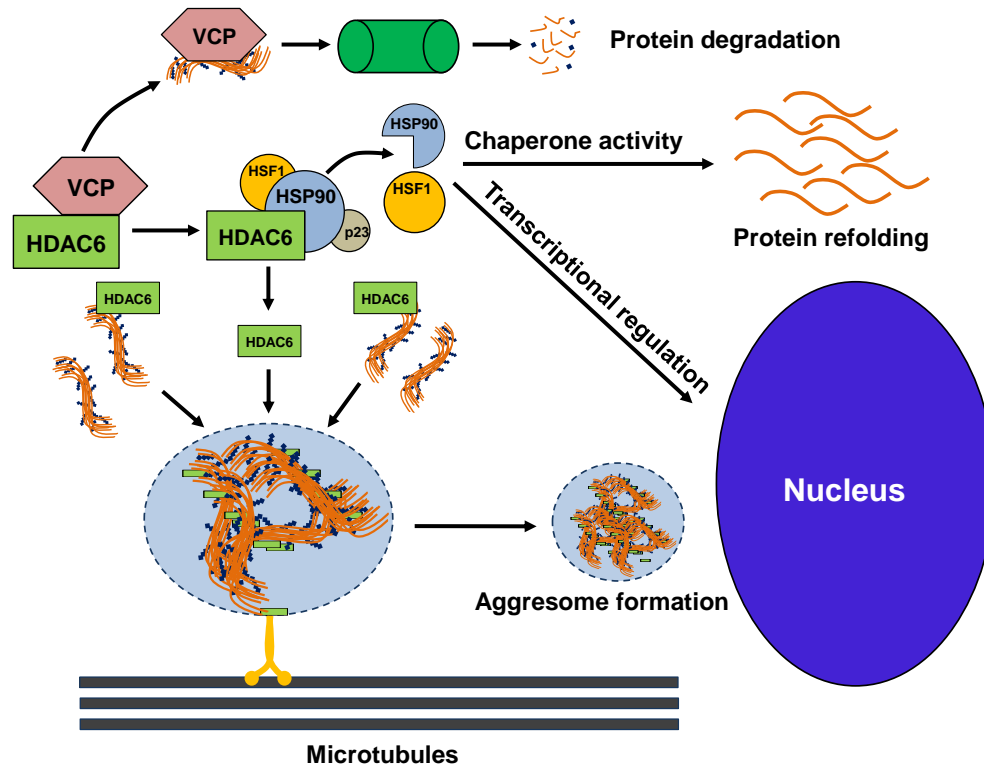


Fig. 1.6. Protein aggregates clearance mechanism in cell. Protein misfolding leads to deregulation of protein homeostasis and accumulation of toxic protein aggregate species (oligomers and fibrillar aggregates) in cells. Presence of misfolded proteins in the cells triggers the molecular chaperones-like HSP90 and HSF1, which facilitates the refolding of protein into right conformation. The proteins, which are not effectively refolded by chaperones, are directed towards degradation *via* UPS by addition of poly-ubiquitination tags. Both chaperone system and UPS are regulated by HDAC6, which is considered as switch between the two pathways. As the aggregate burden increase in the cell, the rate of degradation by UPS falls short to effectively clear out toxic aggregates. In order to cope up with the increased aggregate burden upon failure of chaperone-mediated refolding and UPS, cells employs aggresome pathway. Aggresomes are aggregate rich structures located in the nuclear periphery which are degraded by cell-mediated autophagy. HDAC6 plays an important role in aggresome pathway as it associates with ubiquitin in poly-ubiquitinated aggregates through its ZnF UBP domain. HDAC6 interacts with dynein motor protein and recruits it to carry and sequester poly-ubiquitinated aggregates in the form of aggresomes.

Upon failure of UPS, the aggregates are directed towards the formation of aggresomes, which serves as the cytoprotective response upon the failure of UPS [66]. HDAC6 is a class II histone deacetylase mainly present in the cytoplasm involved in the regulation of various cellular functions. It consists of two catalytic deacetylase domains and a unique ZnF UBP (Zinc finger

ubiquitin binding protein) domain, which sets it apart from other HDACs [67, 68]. Aggregation and subsequent accumulation of Tau protein is primarily tackled by chaperones and ubiquitin proteasomal system. In case of disruption of UPS, the aggregates are directed towards the formation of aggresomes, which serves as the cytoprotective response upon the failure of UPS. One of the major functions of HDAC6 is that it is primarily involved in recruiting the polyubiquitinated protein aggregates to Dynein/Dynactin complex to carry and sequester them to MTOC in the perinuclear region for aggresome formation [69, 70], The function of HDAC6 in both UPS and autophagy indicate its role as a possible link between the two mechanisms [71]. The impairment of UPS function acts as a cue for the activation of a compensatory mechanism for the clearance of protein aggregates [69].

1.9 Altered neuronal functions in Alzheimer's disease

Alzheimer disease is associated with physiological changes, which interfere with the normal functions of neurons (**Fig. 1.7 and 1.8**). As the disease progresses, the protein aggregate inclusions accumulates which cause defects in the transport mechanisms and signalling cascades leading to aberrant cellular functions. One of the deleterious effects of aggregate toxicity is the

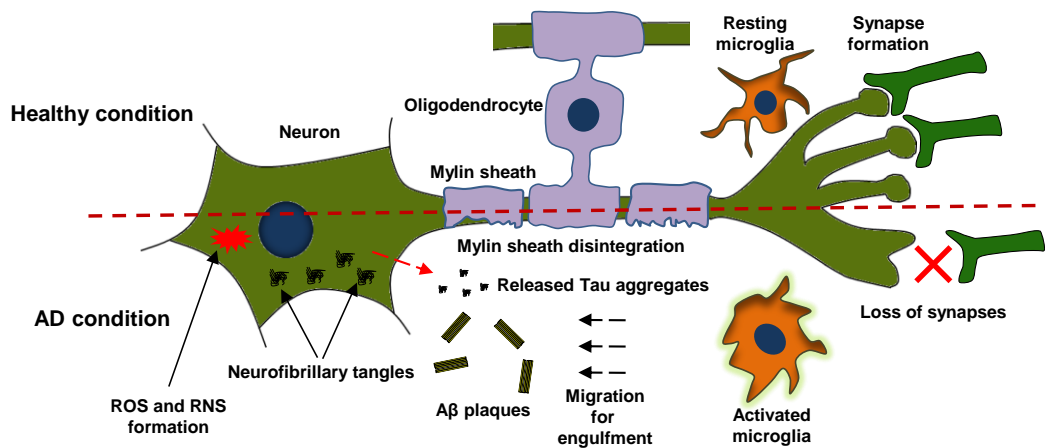


Fig. 1.7. Neuronal dysfunctions and other pathological aspects of Alzheimer's disease. The accumulation of Tau and Amyloid- β aggregates modulates the neuronal environment and triggers processes deleterious to the cells. Neurotoxicity caused by aggregates results in oxidative stress due to production of reactive oxygen species (ROS) and reactive nitrogen species (RNS). ROS and RNS production may result in cell membrane damage and mitochondrial defects. Demyelination or myelin sheath disintegration is one of the outcomes of aggregates induced toxicity. The aggregates present in the extracellular matrices either formed extracellularly or released from neurons stimulate resting microglia to get activated and take amoeboid form in order to migrate and engulf the aggregates. The neuronal network in the brain start collapsing as there is subsequent loss of synapses between neurons leading to their degeneration.

generation of oxidative stress which further damages the neurons [72]. There is a cross-talk between Tau and Amyloid- β aggregates with mitochondrial function where aggregates interfere with mitochondrial fission [73]. Conversely, the conditions which give rise to oxidative stress result in the generation of reactive oxygen species (ROS) and reactive nitrogen species (RNS) [74]. ROS and RNS further damage the cells and are known to mediate abnormal hyperphosphorylation of Tau [75]. Myelin disintegration is another factor, which develops as there is oxidative damage to cells. Axonal damage associated with myelin sheath depletion and monocarboxylic acid transporter 1 (MCT1) has been observed in APP/PS1 mice models [76].

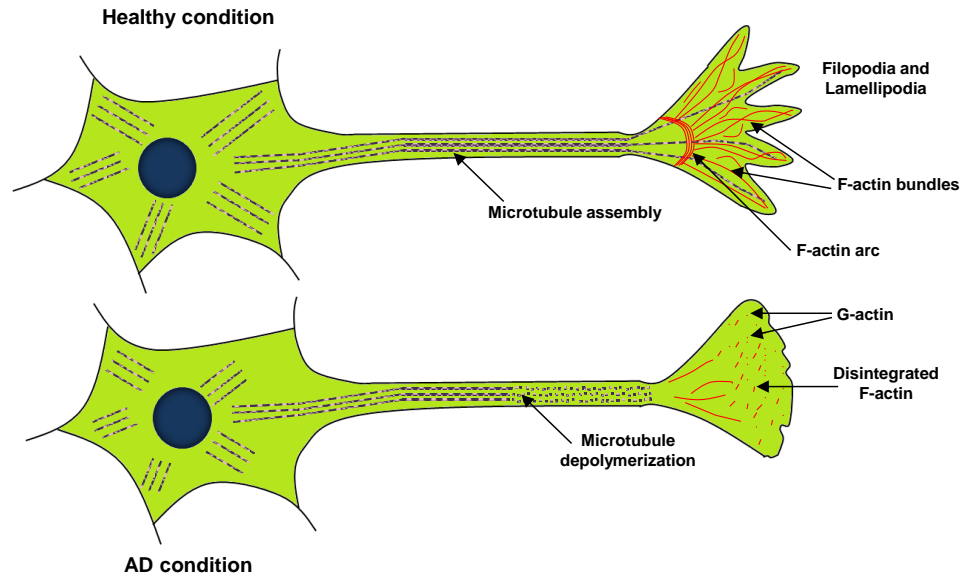


Fig. 1.8. Cytoskeletal organization in physiological and pathological conditions. One major pathological effect apparent in AD involves deregulation of cytoskeletal elements viz. actin fibers and microtubules (MTs). Microtubule network is required for the maintenance of cargo transport from cell body to the axonal region *i.e.* anterograde transport. Under pathological condition of AD, as Tau detaches from microtubules, there is rapid depolymerization and destabilization of MT network affecting axonal transport. Similarly, polymerization of globular actin (G-actin) monomers into fibrous actin (F-actin) is required to form filopodia and lamellipodia structures and synapse formation. Disintegration of F-actin into G-actin monomers takes place in AD due to energy deficient and increasingly oxidative environment in pre-synaptic neurons leading to synaptic loss and neurodegeneration.

Microglia is the resident phagocytic cells of CNS, which functions in maintenance of neurological synapses by engulfment of cellular debris by phagocytosis. Formation of protein aggregates triggers the activation of microglia resulting in the production of pro-inflammatory cytokines causing an inflammatory response [77]. Another pathological impact that arises in AD is the loss of synapses leading ultimately to cognitive decline. Loss of Tau function associated with AD leads to defective axonal transport due to dysregulation of microtubule assembly. The loss of anterograde transport to synaptic terminals leads to their degeneration resulting in neuronal loss [78]. Further, the synaptic vesicles and release of neurotransmitters is affected in AD [79]. This function depends on the actin organization and dynamics for the intricate packing and release of signal molecules in the synaptic cleft [80]. Disintegration of F-actin has been observed in AD leading to hindrance in the synaptic functions [81].

1.10 Histone deacetylases – Origin and Classification

Apart from the role of HDAC6 in aggregate clearance and protein homeostasis, there are several other histone deacetylases, which are implicated in neuronal functions [82]. Histone deacetylases (HDACs) are the enzymes responsible for removal of acetyl groups in lysine residues of a large number of proteins [67]. HDACs were first discovered with respect to their role of histone deacetylation in order to regulate the epigenetic mechanism in cells along with enzymes responsible for acetylation *i.e.* histone acetyl transferases (HATs). In humans, there are 18 HDACs classified into four classes based on their sequence homology with yeast transcriptional repressors and named as per the chronological sequence of their discovery (**Fig.1.9**) [68].

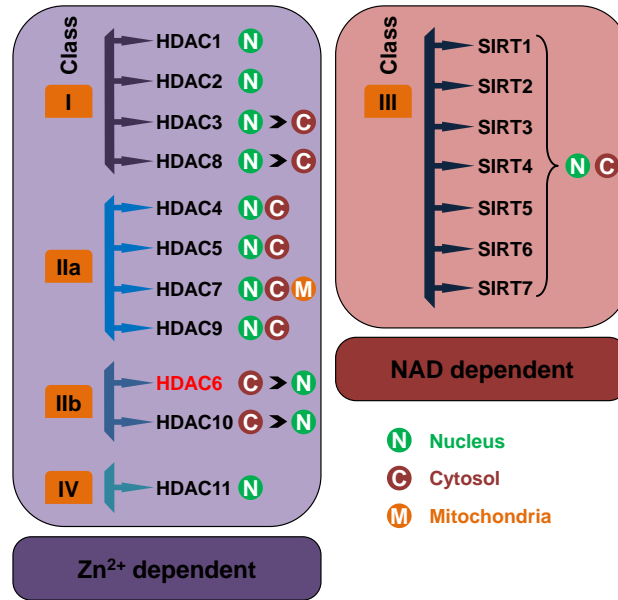


Figure 1.9. Classification of Histone Deacetylases. Histones deacetylases (HDACs) are the class of enzymes well studied for its role in transcriptional modulation and epigenetic regulation by carrying out deacetylation on histone protein. However, there are many non-histone substrates of HDACs present in cells and their activity is regulated by deacetylation. HDACs consist of family of 18 proteins, which are grouped on the basis of their homology with yeast histone deacetylases. Functionally, they are classified on the basis of their enzymatic mechanism as Zn²⁺-dependent and NAD-dependent HDACs. Most HDACs are present in both nucleus and cytosol, some of which can shuttle between the two compartments while others are exclusively found in nucleus. In cytosol, HDACs perform a wide variety of functions-like cytoskeletal regulation, growth and development *etc.* by either functioning alone or as a part of multi-protein complexes. HDAC6 is majorly a cytosolic HDAC distinct from other HDACs by possessing two functional catalytic domains and a C-terminal ZnF UBP domain. HDAC6 is involved in the regulation of cytoskeletal dynamics by acting on α -tubulin and cortactin, transcriptional regulation, and chaperone function. The ZnF UBP domain of HDAC6 is involved in protein homeostasis by mediating the formation of aggresomes in order to degrade the protein aggregates by autophagy.

The HDACs of class I are similar to γ RPD3, class II are similar to γ HDA1 and class III are similar to γ SIR2. Only HDAC11 is included in class IV and shares its properties with class I and class II HDACs [67]. On the basis of mechanism of action, HDACs are classified as Zn²⁺-dependent and NAD-dependent. Further on the basis of domain organization, class II HDACs are further subdivided into class IIa and IIb. The members of class IIa consist of a highly conserved C-terminal catalytic domain and an N-terminal domain dissimilar to other classes of histone deacetylases [83]. Under class IIb, there are two HDACs – HDAC6 and HDAC10. Class IIb HDACs have a duplicated catalytic domain. However, the second deacetylase domain is partial and inactive in case of HDAC10. HDAC6, on the other hand, stands apart from all other HDACs by having two functional catalytic domains and a C-terminal binder of ubiquitin zinc finger (BUZ) or zinc finger ubiquitin binding protein (ZnF UBP) domain [84].

1.11 Role of HDACs in neurodegenerative diseases

Neurodegenerative diseases-like AD, PD and HD originates due to various closely related factors and usually involves interplay of a myriad of cellular processes involving many proteins performing various functions. Likewise, HDACs have been widely studied for their role in neuronal health and in various neurodegenerative diseases. There are various non-histones

substrates of HDACs, which are regulated by acetylation/deacetylation that includes receptors, enzymes, ion channels *etc* [85]. The function of HDACs has been mainly implicated through direct interaction-like in gene transcription or through its deacetylase activity. It is notable that most of the members of class IIa HDACs have minimal deacetylase activity and usually associates with other HDACs to perform their function. HDACs may show neurotoxic or neuroprotective effect depending upon their localization, interacting partners and cell specificity. For example, HDAC1 is a nuclear HDAC which get transported to cytoplasm under pathological condition and cause synaptic dysfunction, impaired axonal transport and mitochondrial dysfunction in neurons [86, 87]. However, when present in nucleus, it associates with histone deacetylase related proteins (HDRP) to impart neuroprotective effect [88]. It is also known to interact with a class III HDAC called Sirtuin1 to protect genomic stability [89]. HDAC2 is closely related to HDAC1 and HDAC3 in terms of its function and has been studied for its role in Niemann-Pick type C disease which is a lipid storage disease associated with abnormal cholesterol deposition [90]. Overexpression of HDAC2 is also associated with impairment of synaptic plasticity and cognitive function by acting as a transcriptional repressor for genes involved in synaptic and cognitive function [91]. HDAC3 is the most expressed class I HDAC known for its role in the embryonic development [92]. It is present in all cell types including neurons, astrocytes and oligodendrocytes [93]. Over-expression of HDAC3 has shown to induce neurotoxicity by a mechanism-associated with GSK-3 β -mediated phosphorylation [94]. HDAC4 is a cytoplasmic HDAC but can shuttle to nucleus *via* Ca²⁺/Calmodulin-dependent kinase-mediated signaling [95]. It is shown to have both neurotoxic as well as neuroprotective function depending on its cellular location. HDAC4 plays an important role in cell survival and protection against apoptosis. The protective mechanism of HDAC4 is independent of its catalytic activity as its inhibition does not affect the neuroprotection [96]. It is found to promote the survival of retinal neurons by interacting with hypoxia-inducible factor 1 α (HIF1 α) [97]. In HD, it is shown to exhibit protective function against poly-glutamine aggregates by positively modulating the function of a subclass of heat shock proteins called DNJB6 [98]. On the other hand, nuclear translocation of HDAC4 has deleterious effect in case of Ataxia Telangectasia which is mediated by the action of PP2A on HDAC4 [99]. Also, reduced expression of HDAC4 results in increased levels of brain-derived neurotropic factor in mouse model of HD [100]. HDAC5 is important in axonal regrowth following injury and its reduced levels are associated with impaired cognitive functions [101]. The functions of HDAC7, HDAC8, HDAC9, HDAC10 and HDAC11 have not been explored extensively but some of the studies shows that HDAC7, HDAC9 and HDAC11 plays a role in neuronal health [93, 102].

1.12 Structure and function of Histone deacetylase 6

HDAC6 is one of the most important HDACs with respect to neuronal health as it is involved in the clearance of aggregated proteins through its ZnF UBP domain. It is also involved in protein homeostasis as it promotes chaperone activity and expression via heat shock factor 1 (HSF1) and heat shock protein 90 (HSP90) [103]. Apart from its role in protein homeostasis, it performs a myriad of several other functions in structural organization and regulation (**Fig. 1.10**). The function of HDAC6 depends on its two catalytic domains and C-terminal ZnF UBP domain, which imparts variability in its role. HDAC6 has a large number of substrates in the cell including α -tubulin, cortactin and Tau [54]. Hypoacetylation of tubulin by the action of HDAC6 results in impaired transport along microtubules and its action on Tau affects clearance and aggregation propensity [104]. Neurodegenerative function and neuroprotective function of

HDAC6 depends differently based on the deacetylase function of catalytic domains and interaction through its ZnF UBP domain respectively. HDAC6 consists of a nuclear localization sequence (NLS), nuclear export signal (NES1), two deacetylase domains (DD1 and DD2), cytoplasmic anchoring domain (SE14) and a ZnF UBP domain. It performs a wide range of functions both dependent and independent of its deacetylase activity (**Fig. 1.11**). It has a large number of interacting partners, which contributes to its functions either by physical association or PTMs. In the N-terminal region, HDAC6 is involved in the regulation of cell migration, chemotaxis and F-actin regulation through its DD1 domain [105]. HDAC6 acts on the elements of cytoskeletal network like α -tubulin, in case of microtubules and cortactin, in case of actin cytoskeleton to regulate their dynamics [106]. It also deacetylates cell survival factors like Ku70 and survivin to mediate anti-apoptotic function [107]. HDAC6 regulates HSP90 function in protein homeostasis under stress conditions. HSP90 is a substrate for deacetylation by DD1 and also associates with ZnF UBP domain [103]. The function of DD2 is regulated mainly by PTMs, as phosphorylation by kinases such as GSK-3 β , Aurora kinase A and Casein kinase 2 (CK2) enhances its deacetylase activity [108]. However, acetylation by p300 and association with Dysferlin suppresses its catalytic function resulting in reduced microtubule deacetylation [109, 110]. The ZnF UBP domain associates with TRIM50 and Ubiquitin to mediate aggresome formation for clearance of protein aggregates [69]. It also binds with protein phosphatase 1 (PP1) to indirectly regulate the Akt dependent phosphorylation in survival signalling and transport mechanisms [111]. The region between DD1 and DD2 constitutes dynein motor binding motif (DMB) which associates with dynein motor in order to transport ZnF UBP bound poly-ubiquitinated aggregates into nuclear periphery for aggresome formation [112].

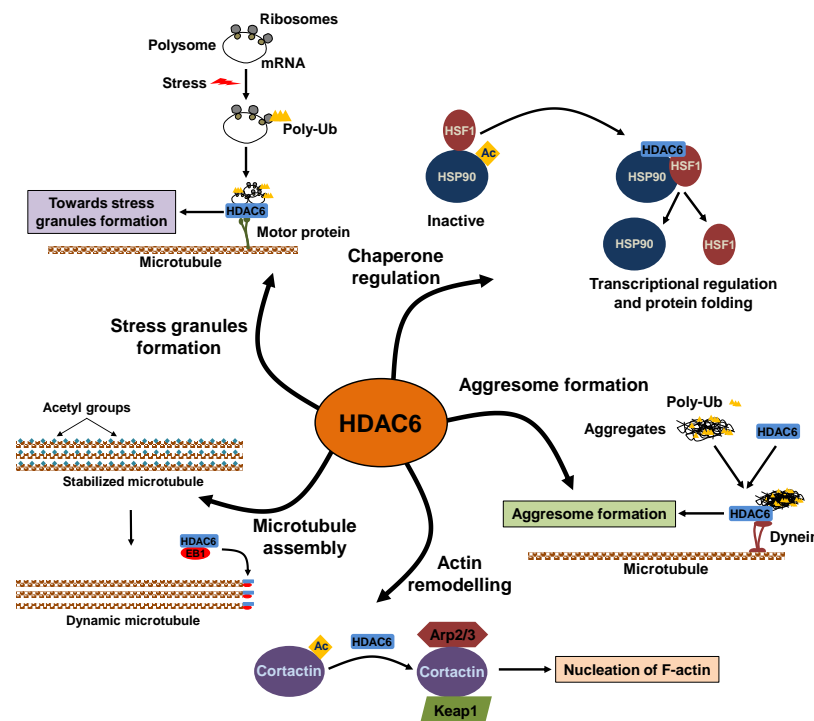


Fig. 1.10. Regulatory role of HDAC6 in diverse neuronal functions. HDAC6 plays a major role in various aspects of neurodegenerative diseases as it modulates many cellular functions. HDAC6 is known to regulate activation of chaperones either directly or indirectly. Heat shock protein 90 (HSP90) under basal conditions remains inactive in its acetylated form. Under stress conditions, HDAC6 binds to HSP90 and activates it via deacetylation. It

also releases heat shock factor 1 (HSF1), which functions in transcriptional regulation and protein folding along with HSP90. Upon failure of chaperone system in protein refolding as well as proteasomal degradation of protein aggregates, HDAC6 mediates the formation of aggresomes, which are cleared by autophagy. HDAC6 binds to poly-ubiquitinated (Poly-Ub) aggregates and help to carry them towards perinuclear region via dynein motor in order to form aggresomes. Actin dynamics during the process of cell migration, cell attachment, neurite extensions and formation of other membrane projections-like filopodia, lamellipodia and podosomes require HDAC6 deacetylase activity. Cortactin is a nucleation factor for F-actin formation, which is deacetylated by HDAC6. Cortactin initiates F-actin formation by associating with other nucleating factors such as Keap1 and Arp2/3. Acetylated α -tubulin in microtubules result in stabilized microtubules. Microtubules are maintained in a dynamic stage by HDAC6 through deacetylation and regulation of growing MT ends through association with end-binding protein 1 (EB1). Stress granules are the structures formed during cellular stress, which contains mRNA, ribosomes and proteins associated with protein translation. Protein translation gets halted during stress conditions, which triggers stress granules formation where mRNA and ribosomes are salvaged that can be reused later. HDAC6 helps in the transport of poly-ubiquitinated aggregates containing polysomes and other proteins in order to form stress granules.

1.13 Role of HDAC6 in cytoskeletal organization

There are various other functions carried out by HDAC6 that reflect the state of neuronal health. This mainly includes its role in the modulation of various cytoskeletal elements, cell migration and regulation of neuronal extensions [105]. α -tubulin is the first known substrate of HDAC6 where deacetylation plays a role in modulation of microtubule dynamics. HDAC6 inhibition leads to enhanced tubulin deacetylation [104]. HDAC6 is also known to associate physically

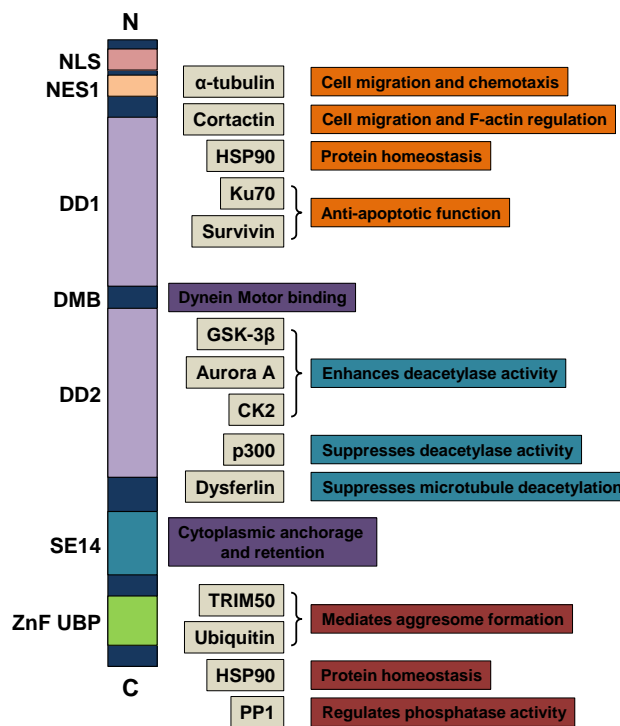


Fig. 1.11. Domain organization and functions of HDAC6. HDAC6 consists of two catalytic deacetylase domains (DD1 and DD2) and a C-terminal Zinc-finger ubiquitin binding protein domain (ZnF UBP). It also consists of nuclear export sequence (NES1), nuclear localization sequence (NLS) and a cytoplasmic anchoring domain (SE14) in the form of a tetradecapeptide marked by serine and glutamine. HDAC6 performs a large number of cellular functions-based on its deacetylase activity or direct interaction to regulate other proteins. There are proteins known to enhance HDAC6 activity through its phosphorylation *e.g.* GSK-3 β or suppress its activity *e.g.* p300. HDAC6 regulates functions such as cell migration, apoptosis, and protein homeostasis by deacetylation of its target proteins-

tubulin, cortactin, HSP90 *etc.* HDAC6 ZnF UBP domain interacts with other proteins to mediate aggresome formation, protein homeostasis and regulation of phosphatase activity of protein phosphatase 1 (PP1).

with β -tubulin as studied in yeast two-hybrid system suggesting its regulatory role independent of deacetylase activity [113]. The binding of HDAC6 is mediated through its catalytic domain but does not involve any catalytic activity. The growth and shrinkage rates of MTs are regulated by HDAC6 where it maintains the dynamic state of MTs facilitating chemotactic movement [114]. The inhibition of HDAC6 shows effect similar to the MT stabilizers like tubacin [104]. HDAC6 can interact with another α -tubulin deacetylase SIRT2 and work together to regulate MT dynamics [115]. HDAC6 associates with the end-binding protein 1 (EB1) and Arp1 present in the growing ends of MTs suggesting its role in MT dynamics [115]. Actin is also identified as an acetylated protein. Although, actin deacetylation by HDAC6 is not known, it plays a crucial role in actin dynamics by interacting or deacetylating proteins involved in nucleation and polymerization to form fibrous actin (F-actin) [105]. Nucleation of F-actin initiates *via* a series of proteins-like cortactin, profilin, N-WASP and Arp2/3 [116]. HDAC6 is found to be co-localized with the growing tips of F-actin and initiating the process through deacetylation of cortactin [105]. HDAC6 associates with cortactin and stimulates F-actin formation aiding in various processes like cell motility, protrusions, neuronal extensions etc [117]. Although, cortactin acetylation/ deacetylation has a regulatory role in actin dynamics but HDAC6 deacetylase activity is not required for initiating actin polymerization. Thus, there is a possible role of other deacetylases along with HDAC6 for deacetylation of cortactin. HDAC6 co-localizes with actin-rich structure such as podosomes, filopodia and lamellipodia denoting its essential role in actin reorganization [118].

1.14 Inter-relationship between Tau and HDAC6

In AD, Tau aggregates are formed and deposited in the cytoplasm as NFTs. As Tau aggregation proceeds, the mechanism for its clearance comes into play. HDAC6-mediated formation of aggresomes and its clearance by autophagy acts as the last resort to salvage neurodegeneration. Poly-ubiquitinated Tau aggregates are captured by HDAC6 through its ZnF UBP domain in order for their transport and formation of aggresomes. Tau and HDAC6 are known to interact directly through the MTB domain of Tau and SE14 domain of HDAC6 [54]. However, the functional attribute of their interaction is not yet clear. Deacetylase activity of HDAC6 is not required for their interaction indicating that HDAC6 may be involved in regulatory functions independent of its catalytic activity. Conversely, Tau acts as an inhibitor of HDAC6 deacetylase activity as well as hinders aggresome formation upon over-expression [119]. This inter-relationship indicates that there may be other ways through which HDAC6 could show its regulatory effect in Tauopathies. It is notable that most of the deleterious effects of HDAC6 in neurodegenerative diseases are based on the catalytic function. On the other hand, HDAC6 regulated processes through its interaction with other proteins are beneficial to neurons and can pave a way for therapeutic strategies against neurodegeneration. In our studies, we aim to explore the direct inter-relationship of Tau and HDAC6 ZnF UBP domain as well as other possible implications of this domain on neuronal functions [120].

1.15 Therapeutic approaches against Alzheimer`s disease

Alzheimer`s disease constitutes the major neurodegenerative condition associated with progressive dementia [121]. It is marked by the decline in cognitive functions and memory

deficit due to substantial neuronal degeneration. The progression of AD depends on multiple factors and there are a large number of proteins, which are considered to be involved in the etiology of disease [122]. The occurrence of these aggregate species, namely Amyloid- β plaques and neurofibrillary tangles, affects the normal functioning of neurons and leads to synaptic loss and neuronal dysfunctions.

The multifactorial etiology of AD presents several therapeutic targets for the prevention and treatment of disease. Most of the therapeutic strategies focus on reducing the aggregate burden of Amyloid- β plaques and neurofibrillary tangles by targeting the mechanisms or factors that promotes their formation. Further, in AD conditions, there is an occurrence of imbalanced neuronal functions reflected by hyperactivity in inflammatory response and defective neuronal transmission [123]. The abnormal and imbalanced neuronal functions eventually lead to the progression of disease by inflicting neurodegeneration. Thus, various therapeutic approaches have been designed dealing with different aspects of neurodegenerative diseases (**Fig. 1.12**). Amyloid- β peptides are generated by the action of β and γ -secretase on APP leading to their accumulation and deposition as Amyloid- β plaques [124]. The generation of Amyloid- β peptides is associated with mutations in APP, Presenilin-1 and Presenilin-2 (PS-1 and PS-2) genes causing familial AD [125]. The therapies focused on Amyloid- β cascade targets both on the underlying mechanisms leading to the generation of Amyloid- β peptides as well as its inhibiting

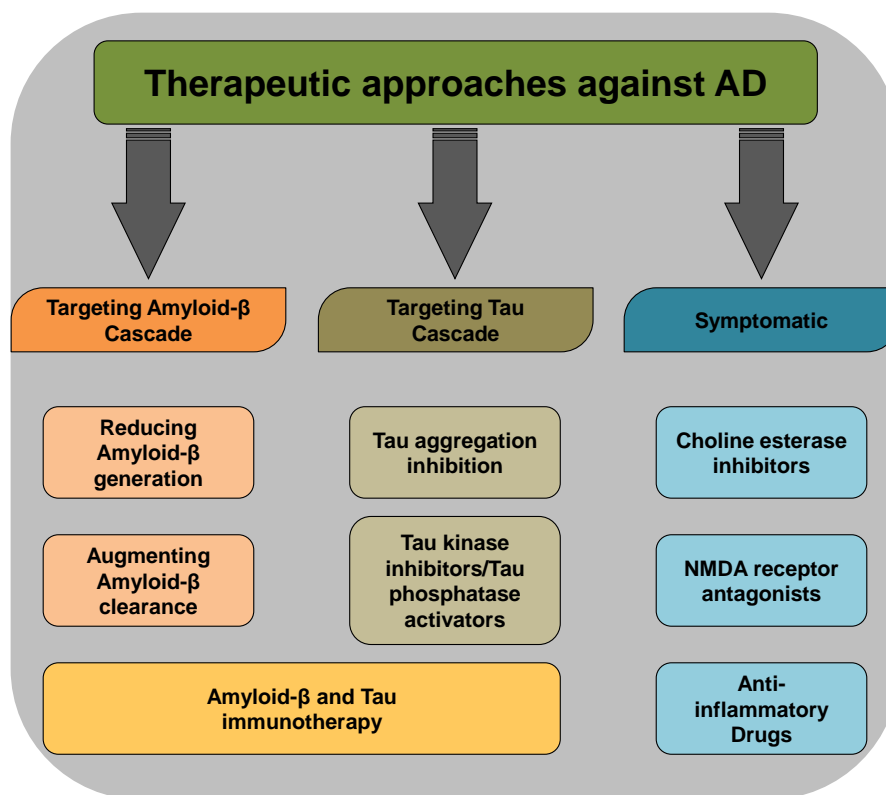


Fig. 1.12 Current therapeutic strategies against Alzheimer's disease. Therapies designed against AD primarily focus on the pathological aggregates of Amyloid- β and Tau or various symptoms that arise due to pathological conditions. Small molecule modulators of Amyloid- β and Tau aggregation as well as specific antibodies against their aggregates aim to promote aggregate clearance and reducing aggregate burden. Symptomatic treatment deals with the pathological aspects by relieving against excito-toxicity and neuronal inflammation.

its aggregation and facilitating clearance. APP is an integral membrane protein which is usually cleaved by α -secretase and do not produce any amyloidogenic peptides [124]. However, sequential cleavage by β and γ -secretases generates Amyloid- β peptides leading to the formation of Amyloid plaque. Presenilin associates with β and γ -secretases and forms the core of proteolytic complex [126]. Thus, β and γ -secretases along with PS1 and PS2 are the suitable targets in order to reduce the generation of toxic Amyloid- β peptides. Many β and γ -secretase inhibitors and modulators of Presenilins and α -secretase have been designed aiming to reduce the Amyloid- β production [127]. Immunotherapy is another strategy employed in order to accelerate the clearance of Amyloid- β aggregates by designing antibodies against Amyloid- β fibrils [128]. On the other hand, there are a large variety of natural as well as synthetic small molecules that are currently in various phases of clinical trials to be used as aggregation inhibitors against Amyloid- β [129]. Similar to the therapies employed against Amyloid- β cascade, Tau aggregation is targeted either by inhibiting the formation of pathological form of Tau or by using therapeutic agents which are effective in dissolving Tau aggregates. Tau aggregates comprise of PHFs and straight filaments consisting hyperphosphorylated Tau [130, 131]. Several small molecules candidates have been studied for their potency against Tau aggregation [132-134]. Most of the therapeutic molecules lack efficacy due to their poor ability to cross blood brain barrier (BBB). Therapeutic approaches against Tau aggregation focus on molecules, which can interact with the toxic species of Tau and able to sequester them to reduce further neuronal damage. Several other therapeutic molecules target the underlying mechanism responsible for Tau aggregation. In this regard, various kinase inhibitors and phosphatase activators are considered to be promising candidates. However, these molecules pose limitation due to their non-specificity and side-effects. Apart from targeting the Amyloid- β and Tau aggregates, preventive measures are widely employed for the symptomatic treatment of AD. AD is associated with neuro-inflammation, synaptic dysfunction and defective neurotransmission, which requires therapeutic intervention [127]. Anti-inflammatory drugs and modulators of neuro-transmitters such as Acetylcholine esterase inhibitors and NMDA (N-methyl -D-Aspartic acid) receptor antagonists provide a suitable therapeutics in order to slow-down the progression of neuronal loss [135]. The most suitable approach in designing therapeutics against AD requires a multi-targeting drug or combination of drugs for the effective treatment and prevention of neurodegeneration.

1.16 Melatonin as a multi-faceted drug against AD

Melatonin is a methoxyindole secreted by pineal gland in the absence of light. First identified in the bovine pineal gland tissue, it was initially believed to be involved only in hormonal functions like regulation of circadian rhythm, sleep homeostasis, vaso-activity and development of reproductive glands [136]. Apart from being the hormone that regulates the sleep wake cycle, Melatonin also functions as a free radical scavenger, an antioxidant and immuno-modulatory agent [137] as well as promotes differentiation and proliferation of neuronal cells [138]. Antioxidant properties of Melatonin are connected with its neuroprotective activity in several degenerative disorders [139]. The origin and progression of neurodegeneration is a complex process and depends on a myriad of factors. One of the causes of neurodegeneration is oxidative stress, which results from an imbalance between free radical formation and anti-oxidative mechanisms [140]. Melatonin is found to be a potent anti-oxidant as well as it plays a key role in the regulation of other proteins involved in the protection against cellular stress and apoptosis [141]. It is notable that the Melatonin production decreases with age and is found to be lowered in age associated neurological disorders. The administration of Melatonin in age-associated

neurological disorders has been found to improve cognitive functions and sleep [142]. As Melatonin is produced in absence of light, the effect of prolonged light exposure in rats and its implications on neuronal function has been studied [143]. Tau undergoes various post-translational modifications such as acetylation, methylation, sumoylation, ubiquitination and truncation, which modulate the properties of Tau in terms of its microtubule-binding and aggregation propensity. Also, the level of monoamine oxidase and superoxide dismutase increased indicating oxidative stress. Amyloid- β plaques, which are formed and deposited in extracellular regions of neurons, are also known to get ameliorated by administration of Melatonin. When Melatonin was supplemented simultaneously with light exposure, molecular and behavioral impairments are mildly arrested. However, Melatonin fails to ameliorate the amyloid- β pathology in Tg2576 mice when administered at the later stages of disease development. Melatonin treatment started at 14 months in amyloid- β plaques bearing Tg2576 mice showed no effect in relieving oxidative damage as well as removal of existing A β plaques even at elevated levels of plasma Melatonin. Further deposition of A β plaques were continued to be observed in cortical and hippocampal region even after 4 months of Melatonin treatment [144]. In contrast, it is found to be effective in suppressing the A β aggregates when administered in Tg2576 mice after 4 months of disease development [145]. Effect of melatonin on α -synuclein aggregation has also been studied extensively. AMPH (amphetamine) induced α -synuclein

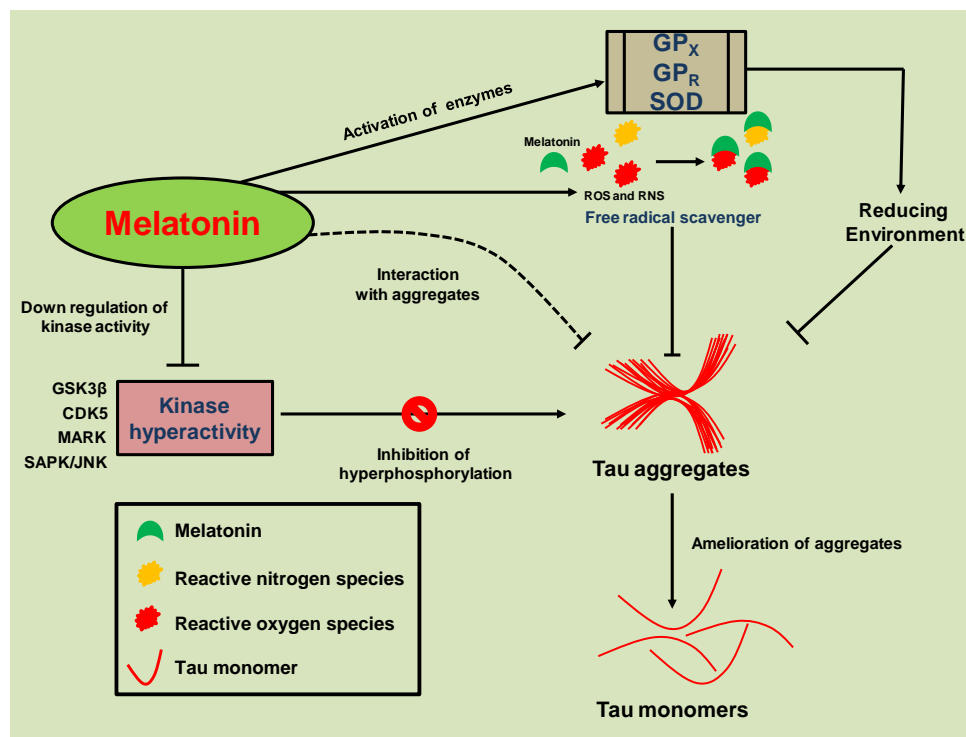


Figure 1.13. Multi-faceted role of Melatonin against AD. The amelioration of Tau aggregates by Melatonin can be attributed to its pleiotropic effect. Activation of enzymes involved in anti-oxidant function like GPX, GPR and SOD provides reducing cytoplasmic environment, which is preventive for aggregate formation. Melatonin itself can function as a free radical scavenger, which exerts its effect on ROS and RNS. It can cross-neuronal cell membrane and can interact with tau aggregates (dotted line), possibly by hydrophobic interaction as reported for amyloid- β and helps in inhibition/disassembly of aggregates. The down-regulation and inhibition of kinases involved in tau hyperphosphorylation like GSK-3 β , cdk5, MARK (microtubule affinity-regulating kinases) and SAPK/JNK (stress-activated protein kinases/Jun amino-terminal kinases) may have a preventive role in tau aggregation resulting in reduced aggregate load inside neurons (Adopted from Balmik et al., JAD, 2018).

toxicity was found to be attenuated in dopaminergic SK-N-SH cells. It also prevented the decrease in mitochondrial complex I level and phosphorylated tyrosine hydroxylase levels after AMPH treatment [146]. The expression level of α -synuclein was found to be reduced after the administration of Melatonin in 4 day old post-natal rat [147]. In another study, Melatonin was found to inhibit α -synuclein fibrillization and destabilized α -synuclein aggregates [148].

The etiology of Alzheimer`s disease includes multiple factors and so are its pathological implications. So, in order to target against AD, we need a multi-faceted approach for effective treatment. Melatonin`s role in neuroprotection is well studied. It is naturally produced by pineal gland and has no side effects as a therapeutic agent. Its multifunctional behavior as an anti-oxidant, anti-inflammatory agent, free radical scavenger, enzyme regulator, epigenetic regulator and aggregation inhibitor makes it a good candidate as a therapeutic agent (**Fig. 1.13**). The effect of Melatonin as an aggregation inhibitor of Amyloid- β has been studied but its role with respect to Tau aggregates is less explored. Its ability to cross BBB can be employed to design a more effective conjugate drug. Further research is required to explore the possibilities of using Melatonin effectively against AD. On the basis of previous studies, its multiple effects in neuroprotection can be understood, but requires a more potent therapeutic approach, which may involve its metabolites or combination with other neuroprotective drugs.

1.17 Small molecule Baicalein functions as a potent drug against neurodegeneration

Baicalein is one of the flavonoid molecules present naturally in Chinese herb *Scutellaria baicalensis* [149]. Flavonoids are known for their therapeutic properties against various ailments such as cancer, diabetes, inflammatory conditions and neurodegenerative diseases [150]. It has been widely studied with respect to neuroprotection due to its ability to permeate BBB and low side-effects [151, 152]. The neuroprotective effects of Baicalein has been explored in various *in vitro* as well as *in vivo* models of AD and PD. Baicalein has shown neuroprotection in 6-hydroxydopamine (6-OHDA)-induced model of Parkinson in SH-SY5Y cells by alleviating oxidative stress, caspase activation and mitochondrial dysfunction [153]. It is also found to promote neurite outgrowth in PC12 cells [154]. In another study, Baicalein promoted cell survival, attenuated cell death and NMDA-mediated oxidative stress in SH-SY5Y cells [155]. Administration of Baicalein in rat primary cortical neurons showed neuroprotection by reducing MPTP (1-methyl-4-phenyl-1, 2, 3, 6-tetrahydropyridine) induced NF- κ B translocation [156]. Baicalein showed neuroprotective activity in C17.2 neural progenitor cells by preventing necrotic cell death after irradiation induced impairment [157].

In various *in vivo* models of neurodegeneration, Baicalein exhibited its protective effect by modulating varied cellular functions. In a 6-OHDA-induced model for neurodegeneration in mice, Baicalein reduced the lipid peroxidation level at 3 and 7 days of 6-OHDA injection [158]. It is also shown to modulate the neurotransmitter levels as it restored glutamate and GABA (γ -amino butyric acid) and improved motor functions in a PD model of rat [159]. In another study, Baicalein aided in suppressing inflammatory pathway in rotenone-induced PD mice model, by reducing TNF- α and IL6 levels and blocking NF- κ B and MAPK signals [160]. It has also been found to improve behavioural functions in MPTP-induced mice model by regulation of various genes and their expression levels [161].

Baicalein has shown its potency against aggregation of disease specific amyloid proteins. It has been studied for its aggregation inhibition properties against α -synuclein, amyloid- β and Tau

aggregates. Aggregation of α -synuclein implicated in PD has been shown to be ameliorated by Baicalein in low micromolar concentrations. It shows effect on both oligomeric and fibrillar aggregates of α -synuclein in aggregation inhibition and disaggregation studies [162]. The effect on α -synuclein aggregates has been observed in both cellular systems and cell-free system *in vitro* [163]. Baicalein has been found to reduce α -synuclein aggregation in SH-SY5Y and HeLa cells resulting in protection from aggregate-induced toxicity [164]. In various models of familial Parkinsonism caused by α -synuclein mutants such as A30P, A53T and E46K, Baicalein reduced aggregation and exerted neuroprotective effects [165]. In AD transgenic mice, Baicalein reduced amyloid- β production by enhancing α -secretase processing of APP [166]. Additionally; it showed inhibitory effect on amyloid- β aggregation as well as disaggregates amyloid- β fibrils

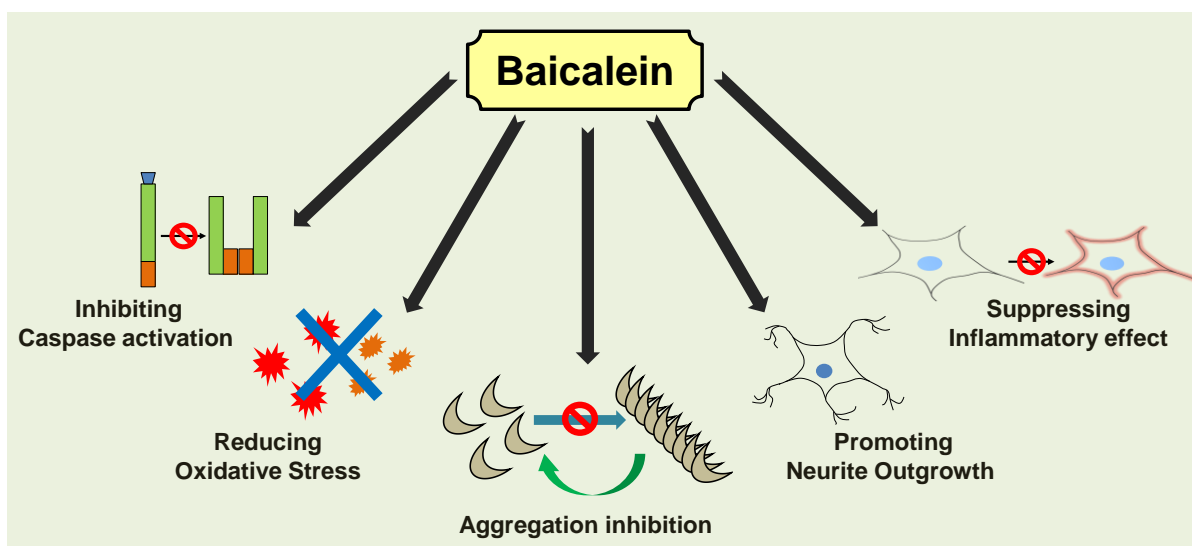


Fig. 1.14. Role of Baicalein against neurodegeneration. Baicalein has shown its potential neuroprotective function in various aspects of neuropathology. It is an effective antioxidant agent, promotes neurite outgrowth, suppresses inflammation, exerts anti-apoptotic effect by inhibiting caspase activation and functions as a modulator of aggregation.

alleviating the aggregate induced toxicity in PC12 cells [164]. The mechanism of Baicalein against α -synuclein aggregates involves formation of aggregation incompetent oligomers by associating with Lys or Tyr side-chains to form a Schiff's base [162]. The Baicalein induced oligomers are non-toxic and does not affect the cellular integrity. Overall, Baicalein as a natural small molecule possess multiple neuroprotective properties and directly acts as the inhibitory agent against protein aggregates in neurodegenerative diseases (**Fig. 1.14**).

Outline and Objectives of the study

The progression of Alzheimer's disease involves microtubule-associated protein Tau as one of the causative mediator of disease as it forms toxic intracellular aggregates in neurons. There are various pathological implications of Alzheimer's disease in the form of cytoskeletal dysfunction, increase in the level of Tau phosphorylation at specific sites and upregulation kinases. In our studies, we focused on the amelioration of Tau aggregates by the Zinc-finger ubiquitin binding protein domain of HDAC6 and small molecules melatonin and baicalein. The role of HDAC6 ZnF UBP domain has also been studied with respect to various neuronal functions.

The primary objectives of our studies includes-

1. To study the effect of HDAC6 ZnF UBP on the aggregation properties (aggregation inhibition and disaggregation) of Tau.
2. To determine the interaction of Tau and HDAC6 ZnF UBP and its implications on Tau stability.
3. To study the involvement of Tau and HDAC6 ZnF UBP in neuronal functions such as cytoskeletal organization, Tau phosphorylation and ApoE localization.
4. To analyze the potency of small molecules Melatonin and Baicalein against Tau aggregates and their interaction with Tau.

Material and Methods

1. Materials

1.1 List of Chemicals

Chemicals or Reagents	Company	Chemicals or Reagents	Company
3-(4, 5-dimethylthiazol-2-yl)-2, 5-diphenyltetrazolium bromide	Sigma	Calcium chloride dihydrate	Sigma
4',6-diamidino-2-phenylindole	Thermo Fisher	Clarity™ Western ECL Substrate	Bio-Rad
8-Anilino-naphthalene-1-sulfonic acid	Sigma	Coomassie brilliant blue R-250	MP Biomedicals
Acetic acid	MP Biomedicals	Copper sulfate (II)	Sigma
Acrylamide	Invitrogen	Dimethyl sulfoxide	Thermo Fisher
Agarose	Invitrogen	Dithiothreitol	Calbiochem
Ammonium acetate anhydrous	MP Biomedicals	DMSO	Life Tech
Ammonium bicarbonate	Sigma	Dulbecco's Modified Eagle Medium	Thermo Fisher
Ammonium persulfate	MP Biomedicals	EnzChek™ Caspase-3 Assay Kit	Thermo Scientific
Ammonium sulfate	MP Biomedicals	Ethanol	MP Biomedicals
Ampicillin	MP Biomedicals	Ethylene glycol tetraacetate	MP Biomedicals
BES	Sigma	Fetal Bovine Serum	Thermo Fisher
Baicalein	Sigma	Gel Loading Dye (6X)	New England Biolabs
Bicinchoninic acid	Sigma	Glycerol	MP Biomedicals
Bis-acrylamide	Invitrogen	Glycine	Invitrogen
Bovine Serum Albumin	Sigma	H ₂ SO ₄	MP Biomedicals
Bradford Reagent	Bio-Rad	HCl	MP Biomedicals
Bromophenol blue	MP Biomedicals	Heparin (MW~17500 Da)	MP Biomedicals

Chemicals or Reagents	Company	Chemicals or Reagents	Company
Imidazole	MP Biomedicals	Potassium phosphate dibasic trihydrate	MP Biomedicals
IPTG	MP Biomedicals	Potassium phosphate monobasic anhydrous	MP Biomedicals
Isopropanol	MP Biomedicals	Protease inhibitor Cocktail	Roche
Kanamycin	Gibco	Precision Plus Protein™ Dual Color Standards	Bio-Rad
Lactate dehydrogenase release assay kit	Thermo Scientific	RIPA buffer	Thermo Scientific
LB Broth	HiMedia	Sodium acetate trihydrate	MP Biomedicals
LB Agar	Invitrogen	Sodium azide	MP Biomedicals
Magnesium acetate tetrahydrate	Sigma	Sodium bicarbonate	MP Biomedicals
Magnesium chloride hexahydrate	MP Biomedicals	Sodium carbonate anhydrous	MP Biomedicals
Magnesium sulfate heptahydrate	MP Biomedicals	Sodium chloride	MP Biomedicals
Melatonin	Sigma	Sodium dodecyl sulfate	Sigma
MES hydrate	Sigma	Sodium hydroxide	MP Biomedicals
Methanol	MP Biomedicals	Sodium MOPS	MP Biomedicals
Nickel sulfate hexahydrate	Sigma	Sodium phosphate dibasic anhydrous	MP Biomedicals
Nucleospin Plasmid DNA isolation kit	Machery Nagel	Sodium phosphate monobasic mono hydrate	Sigma
Okadaic acid	Sigma	Sodium thiosulfate pentahydrate	MP Biomedicals
Penicillin-Streptomycin	Thermo Fisher	SYBR Safe	Invitrogen
Polysorbate 20	MP Biomedicals	Tetramethylethylenediamine	Invitrogen
Polyvinylidene fluoride membrane	Invitrogen	Thioflavin S	Sigma
Potassium acetate	MP Biomedicals	Thioflavin T	Sigma
Potassium chloride	MP Biomedicals	Terrific broth	Invitrogen
Potassium phosphate dibasic trihydrate	MP Biomedicals	Thiamine HCl	Sigma

Chemicals or Reagents	Company
Tris base	Biorad
Tris HCl	Invitrogen
Triton X 100	Sigma
Trypan blue	Invitrogen
Trypsin	Invitrogen

1.2 List of Antibodies

Antibody	Company	Antibody	Company
Anti-ApoE (C-terminal) (SAB2701946)	Sigma	GSK-3 β Ab (MA5-15109)	Thermo Fisher
Anti-HDAC6 (C-terminal) (ab196351)	Abcam	Pan Tau (K9JA) (A0024)	Dako
Anti-His Ab (27471001)	GE	Phospho-GSK-3 β Ab (Ser9) (MA5-14873)	Thermo Fisher
Beta actin loading control (BA3R)	Thermo Fisher	Phospho-Tau (Ser202/Thr205) (MN1020)	Thermo Fisher
Beta tubulin Loading Control (BT7R)	Thermo Fisher	Phospho-Tau (Thr181) (701530)	Thermo Fisher
Donkey anti goat IgG (ab6885)	Abcam	Rabbit anti-Goat IgG - Alexa Fluor 594 (A27016)	Thermo Fisher
Goat anti-mouse - alexa fluor 555 (A28180)	Thermo Fisher		
Goat anti-mouse IgG HRP (32430)	Thermo		
Goat anti-rabbit - alexa fluor 488 (A-11008)	Thermo Fisher		
Goat anti-rabbit IgG HRP (31460)	Thermo Fisher		

1.3 List of Constructs

Construct	Provider
pT7C hTau40WT	Kindly gifted by Prof. Roland Brandt, University of Osnabruck, Germany
pT7C K18WT	Kindly gifted by Prof. Roland Brandt, University of Osnabruck, Germany
pET28a LIC HDAC6 ZnF UBP	Kindly gifted by Prof. Cheryl Aerosmith, University of Toronto, Canada

1.3 Cell line

Construct	Provider
Neuro2a (CCL-131)	ATCC

2. Equipments, Instruments and Softwares

2.1 Equipments

Equipment	Company	Equipment	Company
AKTA Pure FPLC system	GE Healthcare	Optima XPN10 Ultracentrifuge	Beckman Coulter
AKTA Start FPLC system	GE Healthcare	MicroCal PEAQ-ITC	Malvern
Amersham Imager 600	GE Healthcare	Shaker Incubator (H1010-MR)	Benchmark Scientific
Amersham Semi Dry blotting apparatus	GE Healthcare	Shaker Incubator Multitron Standard	Infors HT
Avanti JXN26 High speed Centrifuge	Beckman Coulter	UV-Visible spectrophotometer V-530	Jasco
High Speed Centrifuge 5804R	Eppendorf	Zeiss Axio observer 7 microscope with Apotome 2.0	Zeiss
Homogenizer	Constant Systems Ltd.		

Microcentrifuge 5418 R	Eppendorf		
MicroCal PEAQ-ITC	Malvern		
Microplate reader Infinite 200 PRO	Tecan		
Molecular Imager Gel Doc™ XR+	BioRad		

2.2 Miscellaneous Equipments

Equipment	Company	Equipment	Company
Analytical balance ME204	Mettler Toledo	MiniVE Vertical electrophoresis System	Amersham
Analytical balance ME4001E	Mettler Toledo	MiniSpin Plus Table top centrifuge	Eppendorf
Autoclave	Spire	Nanodrop	Simplinano
Dry bath	Genei	pH meter Five Easyplus	Mettler Toledo
Forma 900 series -80°C	Thermo Scientific	Vacuum Pump	Millipore
Gel rocker	Benchmark	Vortexer mixer	Genei
Heratherm Hot Air Oven	Thermo Scientific	Water bath	Genei
Heraeus Incubator	Thermo Scientific		
Magnetic Stirrer	Genei		
MiliQ Unit Direct 16	Millipore		
Miniprotean Tetra vertical electrophoresis system	Biorad		

2.3 Instruments from Central Facilities

Equipment	Company
Far-UV CD spectrometer J-815	Jasco
T20 Transmission Electron Microscope	Tecnai
Avance III HD 700 MHz NMR spectrometer equipped with TXI probe	Bruker

2.3 Softwares

Software	Company/Organization
ImageJ	NIH
Image Lab	BioRad
ImageQuant TL	GE
Magellan™ Data analysis software	Tecan
MicroCal PEAQ-ITC analysis software	Malvern
MS Excel	Microsoft
Sigma Plot 10.0	Systat softwares
Spectra Manager™	Jasco
Topspin 3.2	Bruker
Zen 2.3	Zeiss

3. Methods

3.1 Competent cells Preparation

Bacterial cells have a natural competency to take up extracellular DNA from their environment, but with low efficiency. In molecular biology, bacterial competency is enhanced by chemical and physical methods. Competent cells can be prepared by using a divalent ion such as calcium to transiently distort the membrane organization making bacterial cell to easily take up DNA.

Procedure

1. Single isolated colony of bacterial strain to be made competent (*BL21**, *DH5 α* or *BL21* Codon Plus RIL) were obtained by streak plate method.
2. Primary culture was made from the single colony by inoculating into 5 ml of LB and keeping for incubation at 37°C overnight in a shaker incubator (Benchmark Scientific).
3. 250 ml of secondary culture was made in LB media by inoculating from primary culture in 1:100 ratio of inoculum and media.
4. Secondary culture is kept for incubation at 37°C in a shaker incubator.
5. When the optical density at 600 nm (OD₆₀₀) reached 0.4, the culture was cooled in ice bath for 15 minutes, transferred to pre-cooled tubes and centrifuged for 10 minutes at 4500 rpm and 4 °C.
6. The cells obtained in the pellet were resuspended in 30 ml of ice cold transformation buffer 1 (TB1).
7. Bacterial cells in TB1 were kept in ice bath for 60 minutes and centrifuged again for 5 minutes at 4500 rpm and 4 °C.
8. The cells were resuspended in ice cold transformation buffer 2 (TB2).
9. Aliquots of 100 μ l were made by keeping the tubes in ice.
10. The aliquots were snap-frozen in liquid nitrogen and immediately transferred to -80 °C (Forma 900 series -80°C) for storage.

Buffers

Transformation Buffer 1 (TB1)	Transformation Buffer 2 (TB2)
100 mM KCl	10 mM KCl
300 mM K ⁺ CH ₃ COO ⁻	10 mM Na-MOPS
10 mM CaCl ₂	75 mM CaCl ₂
10 mM NaCl	15% Glycerol
15% Glycerol	

3.2 Transformation into *E.coli* Competent cells

Bacterial cells have a tendency to take up free DNA from the environment with a limited efficiency. This property of bacterial cells has been employed in molecular biology to insert foreign DNA in the form of plasmid into bacteria. The bacterial cells must be made competent by chemical or physical methods to take up the DNA. Upon transformation of foreign DNA into bacteria, it can be utilized for maintenance of genetic material or can be induced to express a recombinant protein of interest.

Procedure

1. Competent cells (*DH5 α* , *BL21** or *BL21* Codon plus RIL) were removed from -80 °C and kept on ice bath for 20 minutes.
2. Keeping the cells on ice bath, 1-2 μ l of plasmid DNA is added.
3. Cells were incubated in ice bath for 30 minutes for binding of plasmid DNA.
4. Heat shock is given to the cells by keeping in water bath at 42 °C for 90 seconds to transiently disrupt the cell membrane and plasmid DNA intake.
5. The cells are immediately kept on ice bath for 5 minutes.
6. 750 μ l of SOC media is added to the cells, mixed and kept in incubation for 1 hour in a shaker incubator.
7. 50-100 μ l of media containing transformed cells were taken and spread on an antibiotic containing LB agar culture plate.
8. The plates were kept in an inverted position at 37 °C for 8-10 hours.

The bacterial cells transformed with plasmid DNA gives pin-point colonies at the end of 8-10 hours which are picked for further scale up.

3.3 Miniprep for plasmid isolation and purification

After the transformation of desired plasmid vector containing the gene of interest (Tau or HDAC6), isolated colonies of *DH5 α* strain were used for maintenance of plasmid. *DH5 α* has high transformation efficiency and contains *recA* mutation which eliminates homologous recombination, *endA1* mutation to inactivate intracellular endonuclease which degrades plasmid DNA. Thus, it is considered a suitable strain of *E.coli* for maintenance of plasmid DNA due to high insert stability. Δ (*lacZ*) M15 allele, which enables blue-white screening for *lacZ* based vectors.

Purification of plasmid DNA was carried out according to the manufacturer's protocol (Machery Nagel). The technique for plasmid DNA isolation is based on the alkaline lysis method. The bacterial cells are lysed using a lysis buffer containing SDS and sodium hydroxide (NaOH). SDS dissolves the bacterial cell membrane while NaOH helps in disruption of cell wall as well as

denaturation of cellular proteins and DNA. Neutralization buffer is added to the lysates, which allows renaturation of genomic and plasmid DNA. Plasmid DNA, being smaller in size reanneals completely resulting in its solubilization while genomic DNA does not get renatured properly due to large size and stay precipitated. The cellular debris, precipitated proteins and DNA can now be easily separated from plasmid DNA by centrifugation. Plasmid DNA is captured on a silica membrane by ethanolic precipitation and can be eluted by using buffer of low ionic strength in slightly alkaline conditions.

Procedure

1. Single isolated pin-point colonies obtained after transformation are selected for inoculation into 5 ml of LB media and kept for incubation at 37 °C overnight in a shaker incubator. At least four isolated colonies were inoculated in four tubes.
2. Bacterial cells obtained after overnight culture were harvested by centrifugation at 11000X g for 30 seconds at room temperature.
3. 250 µl of Buffer A1 was added in each tube and mixed thoroughly by vortexing until the cells were completely lysed.
4. 250 µl of Buffer A2 was added and mixed by inverting the tubes. Tubes were incubated for 5 minutes at room temperature.
5. 300 µl of Buffer A3 was added and mixed again by inverting the tubes.
6. Cell lysates were clarified by centrifugation at 11000X g for 30 seconds at room temperature.
7. Clarified lysates were passed through columns with silica membrane, placed over collection tubes, by centrifugation at 11000X g for 30 seconds at room temperature. Flow-through was discarded.
8. Silica membranes were washed with 600 µl Buffer A4 supplemented with ethanol by centrifugation at 11000X g for 1 minute at room temperature. Flow-through was discarded and columns were placed in an empty collection tube.
9. Silica membranes were dried by centrifugation at 11000X g for 2 minutes at room temperature. Collection tubes were discarded.
10. 50 µl of Buffer AE was added to each tube and incubated for 1 minute at room temperature.
11. Plasmid DNA was eluted by centrifugation at 11000X g for 1 minute at room temperature.
12. The respective concentration of plasmid DNA obtained from each tube was measured in Nanodrop (Simplinano).

3.4 Protein expression and culture scale-up for protein preparation

To check the expression level of protein of interest, *BL21** or *BL21* Codon plus RIL strains of *E.coli* were used. *BL21** strain contains DE3 lysogen carrying the gene for *T7 RNA polymerase* under the control of lacUV5 promoter. It is widely used for over-expression of recombinant

protein cloned in T7 expression vectors by using IPTG as an inducer. *BL21* Codon plus RIL has same elements for protein expression as *BL21** but also contains extra copies of *argU*, *ileY* and *leuW* tRNA genes to resolve the condition of codon bias in AT rich genes.

The expression of recombinant protein was checked by culturing the single isolated colonies after transformation of *BL21** or *BL21* Codon plus RIL strains containing plasmids for Tau (pT7C) and HDAC6 ZnF UBP (pET28-LIC) respectively. The plasmids confer antibiotic resistance to the transformed cells inhibiting the growth of non-transformed cells or contaminants. The gene for protein of interest is under the regulation of lac operator and the *T7 RNA polymerase* can bind to the operator and start transcription under inducible conditions *i.e.* when an inducer is present in the cell. Isopropyl β -D-1-thiogalactopyranoside (IPTG) is a molecular mimic of allolactose, which is the metabolite of lactose responsible for triggering lac operon system. Expression of protein of interest was carried out in the presence of IPTG as an inducer and the levels of protein expression were visualized by comparing with uninduced bacterial culture by using SDS-PAGE. Further, the selected colony with optimum protein expression was scaled-up using large volumes of culture.

Tau preparation

1. Single isolated pin-point colonies obtained after transformation were selected for inoculation into 10 ml of LB (for Tau) or TB (for HDAC6 ZnF UBP) media supplemented with antibiotic (100 μ g/ml Ampicillin for Tau and 50 μ g/ml Kanamycin for HDAC6 ZnF UBP). At least eight isolated colonies were selected for inoculation.
2. The culture tubes were kept for incubation at 37 °C for 4-6 hours until OD₆₀₀ reaches 0.6.
3. Expression of Tau protein was induced by adding 0.5 mM IPTG to four culture tubes and labelled as induced (I1, I2, I3 and I4). The remaining tubes were labelled as uninduced (UI1, UI2, UI3 and UI4). For HDAC6 ZnF UBP, the tubes were kept in 16 °C for 1 hour prior to induction by 0.2 mM IPTG.
4. For Tau, the tubes were kept in incubation at 37 °C for 4 hours. Incubation was carried out overnight at 16 °C in case of HDAC6 ZnF UBP.
5. The culture tubes were removed and bacterial cells were harvested by centrifugation. The supernatant was discarded and Eppendorf tubes containing cells were labelled accordingly.
6. The cells were lysed by using cell lysis buffer (50 mM Tris-Cl, 500 mM NaCl pH 8.0 for HDAC6 and 50 mM MES pH 6.8 for Tau). 6X gel loading dye was added to 10 μ l of lysed cells, heated for 10 minutes in dry bath (Genei) and loaded on to 10% (Tau) or 12% (HDAC6 ZnF UBP) SDS-PAGE.
7. The protein expression for individual colonies was confirmed by visual observation of protein bands (corresponding to Tau at 55 KDa and HDAC6 ZnF UBP at 14 KDa).
8. Glycerol stock for the selected colony was prepared by adding 200 μ l of culture from induced cells to 800 ml of 80% sterile Glycerol and stored in -80 °C.
9. The selected colony with highest protein expression was up-scaled to 6-8 Litres culture.

10. For scale-up culture, primary inoculum was prepared by overnight incubation of 100 ml LB (for Tau) or TB (for HDAC6 ZnF UBP) media supplemented with antibiotic (100 µg/ml Ampicillin for Tau and 50 µg/ml Kanamycin for HDAC6 ZnF UBP) inoculated by the selected colony.
11. Secondary culture was prepared in respective media and antibiotic using primary inoculum in 1:100 ratios with the media and kept for incubation at 37 °C in a shaker incubator (Multitron Standard).
12. Likewise, for Tau Induction with 0.5 mM IPTG was carried out when OD₆₀₀ reaches 0.6 while for HDAC6 ZnF UBP, culture flasks were acclimatized at 16 °C for one hour prior to induction by 0.2 mM IPTG.
13. In case of Tau, Culture flasks were kept for incubation at 37 °C for 4-5 hours in a shaker incubator while incubation at 16 °C was carried out for HDAC6 ZnF UBP.
14. The cells were pelleted down by centrifugation at 4500rpm at 4 °C (Avanti JXN26 High speed Centrifuge).
15. The cells were further processed for protein preparation or collected in a tube, snap-frozen and stored at -80 °C.

3.5 Biochemical and Biophysical Methods

3.5.1 Protein expression and Purification

3.5.1.1 Recombinant Tau protein preparation

1. Full-length Tau (hTau40) and repeat Tau (K18) cloned in pT7C and transformed into BL21* cells, were induced for expression by 0.5 mM IPTG in the presence of 100 µg/ml Ampicillin. The purification was done by cation exchange chromatography followed by Size-exclusion chromatography.
2. The primary inoculum was prepared from glycerol stock in Luria broth (LB) supplemented with 100 µg/ml Ampicillin at 37 °C.
3. The secondary culture was carried out in LB supplemented with 100 µg/ml Ampicillin at 37 °C.
4. Cells were induced for expressing Tau using 0.5 mM IPTG when OD₆₀₀ reaches 0.6 and incubated further for 4 hours. The cells were harvested and weighed before further processing.
5. The cells were resuspended in cell lysis buffer and lysed by homogenization at 15 KPSI (using Constant cell disruption system).
6. The lysate was supplied with 0.5 M NaCl and 5 mM DTT and kept at 90 °C for 20 minutes to denature all the structured protein.
7. The resulting sample was centrifuged at 40000 rpm for 45 minutes. The supernatant was kept for overnight dialysis in 20 mM MES pH 6.8.

8. The supernatant was kept for overnight dialysis in 20 mM MES pH 6.8.
9. The dialyzed sample was centrifuged again at 40000 rpm for 45 minutes and the supernatant was filtered and loaded onto Sepharose fast flow (SPFF) column (GE17-0729-01) pre-equilibrated with 20 mM MES pH 6.8, 50 mM NaCl.
10. Elution was carried out with a linear gradient using 20 mM MES pH 6.8, 1 M NaCl.
11. Tau protein were pooled, concentrated and subjected to Size-exclusion chromatography.
12. Size-exclusion chromatography was carried out Superdex 75 Hi-load 16/600 column (GE28-9893-33) in 1X PBS buffer with 2 mM DTT.
13. The fractions under the chromatogram peaks were collected and run on SDS-PAGE. The fractions corresponding to Tau protein were pooled and concentrated using 5-10 KDa cut-off centricons.
14. The concentration of Tau protein was determined using Bicinchoninic Acid assay.

Buffers used for Tau preparation

Extraction/Lysis Buffer
50 mM MES pH 6.8
1 mM EGTA
2 mM MgCl ₂
5 mM DTT
1 mM PMSF
Protease Inhibitor Cocktail

Dialysis buffer
50mM MES pH 6.8
50 mM NaCl
1 mM EGTA
1 mM MgCl ₂
2 mM DTT
0.1 mM PMSF

Cation Exchange Chromatography

Wash buffer (Buffer A)	Elution buffer (Buffer B)
50mM MES pH 6.8	50mM MES pH 6.8
50 mM NaCl	1 M NaCl
1 mM EGTA	1 mM EGTA
1 mM MgCl ₂	1 mM MgCl ₂
2 mM DTT	2 mM DTT
0.1 mM PMSF	0.1 mM PMSF

Size-Exclusion Chromatography

Size-Exclusion Chromatography buffer
1X PBS
2 mM DTT
Protease Inhibitor Cocktail

3.5.1.2 Recombinant HDAC6 ZnF UBP preparation

1. HDAC6 ZnF UBP cloned in pET28a-LIC was transformed and expressed in BL21 Codon plus RIL cells and purified in two steps by Ni-NTA affinity chromatography and size-exclusion chromatography.
2. Primary inoculum in Terrific broth (TB), supplemented with 50 µg/ml Kanamycin was prepared from the glycerol stock containing transformed BL21 Codon plus RIL cells by incubating overnight at 37 °C.
3. Secondary culture in TB containing 50 µg/ml Kanamycin inoculated from primary in 1:100 ratio of inoculum and kept in incubation at 37 °C till OD₆₀₀ reaches 0.6.
4. Culture kept at 16 °C for one hour prior to induction by 0.2 mM IPTG.
5. Kept for incubation at 16 °C for 16 hours followed by harvesting of cells. Re-suspend the cell pellets in 20-100 ml of lysis buffer depending on the pellet size.
6. Cell pellets were homogenously re-suspended by vortexing and lysed by subjecting to high pressure (15000 KPSI) (using Constant cell disruption system).
7. The cell lysate is collected and subjected to centrifugation at 20000 rpm for 30 minutes.
8. The supernatant is collected and mixed with Roche Ni-NTA beads in the ratio 1:30 and kept for protein binding for 1 hour at 4 °C.

9. Affinity chromatography was performed using 50 mM Tris-Cl pH 8.0 with 20 mM Imidazole for wash and 1000 mM imidazole for elution.
10. The eluted fractions were dialyzed in 50mM Tris-Cl pH 8.0, 100 mM NaCl, 2 mM TCEP/DTT, 5 % glycerol to remove imidazole.
11. Size-exclusion Chromatography was performed using Superdex 75 Hi-load 16/600 column in 50 mM Tris-Cl pH 8.0, 100 mM NaCl, 2 mM TCEP/DTT which yielded HDAC6 ZnF UBP at retention volume ~110 ml.
12. The fractions containing HDAC6 ZnF UBP were pooled concentrated and stored at -80°C. The protein concentration was determined by using Bradford assay.

Buffers used for HDAC6 ZnF UBP preparation

Extraction/Lysis Buffer
50 mM Tris-Cl pH 8.0
500 mM NaCl
1 mM PMSF
20 mM Imidazole
Protease Inhibitor Cocktail

Ni-NTA Affinity Chromatography

Wash buffer	Elution buffer
50 mM Tris-Cl pH 8.0	50 mM Tris-Cl pH 8.0
500 mM NaCl	500 mM NaCl
20 mM Imidazole	1 M Imidazole
	5% Glycerol

Dialysis buffer	Size-Exclusion Chromatography buffer
50 mM Tris-Cl pH 8.0	50 mM Tris-Cl pH 8.0
100 mM NaCl	100mM NaCl
2 mM TCEP/DTT	1mM TCEP/DTT
5% Glycerol	

3.5.1.3 ^{15}N labelled Repeat Tau preparation

Repeat Tau labelling with ^{15}N was carried out by using ^{15}N containing minimal media. The labelled repeat Tau was prepared to be used in NMR studies [167-169].

Procedure

1. The pT7C repeat Tau transformed BL21*cells were initially grown in LB (6L) with 100 $\mu\text{g/ml}$ Ampicillin at 37 °C till the OD reaches 6 at 600 nm.
2. The cells were pelleted down and washed with 1X M9 salts.
3. The 1X M9 salts washed cells were re-suspended in minimal media containing ^{15}N labelled ammonium chloride.
4. In order to clear unlabelled metabolites, the cells were grown at 37 °C for 1 hour prior to induction with 0.5 mM IPTG and harvesting after 4-5 hours.
5. The labelled protein was prepared similarly as previously described method for unlabelled Tau protein.

Stock Solutions

5X M9 salts (autoclaved)

Salt	Weight (gm/100ml)
KH_2PO_4	1.5
Na_2HPO_4	3
NaCl	0.25
NH_4Cl (^{15}N labelled)	0.5

The pH of the 5X M9 salts is adjusted to 7.2 before autoclaving.

1X M9 salts unlabelled (autoclaved)

Salt	Weight (gm/1000ml)
KH_2PO_4	3
Na_2HPO_4	5
NaCl	0.5

The pH of the 1X M9 salts is adjusted to 7.2 before autoclaving.

Minimal Growth Media (1500 ml)

5X M9 Salts	300 ml
20% D-Glucose (filter sterilized)	30 ml
Thiamine hydrochloride (5 mg/mL) (filter sterilized)	9 ml
1M MgSO ₄ (autoclaved)	3 ml
1M CaCl ₂ (autoclaved)	150 µl

The final volume is made up to 1500 ml using autoclaved MiliQ water.

3.5.2 Protein estimation methods**3.5.2.1 Bicinchoninic acid Assay (BCA assay)**

The Bicinchoninic acid Assay is used for the determination of total protein concentration in a sample [170]. It is a sensitive protein detection method based on the reduction of Cu²⁺ into Cu⁺ by protein under alkaline conditions and formation of a purple colored complex with Bicinchoninic acid. The intensity of colored complex is directly proportional to the concentration of the protein. The Cu²⁺ is reduced to Cu⁺ by Cysteine, Cystine, Tyrosine and Tryptophan content of the protein. However, the peptide backbone of the protein also contributes in the reaction, making it a sensitive method and suitable for proteins lacking the mentioned amino acids.

Standards, Protein dilutions and Reagent preparation

1. The working reagent is prepared by mixing BCA and Copper sulfate (II) in 50:1 ratio.
2. The protein standards are made in a range of 0- 250 µg/ml (Stock - 1mg/ml) concentrations in MiliQ water.
3. The protein dilutions are made in MiliQ water in at least three ratios ranging from 1:25 – 1:400.
4. All the standards and protein dilutions are made in duplicates.

Procedure

1. 25 µl of BSA standards and protein dilutions are mixed with 200 µl of working reagent and pipetted into a 96 wells clear bottom plates.
2. The plate is kept for incubation at 37 °C for 1 hour.
3. The absorption by colored complex is measured at 562 nm in Tecan Infinite 200 PRO spectrophotometer.

4. The protein concentration of the sample is determined by plotting a standard graph using MS Excel.

3.5.2.2 Bradford Assay

Bradford assay is a protein estimation method based on the binding of protein with Coomassie dye under acidic conditions [171]. The Coomassie G-250 dye is doubly protonated in acidic conditions and has red color. Upon binding with protein it gets unprotonated and acquires blue color. The principle of the method is based on transfer of electron from dye to the basic amino acids Arginine, Lysine and Histidine in protein. This leads to the disruption in protein structure and expose hydrophobic patches; to which the dye can bind. The dye bound to protein forms a stable blue colored complex which is proportional to the protein concentration. The intensity of the colored complex can be spectroscopically measured and used to quantify the protein concentration.

Standards, Protein dilutions and Reagent preparation

1. Working reagent is prepared by mixing 4parts MiliQ Water and 1 Part Bradford Reagent (Bio-Rad).
2. The protein standards are made in a range of 0- 250 $\mu\text{g/ml}$ (Stock - 1mg/ml) concentrations in MiliQ water.
3. The protein dilutions are made in MiliQ water in at least three ratios ranging from 1:25 – 1:400.
4. All the standards and protein dilutions are made in duplicates.

Procedure

1. 10 μl of BSA standards and protein dilutions are mixed with 200 μl of working reagent and pipetted into a 96 wells clear bottom plates.
2. Incubate at room temperature for at least 5 minutes.
3. Absorbance will increase over time; samples should incubate at room temperature for no more than 1 hour.
4. The absorption by colored complex is measured at 595 nm in Tecan Infinite 200 PRO spectrophotometer.
5. The protein concentration of the sample is determined by plotting a standard graph using MS Excel.

3.5.3 Agarose Gel electrophoresis

Agarose gel electrophoresis is a technique used to separate DNA fragments or RNA on the basis of their molecular size. The migration is initiated by applying an electric field and the rate of nucleic acid migration is proportional to their size as well as pore size of Agarose gel. DNA ladder of known molecular weight is run along with the samples to determine the molecular

weight of unknown DNA. In order to visualize the separated DNA an intercalating dye is used like SYBR green or EtBr. The DNA bands are visualized by illuminating under UV light.

Procedure

1. 1-2% Agarose gel is prepared in 1X TAE buffer by boiling to completely dissolve the Agarose.
2. SYBR safe™ is added to the gel and mixed just before adding it to casting tray and sample comb.
3. Samples are made in 6X gel loading dye.
4. TE buffer is added to the buffer tank of electrophoresis unit and the combs are removed.
5. Samples are loaded on to the wells along with DNA ladder of suitable size range.
6. Electrophoresis is carried out samples have run until 70-80% of gel length.
7. Gel is removed and visualized under UV in Molecular Imager Gel Doc™ XR+ (Bio-Rad).

Buffers and Reagents

50 X TAE Buffer (for 100ml)
24.2 gm Tris
5.7 ml Acetic acid
10 ml of 0.5 M EDTA

Final volume is made up to 100ml with MiliQ water.

Gel running buffer is prepared by diluting 50X TAE buffer in MiliQ water to make 1X TAE buffer.

3.5.4 SDS-PAGE Analysis and Quantification

SDS-PAGE is an analytical method to separate proteins on the basis of their molecular weight. The proteins migrate under the influence of electric field, through the matrix of poly-acrylamide gel after denaturation by anionic detergent Sodium dodecyl sulfate and reducing agent DTT or β -mercaptoethanol. Upon denaturation, SDS binds to the protein with respect to its relative molecular weight and impart overall negative charge over a wide pH range. Thus, protein migration takes place toward positive electrode (anode) in an electrophoresis system. The smaller proteins migrate fast due to less resistance by gel matrix and *vice versa*.

Discontinuous gel system is used for the separation of proteins which consists of a stacking gel with wells for sample application and a resolving gel. SDS-PAGE running buffer consists of Tris-Cl and Glycine which gets ionized as the electric field is applied. Bromophenol Blue (BPB) is used as the tracking dye. The stacking gel has a lower pH of 6.8 which imparts differential mobility to protein, glycine, chloride and BPB. The ionization potential of glycine is less in

stacking gel as its pH is closer to isoelectric pH of glycine. This imparts lesser conductivity to glycine. However, chloride ions, proteins and BPB retains higher conductivity forming a stack of protein between slow migrating glycine ions and faster chloride ions due to local potential difference between them. Upon entering resolving gel at pH 8.8, glycine retains its electrical conductivity but the overall migration rate declines. Each component ion is subjected to constant electric force and protein separation begins as per their molecular weight. A molecular weight marker is loaded along with the protein samples to locate the protein of interest. The electric field is stopped when tracking dye reaches 80-90% of gel length. The gel is removed from the assembly and proceeded further for staining or western blotting.

Buffers and Reagents

SDS-PAGE Running Buffer
25 mM Tris-Cl
250 mM Glycine
10% SDS

Tracking Dye/Sample Buffer
300 mM Tris-Cl pH 6.8
600 mM DTT
6% BPB
12% SDS
60% Glycerol

3.5.5 Western Blot Analysis

Western blot is an analytical technique used for the detection of specific protein in a sample containing a mixture of proteins. The protein mixture is first separated by using SDS-PAGE or Native-PAGE and then transferred or blotted on to a PVDF or nitrocellulose membrane. The protein detection is carried out by immunostaining the membrane with the antibody specific to the protein of interest. The protein can be visualized and quantified either by using a secondary antibody conjugated with enzymatic or fluorescent tag or using a tagged primary antibody [172, 173].

Procedure

1. Perform SDS-PAGE for the protein samples.
2. Place the PVDF membrane in 100% methanol for activation.

3. Equilibrate the filter paper stacks and PVDF membrane in transfer buffer.
4. After the completion of SDS-PAGE, transfer the gel on blotting assembly and arrange the stack consisting of filter papers and PVDF membrane.
5. Remove the air bubbles by using rolling pin.
6. Fill the reservoir with transfer buffer and start the transfer by applying electric field in blotting apparatus.
7. Transfer is carried out at 200mA for 2 hours.
8. Remove the membrane and place in blocking buffer for 1 hour at room temperature.
9. Remove the blocking buffer and incubate the membrane for 1 hour with primary antibody with suitable dilution made in blocking buffer.
10. Wash the membrane thrice with 1X PBST for 15 minutes to remove unbound antibodies.
11. Incubate the membrane for 1 hour with HRP tagged secondary antibody with suitable dilution made in blocking buffer.
12. Wash the membrane thrice with 1X PBST for 15 minutes to remove unbound antibodies.
13. Proceed for developing the blot using ECL reagent (Bio-Rad).

Buffers used

SDS-PAGE Running Buffer
25 mM Tris-Cl
250 mM Glycine
10% SDS

Transfer Buffer
25 mM Tris-Cl
250 mM Glycine
20% Methanol

Wash Buffer (1X PBST)
1X PBS
0.1% Tween 20

Blocking Buffer
5% Skimmed Milk in 1X PBST

3.5.6 Tau degradation analysis by SDS-PAGE and Western blotting

In order to observe the effect of HDAC6 ZnF UBP on Tau stability, degradation analysis was carried out by incubating the two proteins and observing the degradation pattern at regular time-interval by using SDS-PAGE and Western blotting.

Procedure

1. Tau and HDAC6 ZnF UBP were mixed in varying ratios in 20 mM BES pH 7.4 with 1 μ M DTT, 25 μ M NaCl, 0.01 % Sodium Azide and protease inhibitor cocktail as additives.
2. Tau and HDAC6 ZnF UBP were incubated at 37 °C and analyzed by 12% SDS-PAGE and western blot at 0, 24 and 72 hours.

3. For full-length Tau degradation analysis, the ratio between Tau and HDAC6 were varied as 1:2, 1:1 and 2:1. For hTau40 Cysteine double mutant (C291A C322A), the ratio was kept as 1:2 and 2:1.
4. 20 μM hTau40wt alone was loaded as control. For western blot, samples were loaded in 1:10 dilution and the blots were probed with K9JA antibody (1:8000 dilutions) against total Tau.
5. The degradation pattern was visualized by probing the blot with Goat anti-rabbit IgG-HRP conjugate (1:10000).

3.5.7 Aggregation studies

3.5.7.1 Aggregation and Disaggregation assay set-up

Aggregation propensity of full length and repeat Tau was studied *in vitro* using poly-anionic co-factor heparin (MW-17500) as an inducer in 1:4 ratio of heparin to Tau. The aggregation reaction mixture consists of 20 mM BES pH 7.4, 1 μM DTT, 25 μM NaCl, 0.01 % Sodium Azide and Protease inhibitor cocktail. Tau aggregates were set-up in 20 μM concentration and 2 μM Tau was taken as measuring concentration.

Tau aggregates were prepared by the above mentioned procedure in 100 μM concentration. The final concentration of Tau was made as 20 μM for setting-up disaggregation assay unless stated otherwise [167, 168].

All the readings for aggregation and disaggregation assays were taken in triplicates unless stated otherwise.

3.5.7.2 Thioflavin S (ThS) fluorescence Assay

The kinetics of Tau aggregation over time was monitored using fluorescent dye ThS in 1:4 ratio of Tau to ThS (2 μM Tau and 8 μM ThS). ThS binds to the β -sheet structures abundant in protein aggregates gives enhanced fluorescence upon binding. The working solution of dye is made in 50 mM Ammonium acetate pH 7.0 and mixed with the Tau aggregation assay samples in above mentioned ratio at different time-points of the assay. The mixture is pipetted into a 384 black well plate and incubated for 10 minutes. ThS fluorescence is monitored by excitation at 440 nm and recording the emission at 521 nm in Tecan Infinite 200 PRO spectrophotometer.

3.5.7.3 8-anilino 1-naphthasulfonic acid (ANS) fluorescence Assay

ANS is a fluorescent dye which gives fluorescence upon binding to the hydrophobic region of a protein. Upon protein aggregation, conformational changes occur exposing the hydrophobic surfaces. ANS is used in monitoring the protein aggregation by binding to these hydrophobic surfaces and exhibiting fluorescence. ANS fluorescence is taken by excitation at 375 nm and observing emission at 490 nm in Tecan Infinite 200 PRO spectrophotometer. For monitoring

ANS fluorescence, the ratio between the protein and ANS was taken as 1:20 and fluorescence is recorded at different time-points during the course of aggregation.

3.5.7.4 Thioflavin T (ThT) fluorescence Assay

ThT is a fluorescent dye which binds to the β -sheet structures to produce fluorescence. The protein aggregates rich in β -sheets can be probed and their aggregation propensity can be monitored using ThT. We used ThT fluorescence to monitor aggregation studies with Melatonin as interference was observed with ThS dye [167].

3.5.7.4.1 Aggregation inhibition assay

The reactions were set up as 20 μ M Tau in microcentrifuge amber tubes and incubated at 37°C. Melatonin was prepared in 10% DMSO was added in reaction tubes for repeat Tau in varying concentrations. Aliquots of repeat Tau aggregates were taken at different time intervals to measure ThT fluorescence. All the measurements were taken in triplicates. ThT fluorescence was measured by excitation at 450 nm and emission at 475 nm. The ratio of protein and ThT was taken as 1:1. ThT fluorescence for BES buffer was measured for blank subtraction.

3.5.7.4.2 Disaggregation assay

Classical Method

Repeat Tau aggregates were prepared as mentioned above for inhibition assay in a concentration of 100 μ M incubated with 25 μ M of heparin. After 6 days of incubation at 37°C, the protein was diluted to 20 μ M in a series of reaction tubes with 20 mM BES pH 7.4 in which various concentrations of Melatonin prepared in 10% DMSO (100, 200, 1000 and 5000 μ M) were added and again kept at 37°C. The reaction tubes also contained 25 mM NaCl, 1 mM DTT and 0.01% Sodium azide. ThT fluorescence was measured at 450 nm excitation and 475 nm emission in 30 minutes interval for 4 hours.

Continuous Method

For continuous measurement mode, the reaction was set-up in 20 mM BES, pH 7.4 in 96 well black flat bottom plates in a total volume of 200 μ l without any additives. The measuring concentration of Tau was taken as 5 μ M while melatonin was added in 500, 1000, 2000 and 5000 μ M concentrations. ThT fluorescence of BES buffer was measured as blank while 5 μ M Tau with BES was measured as aggregate control. A control measurement for 10% DMSO was taken to rule out the effect of DMSO. ThT fluorescence was measured continuously at 450 nm excitation and 475 nm emission wavelength at an interval of 1 minute with a shaking time of 30 seconds in a Tecan M200pro spectrophotometer. A total of 20 such measurements were taken over the time of ~30 minutes. Two sets of disaggregation assay in continuous mode were performed.

3.5.8 Transmission Electron Microscopy

Transmission electron microscopy is a microscopy technique in which high energy electron beam is transmitted through an ultrathin section of specimen to obtain a high resolution image. The image is formed by the detection of electrons transmitted through the specimen. In order to obtain contrasting images in biological samples, negative staining is carried out using heavy metal salts such as Uranyl acetate. The staining with heavy metals salts scatters the electrons producing a darker background against the specimen.

Procedure

1. 2 μ M of Tau samples were applied on 400 mesh carbon coated copper grids for 45-60 seconds.
2. The grids are washed twice with filtered MiliQ water for 45 seconds each.
3. Negative staining is performed with 2% aqueous Uranyl acetate for 1-2 minute.
4. The grids were allowed to dry for 24 hours before analysis by TEM.
5. The samples were visualized by using TECNAI T20 Transmission Electron Microscope at 120 KV.

3.5.9 Far-UV Circular Dichroism Spectroscopy

Circular Dichroism spectroscopy is based on the differential absorption of right and left component of a circularly polarized light by a chiral or asymmetrical molecule. This technique is widely used for the determination of protein secondary structure. The peptide backbone in a protein absorbs in far-UV region of spectra and the tertiary folding of polypeptide chain acquiring a secondary structure give rise to a signature spectra characteristic of that conformation. The differential absorption of circularly polarized light components are represented in millidegree as-

$$\Delta A = A_L - A_R$$

Where, ΔA is the difference between absorbance of left (A_L) and right (A_R) component of circularly polarized light [174].

Procedure

1. Far-UV CD spectrum was acquired for soluble Tau, Tau aggregates and Tau along with its modifier (HDAC6 ZnF UBP, Melatonin or Baicalein) in varying concentrations.
2. The CD spectra were recorded using Jasco J-815 CD spectrometer in a cuvette with a path length of 1 mm under nitrogen atmosphere.
3. The scans were carried out at a scan speed of 100 nm/min and bandwidth 1 nm with a scan range from 190 to 250 nm.

4. The final spectra were taken as an average of 5 acquisitions. In each experiment, measurements were done at 25°C. The buffer baseline was set with 50 mM sodium phosphate buffer, pH 6.8 and subtracted from the measured spectra for each sample.
5. The concentration was maintained as 2 μ M for full-length Tau 5 μ M for repeat Tau for all CD measurements.
6. The final subtracted values were plotted using Sigma plot 10.0 (Systat software).

3.5.10 Size-exclusion Chromatography

Size-exclusion chromatography is a technique used for the separation of biomolecules on the basis of their molecular size. The mixture of biomolecules is passed through a column having molecular sieves made up of inert matrix with pore size corresponding to the molecules to be separated. Isocratic elution is carried out using suitable buffer and the separated components are detected by using UV absorption to obtain a chromatogram with peaks corresponding to each separated component. As the mixture runs through the column by applying pressure or under the effect of gravity, the molecules with the large molecular size travel through the void of the matrix while the smaller molecules pass through the pores of the molecular sieve. Thus, the higher weight molecules are eluted earlier. The technique is widely used for purification of proteins as well as for studying the interaction of two or more proteins. The complex formed by the interacting protein gets eluted earlier giving a separate peak in the chromatogram. The constituents eluted under the corresponding peaks can be collected for further analysis.

Procedure

Size-exclusion chromatography for Tau Oligomers

Size Exclusion chromatography was carried out for repeat Tau in presence of Baicalein at different time points in order to characterize the effect of Baicalein on the tendency of oligomerization.

1. Repeat Tau samples were prepared by incubating the protein in 20 μ M concentration in 20 mM BES buffer, pH 7.4 with or without Baicalein in 200 μ M final concentration.
2. Heparin was added in 1:4 ratios as an inducer of aggregation. Baicalein was added to the reaction mixture after 4 hours of incubation at 37°C.
3. The initial incubation was provided for the preparation of lower order oligomers. The time point at which Baicalein is added is considered as 0 hour.
4. The protein sample was filtered prior to loading on to Superdex 75 10/300 GL column (GE). The final sample load was set as 100 μ l.
5. BSA and Lysozyme were loaded as standards in 3 mg/ml concentration and soluble repeat Tau was loaded as a control.
6. The separation was carried out in PBS buffer. Samples at 0, 6, 12, 24 and 60 hours of incubation were subjected to size exclusion chromatography.

Size-exclusion chromatography for Tau/HDAC6 interaction

In order to determine the interaction of HDAC6 ZnF UBP on Tau, size Exclusion chromatography was carried out.

1. Full-length Tau and HDAC6 ZnF UBP were incubated in 1:1 ratio in 50 mM Tris-Cl pH 8.0 at 40 μ M concentration at 37 $^{\circ}$ C for 2 hours.
2. Size-exclusion chromatography was carried out at 0, 1 and 2 hours of incubation using Superdex Increase 10/300 GL column.
3. 100 μ l of sample was injected for each run and the elution was carried out by using 50 mM Tris-Cl pH 8.0

3.6 Methods for Interaction Analysis

3.6.1 ^1H - ^{15}N HSQC Nuclear Magnetic Resonance Spectroscopy

Heteronuclear Single Quantum Coherence (HSQC) Nuclear Magnetic Resonance is a technique used mainly for protein interaction study using the proton (^1H) NMR spectra and a heteronucleus (atomic nucleus other than proton). Each proton gives a unique spectrum corresponding to the heteronucleus attached to it. The proteins under study are isotopically labelled with ^{15}N , which gets incorporated to the amide linkage and side chains of amino acids residues in protein. Each residue gives a spectrum which is characteristic for the protein, such that each amide peak corresponding to a residue can be assigned. The side chain ^{15}N does not give any observable spectra due to solvent exchange. ^1H - ^{15}N HSQC NMR can be utilized for studying the interaction of protein with a ligand or another protein by comparing the spectra for free protein and protein in complex with its interacting partner. Chemical shift perturbations in the spectra are observed for the residues, which are involved in the binding.

Procedure

1. A 200 μ M solution of ^{15}N labelled repeat Tau protein in 50 mM phosphate buffer (10:90 $\text{D}_2\text{O}:\text{H}_2\text{O}$) containing 1 mM DTT was used for NMR spectroscopic experiments.
2. Titration of labelled repeat Tau was carried out with Melatonin in 1:0, 1:5, 1:10, 1:25 and 1:50 of Tau to Melatonin ratios.
3. Residue specific chemical shift perturbations obtained due to Tau and Melatonin interaction were monitored by ^1H - ^{15}N HSQC experiments.
4. All NMR studies were carried out at 278 K on Bruker Avance III HD 700 MHz spectrometer equipped with a TXI probe.
5. ^1H - ^{15}N HSQC experiments were acquired with 512 increments (16 scans per increment) in the indirect dimension and 2k complex points were collected in the direct dimension.

All the data was analyzed using Sparky program [175] after processing by Bruker topspin 3.2 software.

3.6.2 Isothermal Titration Calorimetry

Isothermal Titration Calorimetry (ITC) is a biophysical technique to determine the binding parameters of two molecules. It is a sensitive method for the determining the interaction of two

proteins or the interaction of a protein with a ligand. Binding reactions and enzyme catalyzed reactions are associated with heat changes. ITC can measure the heat change (endothermic or exothermic) up to a degree of 0.1 $\mu\text{cal/sec}$. The titration of one component against the other is carried out in an adiabatic system until saturation attained. The associated heat changes associated with each titration point can be used to determine the affinity (K_d), stoichiometry (n), enthalpy change (ΔH), entropy change (ΔS) or K_m/K_{cat} of a reaction [176].

Procedure

1. Isothermal titration Calorimetry experiments were carried out by using Malvern PEAQ-ITC instrument (MicroCal).
2. Final concentration of repeat Tau and Melatonin used for titration was adjusted by 20 mM BES buffer pH 7.4.
3. Stock solution of Melatonin (3000 μM) was made in the same buffer to minimize buffer mismatch during titration.
4. Both repeat Tau and Melatonin were filtered prior to titration. Reverse titration was performed at 25°C by using Melatonin in the sample cell while repeat Tau in the syringe.
5. Different ratio of repeat Tau and Melatonin was used so as to reach the equimolar ratio of repeat Tau and Melatonin.
6. Each titration comprises of 19 injections of 2 μl for 5 seconds at an interval of 180 seconds between each injection. An initial injection of 0.4 μl was given for stabilization.
7. The data obtained was analysed by PEAQ-ITC software and fitted using one set of sites model.
8. The values of ΔG , ΔH and $T\Delta S$ were used to calculate the binding constant or the association constant as-

$$-RT\ln K = \Delta G = \Delta H - T\Delta S$$

3.6.3 UV-Visible Spectroscopy

UV-Visible spectroscopy is a quantification and detection technique for inorganic or organic molecules containing π electrons or non-bonding (n) electrons. The electrons absorb the energy in UV-Visible wavelength range (200-800 nm) resulting in their excitation from ground state to higher energy states. The molecules absorbing in this range give a characteristic absorption spectrum, which can be used to obtain the concentration of unknown compound, binding parameters of two molecules and rate constant of a reaction.

Procedure

1. 50 μM Baicalein in 20 mM BES buffer was placed in a cuvette and an absorption spectrum was recorded in 230-450 nm range using Jasco V-530 spectrophotometer.
2. Tau protein is added to the cuvette for recording first titration. The titrations are carried out until saturation is obtained in absorption changes.

3. Aliquots of repeat Tau were subsequently added to the cuvette in 3.5, 7, 14, 28, 42, 56, 70, 84, 98 μM concentration and respective spectra were recorded for each addition.
4. The stock concentration of Tau is kept high so that the total volume of repeat Tau added was less than 100 μl so that there is no dilution effect.

Determination of dissociation constant (K_d)

The dissociation constant of protein-ligand binding can be determined by the following formula:

$$[\text{PL}] = \frac{[\text{P}_o] \times [\text{L}]}{K_d + [\text{L}]}$$

where, $[\text{P}_o]$ is the initial protein concentration, $[\text{L}]$ is the free ligand concentration, $[\text{PL}]$ is the concentration of protein-ligand complex and K_d is the dissociation constant.

L and PL are determined as -

$$[\text{PL}] = \alpha [\text{P}_o]$$

$$L = [\text{L}_o] - [\text{PL}]$$

L_o is the total ligand concentration taken in the cuvette and α is the fraction of bound ligand for a given concentration of protein determined from the change in absorption [168].

3.6.4 Ni-NTA Pull down assay

Ni-NTA Pull down assay employs binding of His-tagged protein to the Ni^{2+} immobilized on nitrile triacetic acid (NTA) through coordinate bond to determine the interaction of two proteins by their co-elution. To perform pull down using Ni-NTA resin beads, one of the proteins should be His-tagged and considered as bait protein while the other protein, with which the interaction is called in question, is regarded as prey protein. The proteins and the beads are incubated together and given suitable number of washes with buffer containing low imidazole concentration, to remove unbound and non-specifically bound proteins. The protein complex bound to beads can be either eluted or taken as such in resin bound state.

Procedure

1. The pull-down assay was carried out using Ni-NTA resin to bind HDAC6 as the bait protein and full-length human Tau as prey protein.
2. HDAC6 (20 μM) and full length Tau (10 μM) in a total volume of 200 μl was first incubated together in 1X PBS pH 7.4 as assembly buffer along with 20 μl of Ni-NTA resin at 4 $^\circ\text{C}$ for 1 hour with constant mixing.

3. After washing five times with 1X PBS, pH 7.4, 30 mM imidazole, the beads were collected by centrifugation. The samples from all the steps were loaded on to SDS-PAGE.

3.7 *In Silico* Methods

3.7.1 Molecular modelling and docking

The model for HDAC6 Zinc finger ubiquitin-binding domain was built using the SWISS-MODEL server (<https://swissmodel.expasy.org/>). The crystal structure of human HDAC6 Zn finger domain (PDB ID. 3C5K) downloaded from the RCSB-PDB database (<https://www.rcsb.org/>) was used to build the model for the interaction studies [177, 178]. The model with a global model quality estimate (GQME) of 0.99 was used for further studies. Tau protein (Repeat-Tau) model built by our group for the previous studies has been adopted here for the interaction study [168]. The models were docked using the online server, PatchDock (<https://bioinfo3d.cs.tau.ac.il/PatchDock/php.php>) [179, 180]. The clustering RMSD was set to 4Å since it is a protein-protein interaction. The top 10 models generated from PatchDock was refined using another server, FireDock (<http://bioinfo3d.cs.tau.ac.il/FireDock/php.php>). The model with the lowest binding energy of was used for further simulation studies. The protein complexes are visualized and analyzed using VMD (version 1.9.4a38 (October 20, 2019)) and PyMOL (TM) Molecular Graphics System (Version 1.8.4.0).

3.7.2 Molecular dynamics simulations

The molecular dynamic simulations for the docked complex were performed using GROMACS 2019.3 software with the AMBER03 force field[181-183]. Tip3p water model was used in the simulation. The docked protein-protein complex was placed in the center of a cubic box and the distance between the protein and the box was set as 10Å. The dimensions of the simulation box were initially set to 88X88X88 Å. The box was then solvated with water and the charges are neutralized by adding Cl⁻ ions. The energy minimization for the system was performed using steep descent minimization algorithm until the maximum force, F_{\max} reaches less than 10 KJ/mol/nm. The system converged to $F_{\max} < 1000$ in 418 steps. The temperature and pressure of the system was equilibrated using leap-frog integrator for 100 ns each (50,000 steps). Verlet cut-off scheme (Buffered neighbour searching) was used for non-bonded interactions and PME algorithm (Particle Mesh Ewald) was applied for electrostatics. The temperature of the system was equilibrated to 310 K using V-rescale thermostat (modified Berendsen thermostat). Velocity was generated from Maxwell distribution across the periodic boundaries on all x, y and z axes. The pressure was equilibrated to 1.0 bar using Berendsen pressure coupling across the periodic boundaries x, y and z axes. The final MD-run was performed for 50 ns (25000000 steps) and the trajectories were visualized using VMD. The RMSD, RMSF and Rg graphs were plotted to check the stability of interaction. The Coulombic and LJ energies between the complex were plotted and analysed. Hydrogen bond analyses were performed for different residues and were

plotted. The interacting residual structures from the last 10 ns were plotted using LigPlot+ (version 2.2) [184].

3.8 Cell Biology Methods

3.8.1 3-(4, 5-dimethylthiazol-2-yl)-2, 5-diphenyltetrazolium bromide (MTT) Assay

MTT assay is a colorimetric method to measure metabolic functions of cell as an indicator of their viability. 3-(4, 5-dimethylthiazol-2-yl)- 2, 5-diphenyltetrazolium bromide (MTT) is a tetrazolium salt which get reduced to a purple colored MTT-formazan crystals by NADP dependent oxidoreductase enzymes. The crystals formed during the reaction are solubilized and the color intensity is measured at 500-600 nm. The intensity of the colored product is directly proportional to the viability of cells.

Procedure

1. 10^4 neuro2a cells (ATCC CCL-131) were seeded in a 96 well culture plate in DMEM supplemented with 10% FBS and antibiotic penicillin-streptomycin for 24 hours at 37 °C CO₂ incubator.
2. The cells were treated with HDAC6 ZnF UBP (0- 500 nM) in serum-starved media for 24 hours.
3. MTT was added to the cells at a concentration of 0.5 mg/mL and incubated for 3 hours.
4. The reduction of MTT by cellular enzymes forms purple formazan crystals, which were dissolved by adding DMSO.
5. The developed color was quantified by reading at 570 nm in a Tecan Infinite 200 PRO spectrophotometer.

3.8.2 Lactate Dehydrogenase (LDH) Assay

Lactate Dehydrogenase (LDH) is a cytoplasmic enzyme involved in cellular respiration and present in all cells. LDH is released from the cells if damage to cell membrane occurs. Thus, LDH release from the cell can be used as an indicator of cyto-toxicity. LDH assay is a colorimetric assay which quantifies the LDH released by cell by using a tetrazolium salt 2-(4-iodophenyl)-3-(4-nitrophenyl)-5-phenyl tetrazolium chloride (INT). INT gets converted into a red formazan product upon reduction by NADH produced as LDH converts lactate to pyruvate. The intensity of red color is proportional to the released LDH and thus the number of damaged cells.

We studied the effect of HDAC6 ZnF UBP treatment on cell membrane integrity by LDH assay.

Procedure

1. 10^4 neuro2a cells (ATCC CCL-131) were seeded in a 96 well culture plate in DMEM supplemented with 10% FBS and antibiotic penicillin-streptomycin for 24 hours at 37 °C CO₂ incubator.
2. The cells were treated with HDAC6 ZnF UBP (0- 500 nM) in serum-starved media for 24 hours.
3. After the treatment with HDAC6 ZnF UBP, supernatant media was separated and used for the assay as per the manufacturer's protocol.
4. In brief, 50 µL of cell supernatant was incubated with 50 µL of the provided reaction mixture for 30 minutes at room temperature.
5. 50 µL of stop solution was added to each well and the color developed was measured at 490 nm and background subtraction was done at 680 nm in a Tecan Infinite 200 PRO spectrophotometer..

3.8.3 Caspase 3/7 activity Assay

Apoptotic cell death is mediated by the activation of caspase family of proteases which cleaves and degrades a large number of cellular proteins. Caspase 3 and 7 are the proteases with substrate specificity towards amino acid sequence – Asp-Glu-Val-Asp (DEVD). The assay for Caspase 3/7 is based on the conversion of non-fluorescent bisamide derivative of Rhodamine R110 into a fluorescent monoamide and then into more fluorescent R110. DEVD peptides are covalently linked to each amino group in Rhodamine R110 such that its visible absorption and fluorescence is suppressed. Caspase 3/7 in the apoptotic cell carry out enzymatic cleavage of DEVD peptides to obtain fluorescent products which corresponds to the enzymatic activity in the sample.

In order to study the effect of HDAC6 ZnF on inducing apoptotic cell death, the activity of executioner caspase 3 was determined by EnzChek™ Caspase-3 Assay Kit.

Procedure

1. 10000 cells/well cells were seeded in a 12 well culture plate for 24 hours and further treated with HDAC6 (0-500 nM) for 24 hours in serum-starved media.
2. Caspase activity was performed as per manufacturer's protocol.
3. The cells were lysed with provided lysis buffer in freeze-thaw cycles.
4. The cell debris was centrifuged out and the supernatant was incubated with the substrate (DEVD-Rhodamine)
5. The fluorescence was quantified at (Ex/Em) 496 /520 nm at different time intervals in TECAN Infinite 200 PRO plate reader.

3.8.4 Immunofluorescence Analysis and Quantification

Immunofluorescence refers to the technique used for visualizing the proteins in cells or tissues by using fluorescent tagged primary or secondary antibodies. This technique provides the cellular or subcellular localization, distribution and levels of protein in question. The immunostained proteins can be visualized by a microscope based on the principle of fluorescence *i.e.* simple fluorescence microscope, confocal microscope *etc.*

Procedure

1. Neuro2a cells from passage number 10-20 were cultured in advanced DMEM supplemented with penstrep-glutamine, anti-mycotic and 10% FBS at 37 °C, 5% CO₂, until the cells were 70-80 % confluent.
2. For immunofluorescence studies, 5*10⁴ cells were seeded on a glass coverslip (Bluestar) in a 12 well cell culture plate and allowed to attach for 24 hours.
3. Cells were given the respective treatment in serum starved media (0.5% FBS) for 24 hours.
4. After incubation period, cells were washed with 1X PBS and fixed with 4% paraformaldehyde or molecular biology grade absolute methanol for 10 minutes.
5. Further cells were washed thrice with 1X PBS and permeabilized using 0.2% Triton X-100.
6. Blocking is carried out using 2% horse serum and incubated with primary antibodies in a moist chamber at 4 °C overnight.
7. Next day, cells were washed thrice with 1X PBS and incubated with alexa fluor labelled secondary antibodies for 1 hour at 37 °C.
8. The unbound secondary antibody was washed off with three washes of 1X PBS and counterstained with DAPI.
9. The coverslips were mounted in 80% glycerol and observed under 63X oil immersion lens in Axio Observer 7.0 Apotome 2.0 (Zeiss) microscope.
10. The quantification of immunofluorescence intensity was carried out by Zen 2.3 software and mean fluorescence intensity per unit area were determined for various treatment groups in respective number of fields (n = 5-12).

3.9 Statistical Analysis Methods

Two-tailed unpaired student t-test was used to determine the significance for experiments involving comparison of two groups (n.s. – non-significant, * indicates $P \leq 0.05$, ** indicates $P \leq 0.01$, *** indicates $P \leq 0.001$). One way ANOVA was conducted for the experiments involving comparison of multiple treatment groups. Tukey's HSD (Honest significant difference) test was performed to compare the significance within groups ((Significant at mean difference between groups > Tukey's criterion; T). All the experiments were performed in triplicates and analyzed by Sigmaplot 10.0 (Systat software).

Chapter 2

Tau aggregation inhibition and disaggregation of preformed aggregates by HDAC6 ZnF UBP

2.1 Background

In AD, protein aggregation is an intriguing process involving multiple factors influencing the eventual direction of proteostasis. The process of aggregation varies depending upon the type of protein and cellular environment. Microtubule associated protein Tau (MAP-Tau) associates with microtubules and promotes their structural integrity [12, 185]. The structure and function of Tau protein is modified by various cellular and molecular factors such as oxidative stress, post-translational modifications and interaction with its binding partners [31]. Tau protein aggregates are deposited as intracellular inclusion bodies called neurofibrillary tangles. Tau aggregation is a process involving conversion of highly soluble Tau protein into insoluble Tau fibrils. This process mainly depends on the charge compensation of Tau brought about by cellular environment, mutations, PTMs or protein interactions. Tau undergoes a wide range of PTMs, which regulates its structure and function [186]. Tau protein has regions with inherent tendency to form β -sheet structure which is usually opposed by interactions within the proteins and charge restrictions [12]. However, in case of mutations or other modifications in the form of proteolytic cleavage or PTMs like phosphorylation at specific residues, Tau is driven to form β -sheet structure. The changes within the Tau molecule result in its detachment from microtubule and self-association leading to initiation of aggregates formation.

Tau aggregation has drawn attention in past two decades as a therapeutic target [187]. The therapeutic approach against Tau aggregation includes either search for inhibitors to tackle the processes that drive Tau towards aggregation or inhibitors directly working on Tau aggregates [188]. The first approach involves designing inhibitors against kinases involved in Tau hyperphosphorylation [189]. Such an approach is often non-specific and difficult to target against a particular cell type [190]. On the other hand, targeting Tau protein specifically so as to inhibit its aggregation or to dissolve pre-formed aggregates is a suitable approach to curb down neuronal damage. However, there are constraints to such an approach as most of the molecules that are found to be effective against Tau aggregation have to cross the blood brain barrier to be of use [191]. Further, merely targeting the aggregation of Tau may not be sufficient enough to curb the ill effects associated with AD since it is a multi-factorial disease. Thus, in order to understand the molecular mechanisms associated with Tau aggregation and the factors that affect the fate of Tau in neurons is desirable to design a holistic therapeutic strategy. Tau has a large number of interacting partners that includes various enzymes like kinases or non-enzyme proteins such as molecular chaperones, which determines its function under various specific conditions [192]. Understanding the association of Tau with its interacting partners can give useful information in order to designing potential inhibitors. The interaction with other proteins can either be beneficial or detrimental in terms of their physiological function. For instance, refolding through associating with chaperones is a beneficial aspect while Tau hyperphosphorylation may occur due to enhanced association with kinases under pathological conditions.

HDAC6 is a known interacting partner of Tau and regulates its association with microtubules *via*

deacetylation [54]. Apart from its enzymatic function, HDAC6 is involved in reducing aggregate burden in cells by mediating the formation of aggresomes *via* its ZnF UBP domain [103]. Protein aggregates are poly-ubiquitinated in order to target them to UPS. The failure or inefficiency of UPS triggers aggresome formation where HDAC6 binds to poly-ubiquitinated aggregates *via* ZnF UBP membrane and targets them to degradation by means of autophagy. We have studied HDAC6 ZnF UBP for its ability to modulate the aggregation propensity of Tau as well as for its potency to dissolve pre-formed aggregates. We propose a mechanism by which HDAC6 ZnF UBP modulates its aggregation properties and elaborates the function of HDAC6 as the direct modulator of Tau aggregation.

2.2 Aggregation propensity of Tau

Tau hypothesis suggests that microtubule-associated protein Tau undergoes loss of function under pathological conditions and forms toxic intracellular aggregates [193]. The exact mechanism through which Tau aggregates impart toxicity to neurons is not well defined. However, presence of various species of Tau aggregates in neurons has been linked to cognitive decline and neurodegeneration. Tau aggregates adopt β -sheet conformation and the fibrillar aggregates are characterized by parallel, in register β -sheets perpendicular to the axis of fibril [22]. The aggregates of Tau acquire different morphological forms depending on the arrangement of oligomeric units. The most predominant form called paired helical filament consist of two protofibrils wound together to demonstrate a characteristic helical twist [194]. The formation of Tau aggregates *in vivo* is a complex process involving multiple causative factors such as post-translational modifications, molecular crowding, presence of nucleating factors and interaction with other proteins modulating Tau structure and function [195]. In order to study the mechanism of Tau aggregation, *in vitro* aggregation studies have been carried out with different Tau isoforms as well as different constructs of Tau. The aggregation conditions are designed in such a way to mimic the physiological conditions. However, in order to induce Tau aggregation *in vitro*, aggregation inducers are employed which includes poly-anionic factors like heparin and arachidonic acid. Conversely, pro-aggregant forms and constructs of Tau are used for promoting aggregation [196]. Such pro-aggregant forms of Tau consist of mutations such as lysine deletion in the second repeat of Tau (Δ K280) or truncated form of Tau (cleavage at D421). There are constructs which consists of only repeat region of Tau such as K18 (4R) and K19 (3R). Such constructs have higher propensity for aggregation compared to wild type form of Tau. In our aggregation studies, we have used recombinant full-length form of Tau (hTau40wt) and 4 repeat Tau (K18wt) (**Fig 2.1A and B**). The course of Tau aggregation was monitored by using the fluorescent dye Thioflavin S (ThS), which binds specifically to β -sheet structures formed upon aggregation. As the aggregation proceeds, the amount of β -sheet increases indicating higher content of aggregates. The time course of aggregation gives an indication of the rate of aggregation. The aggregation kinetics of both the forms of Tau differs with respect to their ability to form fully developed mature aggregates. hTau40wt requires a higher time-course to produce mature fibrils as the initial nucleation steps is a limiting factor (**Fig. 2.1C,D and E**).

However, K18wt has a faster rate of aggregation is able to bear well defined aggregates in shorter time while attaining saturation earlier (**Fig 2.3F, G and H**).

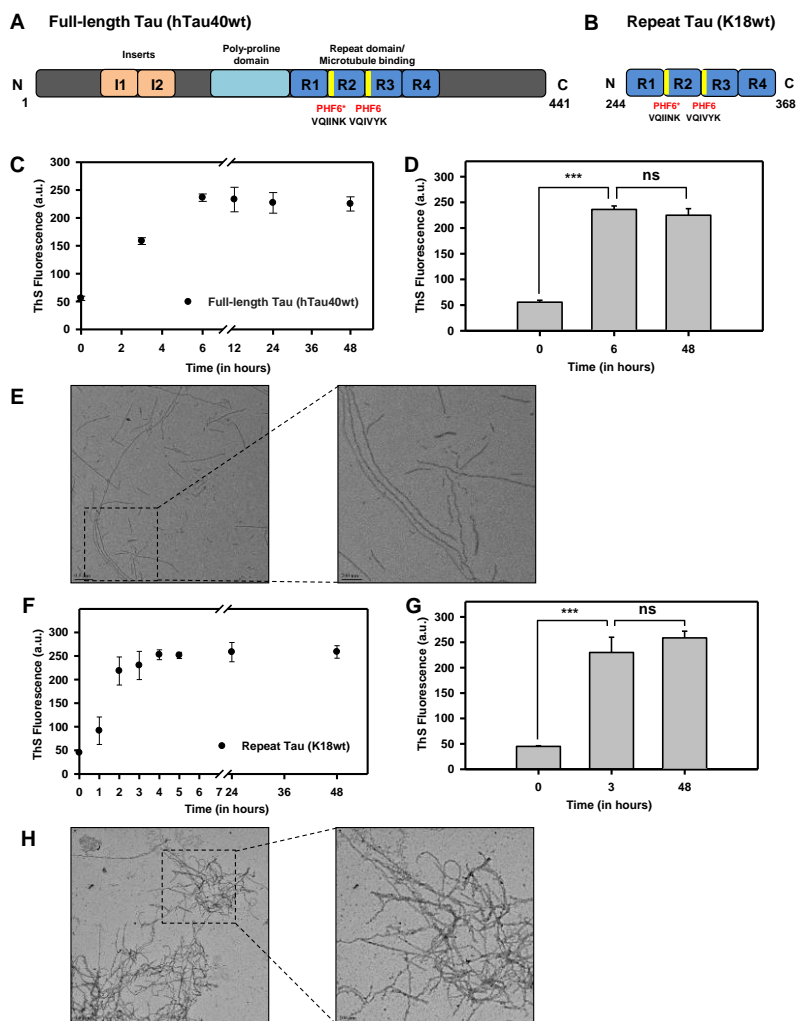


Fig. 2.1. Aggregation propensity of Tau. Bar diagram representation of A) full-length Tau (hTau40wt) and B) repeat Tau (K18wt) and their domain organization. Repeat Tau represents the physiological as well as pathological unit of Tau involved in microtubule interaction and aggregate formation respectively. C) Aggregation assay for hTau40wt monitored by using ThS fluorescence for a time-course of 48 hours. The aggregation reaction was incubated at 37°C and aliquoted for ThS fluorescence measurement at respective time-points. D) Bar graph representation of ThS absolute fluorescence at 0, 6 and 48 hours to indicate the point of saturation in aggregation assay. E) Morphology of hTau40wt aggregates obtained at the end-point of aggregation assay showing fibrillar form of aggregates as seen in scales of 0.5 μm and 200 nm as observed in transmission electron microscopy (TEM). F) Aggregation of repeat Tau domain (K18wt) carried out for 48 hours and aggregation propensity assayed by ThS fluorescence. G) The aggregation of K18wt approaches saturation in 3 hours of incubation at 37°C as represented by bar graph. H) TEM images taken for K18wt aggregates at the end-point of aggregation assay shows fibrillar form of aggregates.

2.3 Inhibition of Tau aggregation and conformational changes by HDAC6 ZnF UBP

Cytosolic deacetylase HDAC6 interacts and modulate the function of wide range of proteins involved in various cellular processes [197, 198]. In this regard, we studied the interaction of

full-length human Tau and HDAC6 ZnF UBP domain with respect to HDAC6's ability to modulate Tau function. Aggregation assay was carried out for hTau40wt in presence of varying concentrations of HDAC6 ZnF UBP. The aggregation assay shows that HDAC6 ZnF UBP is able to inhibit the full-length Tau fibrillar assembly at a concentration of 20 μ M as monitored by ThS fluorescence intensity (**Fig. 2.2A**). Tau in its soluble form exists as a random coil and gives a characteristic signature for random coil conformation with a negative band at \sim 200 nm [174]. In order to analyze the conformational changes in hTau40wt, far-UV CD spectroscopy was performed for the end point samples from aggregation inhibition assay. While soluble Tau gives a signature for random coil conformation with a negative band at 202 nm, upon aggregation the spectra shifts towards β -sheet conformation. hTau40wt aggregate has predominantly β -sheet conformation and gives a signature band at 208 nm. The CD spectra for the Tau samples incubated with HDAC6 ZnF UBP showed spectral shift back towards random coil conformation *i.e.* 204 nm (**Fig. 2.2B**). The wavelength maxima obtained for hTau40wt in its monomeric form, aggregates and with varying HDAC6 concentration is summed up in **Table 2.1**.

In order to visualize the aggregate formation and aggregation inhibition in the presence of HDAC6 ZnF UBP, SDS-PAGE was carried out for aggregation assay samples taken at various time-points of aggregation assay. The same effect of aggregation inhibition was observed in SDS-PAGE for aggregation assay samples at different time points. However, the reduction in aggregate population as observed in SDS-PAGE was quite similar in all concentrations of HDAC6 ZnF UBP (**Fig. 2.2C**). The inhibition effect of HDAC6 ZnF UBP was also evident in transmission electron microscopy (TEM) for HDAC6 ZnF UBP treated Tau aggregates as compared to the control Tau aggregates (**Fig 2.2D**). Tau aggregates as observed in TEM, appear as complete long fibrillar structure while the Tau aggregates with HDAC6 ZnF UBP gives morphology of broken and thinner fibrils. Interestingly, there was a significant difference in the degradation pattern of hTau40wt in HDAC6 ZnF UBP treated samples as compared to the Tau control aggregates. The aggregation assay for Tau with HDAC6 ZnF UBP suggested a possible mechanism through which HDAC6 ZnF UBP brings about aggregation inhibition of Tau as well as mediating its degradation. Aggregation assay for repeat Tau was also carried out in presence of HDAC6 ZnF UBP in 2.5, 5, 10 and 20 μ M concentrations (**Fig. 2.3A**). The aggregation kinetics for repeat Tau shows inhibition effect with 20 μ M of HDAC6 ZnF UBP (**Fig. 2.3B**). TEM analysis of repeat Tau aggregation assay samples in the presence of HDAC6 ZnF UBP showed amorphous Tau aggregates indicative of hindered fibril formation (**Fig. 2.3C**).

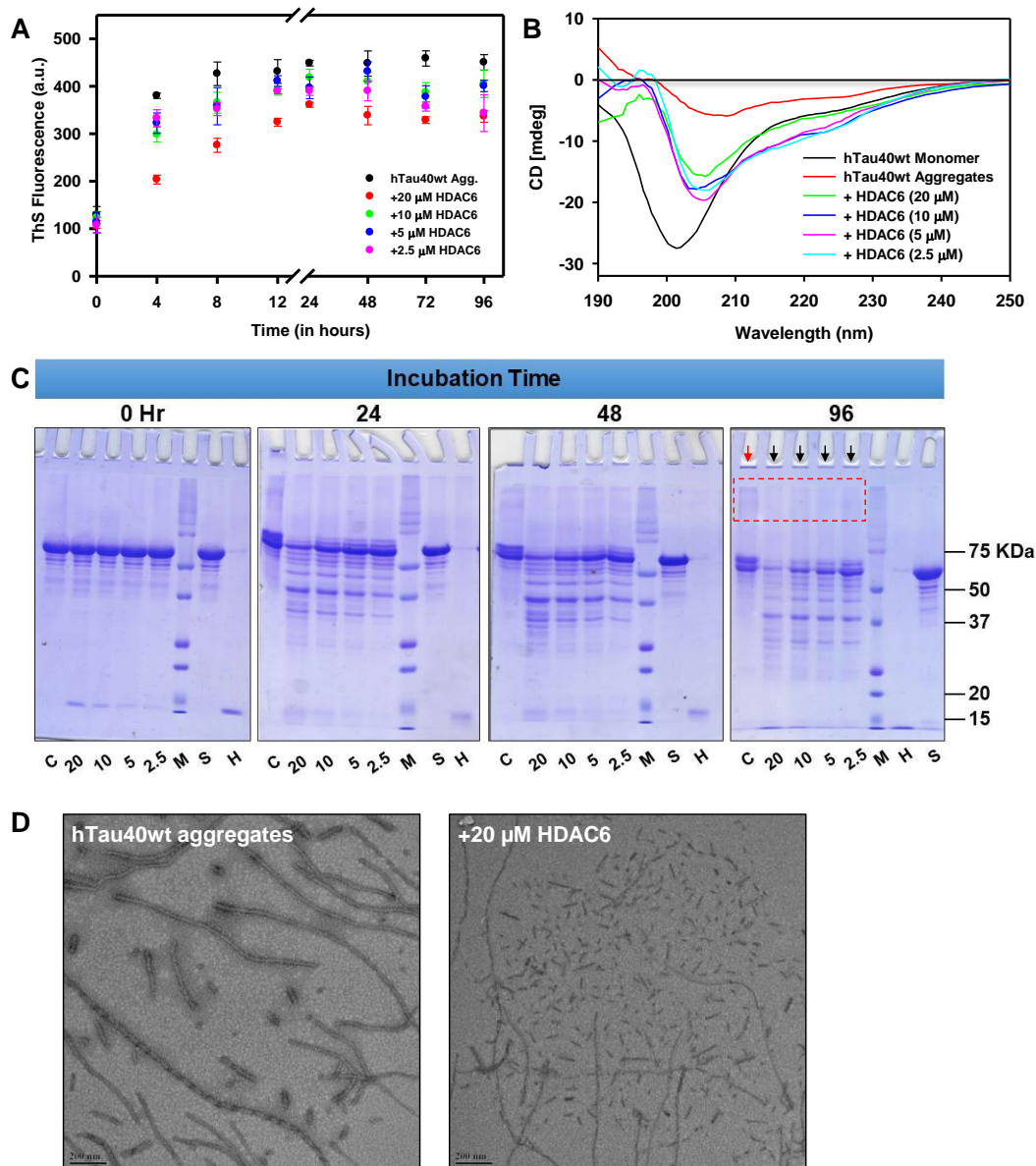


Fig. 2.2. Effect of HDAC6 ZnF UBP on full-length Tau aggregation and conformation. A) hTau40wt was subjected to aggregation with different concentrations of HDAC6 and the aggregation kinetics was monitored using ThS fluorescence. B) Circular dichroism spectroscopy for hTau40wt aggregation assay samples incubated with different HDAC6 concentration showed the shift towards random coil structure in Tau samples incubated with HDAC6 ZnF UBP. C) SDS-PAGE analysis for aggregation of hTau40wt in presence of different HDAC6 concentrations at 0, 24, 48 and 96 Hrs. SDS-PAGE analysis showed absence of higher order aggregates in Tau incubated with HDAC6 ZnF UBP (indicated by black arrows) compared to control Tau aggregates (indicated by red arrow). The control Tau aggregates is marked as C, protein marker lane as M, HDAC6 ZnF UBP lane as H and soluble Tau as S. D) Electron micrographs for aggregation assay samples showed morphologically irregular and broken fibrils as compared to well-defined fibrils in control Tau aggregates sample.

Table 2.1. Wavelength maxima for hTau40wt-HDAC6 ZnF UBP aggregation assay samples.

Sample	Wavelength Maxima (nm)	CD (millideg)
hTau40wt Soluble	202	-29.0441
hTau40wt aggregates	208	-6.5926
hTau40wt agg. + 20 μ M HDAC6	204	-19.7214
hTau40wt agg. + 10 μ M HDAC6	204	-19.3865
hTau40wt agg. + 5 μ M HDAC6	204	-21.5629
hTau40wt agg. + 2.5 μ M HDAC6	204	-18.9884

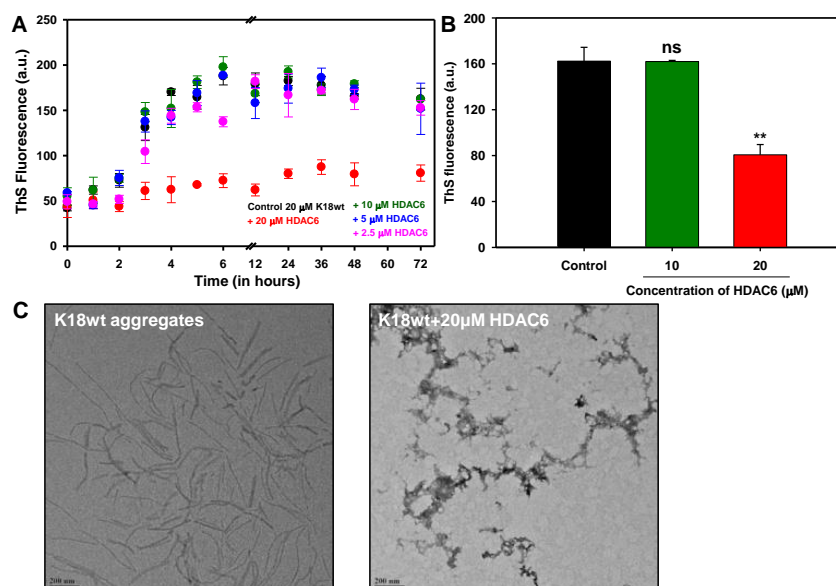


Fig. 2.3. Repeat Tau (K18wt) aggregation inhibition by HDAC6 ZnF UBP. A) ThS fluorescence assay was carried out for K18wt with different concentrations of HDAC6 ZnF UBP. Aggregation inhibition was observed with 20 μ M of HDAC6 ZnF UBP. B) Inhibition of K18wt aggregation as represented by the absolute fluorescence values at the assay end point. (n.s. indicates $P \geq 0.05$ (non-significant), * indicates $P \leq 0.05$, ** indicates $P \leq 0.01$, *** indicates $P \leq 0.001$). C) Electron micrographs for K18wt aggregates shows fibrillar structures while K18wt incubated with 20 μ M HDAC6 ZnF UBP shows amorphous structures.

2.4 Disaggregation of preformed Tau fibrils by HDAC6 ZnF UBP

Apart from aggregation inhibition, another approach to curb down the detrimental effect of protein aggregates involves dissolution of already formed aggregates. HDAC6 ZnF UBP domain is known to interact with aggregated proteins in cells through ubiquitin C-termini of polyubiquitinated aggregates, but there are limited evidence for its direct effect on protein aggregates [199]. We carried out disaggregation assay for hTau40wt where pre-formed Tau aggregates were incubated with HDAC6 ZnF UBP. The disaggregation effect was monitored employing ThS fluorescence such that lowered value of ThS fluorescence over time is indicative of disaggregation. Disaggregation assay carried out for a time course of 96 hours showed

decrease in fluorescence in Tau aggregates incubated with 20 μM HDAC6 ZnF UBP (**Fig. 2.4A**). The absolute fluorescence values for Tau aggregates incubated with 20 μM HDAC6 ZnF UBP showed a decrease by ~ 70 a.u. as compared to control Tau aggregates (**Fig. 2.4B**). However, in SDS-PAGE analysis, the effect was observed for both the concentrations of HDAC6 (2 and 20 μM) with almost complete degradation of Tau. At the end of 96 hours, the Tau aggregates were observed to dissolve completely for samples with both 2 and 20 μM of HDAC6 while they were intact in control Tau aggregates as seen in SDS-PAGE analysis (**Fig. 2.4C**). TEM images also suggested the disaggregation of Tau aggregates with HDAC6 ZnF UBP evident by the presence of broken fibrillar structures (**Fig. 2.4D**). Overall, the results indicated that HDAC6 ZnF UBP can effectively dissolve the pre-formed aggregates of Tau owing to their interaction and degradation effect.

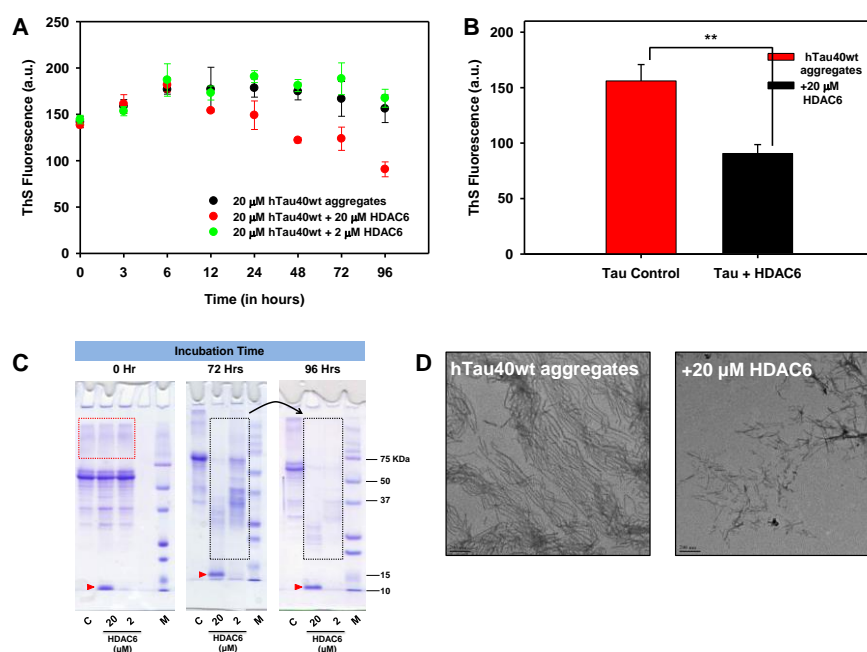


Fig. 2.4. Disaggregation assay for full-length Tau fibrils in presence of HDAC6 ZnF UBP. A) Disaggregation assay kinetics for hTau40wt with 2 and 20 μM of HDAC6 ZnF UBP shows the effect at higher concentration of HDAC6 as monitored by ThS fluorescence. B) Bar graph showing marked reduction in ThS fluorescence after 96 hours with 20 μM of HDAC6 ZnF UBP as compared to Tau control aggregates. (n.s. indicates $P \geq 0.05$ (non-significant), * indicates $P \leq 0.05$, ** indicates $P \leq 0.01$, *** indicates $P \leq 0.001$). C) SDS-PAGE for hTau40wt disaggregation at various time points (0, 72 and 96 hours) shows remarkable reduction in aggregate load over time. D) Electron micrographs for hTau40wt disaggregation by HDAC6 shows marked changes in the morphology of Tau fibrils. Broken shorter aggregates were observed for the Tau aggregates incubated with HDAC6.

2.5 Summary

The aim of our study is to elucidate the role of HDAC6 ZnF UBP domain with respect to Tau in physiological and pathological conditions i.e. in its soluble and aggregated form respectively. We have addressed the direct effect of this HDAC6 on Tau through its ZnF UBP domain. HDAC6 ZnF UBP domain is able to inhibit the aggregation of Tau as well as cause disaggregation of pre-formed aggregates in vitro suggesting the possibility of its protective role

in Tauopathies. Also, the aggregation inhibition as well as disaggregation of pre-formed aggregates was associated with rapid degradation of Tau in both aggregated and non-aggregated state. Degradation of Tau in presence of HDAC6 ZnF UBP suggests the possible role of this domain in Tau stability and function. However, the nature of interaction and the site specific to which it binds in Tau need to be further explored.

Chapter 3

Interaction of HDAC6 ZnF UBP with Tau affects its stability

3.1 Background

HDAC6 associates with other proteins and regulates their function through deacetylation [200, 201]. Although, the ZnF UBP domain of HDAC6 is not known to possess any known catalytic activity, it is essential in strengthening the association of target protein with HDAC6 facilitating the enzymatic efficiency of catalytic domains [202, 203]. The ZnF UBP domain is mostly involved in physical association with proteins and regulating their transport or providing tether to enable their association with other proteins by making a ternary or multi-protein complex [204]. The UBP or BUZ domain is known to recognize specific C-terminal sequence of proteins [199]. Interaction studies with HDAC6 ZnF UBP and other ZnF UBP containing proteins revealed that it requires a C-terminal diglycine motif for binding. This includes proteins like ubiquitin, which interacts with HDAC6 ZnF UBP after ataxin-3-mediated C-terminal cleavage exposing diglycine motif RLRGG-COOH [69]. Histone H3-H4 tetramer is another binding partner of ZnF UBP domain having regulatory function [199]. Isopeptidases are ubiquitin interacting enzymes involved in the cleavage of isopeptide bond (a peptide bond involving the side chain of at least one amino acid). Structural analysis has shown that their binding involves interaction of Arg, Leu, Ile and Phe residues from ubiquitin forming hydrophobic bonds which strengthens the interaction through diglycine motif [199, 205]. HDAC6 ZnF UBP domain interaction with ubiquitin is well characterized by crystallographic analysis which explains its function in aggresome formation [69]. We aimed to study its interaction with Tau protein owing to its effect in aggregation studies. Also, the natively unfolded structure of Tau may allow its modification by constituting multiple interacting residues.

Microtubule-associated protein Tau can undergo a large number of modifications which directs its stability and function. While some of the modifications are essential for the physiological function of Tau, an imbalance in these modifications often lead to pathological state of Tau [206]. For example, phosphorylation is important for Tau function and it is always associated with a minimal amount of phosphorylation at specific sites to perform its physiological function [207]. However, under pathological conditions, Tau becomes hyperphosphorylated either due to over-activity of kinases or suppressed phosphatase activity [208]. This leads to detachment of Tau from microtubules and self-association to form Tau aggregates. Similar to phosphorylation, another important event that decides the fate of Tau is its truncation or cleavage. However, the mechanism of toxicity and pathology mediated by Tau truncation is less understood.

Tau truncation or cleavage is considered as an important modification leading to pathological condition [209]. Tau may undergo cleavage either enzymatically through the action of proteases, which includes caspases, calpain and cathepsins or non-enzymatically through a less understood mechanism. The Tau fragments generated during the course of cleavage have been widely studied with respect to their pro-aggregation properties and toxicity to neuronal cells [210, 211]. The major fragments characterized for Tau cleavage includes – F1 (at N-terminal after Lys²⁵⁷), F2 (at C-terminal after Val³⁶³) and F3 (at C-terminal after Ile³⁶⁰) [55, 212]. The F2 and F3 fragments are more amyloidogenic than F1. Thus, N-terminal plays a protective role in Tau

function and stability [213]. There are other peptide fragments generated by the proteolytic cleavage of Tau, which are well studied and characterized. Calpain 1-mediated cleavage yields a 24 KDa fragment consisting of four repeats along with a C-terminal tail and lacking N-terminal region [214]. This fragment is found to be neurotoxic and pro-aggregant with prominent seeding effect. Similarly, a 17 KDa fragment is obtained by the action of calpain 2, which was found to be non-toxic to cells [215]. The events that trigger the cleavage of Tau mark other cellular events like Tau phosphorylation and apoptosis, leading to the pathological cascade in Tauopathies. Tau cleavage is associated with lysosomal pathway of protein degradation where Tau gets attached to lysosomal membrane and undergoes incomplete translocation into lysosomal lumen in order to get degraded. The membrane bound Tau is then cleaved by Cathepsin L residing in lysosomal lumen to generate F2 and F3 fragments [216]. Tau cleavage may also occur independent of proteolytic enzymes. Tau undergoes auto-acetylation associated with its cleavage to generate a 12 and 17 KDa fragment derived from C-terminal [50]. The autoproteolysis of Tau is a cysteine dependent mechanism in which C291 and C322 mediates Tau cleavage [61]. In the current study, we have worked to explore the properties of ZnF UBP domain of HDAC6 with respect to its potency to interact with Tau and to regulate Tau stability.

3.2 Interaction analysis of Tau (Full-length and Repeat) with HDAC6 ZnF UBP

To study the interaction of HDAC6 ZnF UBP with full-length Tau *in vitro*, pull-down assay and size-exclusion chromatography were performed. Pull-down assay was carried out for analyzing the interaction of HDAC6 ZnF UBP with both full-length Tau and repeat Tau. The assay was based on employing 6X his-tag HDAC6 ZnF UBP to bind Ni-NTA resin beads. The experiments were performed with purified recombinant proteins at concentration of 20 μ M and 1:1 ratio. SDS-PAGE was used to visualize the interaction of hTau40wt and HDAC6 ZnF UBP. Pull-down assay was performed by incubating first HDAC6 ZnF UBP with Ni-NTA beads and then with hTau40wt for 1 hour at 4 $^{\circ}$ C. The Ni-NTA beads were given wash by buffer containing 20 mM imidazole to remove unbound and non-specific interacting proteins after each incubation step. This was followed by two elution steps to elute out the protein complex. SDS-PAGE revealed the interaction between Tau and HDAC6 ZnF UBP as both proteins were found to be present in the lane for eluted samples as well as lane for beads (**Fig. 3.1A**).

For repeat Tau and HDAC6 ZnF UBP interaction, both the proteins were incubated at 4 $^{\circ}$ C for 1 hour with constant mixing. The protein mixture is then incubated with Ni-NTA beads at 4 $^{\circ}$ C for one more hour followed by washing of Ni-NTA beads with 1X PBS containing 20 mM imidazole. A separate experiment with K18wt incubated with Ni-NTA beads was also carried out to determine whether Tau interacts non-specifically to the beads. The samples from different stages were loaded and run on 12% SDS-PAGE. The proteins from SDS-PAGE were transferred to PVDF membrane and probed with antibody against total Tau (K9JA). The lane corresponding to Ni-NTA beads showed a prominent band for K18wt when incubated with HDAC6 ZnF UBP domain indicating their interaction but the beads incubated only with K18wt showed a very faint

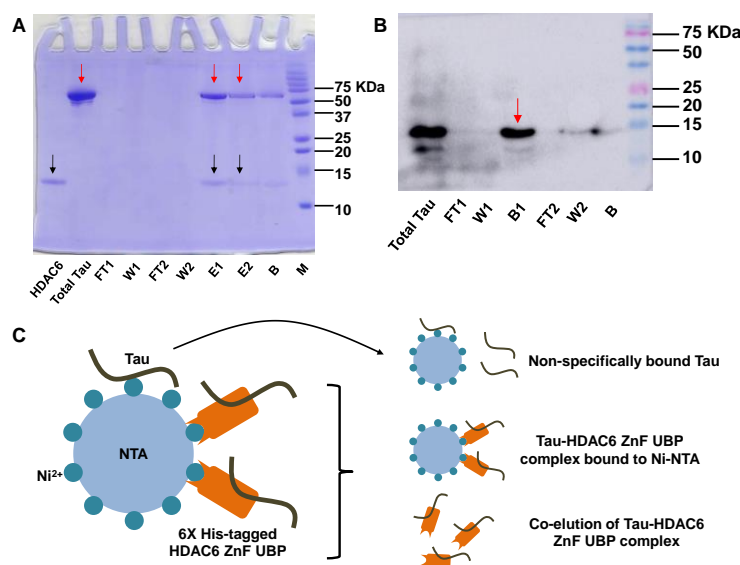


Fig. 3.1. Interaction analysis of Tau and HDAC6 ZnF UBP. A) Pull-down assay for hTau40wt and HDAC6 ZnF UBP interaction was performed with 6X his-tag HDAC6 ZnF UBP as bait and Tau as prey protein. The samples from various steps of pull-down were loaded on to SDS-PAGE. The flow through obtained after incubation of beads with HDAC6 and Tau are represented by FT1 and FT2 respectively. Total numbers of three washes were given after incubation with HDAC6 and Tau. The last wash in each case is represented as W1 and W2 respectively. The eluents (E1 and E2) obtained showed the co-elution of Tau along with HDAC6 ZnF UBP. Significant amount of HDAC6 ZnF UBP and Tau were retained in the Ni-NTA beads (B). B) Interaction between K18wt and HDAC6 ZnF UBP was studied by pull-down assay followed by Western blot analysis using antibody against total Tau (K9JA) in 1:8000 dilution. Both proteins were co-incubated prior to binding with beads. A control experiment with K18wt incubated with beads was carried out to overrule non-specific interaction. The flow through, last wash and beads (represented by FT1, W1 and B1 for Tau with HDAC6 ZnF UBP and FT2, W2 and B2 for control experiment) were loaded on SDS-PAGE and transferred to PVDF. Upon exposure for 0.5 seconds, the lane for beads incubated with both proteins showed presence of K18wt indicating its interaction with HDAC6 ZnF UBP while the beads for control experiment showed a minimal amount of K18wt due to non-specific interaction. C) The Tau-HDAC6 ZnF UBP complex either co-eluted or loaded as such on SDS-PAGE in complex with the Ni-NTA beads. In a control experiment, a small fraction of Tau was found to bind non-specifically with the Ni-NTA beads. D) Size-exclusion chromatography for Tau and HDAC6 ZnF UBP after co-incubation showed peak broadening and enhanced degradation of Tau indicating Tau degradation accompanied with the association of HDAC6 ZnF UBP with products of Tau degradation.

band due to some non-specific binding (**Fig. 3.1B**). In both the experiments for full-length Tau and repeat Tau, there was some non-specific interaction of Tau with the Ni-NTA resin but comparatively major amount of Tau was either co-eluted with HDAC6 ZnF UBP or existed in complex with HDAC6 ZnF UBP bound to Ni-NTA beads (**Fig. 3.1C**).

Size-exclusion chromatography was carried out for Tau-HDAC6 ZNF UBP at 0, 1 and 2 hours of incubation at 37 °C. SEC did not showed any peak corresponding to the formation of protein complex but showed peak broadening with time. Also, there was an increase in the peak corresponding to HDAC6 ZnF UBP (**Fig. 3.2**). The data for SEC suggests possible transient interaction between Tau and HDAC6 ZnF UBP. The occurrence of peak broadening instead of a complex formation indicates Tau degradation and the increased peak intensity denotes its possible interaction with the degradation products of Tau.

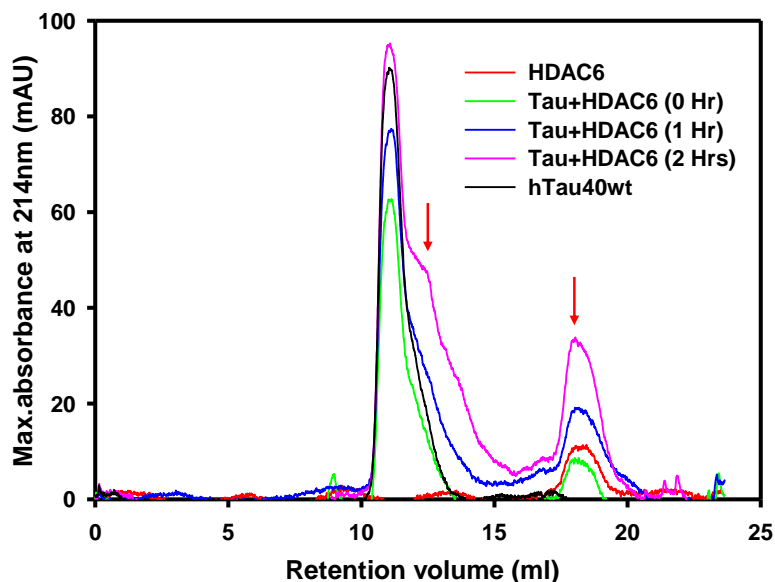


Fig. 3.2. Size-exclusion chromatography for detecting Tau-HDAC6 ZnF UBP association. hTau40wt and HDAC6 ZnF UBP were incubated at 4 °C in equimolar concentration (20 μ M). Size-exclusion chromatography was carried out at 0, 1 and 2 hours to detect the presence of any protein complex formation. However, after co-incubation Tau and HDAC6 ZnF UBP showed peak broadening and enhanced degradation. This indicates Tau degradation accompanied by the association of HDAC6 ZnF UBP with products of Tau degradation as evident from the increased peak intensity corresponding to HDAC6 ZnF UBP.

3.3 ^1H - ^{15}N HSQC NMR Spectroscopy for Tau-HDAC6 ZnF UBP interaction

NMR spectroscopic studies were carried out to study the influence of HDAC6 ZnF UBP on repeat Tau for which a 200 μ M of ^{15}N labelled repeat Tau dissolved in phosphate buffer (see experimental section) was employed. The protein solution was titrated with HDAC6 ZnF UBP at 0, 10, 25 and 50 μ M concentrations. The effect of the increasing concentration of HDAC6 ZnF UBP on repeat Tau was characterized by ^1H - ^{15}N HSQC experiments and the changes in the cross-peak positions was thoroughly monitored [217]. Our experiments showed a change in the position of the cross-peaks corresponding to the residues H268, H299, H329, H330, H362, V300, K331 and V363 (Fig. 3.3).

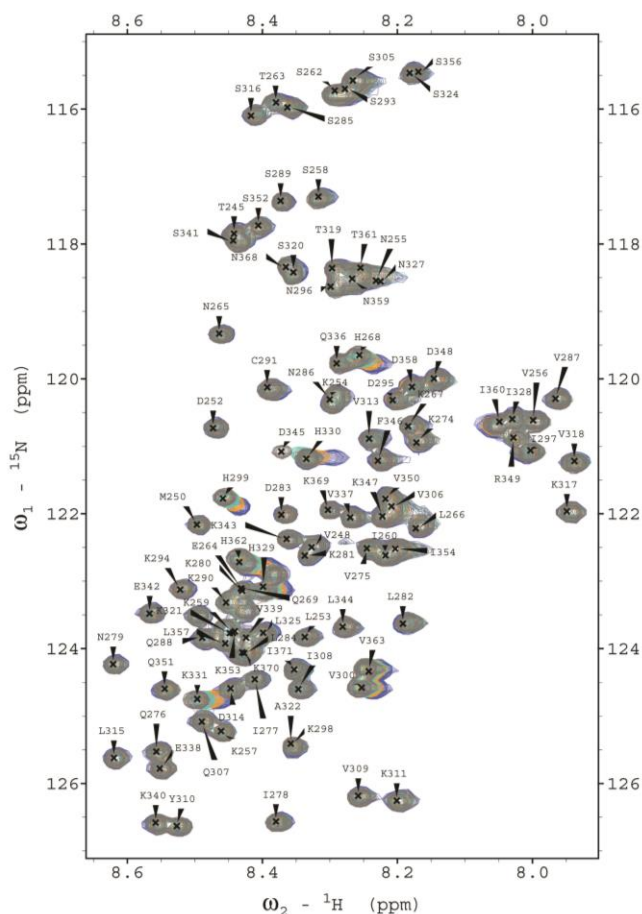


Fig. 3.3. ^1H - ^{15}N HSQC NMR for Tau and HDAC6 ZnF UBP. Overlay of ^1H - ^{15}N HSQC spectra obtained for the titration of 200 μM solution of ^{15}N labelled repeat Tau with HDAC6 ZnF UBP at 0 μM (gray), 10 μM (turquoise), 25 μM (orange) and 50 μM (blue) concentrations. Annotations on the cross peaks in the parent ^1H - ^{15}N HSQC spectrum corresponds to the respective residues from repeat Tau[217]. While the residues which are unaffected by the addition of HDAC6 ZnF UBP give rise to unchanging cross-peak position, the amino acids which are affected by HDAC6 result in a change in the position of the corresponding cross-peaks.

3.4 Molecular modelling and docking of HDAC6 ZnF UBP and repeat-Tau

The SWISS-model generated for the HDAC6 ZnF UBP domain had a global model quality estimate (GQME) of 0.99. The quality assessment was performed for this model and the Ramachandran plot showed 97.14% favoured residues. Repeat-Tau model used by Sonawane *et al.*, has been adopted for protein-protein docking [168]. The refined complex from Patchdock with the lowest global energy of -16.26 (binding score) was taken for md-simulation (**Fig. 3.4A**). From the model it was observed that the active region of HDAC6 ZnF UBP (R1155, Y1184 and other aromatic residues) interacts with residues from the hexapeptide region ($^{275}\text{VQIINK}^{280}$) and other specific residues of repeat-Tau [218] which was further analysed by molecular dynamics simulation.

3.5 Interaction study of HDAC6 ZnF UBP and repeat-Tau complex by md-simulations

The docked complex of HDAC6 ZnF UBP domain and repeat-Tau was examined by molecular dynamics simulation for a time scale of 50 ns. The stability of the complex, interacting residues and the type of interactions formed between the residues are analysed. The RMSD graph was plotted from the protein backbone (nm) of HDAC6 ZnF UBP, repeat-Tau and the complex with the corresponding time (ps) along the Y- and X-axis respectively and the stability of the complex was analyzed (**Fig. 3.4B**). From the graph, it is inferred the docked complex stabilized over the initial 15 ns and the stability was maintained with a deviation of ~ 0.4 nm between the initial and final structure over the 50 ns simulation. The fluctuation among the individual residues of Tau was calculated from the RMSF graph plotted with residues of Tau and the residual fluctuation (nm) on X and Y- axis respectively (**Fig. 3.4C**). The RMSF values of initial 10 ns (red) was quite stable when compared with the final 10 ns (green), which indicated that the residues were attaining instability over the simulation. The overall RMSF over the 50 ns timescale (black) also denoted that residues were destabilized with a maximum fluctuation 0.8-1.0 nm around Tau residues, 320-332. The radius of gyrate (Rg) of HDAC6 ZnF UBP, repeat-Tau and the complex were also plotted with Rg values and the corresponding time scale on the Y- and X-axis respectively (**Fig. 3.4D**). The Rg value of HDAC6 ZnF UBP was stable at ~ 1.3 nm throughout the simulation, which indicated the closed and compact nature of this protein. The Rg values of

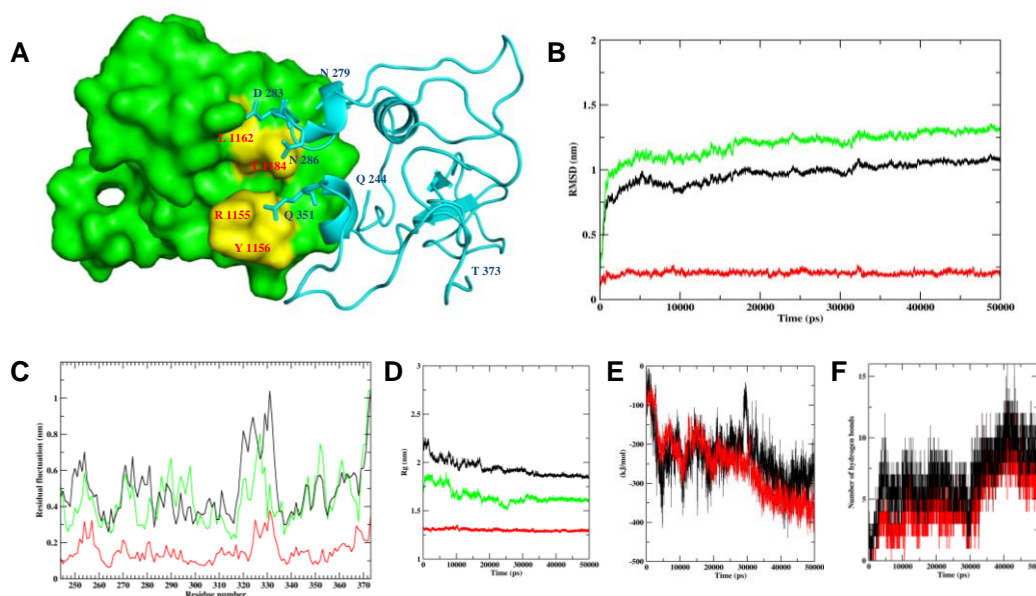


Fig. 3.4. Molecular docking and molecular dynamics simulation of HDAC6 ZnF UBP and repeat-Tau (244-373). A) Docked and refined complex of repeat-Tau 244-373 and HDAC6 ZnF UBP domain. [Green-HDAC6 ZnF UBP domain, Cyan blue-repeat Tau model (244-373), the active region of HDAC ZnF UBP highlighted in yellow] B) RMSD graph for HDAC6 ZnF UBP (red), repeat-Tau (green) and the complex (black) plotted with RMSD values (nm) and the corresponding time scale (ps) in the Y- and X-axis respectively. C) RMSF graph for Tau residues were plotted with residues on X- axis and the corresponding fluctuation (nm) on Y- axis. The residual fluctuation over the initial 10 ns (red), final 10 ns (green) and for the overall simulation, 50 ns (black) were plotted. D) Radius of gyrate (Rg) graph for HDAC6 ZnF UBP (red), repeat-Tau (green) and the complex (black) plotted with Rg values (nm) and

the corresponding time scale (ps) in the Y- and X-axis respectively. E) Energy graph plotted for Lennard-Jonnes (red) and Coulombic (black) interaction energy showing the hydrophobic and electrostatic energies of the interacting complex. The energy values and the corresponding time scale are plotted against Y- and X-axis respectively. F) Hydrogen bond analysis showing the number of hydrogen bonds formed between HDAC6 ZnF UBP and repeat-Tau (black) on Y-axis with the corresponding timescale on X-axis respectively. Hydrogen bonds formed by specific residues of HDAC6 ZnF UBP (Q1131, R1155, R1155/Y1184, N1158, Q1163 and Q1187) with repeat-Tau residues (N327/I328, D283, N286, E264/N265, I277/N279 and L282 respectively) are also plotted in the same graph (red).

Tau and the complex were quite high with more fluctuations at the initial time points and got minimized and stabilized during the second-half of the 50 ns simulation which indicated that Tau is attaining to form a closed and compact structure with HDAC ZnF UBP during the latter part of the simulation. The electrostatic and hydrophobic energies between the protein complexes were plotted to analyze the type of interaction. In order to determine the type of interactions occurring between the protein complexes, the electrostatic (Coulombic) and hydrophobic (LJ) energies between the proteins were plotted with energy values (KJ/mol) and the corresponding time (ns) on Y- and X-axis respectively (**Fig. 3.4E**). During the initial periods of simulation, both electrostatic and hydrophobic energies were dynamic and equally contributing with a steady and constant decrease in the energy after 30 ns towards the end of the simulation which indicated the possibilities for both bonded and non-bonded interactions. However, the hydrophobic energy was dominating over the electrostatics in the latter part of the simulation which denoted that non-bonded interactions are playing a major role in HDAC6 ZNF UBP – repeat-Tau interaction. Then the hydrogen bond analysis was performed to determine hydrogen bonding and the number of hydrogen bonds formed between the protein-protein complex (**Fig. 3.4F - black**). The number of hydrogen bonds and the corresponding time scale (ps) is plotted in the Y- and X-axis respectively.

For the residual interaction analysis, structures from the last 10 ns were examined and the residues involved in hydrogen bonding and hydrophobic interactions are plotted (**Fig. 3.5A**). From the data it has been inferred that the aromatic residues of HDAC6 ZnF UBP such as Y1156, Y1184, Y1185, W1182 and other residues such as T1138, Q1140, H1160 are involved in hydrophobic interactions with repeat-Tau residues such as V250, V275, Q276, V287, etc., The HDAC6 ZnF UBP residues Q1131, R1155, R1155/Y1184, N1158, Q1163 and Q1187 formed hydrogen bonds with residues N327/I328, D283, N286, E267/N268, I277/N279 and L282 of repeat-Tau respectively (**Fig. 3.5B**). The number of hydrogen bonds formed by these residues of HDAC6 ZnF UBP with repeat-Tau residues were individually analysed and plotted throughout

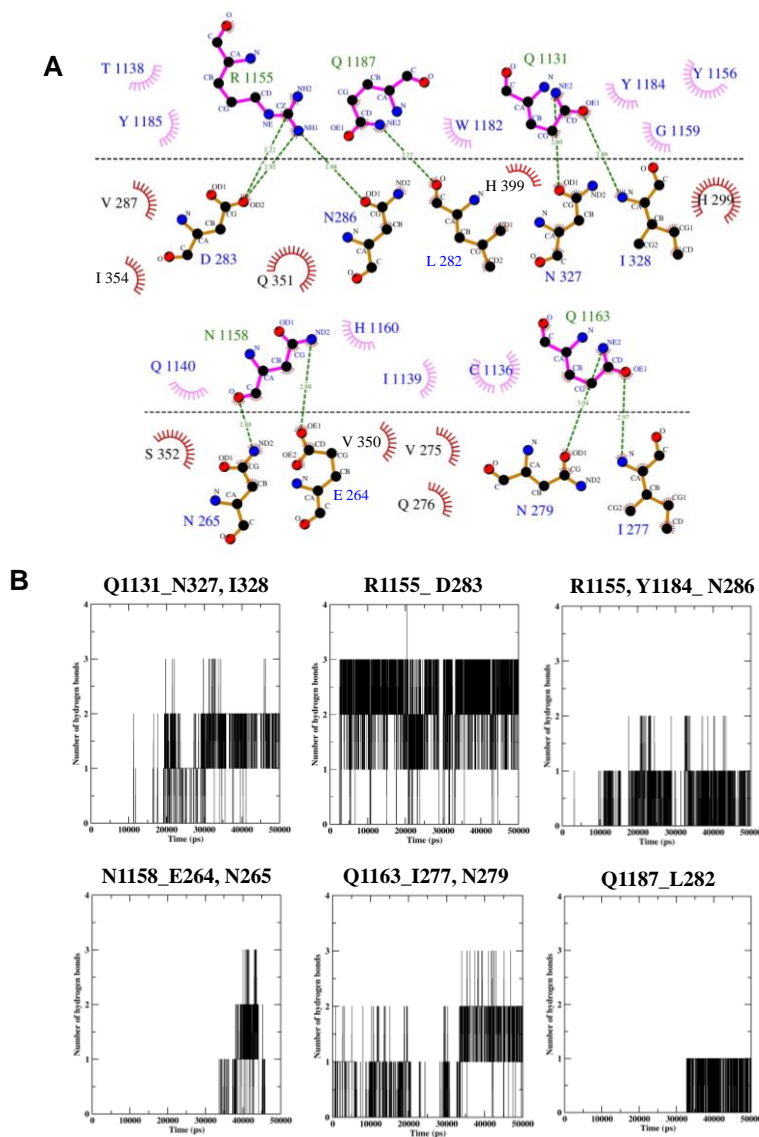


Fig. 3.5. Intermolecular interaction studies of HDAC6 ZnF UBP with repeat-Tau (244-373). A) Residues involved in the hydrogen bond and hydrophobic interactions were plotted using LigPlot+ (last 10ns of the md-simulation taken for analysis). B) Hydrogen bond analysis for specific residues of HDAC6 ZnF UBP (Q1131, R1155, R1155/Y1184, N1158, Q1163 and Q1187) with the repeat-Tau residues (N327/I328, D283, N286, E264/N265, I277/N279 and L282 respectively) were plotted as individual graphs.

the 50 ns simulation (**Fig. 3.5B**). The majority of hydrogen bond interactions from the complex were formed by these residues of HDAC6 ZnF UBP (**Fig. 3.4E - red**). The hydrogen bond analysis was also performed for specific residues of HDAC6 ZnF UBP that forms the binding site for C-terminal of ubiquitin and for specific residues of repeat-Tau such as hexapeptide ($^{275}\text{VQIINK}^{280}$) and other nearby residues of Tau [69, 218] (**Fig. 3.6A, B**).

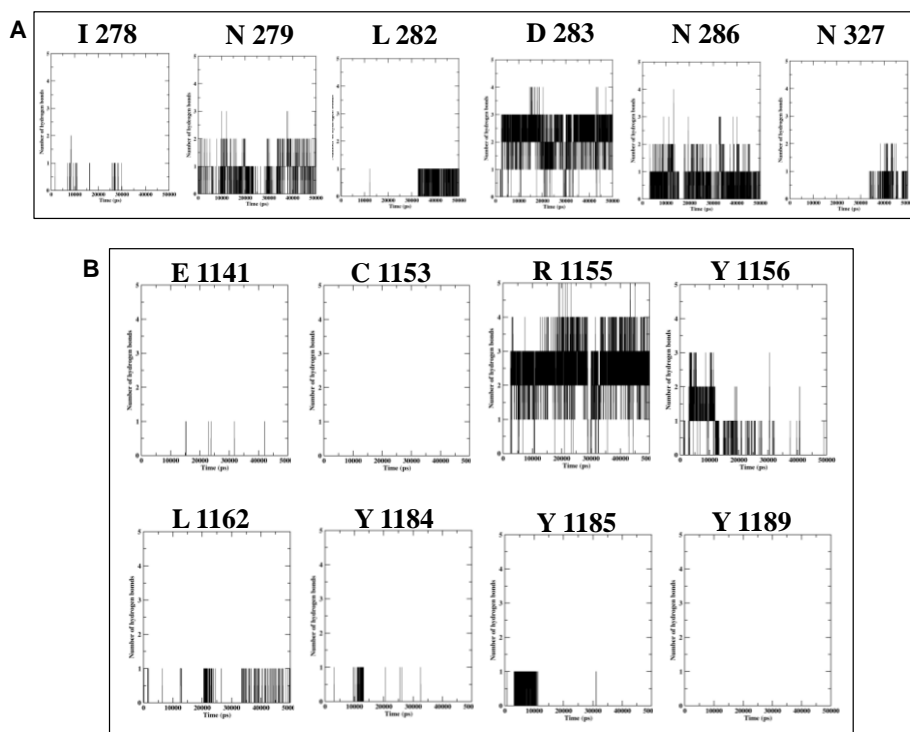


Fig. 3.6. Hydrogen bond analysis for Tau and HDAC6 ZnF UBP residues. A) Hydrogen bond analysis for specific residues of Tau (I278, N279, L282, D283, N286 and N327) with HDAC6 ZnF UBP (1109-1215). B) Hydrogen bond analysis for specific residues of HDAC6 ZnF UBP (E1141, C1153, R1155, Y1156, L1162, Y1184, Y1185 and Y1189) with repeat-Tau (244-373).

These data clearly suggest that the aspartic acid (D2883) - arginine (R1155) interaction occurs throughout the simulation supported by other interacting residues of Tau such as V275, Q276, I277 and N279 from the hexapeptide region and N286, which could possibly alter the aggregation propensity of Tau.

3.6 Degradation of monomeric Tau in the presence of HDAC6 ZnF UBP

Tau showed enhanced degradation in the presence of HDAC6 ZnF UBP in aggregation studies. To explore the possible implication of HDAC6 ZnF UBP on Tau degradation, we incubated soluble hTau40wt and HDAC6 ZnF UBP at 37 °C and analysed the degradation profile over a time course of 72 hours by SDS-PAGE and Western blot for total Tau. Tau and HDAC6 ZnF UBP were taken in equimolar concentrations for analysis by SDS-PAGE while HDAC6 concentration was varied for Western blot analysis. There was a marked difference in the degradation profile of Tau alone and Tau incubated with HDAC6 ZnF UBP at 72 hours as observed in SDS-PAGE (**Fig 3.7A, indicated by red star**).

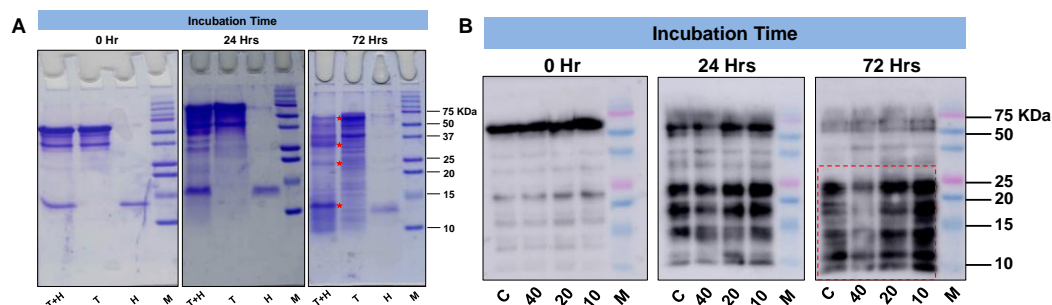


Fig. 3.7. HDAC6 ZnF UBP induced Tau degradation. A) SDS-PAGE analysis was carried out for monitoring Tau degradation upon incubation with HDAC6 ZnF UBP at 0, 24 and 72 hours at 37 °C. SDS-PAGE analysis showed the effect HDAC6 ZnF UBP on Tau degradation as compared to Tau incubated alone. Distinct degradation pattern of Tau can be observed for the HDAC6 incubated sample suggesting the role of HDAC6 ZnF UBP domain in Tau degradation. B) Western blot analysis for Tau degradation assay showed enhanced degradation after 72 hours of incubation. The degradation pattern of Tau did not show any significant difference up to 24 hours but was greatly increased at 72 hours.

The band corresponding to HDAC6 ZnF UBP begins to degrade over time but was found to be prominently stable in the presence of Tau. Thus, HDAC6 ZnF UBP was found to enhance Tau degradation while its own degradation was salvaged in presence of Tau. This suggests the possible interaction between HDAC6 ZnF UBP and Tau modulating the stability of both. In order to visualize the degradation pattern of Tau with HDAC6 ZnF UBP, both proteins were incubated in varying ratio and western blot analysis was carried out to examine primarily the degradation products of Tau. Tau degradation fragments were enhanced in Tau incubated with 10 μM HDAC6 ZnF UBP (2:1 ratio of Tau and HDAC6) (**Fig. 3.7B**). CD spectroscopy analysis of Tau incubated with HDAC6 ZnF UBP did not show significant spectral shift in Tau while HDAC6 ZnF UBP showed signature for α -helical structure (**Fig. 3.8A, B**).

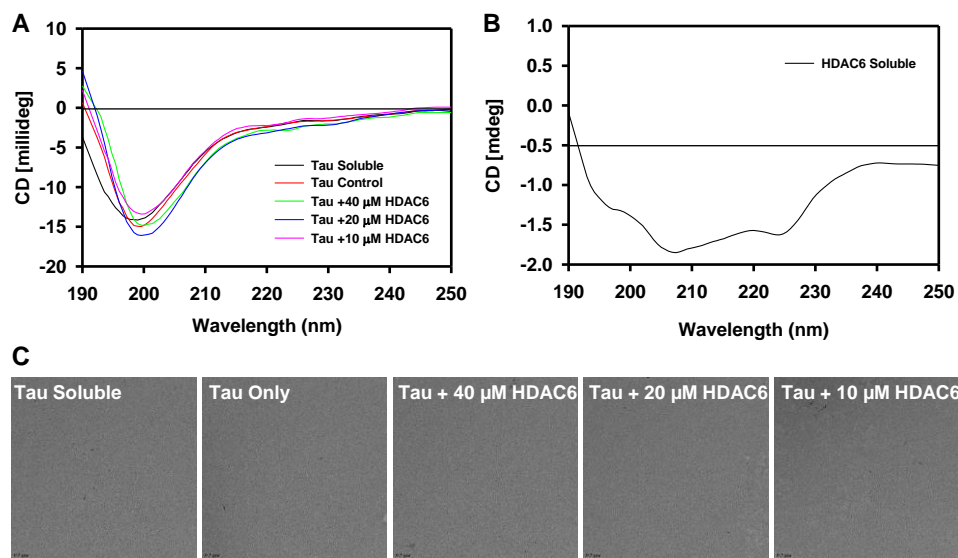


Fig. 3.8. Tau and HDAC6 interaction is not associated with any conformational changes. A) CD spectroscopy for samples obtained from degradation analysis at 72 hours did not show any significant change in natively

disordered conformation of Tau as indicated by the insignificant changes in wavelength maxima for respective samples. B) HDAC6 ZnF UBP gives a signature for α -helical conformation in CD spectroscopy. C) Electron micrographs taken at the end-point of Tau degradation assay showed absence of any morphological structure that would indicate formation of any higher order species mediated by HDAC6 ZnF UBP.

Table 3.1. Wavelength maxima for hTau40wt-HDAC6 ZnF UBP samples for degradation analysis.

Sample	Wavelength Maxima (nm)	CD (millideg)
hTau40wt Soluble	199	-15.0978
hTau40wt only	198	-15.5531
hTau40wt + 40 μ M HDAC6	200	-15.7816
hTau40wt + 20 μ M HDAC6	200	-16.8318
hTau40wt + 10 μ M HDAC6	199	-13.7485

The wavelength maxima for each sample taken for degradation analysis showed minimal shift in spectra and corresponded the random coil signature (**Table 3.1**). TEM analysis of samples from degradation assay showed no characteristic morphology in Tau samples incubated with HDAC6 ZnF UBP suggesting there was no formation of higher order species of Tau in its presence (**Fig. 3.8C**). However, the degradation of Tau did not depend on previously reported Cysteine-mediated catalytic mechanism [219] as hTau40 C291A C322A mutant showed increased degradation with HDAC6 ZnF UBP similar to hTau40wt (**Fig. 3.9A, B**). Cysteine residue may comprise a part of a catalytic diad or triad and mediates proteolytic cleavage *via* formation of thiol ester.

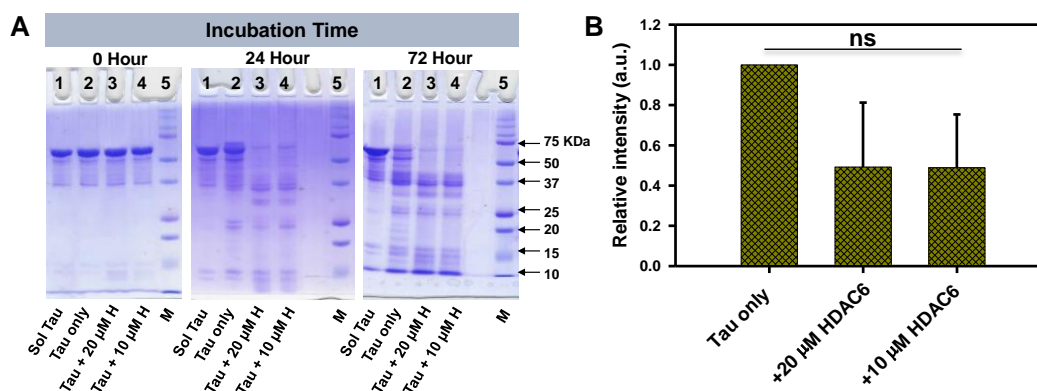


Fig. 3.9. Degradation analysis of hTau40 Cysteine double mutant by HDAC6 ZnF UBP. A) HDAC6 ZnF UBP was incubated with hTau40 Cysteine double mutant (C291A C322A) at 37 °C in order to assess its effect on Tau degradation. Degradation analysis for the time course of 72 hours showed enhanced degradation of Tau in HDAC6 ZnF UBP incubated samples (10 and 20 μ M HDAC6 ZnF UBP) compared to soluble Tau (Sol Tau) and Tau incubated alone (Tau only). Thus, cysteine residues do not mediate the degradation effect in presence of HDAC6 ZnF UBP. B) Quantitative analysis lanes at 72 hours showed remarkably higher degradation in HDAC6 ZnF UBP incubated Tau.

3.7 Summary

Tau stability is an important factor which determines its functional state. Tau has multiple interacting partners which modulate its structure and function either through interaction or PTMs. HDAC6 is known to interact with Tau through its catalytic domain and SE14 domain but the role of its ZnF UBP domain is limited regulation of aggresome pathway. Our studies suggest that HDAC6 ZnF UBP can interact directly with Tau protein and modulates its stability by triggering Tau degradation without affecting its conformation.

Chapter 4
Modulation of neuronal functions by
HDAC6 ZnF UBP

4.1 Background

Tau pathology is implicated in several neurodegenerative diseases including Alzheimer's disease, Parkinson's disease, Progressive supranuclear palsy, Pick's disease, Corticobasal degeneration and Post-encephalitic parkinsonism [185, 220]. In Alzheimer's disease, the structure and function of Tau protein is modified by various cellular and molecular factors such as oxidative stress, post-translational modifications and interaction with its binding partners [12]. This result in the accumulation of Tau protein aggregates as intracellular inclusion bodies called NFTs. The abnormal accumulation of Tau as NFTs affects various cellular processes including microtubule dynamics and intracellular transport mechanism-dependent on the cytoskeletal networks. Tau is a member of Microtubule-associated protein family which functions in maintaining the microtubule framework and dynamic instability of microtubule cytoskeleton.

The proteins upon misfolding are either refolded by chaperones or targeted for degradation *via* ubiquitin proteasomal system [221, 222]. Upon failure of UPS, the aggregates are directed towards the formation of aggresomes [222, 223]. HDAC6 is a class II histone deacetylase mainly present in the cytoplasm involved in the regulation of various cellular functions. It consists of two catalytic deacetylase domains and a unique ZnF UBP domain, which sets it apart from other HDACs [224]. In case of disruption of UPS, aggregates are directed towards the formation of aggresomes, which serves as the cytoprotective response upon the failure of UPS [223]. One of the major functions of HDAC6 is primarily involved in recruiting the polyubiquitinated protein aggregates to Dynein/Dynactin complex and sequestering them to MTOC in the perinuclear region for aggresome formation. The function of HDAC6 in both UPS and autophagy indicate its role as a possible link between the two mechanisms [225, 226]. The impairment of UPS function acts as a cue for the activation of a compensatory mechanism for the clearance of protein aggregates. It has been studied in the *Drosophilla* model of spinobulbar muscular atrophy, where expression of HDAC6 has been found to effectively cause rescue from UPS impairment induced neurodegeneration by triggering the autophagic clearance of protein aggregates [71]. In another study, HeLa cells transfected with PolyQ Huntingtin forms intracellular protein aggregates, which require HDAC6 for autophagic clearance after inhibition of proteasomal system [227]. Overall, the function of HDAC6 with respect to protein aggregate clearance and autophagy induction serves as a protective mechanism. The HDAC6 expression level increases sharply in protein misfolding diseases [111].

Phosphorylation is a well-studied PTM of Tau responsible for its conversion to pathological form in AD condition [228]. Alzheimer's disease is associated with the upregulation of cellular kinases-like GSK-3 β and CDK5 [131]. GSK-3 β is one of the major kinase involved in Tauopathies [229]. Tau is phosphorylated by GSK-3 β on both primed (after pre-phosphorylation) and unprimed sites and affects its ability to bind and stabilize microtubules [230]. Many serine and threonine residues in repeat region of Tau have been mapped and assigned to be phosphorylated by proline-directed kinases [231]. On the other hand, protein phosphatases-like PP1 and PP2A are known to be downregulated in AD failing to reverse the effect of

hyperphosphorylation [232-234]. Thus, there is an imbalance between the kinase and phosphatase function in neurons. We have studied the role of HDAC6 ZnF UBP domain (**Fig 4.1A**) on phospho-Tau epitopes-pT181 and AT8 as well as level of total and downregulated form of GSK-3 β . HDAC6 ZnF UBP was found to lower both phospho-epitopes and promoted GSK-3 β downregulation. We hypothesize the effect of HDAC6 ZnF UBP through a mechanism involving PP1 and Akt. Neurodegenerative diseases also involve the mis-functioning of its cytoskeletal elements leading to various functional and structural aberrations. Microtubule network and actin organization were found to be distorted leading to impaired cellular trafficking and other associated functions [235, 236]. Actin organization is crucial for synaptic signalling in neurons where they are involved in the formation of dendritic spines for neurotransmission.

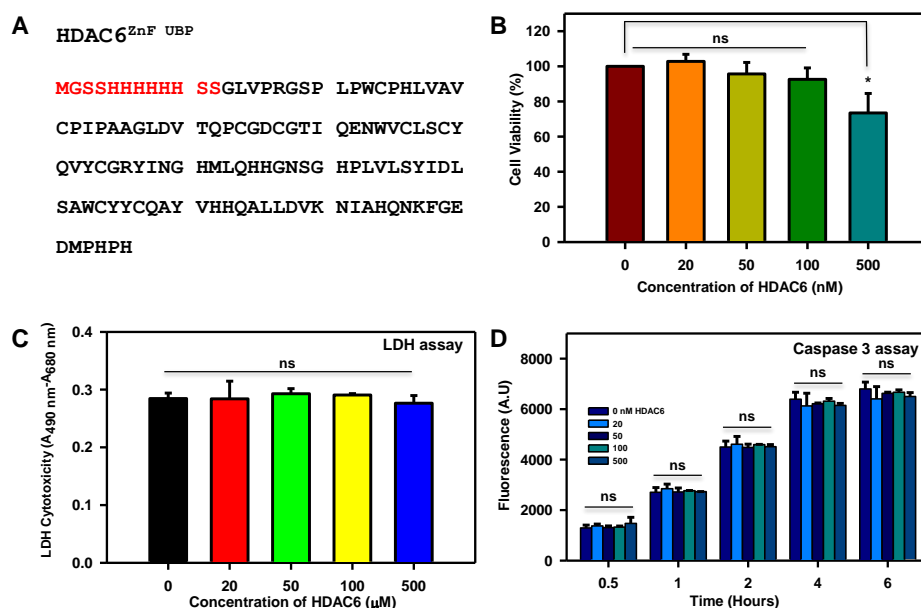


Fig. 4.1. HDAC6 ZnF UBP treatment to neuro2a cells is non-toxic. A) Amino acid sequence of human HDAC6 Zinc finger ubiquitin-binding domain located on the C-terminal of HDAC6, which associates with polyubiquitinated protein, aggregates to mediate the formation of aggresomes. B) MTT assay was carried out to determine the viability of neuro2a upon HDAC6 ZnF UBP treatment. Neuroblastoma cells treated with HDAC6 at different concentrations show minimum toxicity and maintain viability at 80% at highest concentration of 500 nM. C) LDH release assay determines the damage to the cell membrane upon exposure to test molecule. The membrane leakage assay (LDH assay) shows that HDAC6 does not disrupt the cell membrane and affect cell viability. D) Apoptosis rate of neuro2a cells upon HDAC6 ZnF UBP treatment was assayed using Caspase-3 assay. Caspase-3 assay shows increased levels of caspase-3 with successive time interval but do not differ from control samples. Statistical significance determined by two-tailed unpaired t-test. (n.s. – non-significant, * indicates $P \leq 0.05$, ** indicates $P \leq 0.01$, *** indicates $P \leq 0.001$).

Impaired actin assembly and depolymerization leads to loss of dendritic spines ultimately causing neuronal death [237, 238]. Actin dynamics is important in the formation of actin rich structures employed in various functions such as cell migration, invasion and attachment. These include podosomes, filopodia and lamellipodia which are distinguished by their characteristic morphology. HDAC6 is a key protein in the regulation of both actin and microtubule organization through its deacetylase activity [239]. HDAC6 acts on cortactin and mediates its

association with F-actin to facilitate cell motility [198]. In the present study, we studied the role of HDAC6 ZnF UBP domain in modulating cytoskeletal assembly independent of its catalytic domain. The localization of ApoE either in cytoplasm or nucleus serves as an indicator of neuronal health. Nuclear localization of ApoE is associated with increased neuronal survival. Enhanced ApoE nuclear localization was observed in neurons in the presence of HDAC6 ZnF UBP. HDAC6 ZnF UBP can promote ApoE nuclear localization in HSP90 and nucleolin mediated manner.

Overall, HDAC6 ZnF UBP domain was found to affect actin and tubulin organization, Tau phosphorylation and localization of ApoE in neuronal cells. Enhancement in podosome and lamellipodia-like structures were found when neuronal cells were exposed to HDAC6 ZnF UBP domain suggesting its direct role in actin organization. HDAC6 ZnF UBP treatment also resulted in enhanced tubulin localization in MTOC indicating its possible role in tubulin polymerization events. Our findings suggest the role of HDAC6 ZnF UBP as the direct modulator of Tau phosphorylation and cytoskeletal dynamics.

4.2 HDAC6 ZnF UBP is non-toxic and non-apoptotic

Neuronal cells were exposed to HDAC6 ZnF UBP exogenously to observe the effect on different cellular functions. In order to study the effects of HDAC6 ZnF UBP, a minimum toxic dose was determined by viability assay as well as membrane leakage assays. Neuronal cells were treated with a range of concentrations of HDAC6 ZnF UBP (20-500 nM). The cell viability carried out by MTT assay showed no decrease in viability. The cell viability was maintained at 80% even in highest HDAC6 ZnF UBP concentration of 500 nM (**Fig.4.1B**). Similarly, LDH assay was carried out to check the effect of HDAC6 on membrane integrity in terms of LDH release. Neuronal cells showed intact membrane integrity when treated with HDAC6 ZnF UBP in 20-500 nM concentration range (**Fig.4.1C**). Thus, HDAC6 ZnF UBP did not show toxicity in neuroblastoma cells. Further to confirm the non-toxic nature of HDAC6 ZnF UBP in neuronal cells we studied the apoptosis on treatment with HDAC6 ZnF UBP by caspase-3 assay. Cells undergo apoptosis under stressful conditions-mediated by endoproteases called caspases [240]. Caspase-3 is an executioner caspase responsible for DNA fragmentation and degradation of cytoplasmic proteins [241]. The caspase-3 assay showed basal level of activity in all the treated and control samples. No difference was observed in the HDAC6 ZnF UBP treated and untreated control samples in terms of cell viability, suggesting that HDAC6 ZnF UBP treatment do not induce apoptosis in the neuro2a cells (**Fig.4.1D**). The preliminary studies on cell viability and morphology inferred that HDAC6 ZnF UBP treatment do not show cytotoxic effect on neuro2a cells. The HDAC6 internalization was monitored for 20-500 nM concentrations by immunostaining for HDAC6 and anti-His-tag (**Fig. 4.2**). In further experiments, the cells were treated with a moderate concentration of 50 nM HDAC6 ZnF UBP for subsequent experiments unless stated otherwise.

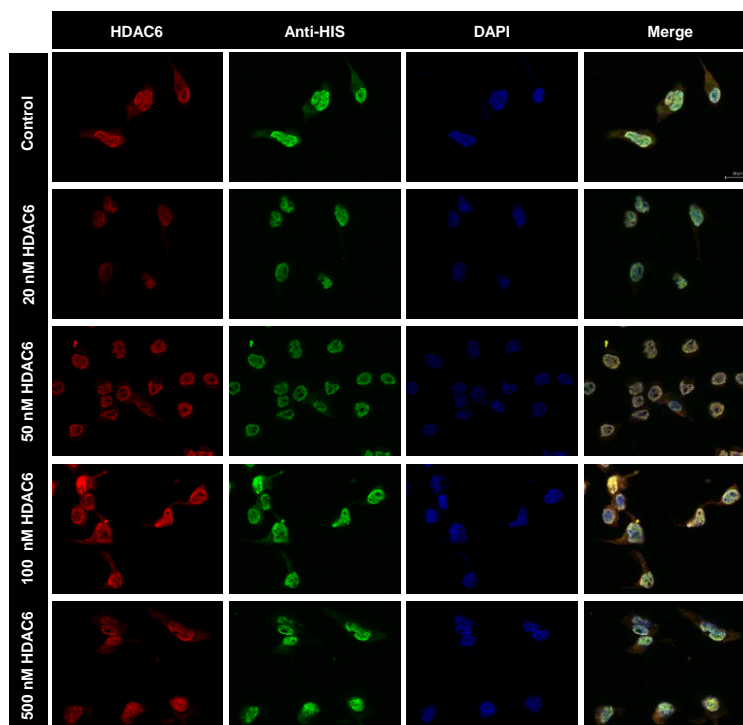


Fig. 4.2. Internalization of HDAC6 ZnF UBP in neuro2a. Neuro2a cells treated with HDAC6 ZnF UBP (20-500 nM) were mapped by antibody against HDAC6 and anti His-tag antibody to determine the internalization of 14 KDa HDAC6 ZnF UBP domain in cells. HDAC6 ZnF UBP was found to be internalized in neuro2a cells at all concentrations and 50 nM concentration was chosen for further studies.

4.3 HDAC6 ZnF UBP enhances levels of pGSK-3 β

The level of GSK-3 β in its phosphorylated and non-phosphorylated form determines its activity as a kinase. GSK-3 β is known to associate with HDAC6 to counteract its function to induce LPS-tolerance in astrocytes [242]. We mapped GSK-3 β and pGSK-3 β (pSer9) levels by immunofluorescence in neuronal cells in basal conditions and upon HDAC6 ZnF UBP treatment (No. of fields selected for quantification of pT181 and AT8, n = 5). There was no marked difference in level of GSK-3 β in HDAC6 treated and untreated cells (**Fig.4.3A**). However, immunofluorescence analysis of HDAC6 ZnF UBP treated cells showed significant increase in the pGSK-3 β levels (**Fig.4.3B**). GSK-3 β function in cells is regulated mainly by inhibitory phosphorylation at ser9 or ser21. The kinase activity of GSK-3 β is reduced with phosphorylation at ser9 as it affects the binding of primed substrates with GSK-3 β . The increase in pGSK-3 β in neuronal cells signifies the reduced GSK-3 β activity on primed Tau substrate [243]. HDAC6 ZnF UBP exposed to the cells resulted in increased levels of pGSK-3 β (Ser9), which suggests reduced Tau phosphorylation.

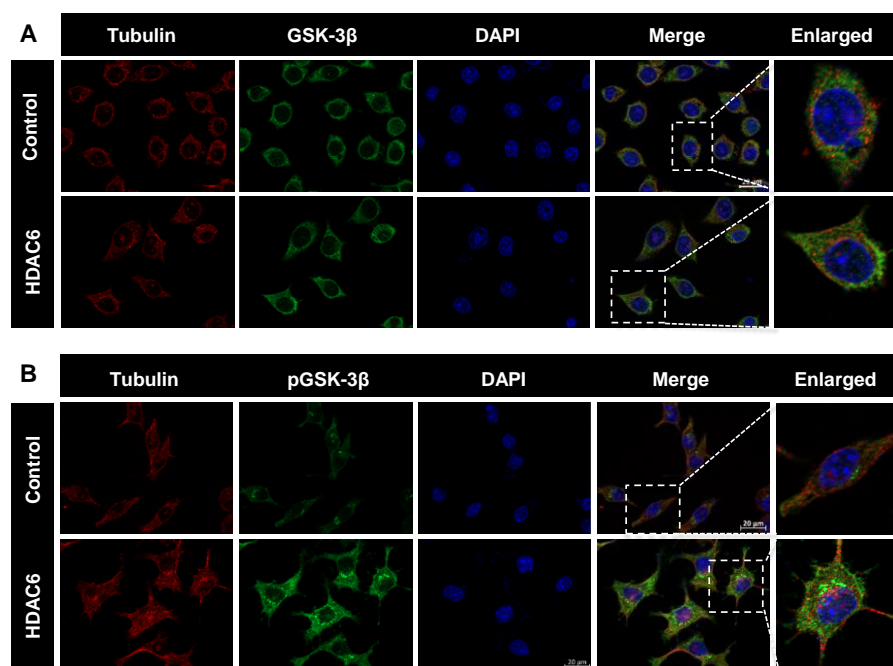


Fig. 4.3. Downregulation of GSK-3 β activity by HDAC6. The levels of GSK-3 β and pGSK-3 β reflect its activity in the cell. Enhanced levels of pGSK-3 β were observed while total GSK-3 β remained unaltered upon the treatment of HDAC6 ZnF UBP domain. A) Neuro2a mapped for total GSK-3 β shows their unaltered levels upon HDAC6 ZnF UBP. B) The activity of GSK-3 β is governed by phosphorylation at specific residues which either upregulates or downregulates its activity. Inhibitory phosphorylation of GSK-3 β at Ser9 increases upon HDAC6 ZnF UBP treatment. The enlarged image shows the elevated level of pGSK-3 β compared to neuro2a cell control.

4.4 HDAC6 ZnF UBP reduces Tau phosphorylation in neuronal cells

Tau phosphorylation is the key event in the pathogenesis of Alzheimer's disease. Tau phosphorylation is required for its function in microtubule interaction and stabilization. Under pathological conditions Tau becomes hyperphosphorylated due to imbalance in kinase and phosphatase level or activity [244]. Okadaic acid (OA) was used as an inducer of hyperphosphorylation as it inhibits protein phosphatase 2A (PP2A), thus increasing the overall phosphorylation level [245]. Untreated control cells and HDAC6 ZnF UBP treated cells alone showed basal levels of phospho-Tau at epitopes pT181 and pS202/T205 (AT8). The levels of pT181 were increased in OA treated cells. Cells supplemented with HDAC6 ZnF UBP with OA showed lower levels of phospho Tau at T181 as compared to positive control (**Fig. 4.4A**). Tau phosphorylated at pT181 was dominantly seen in the nucleus especially in the positive control (enlarged images). Similar results were observed for phospho Tau epitope AT8. The enlarged images clearly show the increased levels of phospho-AT8 in positive control as compared to OA+HDAC6 ZnF UBP treatment (**Fig. 4.5A**). pT181 and AT8 are two of the crucial epitopes of pathological Tau in AD. HDAC6 ZnF UBP treatment lowered down the level of these two phospho-epitopes suggesting its possible role in modulating Tau phosphorylation.

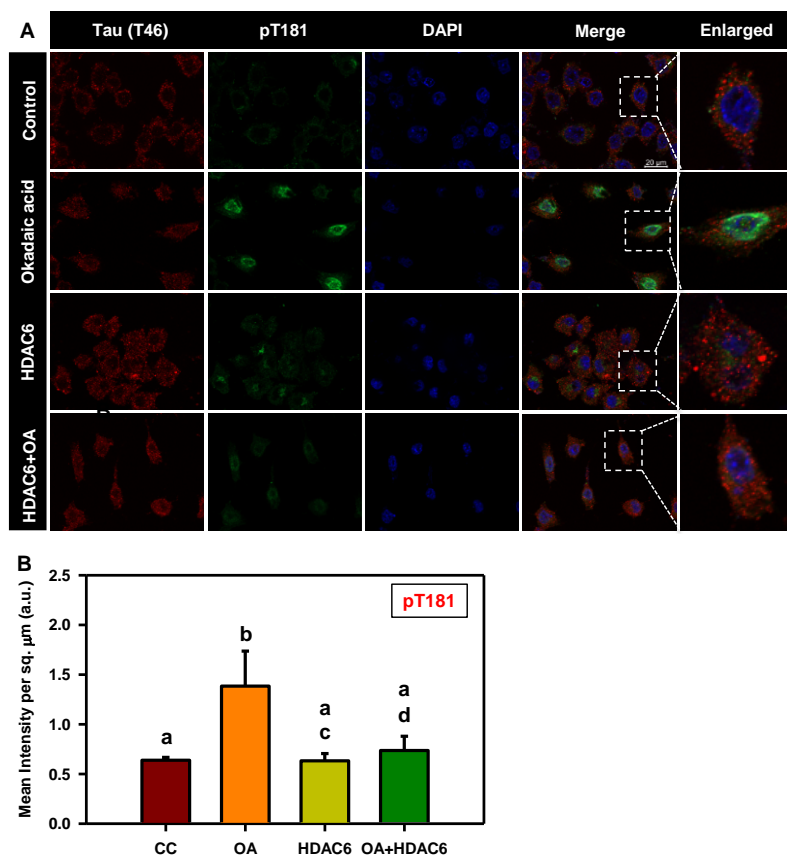


Fig. 4.4. Inhibition of Tau phosphorylation (pT181) by HDAC6. A) Neuro2a cells treated with okadaic acid (OA) enhanced overall phosphorylation by inhibition of PP2A. Tau phosphorylations at pT181 epitope of Tau was mapped after 25 nM OA treatment alone as well as in simultaneous treatment with 50 nM HDAC6 ZnF UBP to observe the effect on Tau phosphorylation. HDAC6 treatment for 24 hours along with OA shows inhibition of Tau phosphorylation at pT181 epitope whereas OA treatment shows increased phosphorylation at pT181. HDAC6 ZnF UBP treatment resulted in reduced AT8 level, which is evenly distributed throughout the cell as opposed to more localized presence in OA cells. B) Mean fluorescence intensity for pT181 in different treatment groups showed decreased levels of pT181 in HDAC6 ZnF UBP treatment (HDAC6) and HDAC6 ZnF UBP treatment along with okadaic acid. Significant at mean difference $> T$ (Tukey's criterion) and $\alpha = 0.05$. Groups with the same letters are not significantly different. The value of T is calculated as 0.365 for pT181 quantification.

The level of both phospho-tau epitopes (pT181 and AT8) was quantified by their immunofluorescence levels in different experimental groups (No. of fields selected for quantification of pT181 and AT8, $n = 5$). Untreated cells (CC) showed no significant difference from HDAC6 treated or OA+HDAC6 treated in pT181 immunostaining. OA treatment resulted in increased pT181 levels, which was found to be reduced with HDAC6 ZnF UBP treatment (Fig. 4.4B). Similar results were obtained for quantification of AT8 immunostaining. HDAC6 ZnF UBP treatment along with OA reduced AT8 level, bringing it down similar to untreated cells (CC) when compared to OA alone treatment group. AT8 levels were also found to be lesser in HDAC6 ZnF UBP treatment as compared to untreated (Fig. 4.5B). Quantification data was

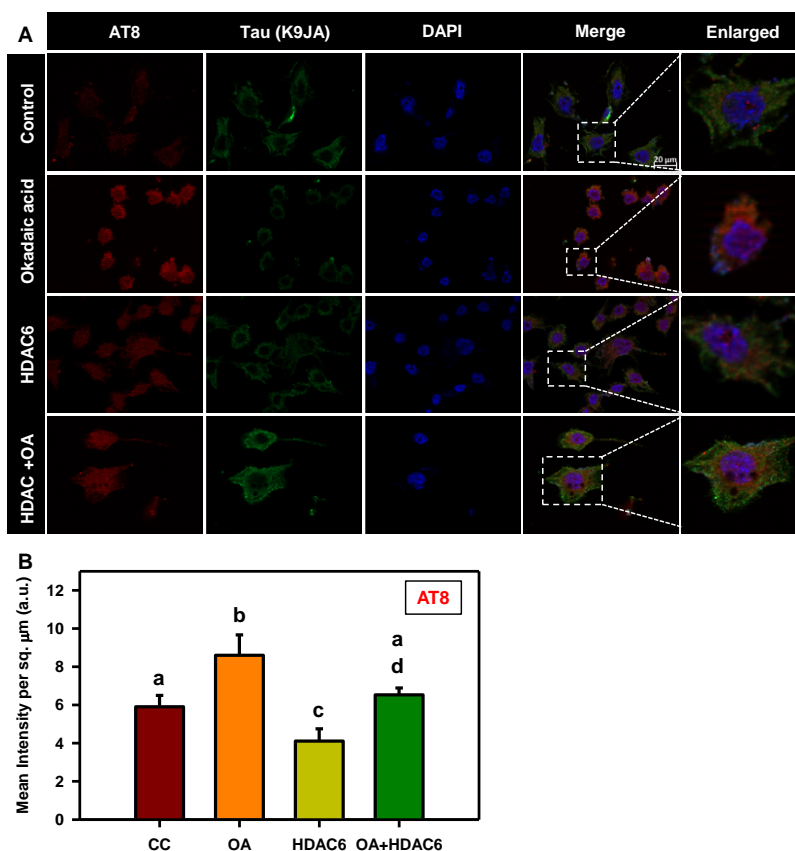


Fig. 4.5. Inhibition of Tau phosphorylation (AT8) by HDAC6. A) Phosphorylation at AT8 epitope is also reduced in presence of HDAC6 ZnF UBP along with OA as compared to OA alone. The enlarged image of neuro2a treated with OA alone and OA along with HDAC6 ZnF UBP shows marked difference in the level of phosphorylation at pT181 and AT8 epitopes. OA treatment resulted in increased AT8 levels, which is more localized into nucleus. OA treatment along with HDAC6 ZnF UBP significantly lowered AT8 level with its overall even distribution in neuronal cells. B) AT8 levels were increased upon OA treatment while it was found to be significantly reduced in HDAC6 ZnF UBP treatment along with okadaic acid. Significant at mean difference $> T$ (Tukey's criterion) and $\alpha = 0.05$. Groups with the same letters are not significantly different. The value of T is calculated as 1.341 for AT8 quantification.

analyzed by one-way ANOVA followed by Tukey's HSD test (significant at $\alpha = 0.05$). The statistical significance is calculated with respect to Tukey's criterion (T). The groups with the same letters show no significant difference.

4.5 HDAC6 ZnF UBP modulates actin dynamics

Actin organization and dynamics is crucial for cell shape and migration in respective cell types. In neuronal cells, actin dynamics is important for cell-to-cell communication through regulating neurite extension. Actin assembly and dynamics requires complex machinery and nucleating factors [246, 247]. In neurodegenerative diseases, the regulation of actin dynamics gets impaired resulting in loss of synapses and dendritic spines [248]. HDAC6 is known to modulate actin organization through its association and deacetylase activity on cortactin and arp2/3 complex [198, 246, 247]. The function of HDAC6 ZnF UBP domain in actin dynamics is not yet

understood. Our present observations showed HDAC6 ZnF UBP treatment lead to increase in neuritic extensions in neuro2a cells. We mapped HDAC6 ZnF UBP treated cells with FITC-Phalloidin to observe the F-actin cytoskeleton. We studied actin organization along with Tau and it was observed that HDAC6 ZnF UBP treatment had no effect on Tau levels but the actin cytoskeleton changed significantly (**Fig. 4.6A**). Further, to check for HDAC6 localization on treatment, we mapped actin with HDAC6 ZnF UBP. The control cells showed a normal F-actin cytoskeleton in the extensions but HDAC6 treated cells showed presence of actin along with HDAC6 in these extensions (**Fig. 4.6B**). As previously observed, HDAC6 ZnF UBP treated cells showed more neuritic extensions and dense actin cytoskeleton. Tau and actin are known to co-localize in neuritic extensions in previous studies where they facilitate growth cone transition [249]. Greyscale images for actin immunostaining shows localization in neurite extensions and growth cones in filopodia-like structures (**Fig. 4.6C, D**).

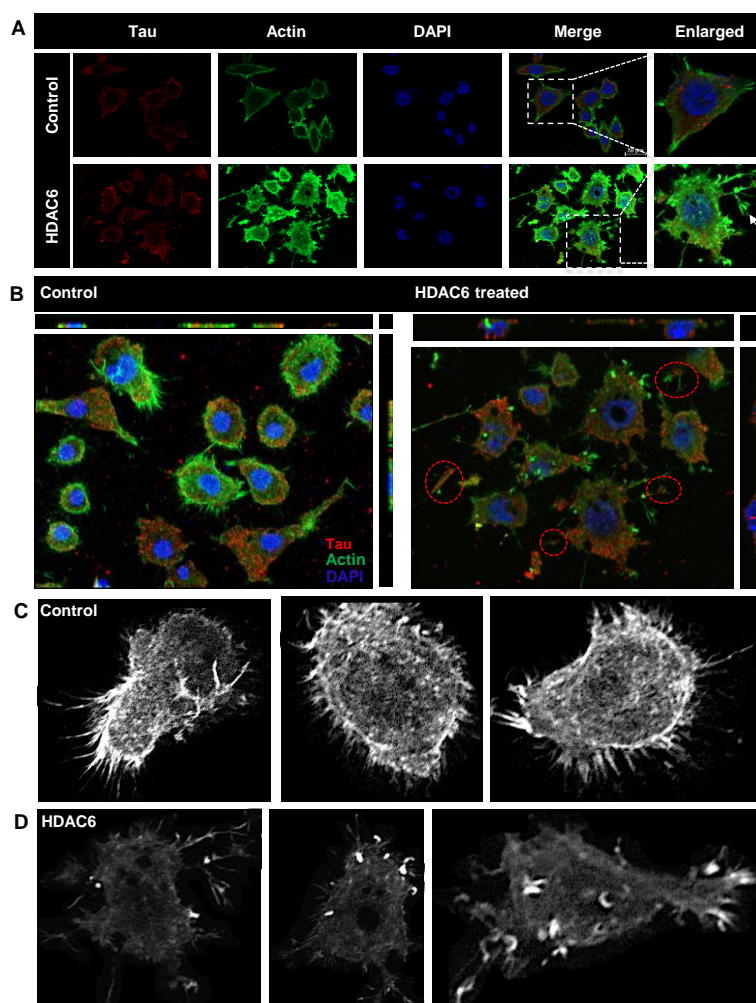


Fig. 4.6. HDAC6 ZnF UBP as a modulator of actin dynamics. HDAC6 deacetylase activity is known to modulate actin dynamics. The effect on actin dynamics was studied after exposure to HDAC6 ZnF UBP domain. HDAC6 ZnF UBP treatment to neuro2a resulted in enhancement of neurite extensions which are mapped by F-actin staining. A) HDAC6 ZnF UBP treatment for 24 hours increases the neuronal extensions as compared to untreated control cells when the extensions are mapped by actin immunostaining. The Tau levels remain unaltered in both the groups. B)

The orthogonal projection shows the increase in number of neurites in the HDAC6 ZnF UBP treated cells. C) Greyscale images for untreated neuro2a cells mapped for F-actin showed small extensions in the growth cones. D) In HDAC6 ZnF UBP treated cells, F-actin containing longer extensions were observed. Growth cones were observed to be concentrated in membrane extensions and filopodia-like structures.

4.6 Enhancement of podosome-like structures by HDAC6 ZnF UBP

Podosomes are actin based structures involved in the remodeling of extracellular matrix (ECM) and cell migration while podonuts consists of a cluster of podosomes interacting with ECM [250]. It consists of an actin-rich core surrounded by actin regulatory molecules-like cortactin and arp2/3 as well as cell adhesion molecules-like Talin and Vinculin [251]. Neuro2a cells were incubated with 50 nM HDAC6 ZnF UBP on 18 mm coverslips for 24 hours prior to immunostaining preparation. Immunostaining showed the localization of actin in the membrane ruffles in HDAC6 ZnF UBP treated cells. Morphological changes in neuronal cells were observed when treated with HDAC6 ZnF UBP. HDAC6 ZnF UBP treated cells showed increased membrane ruffles and podosome-like structures. We observed minimal neuritic extensions in untreated neuro2a as compared to treated cells (**Fig. 4.7A**). Actin localization was observed mostly along the cell periphery in untreated neuro2a while it was focused in the neurite extensions and protruding podosome structure in HDAC6 ZnF UBP treated cells (**Fig. 4.7B**). Orthogonal sections were taken to clearly visualize the actin extensions and podosome formation. The initial orthogonal sections showed numerous extensions and actin localized in tip of the extensions in HDAC6 ZnF UBP treated cells as compared to control (**Fig. 4.7C, D**). Involvement of podosomes in cell adhesion and migration is an important attribute of invasive cells. Neuro2a can form podosomes which functions in cell migration and attachment. In contrast to untreated control neuronal cells (**Fig.4.8A, B, C**), HDAC6 ZnF UBP treated cells showed enhanced cell extensions and actin-rich structures similar to podosomes formed in migrating and invading cells. HDAC6 treated cells showed a variety of actin-based membrane protrusions, which can be morphologically classified as filopodia or lamellipodia, podosomes and podonuts (**Fig. 4.8D-J**). The neuritic extensions and podosomes were quantified in untreated control cells (CC) and HDAC6 treated cells. The neurites and podosomes were counted manually in random multiple fields for untreated control and HDAC6 treated group (No. of fields, n = 6 and 5 for neurites and podosomes respectively). HDAC6 ZnF UBP treated cells showed significantly enhanced neurite extensions and podosomes compared to untreated cells implicating its effect on actin dynamics and re-organization (**Fig. 4.8K, L**). Statistical significance of control and HDAC6 treated cells was analyzed by two-tailed unpaired student t-test.

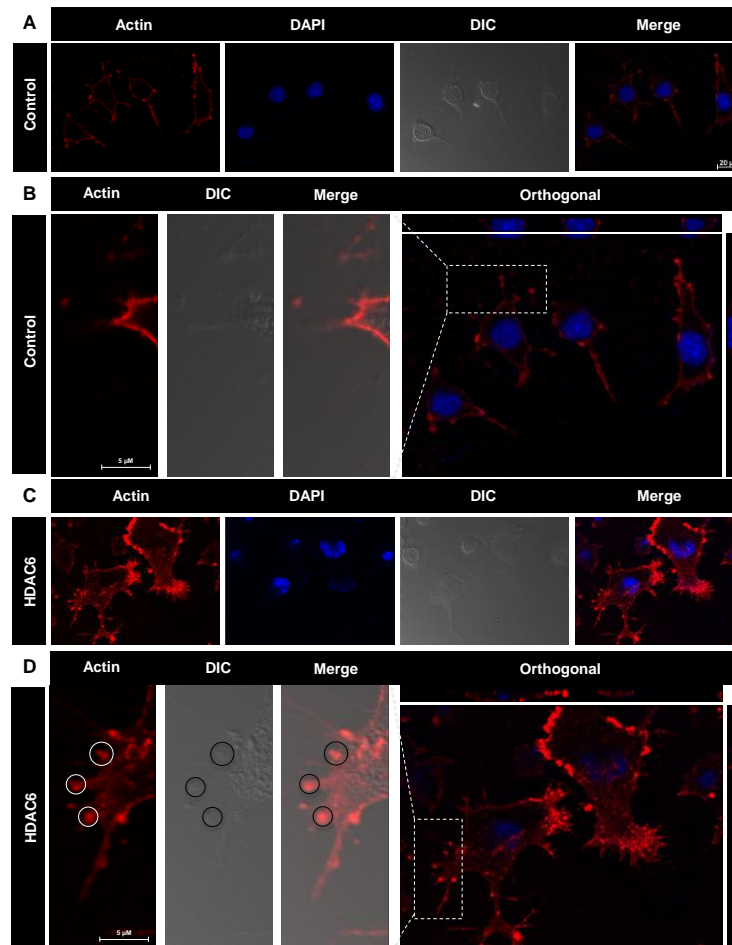


Fig. 4.7. Enhancement of podosome formation by HDAC6. HDAC6 deacetylase activity is known for regulating the actin dynamics in cells and podosome formation. Structures resembling podosomes and podonuts were observed in neuro2a upon HDAC6 ZnF UBP treatment. Podosomes and podonuts are actin-rich structures involved in cell attachment and migration. A) Podosomes marked by the actin-rich structures along plasma membrane, were observed in neuro2a cells at a minimal level. B) Enhancement in podosome-like structures observed in HDAC6 ZnF UBP treated cells. Orthogonal projection images showed marked difference in the membrane morphology and actin concentrated in membrane ruffles and podosome-like structures in HDAC6 ZnF UBP treated cells. C) HDAC6 is found to be present in the neuritic extensions along with actin suggesting its role in regulation of neurite extensions. This is not seen in case of untreated cells as indicated in the enlarged images for both groups. D) In HDAC6 ZnF UBP treated cells, F-actin containing longer extensions were observed. Growth cones were observed to be concentrated in membrane extensions and filopodia-like structures.

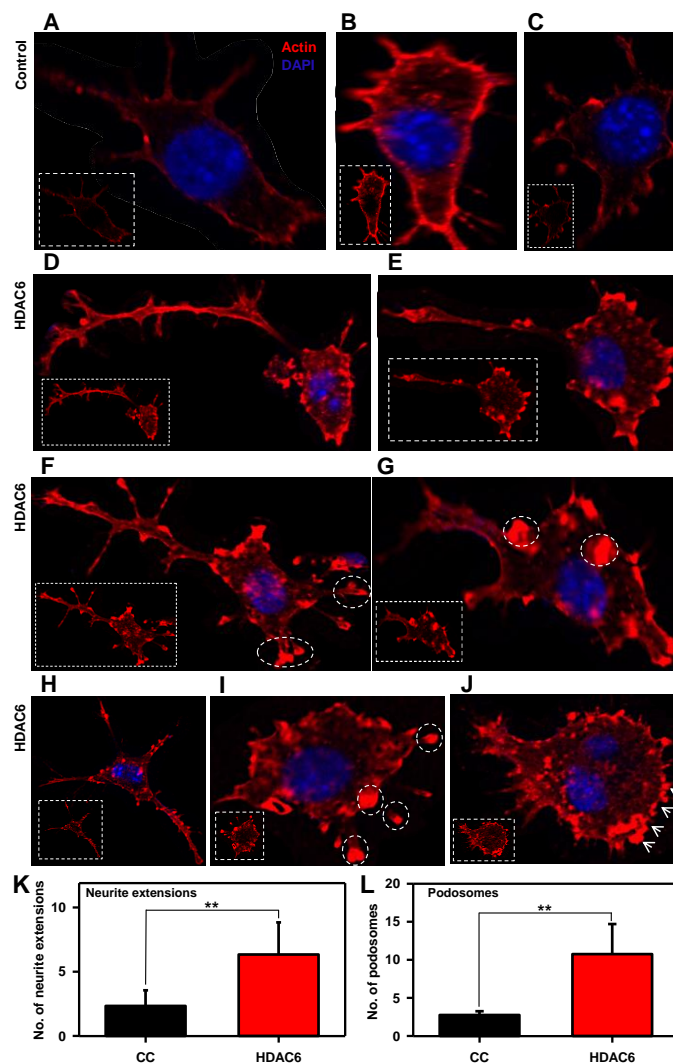


Fig. 4.8. Podosome, lamellipodia and podonut-like structure-induced by HDAC6 ZnF UBP. Neuro2a cells exposed to HDAC6 ZnF UBP exhibit a variety of actin-rich structures characteristics of migratory or invading cells. A, B, C) Untreated neuro2a cells showed actin uniformly distributed along the periphery with smaller neuritic extensions as compared to D, E) HDAC6 ZnF UBP treated cells which showed longer extensions and membranes ruffles resembling podosomes and filopodia involved in cell migration. F, G) Invadopodia and lamellipodia-like structures (encircled) were also observed, which are found in phagocytic cells. H, I, J) Most of the treated cells were observed to consist of assemblance of podosomes (encircled) and podosome clusters called podonuts (white arrow) rich in actin. K) The overall neurite extensions in neuro2a cells were counted in untreated and HDAC6 treated group in β -actin immunostained cells. The number of extensions in HDAC6 treated cells were found to be greatly enhanced compared to untreated group. L) The podosomes formed after HDAC6 ZnF UBP treatment were quantified by counting the podosome crown structures in both untreated and treated groups. HDAC6 ZnF UBP treated cells showed more podosome clusters signifying its actin modulating effect. Statistical significance determined by two-tailed unpaired t-test. (n.s. – non-significant, * indicates $P \leq 0.05$, ** indicates $P \leq 0.01$, *** indicates $P \leq 0.001$).

4.7 HDAC6 ZnF UBP enhances ApoE nuclear localization

ApoE functions mainly as a lipid carrier in central nervous system where it delivers cholesterol to neurons *via* ApoE receptors following neuronal injury [252]. ApoE can be localized to

nucleus and carries out induction of gene expression involved in inflammatory response. ApoE is the major apolipoprotein of central nervous system, produced primarily by astrocytes. ApoE is taken up by neurons where it plays important role in membrane maintenance and repair [253].

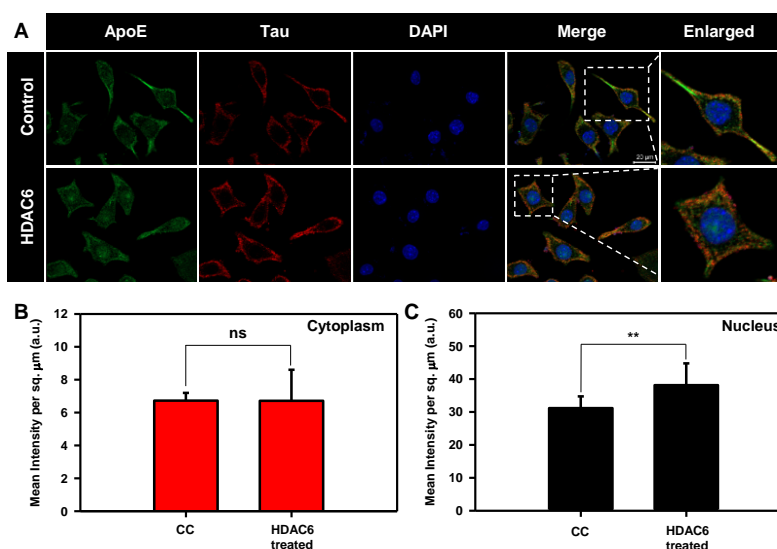


Fig. 4.9. Modulation of ApoE and Tubulin localization by HDAC6. Cells were mapped for ApoE to observe its level and localization. Enhanced nuclear localization of ApoE was observed with HDAC6 ZnF UBP treatment. HDAC6 ZnF UBP also affected the tubulin distribution where the treated cells showed more tubulin localization in MTOC compared to untreated cells where tubulin was evenly distributed. A) Immunofluorescence mapping for ApoE and Tau upon HDAC6 treatment in neuro2a cells shows increased nuclear localization of ApoE. B, C) ApoE intensity in nucleus and cytoplasm was quantified for untreated and HDAC6 ZnF UBP treated neuro2a immunostained with anti-ApoE antibody. There was no significant difference in cytoplasmic level of ApoE in both groups while the nuclear ApoE fraction was notably increased in HDAC6 ZnF UBP treated cells. Statistical significance determined by two-tailed unpaired t-test. (n.s. – non-significant, * indicates $P \leq 0.05$, ** indicates $P \leq 0.01$, *** indicates $P \leq 0.001$).

In normal physiological conditions, ApoE is localized in cytosol. ApoE nuclear localization has been reported in ovarian cancer cells, where it leads to better survival possibly through gene regulation [254]. We treated neuro2a cells with 50 nM of HDAC6 ZnF UBP domain to observe its effect on distribution and localization of ApoE in cell. It was observed that upon HDAC6 ZnF UBP treatment, there is increased nuclear localization of ApoE (**Fig. 4.9A**). The localization of ApoE was quantified by analyzing the intensity of ApoE immunofluorescence in nucleus and cytoplasm of untreated and HDAC6 ZnF UBP treated cells (No. of fields selected for quantification, $n = 10$ and the statistical analysis carried out by using two-tailed unpaired student t-test.). The ApoE level in cytoplasm of both untreated and HDAC6 treated cells showed no change while it was significantly increased in the nucleus of HDAC6 ZnF UBP treated cells (**Fig. 4.9B, C**).

4.8 Enhanced Tubulin localization to MTOC with HDAC6 ZnF UBP treatment

HDAC6 is a known interacting partner of tubulin and regulates microtubule structure and function through deacetylation. Both actin and tubulin networks work in synchronicity in order

to enable cell migration and cellular movement in the form of membrane extensions or projections. We observed Tau-actin co-localization in neuritic extensions indicating the interplaying of microtubule and actin dynamics in formation of cell extensions. When neuro2a cells were mapped for actin and tubulin, untreated cells showed more axonal localization of tubulin along with actin, while HDAC6 treated cells showed tubulin predominantly in MTOC (Fig. 4.10A). In a previous study, it was found that HDAC6 knockdown in cells along with HDAC6 inhibitor tubacin treatment does not affect microtubule growth velocity [114]. This implies that effect of HDAC6 on tubulin independent of its deacetylase activity may also exist. We have given HDAC6 ZnF UBP to neuro2a cells to observe the effect on microtubule network. HDAC6 ZnF UBP treatment to neuro2a cells increased tubulin localization around nucleus in MTOC (Fig. 4.10B). The re-orientation of MTOC is a complex process which occurs in a dynein, cdc42 and dynactin dependent manner [255, 256]. However, the mechanism and function of MTOC re-orientation is poorly understood. The results suggest the possible role of HDAC6 ZnF UBP domain in microtubule organization.

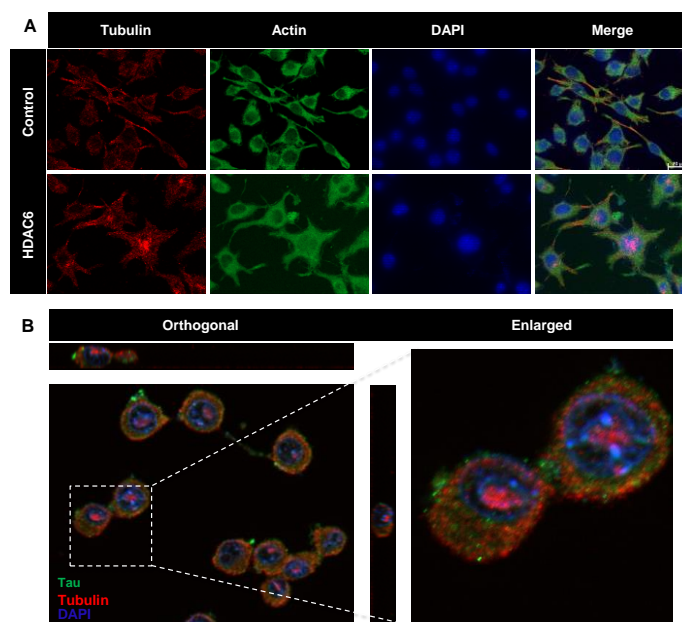


Fig. 4.10. Modulation of Tubulin localization by HDAC6. A) Immunostaining for β -actin and tubulin was performed to examine their localization in HDAC6 ZnF UBP treated neuro2a cells. Actin and tubulin co-localizes in the neuronal extensions in both treated and untreated cells. However, tubulin was found to be localized more in MTOC in case of HDAC6 treatment. B) Neuro2a treated with HDAC6 ZnF UBP shows localization of tubulin focused over the nuclear periphery compared to untreated neuro2a where tubulin is evenly distributed in cytoplasm. Orthogonal projection image shows tubulin localization in nuclear periphery in HDAC6 ZnF UBP treated neuro2a cells.

4.9 Summary

We studied the role of HDAC6 ZnF UBP domain in different aspects of AD pathology. Upon HDAC6 ZnF UBP treatment, inactive phosphorylated form of GSK-3 β increases without any change in total GSK-3 β level. Decreased level of Tau phospho-epitopes pT181 and AT8 with

HDAC6 ZnF UBP treatment indicates that it has a regulatory role in Tau phosphorylation. Also, HDAC6 ZnF UBP was found to be involved in cytoskeletal re-organization by modulating actin dynamics and tubulin localization. Enhanced neuritic extension and formation of podosome-like structure were observed with HDAC6 ZnF UBP treatment and tubulin was more localized in MTOC suggesting its regulatory function. ApoE translocation in nucleus enhanced upon HDAC6 ZnF UBP treatment implying its possible role in ApoE pathological cascade in AD. To summarize, our study suggests that the ZnF domain of HDAC6 performs various regulatory functions apart from its classical function in aggresome formation in protein misfolding diseases.

Chapter 5

Screening of small molecules against Tau aggregation

5.1 Background

The progression of Alzheimer's disease is a multi-factorial process dependent on events like protein aggregation, neuro-inflammation and oxidative stress, which in turn are dependent on each other as cause or effect. However, the exact mechanism for the etiology of AD so far is poorly understood. Tau aggregation leading to neurotoxic effect is considered as the prime reason for pathological state in AD. Aggregation of Tau protein in AD and other related Tauopathies proceeds in a cascade of events involving the formation of intermediate species-like oligomers, proto-fibrils, paired helical filaments, which ultimately lead to the formation of neurofibrillary tangles [12]. Therapeutic strategies are being designed so as to target these intermediates as well as other aspects of neurodegeneration to curb down the progression of disease [257]. The various therapeutic strategies involves development of small molecules able to inhibit Tau aggregation or dissolve the pre-existing aggregates, kinase inhibitors or phosphatase activators to target Tau hyperphosphorylation, immunotherapy, acetylation inhibitors, microtubule stabilizers and deglycosylation inhibitors [258]. Several molecules belonging to different classes-like synthetic molecules, natural compounds, peptide inhibitors *etc.* have found to be potent against Tau aggregation [259-261].

We have explored the role of two of the naturally occurring small molecules-Melatonin, which is a pineal gland derived neurohormone and Baicalein, a flavonoid derived from a Chinese herb *Scutellaria baicalensis*. Both these have been studied for their properties in neurodegenerative diseases as well as in general health and disease. Melatonin is an endocrine hormone mainly known for its role in maintenance of circadian rhythm *via* regulation of transcription factor CLOCK and its homologs [262]. In conditions of depression and sleep disorders, exogenous Melatonin administration is known to relieve the symptoms without any side-effects. Melatonin is rapidly metabolized in the liver through hydroxylation at C6[263]. It can also be synthesized by other tissues in variable quantities as the enzymes for Melatonin biosynthesis are ubiquitously expressed [264]. Melatonin is an amphipathic molecule, which can cross all biological membranes [265]. The role of Melatonin in neuroprotection has been studied in terms of its various functions. It is well known that Melatonin has potent anti-oxidant properties as well as regulator of other enzymes involved in protection against oxidative stress [266, 267]. Anti-oxidant properties of Melatonin and its metabolites have been well-studied [268]. Melatonin also regulates the function of kinases-like GSK3- β and PKA, which are known to play a major role in Tau hyperphosphorylation [269, 270]. Upon Melatonin treatment, GSK3- β and PKA activity get reduced leading to decreased phosphorylation of Tau [270, 271]. Due to its pleiotropic properties, high bioavailability and low toxicity, Melatonin has drawn attention as a potent therapeutic molecule. Administration of Melatonin in age-associated neurological disorders was found to improve the cognitive function and sleep patterns [272]. The effect of Melatonin is most extensively studied with respect to Amyloid- β but its role in Tau pathology needs to be explored in terms of its multiple functions [273, 274]. Melatonin was found to be effective as an aggregation inhibitor has been studied against A β and α -Synuclein aggregation [275-277]. A recent study shows that Melatonin and its close analogues inhibit and destabilize the aggregation

of A β thereby acting as neuroprotective agents [278]. Neurodegenerative diseases are often associated with inflammatory response, which further causes neuronal damage [279]. Melatonin inhibits the production of pro-inflammatory cytokines such as IL-6, IL-8 and TNF- α , hence, suppressing inflammation [280]. We have studied Melatonin with respect to its interaction with microtubule-associated protein Tau and to modulate its aggregation propensity.

Baicalein is a plant derived flavonoid molecule traditionally used in Chinese medicines. Flavonoids are a rich source of anti-oxidants and are known to play a neuroprotective role [281]. It is known for its various medicinal properties and finds its use as an anti-inflammatory, anti-carcinogenic and cardio-protective agent. It has been widely studied with respect to its protective functions in neurodegenerative diseases. Baicalein has been found to be effective against α -synuclein aggregates involved in Parkinson's disease as well as amyloid- β pathology associated with AD [270] [282].

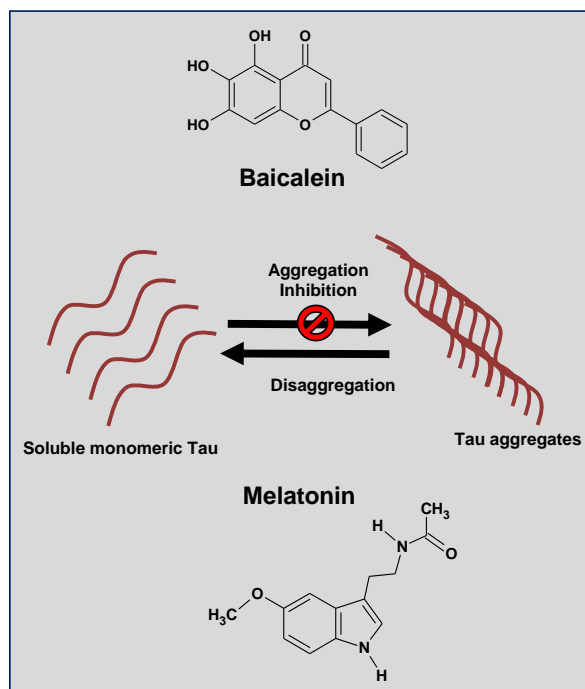


Fig. 5.1. Small molecules Melatonin and Baicalein against Tau aggregates. Baicalein is a flavonoid derived from Chinese herb *Scutellaria baicalensis* while Melatonin is a neurohormone primarily produced by the pineal gland. Both of these naturally occurring small molecules were studied for their interaction with repeat Tau and their potency against Tau aggregation inhibition or disaggregation of pre-formed aggregates.

In the current studies, we explored the role of Melatonin and baicalein with respect to their interaction with repeat domain of Tau and modulation of its aggregation properties (**Fig. 5.1**). We found that both Melatonin and baicalein interacts with repeat Tau with a weak interaction. We explored the potency of Melatonin in repeat Tau aggregation inhibition and disaggregation while baicalein was studied for its effect on oligomeric as well as fibrillar species of repeat Tau aggregates. The results suggest that Melatonin can affect Tau aggregation but its potency as a drug need to be explored further in combination of other potent drugs as it was found to be

effective at a high concentration. The flavonoid Baicalein showed potency against preformed aggregates of repeat Tau in different stages of maturation and can interact with the repeat region of Tau. Baicalein was found to interact both with early oligomers and mature fibrils to disaggregate the preformed aggregates. Tau upon interaction with Baicalein is directed to form stable oligomers which are non-toxic in nature.

5.2 Melatonin in higher concentrations inhibits repeat Tau aggregation

We investigated the potential of Melatonin as an inhibitor of Tau protein aggregation by subjecting Melatonin at a concentration range of 100-5000 μM . Repeat domain of Tau was subjected to aggregation in presence of Melatonin. The aggregation kinetics of repeat Tau was monitored by ThT and ANS fluorescence. It was observed that Melatonin was able to inhibit repeat Tau aggregation at a concentration as high as 1000 μM (**Fig. 5.2A**) without affecting the hydrophobicity of Tau protein as indicated by ANS fluorescence (**Fig. 5.2B**). Transmission electron microscopy images for repeat Tau samples subjected to aggregation in presence of 1000 μM of Melatonin showed distinct morphology of small, broken Tau aggregates while control aggregates showed mature Tau fibrils (**Fig. 5.2C**).

5.3 Effect of Melatonin on structural conformation of Tau

Tau in its soluble form exists in a random coil conformation which changes to β -sheet form when it aggregates. We studied the effect of Melatonin using circular dichroism spectroscopy for its ability to alter the structure of repeat and found that it does not affect the conformation of Tau during interaction. CD spectroscopy for soluble repeat Tau shows a negative band at ~ 198 nm while upon aggregation in the presence of heparin, the spectrum shifts towards β -sheet structure with a signature negative band at ~ 208 nm (**Fig 5.2D**). However, there was no change in the spectra indicating that the β -sheet conformation was retained even in the presence of Melatonin.

5.4 Melatonin disaggregates pre-formed Repeat Tau aggregates

Tau protein upon aggregation forms well defined fibrillar protein aggregates through a series of intermediate species. We prepared repeat Tau aggregates and incubated them with various concentrations of Melatonin. It was observed that at lower concentrations of Melatonin, there was little or insignificant disaggregation effect while at higher concentrations (1000 and 5000 μM) of Melatonin, there was effective disaggregation of repeat Tau fibrils (**Fig 5.3A**). There was

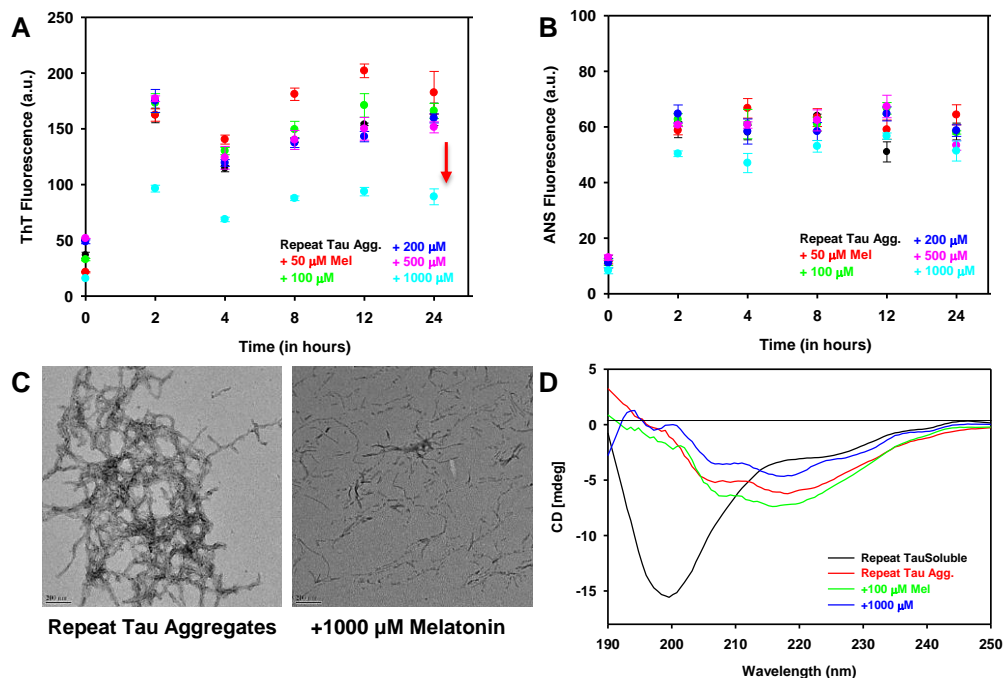


Fig. 5.2. Effect of Melatonin on repeat Tau aggregation. A) ThT fluorescence assay for repeat Tau aggregation inhibition by Melatonin. Melatonin inhibited repeat Tau aggregation at the concentration of 1000 µM (Data represented as SD±Mean of triplicate values). B) ANS fluorescence assay for repeat Tau aggregation with different concentration of Melatonin. Melatonin does not cause any change in hydrophobicity of repeat Tau (Data represented as SD±Mean of triplicate values). C) CD spectroscopy for repeat Tau aggregation samples with or without Melatonin. For Melatonin treated samples, no difference was observed as compared to control aggregates samples. D) Electron micrographs for repeat Tau control aggregates and repeat Tau incubated with 1000 µM of Melatonin. Broken aggregates were observed in the Melatonin treated sample while control shows mature repeat Tau aggregates. (Adopted from Balmik *et al.*, 2020, BBA-General Subjects)

60% disaggregation observed with 5000 µM Melatonin while lower concentrations of Melatonin gives only around 20% disaggregation (Fig 5.3B). In order to study the time course of disaggregation, continuous fluorescence measurement was taken, which showed similar results for the same range of Melatonin concentrations (Fig 5.3C). The samples at the end-point of the assay were observed under TEM, which revealed fewer and shorter fibrils in samples with 1000 and 5000 µM Melatonin distinct from mature Tau fibrils in control aggregates (Fig. 5.3 D).

5.5 Melatonin interacts weakly with the Repeat Tau

Being an amphipathic molecule, Melatonin can interact with a wide variety of molecules. Melatonin exhibited the property as modifier of repeat Tau aggregation, both as an inhibitor and

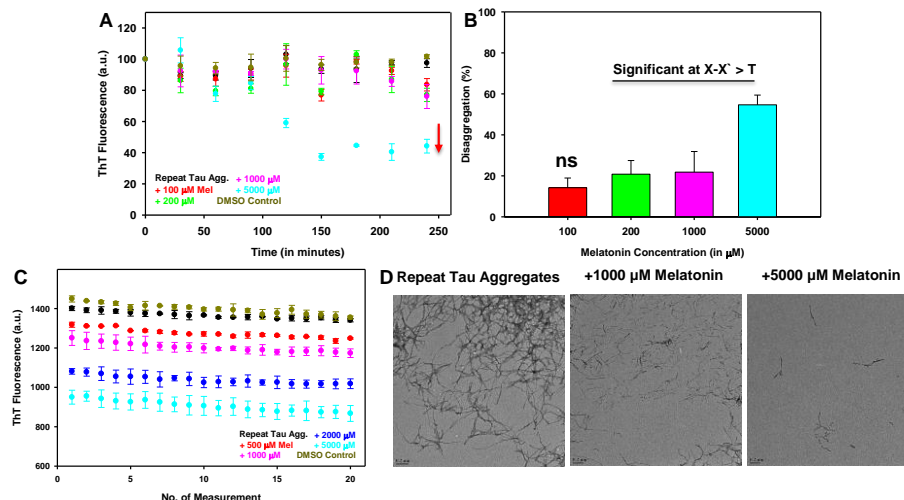


Fig. 5.3. Disaggregation of repeat Tau fibrils by Melatonin. A) ThT fluorescence assay for repeat Tau disaggregation with different Melatonin concentration. Disaggregation of preformed repeat Tau aggregates observed for 1000 and 5000 μM of Melatonin. B) Melatonin shows nearly 60% disaggregation of repeat Tau aggregates at 5000 μM (n.s. indicates $P \geq 0.05$ (non-significant), * indicates $P \leq 0.05$, ** indicates $P \leq 0.01$, *** indicates $P \leq 0.001$). C) Repeat Tau disaggregation assay in continuous mode. Disaggregation assay for pre-formed repeat Tau aggregates was monitored in a continuous mode using ThT fluorescence. Melatonin was used in the concentration range from 500 – 5000 μM . Melatonin showed disaggregation effect only at higher concentrations range. D) TEM images repeat Tau aggregates treated with 1000 and 5000 μM Melatonin shows morphology of broken fibrils as compared to the control aggregates sample (Scale bars – 0.2 and 0.5 μm). (Adopted from Balmik *et al.*, 2020, BBA-General Subjects)

in disaggregation. We studied their interaction using ITC as a function of its activity with repeat Tau. In ITC, the non-specific heat change was ruled out by titrating Melatonin with titration buffer (Fig 5.4A). At lower concentrations of titrants, there was no significant heat change (Fig. 5.4B).

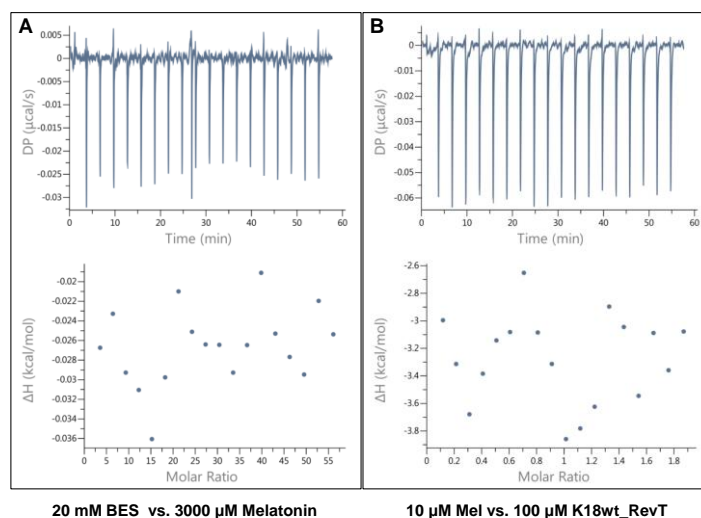


Fig. 5.4. ITC for repeat Tau and Melatonin interaction at low concentrations of protein and ligand. A) ITC carried out for 20 mM BES, pH 7.4 with 3000 μM Melatonin did not produced any background heat of association. B) ITC carried out at lower concentration (10 μM) of Melatonin with 100 μM of repeat Tau did not produced

sufficient heat changes that can be fitted into a plot and analysed. (Adopted from Balmik *et al.*, 2020, BBA-General Subjects)

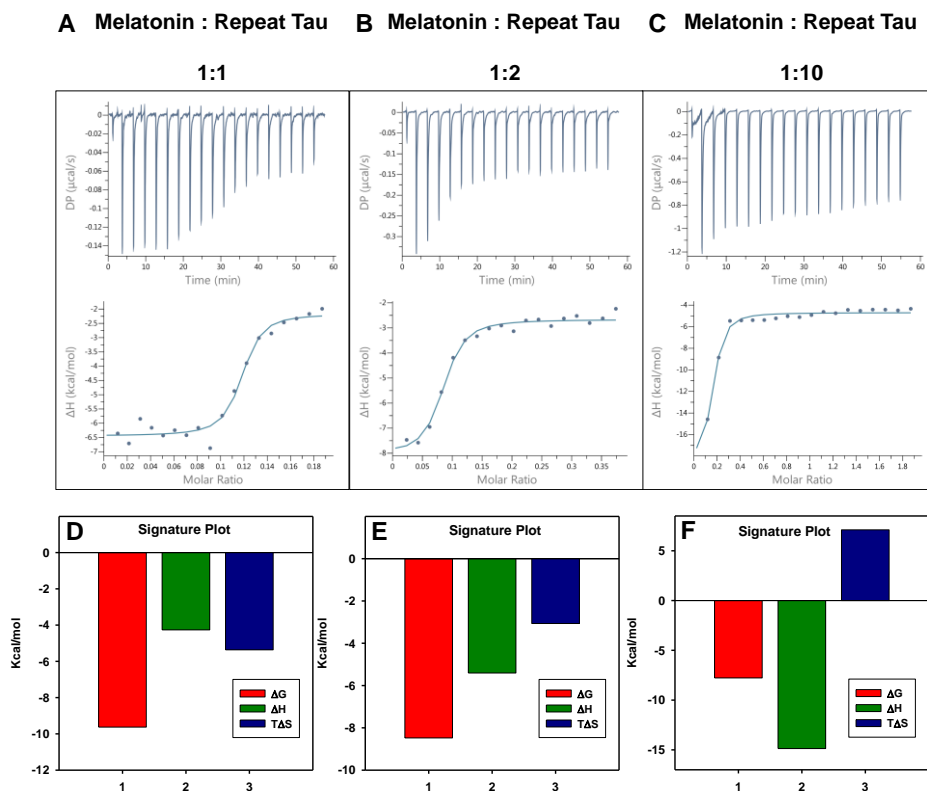


Fig. 5.5. Repeat Tau-Melatonin interaction by ITC. A) Isothermal titration Calorimetry thermographs for the reverse titration of repeat Tau (titrant) and Melatonin (titrand) at 1:1 ratio shows the association between the two although without attaining saturation. B) Reverse titration at 1:2 ratio produce a near exponential heat plot indicative of concentration-dependent association of repeat Tau and Melatonin. C) At 1:10 ratio, rapid heat change was observed with each injection along with exponential heat plot, but saturation was not observed due to dynamic nature of Tau-Melatonin binding. D, E, F) Signature plots for repeat Tau-Melatonin reverse titration at 1:1, 1:2 and 1:10 ratio showing highly negative free energy change indicating the spontaneity of association. (Adopted from Balmik *et al.*, 2020, BBA-General Subjects)

We performed reverse titration in ITC with ratios of Melatonin to repeat Tau as 1:1, 1:2 and 1:10 (Fig 5.5A, B, C). There was significant heat change for the interaction of repeat Tau and Melatonin at all these ratio while increase in entropy was observed in 1:10 ratio (Fig 5.5D, E, F). As the concentration of repeat Tau is increased with respect to Melatonin, the molar ratio approaches unity. However, this result in the equilibrium shifting towards dissociation before the saturation can be attained in the system. These results shows the interaction between Melatonin and repeat Tau without attaining the saturation and Melatonin can bind to repeat Tau with a weak affinity.

5.6 Characterization of residue specific interaction of Melatonin and Repeat Tau using NMR spectroscopy

Repeat Tau was labelled by incorporating ^{15}N and used to determine the interaction with Melatonin by carrying out titration at varying Melatonin concentrations. NMR spectroscopic studies were carried out to characterize the interaction of Melatonin with repeat Tau. 200 μM solution of ^{15}N labelled repeat Tau in phosphate buffer was titrated against stoichiometric ratios (1:0, 1:5, 1:10, 1:25, 1:50 ratios of repeat Tau to Melatonin) of Melatonin and the residue specific chemical shift perturbations were monitored by ^1H - ^{15}N HSQC experiments [283]. NMR data revealed considerable perturbation of all the five histidine residues in repeat Tau H268, H299, H329, H330, H362 and the other residues such as V300, K331 and V363, which are adjacent to histidine residues (**Fig. 5.6**).

Apparently, the interaction of melatonin with repeat Tau is similar to the interaction by polyamines such as spermine and spermidine, which also bind at the histidine sites of repeat Tau or A β [284]. However, Melatonin is weakly binding and requires millimolar concentration for observable effects. Furthermore titration with Melatonin has slowly populated a new HSQC cross peak at $\delta(^1\text{H}, ^{15}\text{N}) = (7.933, 127.178)$ (**Fig. 5.6, bottom right corner**), whose intensity rose with increasing concentration of Melatonin, which otherwise was completely absent in the native conditions. Hence, this cross peak could not be traced to any residue due to the lack of an appropriate backbone chemical shift assignment. We speculate that the cross peak might be resulting from a residue, which was flexible and broadened beyond observation in the absence of Melatonin.

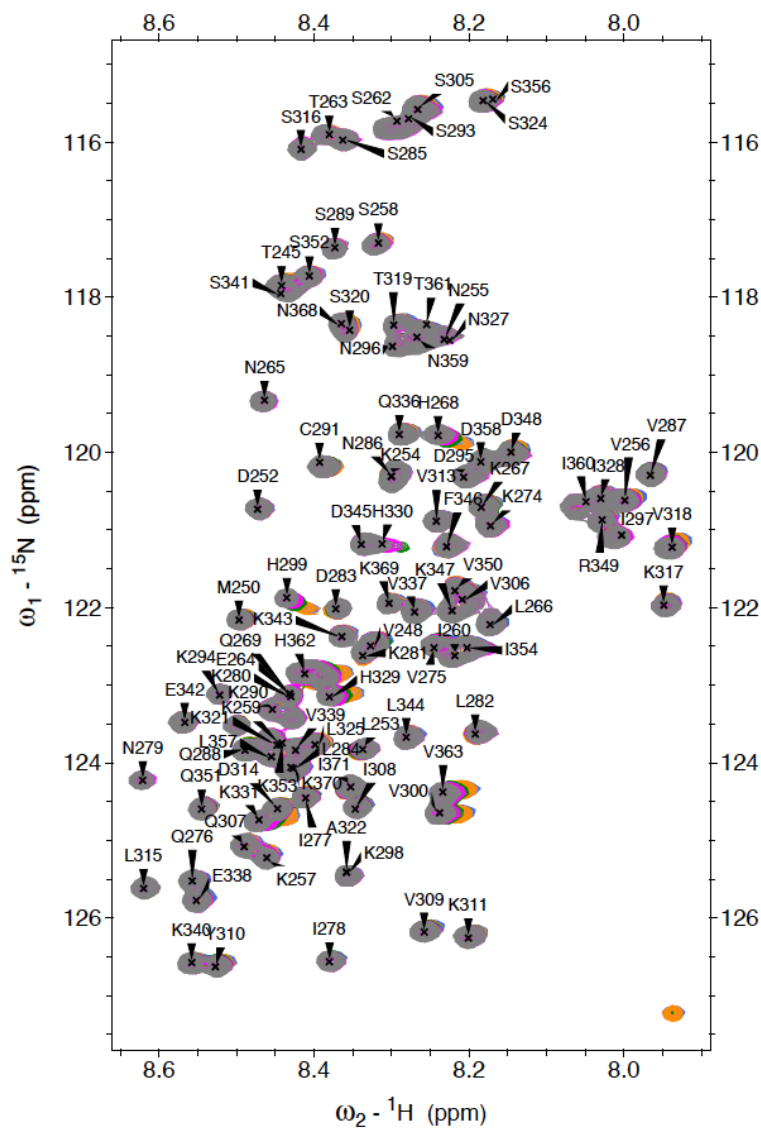


Fig. 5.6. ^1H - ^{15}N HSQC NMR for repeat Tau and Melatonin. ^1H - ^{15}N HSQC chemical shift perturbation plot for the titration of 200 μM solution of repeat Tau with Melatonin in concentration ratios 1:0 (gray), 1:5 (magenta), 1:10 (green), 1:25 (dark orange), 1:50 (dark blue) of repeat Tau to Melatonin. Almost all the cross peaks in ^1H - ^{15}N HSQC have been labelled with the names of the respective residues from repeat Tau. Residues from repeat Tau that are involved in interaction with Melatonin can be identified based on the shifting position of their corresponding cross peaks with increasing concentration of Melatonin. (Adopted from Balmik *et al.*, 2020, BBA-General Subjects)

5.7 Effect of Melatonin on repeat Tau aggregates-mediated toxicity

Melatonin showed inhibitory effect on repeat Tau aggregation, which prompted us to check whether it can revert the aggregates-mediated cytotoxicity. Firstly, neuro2acells were treated with repeat Tau aggregates in 0- 40 μM concentrations to determine its minimal toxicity on neuro2a cells (**Fig. 5.7A**). It was observed that 5 μM repeat Tau aggregates induced 50% cytotoxicity. 0- 100 μM of Melatonin along with 5 μM of repeat Tau aggregates were given to neuro2a cells. Melatonin treatment showed no significant rescuing effect from aggregates

mediated toxicity (**Fig. 5.7B**). Tau aggregates used for treatment were also measured and characterized by SDS-PAGE, ThT fluorescence and CD spectroscopy (**Fig. 5.7 C, D, E**).

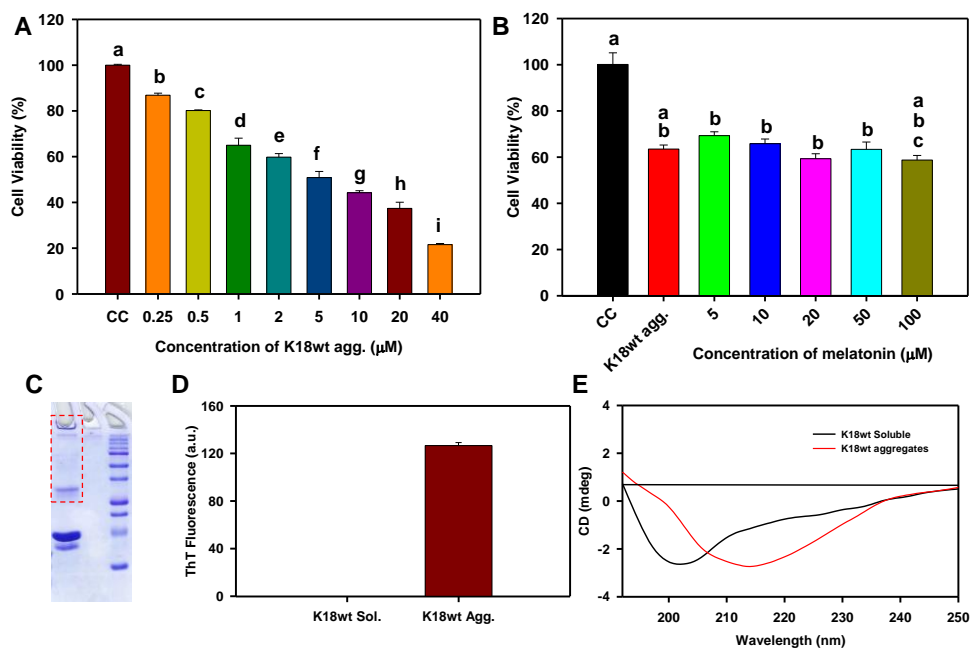


Fig. 5.7. Cytotoxicity of repeat Tau aggregates on neuro2a and effect of Melatonin on Tau aggregates-mediated toxicity. A) Neuro2a cells were treated with repeat Tau aggregates prepared *in vitro* with heparin as an inducer. Treatment with repeat Tau aggregates shows reduced cell viability in a concentration dependent manner. 50% viability was obtained with 5 μM aggregates treatment while the highest concentration of aggregates used in the study (40 μM) showed 20% cell viability. B) 5 μM of repeat Tau aggregates were used to induce cyto-toxicity in neuro2a. Melatonin treatment (0- 100 μM) along with aggregates did not show significant rescue. Repeat Tau aggregates were prepared in the assembly buffer (20 mM BES pH 7.4). The aggregates were used for the treatment of neuro2a cells were characterized by using C) SDS-PAGE showing higher order aggregates (marked by red dotted box) D) ThT fluorescence for soluble repeat Tau and aggregates in 5 μM measuring concentration and E) Circular dichroism spectroscopy for soluble and aggregated repeat Tau showing random coil and β -sheet structure respectively. (Significant at mean difference $> T = 9.245$, groups with the same letters are not significantly different while groups with significance are represented together with different letter. Data represented as $\text{SD} \pm \text{Mean}$ of triplicate values). (**Fig. 5.7A and B** were adopted from Balmik *et al.*, 2020, BBA-General Subjects)

5.8 Baicalein binds to Tau *in vitro*

Tau protein is one of the major microtubule-associated proteins in neuronal axons that mainly functions to stabilize and assemble microtubules. Tau is highly soluble protein and adopts a natively unfolded structure in solution [285]. The repeat domain of Tau plus the proline-rich flanking regions confer the property of microtubule-binding and assembly, where the repeat domain of Tau represents the core of the PHFs. Baicalein shows characteristic λ_{max} at two wavelengths 270 nm and 362 nm (**Fig 5.8A, B**). Upon titrating with repeat Tau from 0-98 μM , the peak at 362 nm was found to decrease in intensity indicating the binding of Baicalein (**Fig. 5.8C**).

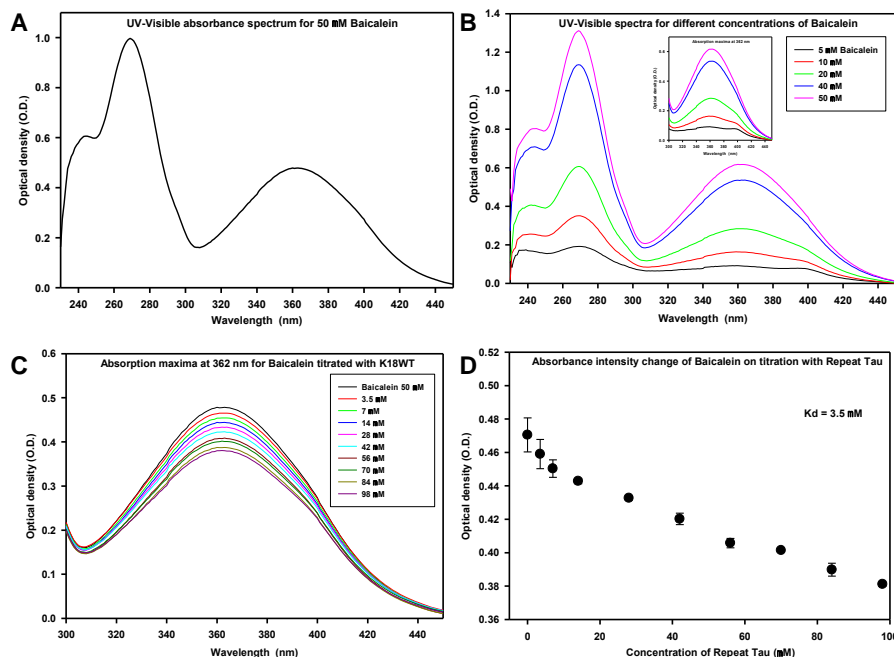


Fig. 5.8. The interaction of Tau with Baicalein by UV–Visible absorption spectroscopy. A) UV-VIS absorption spectrum for 50 μM Baicalein in 20 mM BES buffer, pH 7.4 showing maxima at 270 nm and 362 nm. B) Absorption spectra for different concentrations (5, 10, 20, 40 and 50 μM) of Baicalein. C) Figure shows decrease in the absorbance intensity at 362 nm upon increasing the protein concentration against Baicalein. D) The absorbance intensity at 362 nm obtained for different titrations when plotted against respective concentrations gives a plot representing the binding affinity of Tau with Baicalein. (Adopted from Sonawane, Balmik *et al.*, 2020, Archives of Biochemistry and Biophysics)

The maxima at 362 nm plotted against increasing Tau concentration (0–98 μM) shows a gradual decrease in absorbance intensity (**Fig. 5.8D**). The dissociation constant (K_d) for the binding of Tau with Baicalein was found to be 3.5 μM by using the following formula:

$$[C_{\text{Tau}}C_{\text{Baicalein}}] = \frac{[C_{\text{Tau}}] \times [C_{\text{Baicalein}}]}{K_d + [C_{\text{Baicalein}}]}$$

Where $[C_{\text{Tau}}]$ is the initial Tau concentration, $[C_{\text{Baicalein}}]$ is the free Baicalein concentration, $[C_{\text{Tau}}C_{\text{Baicalein}}]$ is the concentration of Tau–Baicalein complex and K_d is the dissociation constant [286]

5.9 Disaggregation and sequestration of repeat Tau oligomers by Baicalein

Oligomers of repeat Tau were prepared by incubating Tau in aggregation conditions for 4 hours and then subjected to various concentrations of Baicalein to study the disaggregation of repeat Tau oligomers. ThS fluorescence assay suggested that Baicalein is able to disaggregate preformed oligomers in a concentration-dependent manner (**Fig. 5.9A**). Baicalein was found to enhance and moderately induce oligomerization as well as sequester oligomers into an aggregation incompetent form. The underlying mechanism of disaggregation may involve the breaking of aggregates into smaller fragments and then inhibiting the reformation of higher order

aggregates. It was observed that both ThS and ANS fluorescence was decreased upon addition of Baicalein in 4 hours (**Fig. 5.9A, B**) incubated samples suggesting disaggregation and decreased hydrophobicity respectively. However, the ANS fluorescence increased after 12 hours in all the

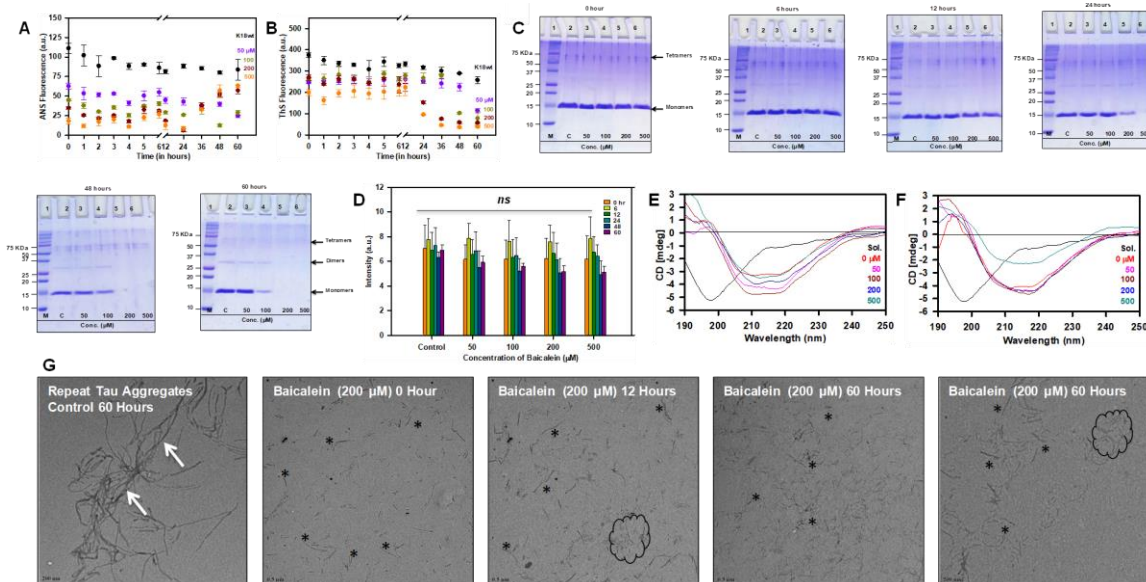


Fig. 5.9. Disaggregation of repeat Tau oligomers by Baicalein. A) Formation of repeat Tau aggregates was monitored by ThS fluorescence after addition of Baicalein at different concentrations after 4 hours of incubation. ThS fluorescence shows a marked decrease in a concentration dependent manner. B) ANS fluorescence assay for repeat Tau oligomers disaggregation on addition of different concentrations of Baicalein at 4 hours of incubation shows a prominent decrease in fluorescence after Baicalein addition in all the concentrations. There was an increase in fluorescence from 24 hours onwards indicating that at higher concentrations Baicalein can increase the hydrophobicity of protein aggregates. C) SDS-PAGE analysis shows a marked decrease in the monomeric form of repeat Tau, which are mostly entrapped as dimeric and tetrameric forms in presence of all different concentrations of Baicalein. D) Quantification of SDS-PAGE showing concentration-dependent decrease in intensity for repeat Tau oligomers. E, F) The CD spectra for repeat Tau oligomer disaggregation samples at 0, and 60 hours of incubation with different Baicalein concentrations. In all the treated samples, the shift in the spectrum towards β -sheet structure can be observed (shown by pink arrow) as compared to soluble repeat Tau. The Sol. represents for soluble protein. G) Electron micrographs for repeat Tau at 0, 12 and 60 hours of incubation with 200 μ M Baicalein show smaller broken filaments (black asterisks and encircled area) as compared to untreated control (white arrow). (**Adopted from Sonawane, Balmik *et al.*, 2020, Archives of Biochemistry and Biophysics**)

incubated samples. The SDS-PAGE analysis showed that Baicalein could bind to the preformed oligomers and sequester them at this stage. The presence of a tetramer band in all the concentrations of Baicalein can be observed but the dimer as well as the monomer completely disappears (**Fig. 5.9C**). We observed the formation of oligomers on the SDS-PAGE and increase in ANS fluorescence but a complete decrease in ThS fluorescence for the Baicalein treated oligomers. This strongly suggests the role of Baicalein in sequestering the Tau oligomers. The SDS-PAGE quantification for repeat Tau oligomer disaggregation (**Fig. 5.9D**) shows a gradual decrease in soluble repeat Tau in a concentration-dependent manner. Further, CD spectra analysis for repeat Tau samples treated with a varying range of Baicalein concentrations shows a shift towards the β -sheet structure in all concentrations (**Fig. 5.9E, F**). Electron micrographs for disaggregation assay samples shows fragility of Tau aggregates and absence of mature Tau filaments (**Fig. 5.9G**).

5.10 Baicalein disaggregate mature fibrils of repeat Tau

Disaggregation of repeat Tau fibrils was carried out using different concentrations of Baicalein and monitored by ThS and ANS fluorescence assay. Repeat Tau fibrils were prepared by subjecting the protein to aggregation conditions for 60 hours. Initially, after addition of Baicalein, there was decrease in the ThS fluorescence within 12 hours in all concentrations of Baicalein suggesting disaggregation of Tau fibrils (**Fig. 5.10A**). However, ANS fluorescence decreased initially for 12 hours and increased afterwards indicating the formation of oligomers (**Fig. 5.10B**). In SDS-PAGE analysis, Baicalein treated samples showed decrease in the population of oligomeric species at different time points (**Fig. 5.10C**). The SDS-PAGE quantification for fibril disaggregation (**Fig. 5.10D**) shows a gradual decrease in soluble repeat Tau in a concentration dependent manner. Further, CD spectra analysis for repeat Tau samples treated with a varying range of Baicalein concentrations shows a shift towards the β -sheet structure in all concentrations (**Fig. 5.10E, F**). The disaggregation effect of Baicalein was also supported by the electron micrographs (**Fig. 5.10G**), which shows fragility of Tau and absence of mature Tau filaments.

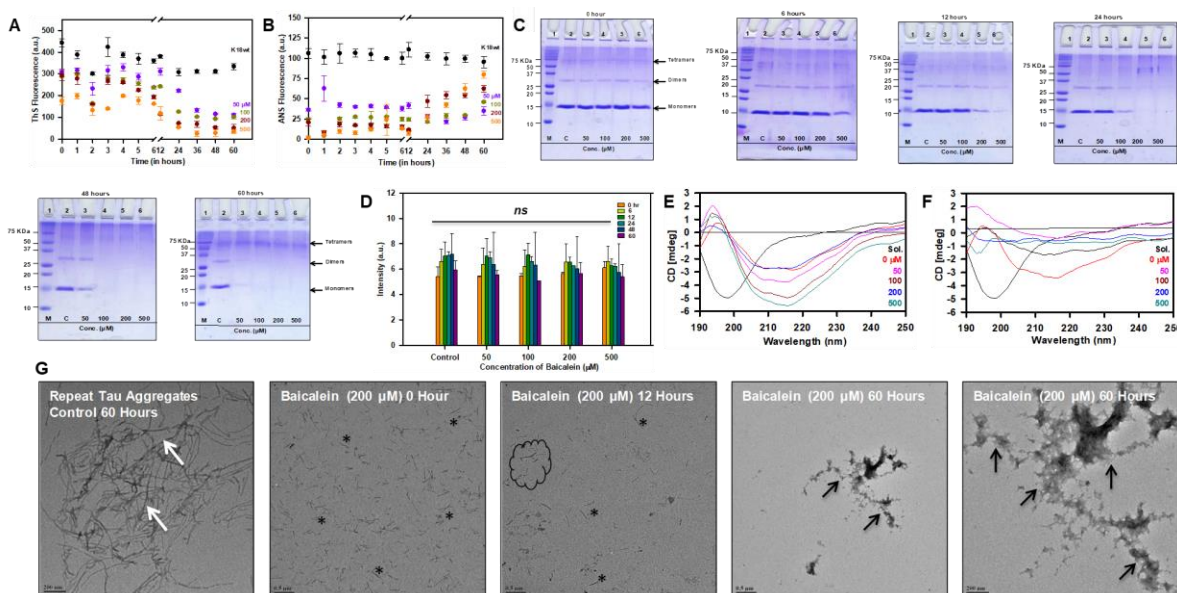


Fig. 5.10. Disaggregation of repeat Tau fibrils by Baicalein. A) ThS fluorescence for repeat Tau fibril disaggregation shows a decrease with increase in Baicalein concentration and the time of incubation. B) The ANS fluorescence assay for repeat Tau fibrils disaggregation shows more prominent decrease in all concentrations of Baicalein. Furthermore, there is similar increase in ANS fluorescence after 12 hour of Baicalein addition. C) The SDS-PAGE analysis for different time point samples shows enhancement of repeat Tau dimer and tetramers until 12 hours after Baicalein addition. At 60 hours, the population of repeat Tau soluble protein as well as dimer is greatly reduced in all Baicalein concentrations while the tetrameric population is enhanced. D) Quantification of SDS-PAGE for samples with 50, 100, 200 and 500 μM of Baicalein was carried out for 0 hours to 60 hours of Baicalein addition. E, F) CD spectra for repeat Tau aggregates at different time points treated with Baicalein at different concentrations shows a shift in structure towards β sheet (shown by pink arrows) as compared to soluble repeat Tau. The Sol. represents for soluble protein. G) Electron micrographs for repeat Tau control and fibrils at different time points with 200 μM of Baicalein show disaggregation of fibrils into small pieces (black asterisks and encircled area) as compared to untreated control (white arrow). (Adopted from Sonawane, Balmik *et al.*, 2020, Archives of Biochemistry and Biophysics)

5.11 Characterizing Baicalein-stabilized oligomers by Size-exclusion chromatography

Formation of Baicalein induced oligomers was evident in size-exclusion chromatography (SEC). Repeat Tau incubated with Baicalein leads to formation of oligomers as seen in the SEC profiles for samples at 0, 6, 12, 24, 48 and 60 hours (**Fig. 5.11A**) as compared to soluble repeat Tau. BSA and Lysozyme were loaded as standards in 3 mg/ml concentration and soluble repeat Tau was loaded as a control (**Fig. 5.11B**).

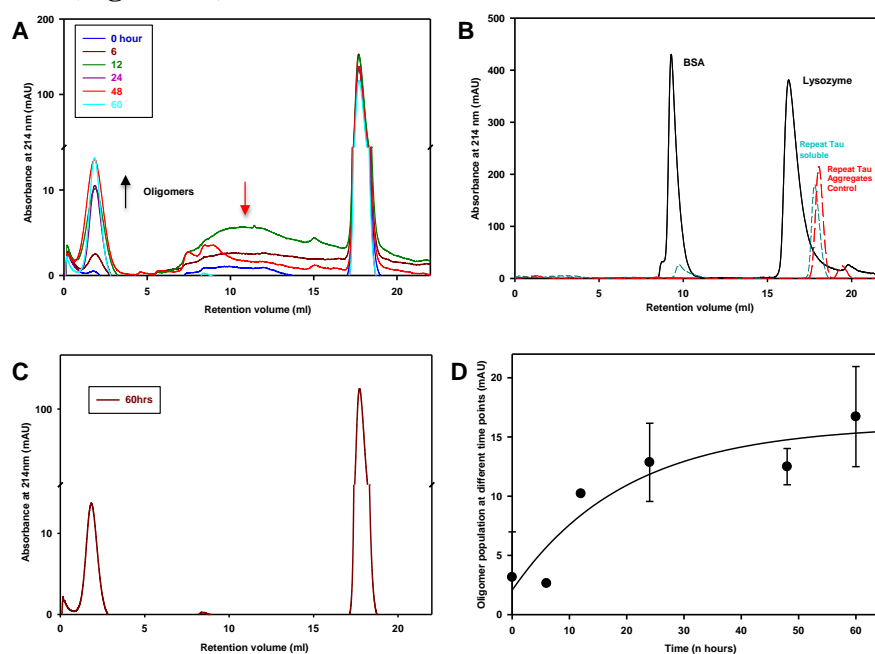


Fig. 5.11. Size-exclusion chromatography for repeat Tau aggregates. A) 20 μ M repeat Tau was incubated with Baicalein at 200 μ M concentration and subjected to size-exclusion chromatography at different time-points. Comparison of the chromatograms for repeat Tau incubated with Baicalein at different time points. Figure shows a decrease in dimeric population of repeat Tau (pink arrow) with subsequent increase in the Baicalein stabilized oligomers (black arrow). B) BSA and Lysozyme (3 mg/ml each) were run for standardization of SEC column. The chromatogram in dark cyan and red shows profile for repeat Tau soluble and repeat Tau aggregates at 0 hour respectively. C) Chromatogram for repeat Tau incubated with Baicalein for 60 hours shows increase in oligomer population. D) Maximum absorbance obtained for the peaks for oligomers at different time points shows a gradual increase in Baicalein stabilized oligomers with time. (Adopted from Sonawane, Balmik *et al.*, 2020, Archives of Biochemistry and Biophysics)

Further the repeat Tau was incubated with Baicalein at 1:10 ratio showed presence oligomers while it was absent in the control aggregation sample at 60 hours, (**Fig. 5.11C**) suggesting enhancement of oligomerization in presence of Baicalein. There is an increase in the intensity of peak corresponding to repeat Tau oligomers with respect to time (**Fig. 5.11D**).

5.12 Summary

Our results showed that Melatonin interacts with the repeat domain of Tau weakly. In spite of its weak interaction and slow kinetics, it was apt enough to dissolve Tau fibrils. The inhibition and disaggregation effects of Melatonin on repeat Tau were mediated by its interaction with the histidine sites on the protein. It required high concentration of Melatonin to exert its effect on aggregation of Tau, but it is known to be non-toxic even at higher concentrations. Melatonin is a potent biomolecule whose therapeutic action has been well studied in neurodegenerative diseases. However, its low half-life period in biological system limits its therapeutic use. Thus, we suggest enhancing its ameliorating effects either by conjugation in order to stabilize the molecule or in combination with other potent drugs to complement their action.

Our current investigation on Baicalein demonstrates the ability of Baicalein to inhibit the Tau aggregation by covalent modification. Baicalein inhibits the Tau aggregation by inducing the off-pathway oligomer formation and preventing the filamentous aggregate formation thus highlighting its potential to be developed as a future therapeutic agent in AD.

Chapter 6

Discussion

6.1 Tau protein in health and disease

Tau is a member of MAPs family of proteins, known for its role in the stabilization of microtubules and neurodegenerative conditions associated with its abnormal aggregation and accumulation in neurons. The neuropathology associated with Tau has been well studied and documented in various neurological disorders. Although, microtubule stabilization is considered as the major function of Tau, it serves diverse functions in other physiological processes. Tau is known to be present in nucleus of neurons where it associates with the minor groove of DNA preventing its metabolism [287]. The levels of nuclear Tau get reduced in Tauopathies, suggesting the role of Tau in DNA stabilization. Tau has been found to associate with cell membrane through its N-terminus [288]. However, the role of Tau with respect to its association with cell membrane is not clear. The membrane association of Tau may be involved in the stabilization of cyto-cortex as it associates with cyto-cortical elements microtubule as well as actin playing an important role in their dynamics local cargo transport. The role of Tau in fast and slow axonal transport is well studied. Tau is majorly an axonal protein and its association with microtubules is an important regulating factor in axonal transport [289]. Another important non-typical role of Tau involves regulation of insulin signaling in brain. There have been evidences for glucose metabolism impairments related to insulin resistance upon Tau deletion. The Tau knock-out model studies suggested the regulatory role of Tau in glucose homeostasis. The effect has been hypothesized to involve inhibitory phosphorylation of insulin receptor substrate-1 (IRS-1) at S636 leading to insulin resistance in AD brain. The other mechanism may involve reduced function of phosphatase and tensin homolog (PTEN) lipidphosphatase, which converts phosphatidylinositol-3, 4, 5-triphosphate (PIP3) to phosphatidylinositol-4, 5-bisphosphate (PIP2) in insulin signaling pathway [290]. Tau is also involved in the process of myelination as Tau-KO mice showed hypo-myelination of sciatic nerves [291]. The non-typical functions of Tau are less understood and further studies could reveal an important aspect of its role in neurodegenerative diseases.

Tau protein undergoes various changes in its repertoire of PTMs as well as in its conformation as it acquires pathological form. There are certain PTMs like phosphorylation, acetylation and proteolytic cleavage, which make Tau susceptible to undergo changes in local conformation directing towards Tauopathies. However, the modifications are highly specific in nature and reflects either its functional or pathological state. For example, Tau phosphorylation at S422 protects it from proteolytic cleavage at D421 and thus protecting against abnormal processing [292]. There is a marked difference in Tau aggregation in various Tauopathies in terms of morphology of aggregates, location, cell types and Tau isoforms. In AD, Tau gets aggregated and deposited intracellularly in the form of NFTs. NFTs comprises of PHFs and straight filaments. PHFs are highly ordered structure made of two inter-twined filaments with a periodicity of 80 nm while straight filaments lack ant periodicity [293]. The NFTs consists of equimolar ratio of 4-repeat (4R) and 3-repeat (3R) isoforms of Tau, which sets it apart from Tau aggregates in other Tauopathies [294].

Thus, Tau pathology is implicated not only in AD, but a wide range of related diseases. In order to prevent the progression of neurodegenerative conditions in Tauopathies, therapeutics focus either on inhibiting Tau aggregation or dissolving the pre-formed aggregates.

6.2 Targeting Tau aggregation – importance as a therapeutic approach

Formation of Tau aggregates and their deposition as NFTs is a complex process, which leads to multiple secondary neurotoxic effects. Further, Tau oligomeric species are considered more toxic than the fibrillar aggregates, which are suggested to be a protective response of neurons. Tau dysfunction leads to collapse of cytoskeletal networks affecting axonal and dendritic transport systems. The impaired transport system in turn results in synaptic loss and ultimately cell death. Thus, inhibiting the aggregation of Tau provides a suitable target in order to curb the associated neurotoxic effects.

A wide range of aggregation inhibitors have been screened against Tau [295]. Tau is a fairly soluble protein in physiological conditions but attains insoluble aggregated form in Tauopathies. The physiological concentrations of free Tau in neuronal cell increase upon the initiation of pathology. However, in physiological system, longer time period for the formation of toxic aggregates. Various cell and animal model systems have been designed by the researchers in order to study the process and etiology of aggregation in AD. Monomeric Tau protein upon aggregation acquires hydrophobicity. The hydrophobic Tau aggregates are not effectively cleared and cause pathological interactions with other proteins like Fyn and Jun N-terminal kinase (JNK) interacting protein (JIP1) interfering with their functions in dendrites and axonal transport respectively [296]. Further, Tau aggregation affects mitochondrial functions resulting in increased ROS production as well as disruption of myelin sheath formation [297, 298]. Thus, inhibition of Tau aggregation at an early stage could be helpful in ameliorating these deleterious effects and slow down the progression of disease. Therapies based on inhibiting Tau aggregation have gained focus in past few years. There are several classes of therapeutic agents, which have been tested against Tau aggregation [132, 133, 169, 295, 299]. These include various classes of naturally derived or synthetic small molecules such as polyphenols, porphyrins, benzothiazoles, N-phenylamines, rhodanines and anthraquinones [300]. Based on their efficacy against Tau aggregation, some of the compounds have been employed in clinical trials but with limited desirable effects or undesirable side effects. Thus, another effective approach to tackle the process of Tau aggregation in neurons involves modulation of underlying mechanisms that lead to its aggregation.

6.3 HDAC6 ZnF UBP as modulator of Tau aggregation and stability

There are a large number of proteins, which interact with Tau in order to regulate its function. These include proteins involved in PTM of Tau such as kinases (GSK-3 β , CDK5, MARKs, and MAPKs *etc.*), phosphatases (PP1, PP2A and PP2B *etc.*), acetyltransferases (CBP and P300), deacetylases (HDAC6 and SIRT1) and methyltransferases (SETD7 and other lysine transferases)

[54, 301]. Modulating the function of these interacting partners of Tau serves as a therapeutic target to inhibit the pathological implications of Tau. There are other Tau interacting proteins like various HSPs, Pin1 and Fyn kinase, which bind to Tau and regulate its folding, localization or turnover. In AD, there is abnormal association or activity of these proteins leading to pathological state [192]. Thus, targeting specific functions like phosphorylation, dephosphorylation or factors affecting the stability or turnover of Tau in neurons may serve as a suitable therapeutic target.

HDAC6 plays an important part in cell homeostasis by mediating the degradation of misfolded and aggregated proteins by regulating cell-mediated autophagy and aggresome formation [103, 225]. HDAC6 has been widely studied with respect to its role in neurodegenerative diseases. Apart from its deacetylase mediated functions, HDAC6 is involved in regulating other proteins by direct interaction leading to modulation of their activity [112, 302]. HDAC6 levels are found to be elevated in the AD patients in response to increased aggregate burden in cells, which implies its protective role in aggregates clearance [111]. HDAC6 has been reported to interact with Tau through its deacetylase domain (DD2) and anchoring domain (SE14) [54]. It is notable that the catalytic function of HDAC6 is considered deleterious with respect to Tau pathology but its ZnF UBP domain is involved in protective mechanism by directing aggresome formation and HSP activation [303]. Thus, augmenting the function of HDAC6 ZnF UBP domain can be beneficial in designing therapeutics against AD. We aimed to explore the novel aspect of HDAC6 ZnF UBP interaction with Tau and its role in Tau aggregation and stability. We studied the effect of HDAC6 ZnF UBP domain in modulation of aggregation propensity of Tau, disaggregation of pre-formed Tau filaments and Tau conformation to address the possible role of this domain in Tau function. Aggregation assays carried out in presence of HDAC6 ZnF UBP showed its inhibitory effect both on full-length Tau (hTau40wt) and repeat Tau (K18wt) aggregation. Therapeutic strategies against Tau aggregation targets initial stages of aggregation to disallow the accumulation of toxic oligomers and protofilaments [304]. Further stages of aggregation involve stabilization of aggregate structures by cross-linking [305]. In our studies, HDAC6 ZnF UBP was found to be effective in hindering the initial aggregates formation in both full-length Tau and repeat Tau as well as destabilizing pre-formed aggregates accompanied by degradation leading to their dissolution. Also, the CD spectroscopy analysis of aggregation mixture of Tau with HDAC6 ZnF UBP showed the conformational shift from β -sheet (signature for aggregated Tau) towards random coil (signature for soluble Tau) [174]. Overall, these results show that HDAC6 ZnF UBP itself can modulate the aggregation propensity of Tau as well as its stability. *In vitro* aggregation assays carried out for Tau showed inhibitory effect of HDAC6 ZnF UBP on Tau aggregation in equimolar concentration. HDAC6 ZnF UBP was found to be equally effective in dissolving pre-formed aggregates (**Fig 6.1**). The effect of HDAC6 ZnF UBP on Tau aggregates was accompanied by its degradation which suggested physical association of HDAC6 ZnF UBP with Tau. Interaction studies between HDAC6 ZnF UBP and Tau revealed involvement of hydrophobic interactions and histidine and lysine residues in Tau. Thus, we hypothesized that the inhibitory mechanism of HDAC6 ZnF UBP involves weakening of

hydrophobic interaction and hindering salt bridge formation in Tau aggregates. We studied the role of HDAC6 ZnF UBP domain in direct interaction with Tau protein to explore their role in modulating aggregation; long before the ubiquitination event occurs. Our biochemical analysis suggested that HDAC6 ZnF UBP can interact transiently with Tau and increased degradation of Tau over time was observed when Tau was incubated with HDAC6 ZnF UBP. This triggers the possibility of involvement of this domain in tackling aggregates in a deacetylase-independent manner. Enhanced degradation of Tau in the presence of HDAC6 ZnF UBP does not involve cysteine protease activity of Tau as degradation was observed for the wild type Tau as well as Tau with

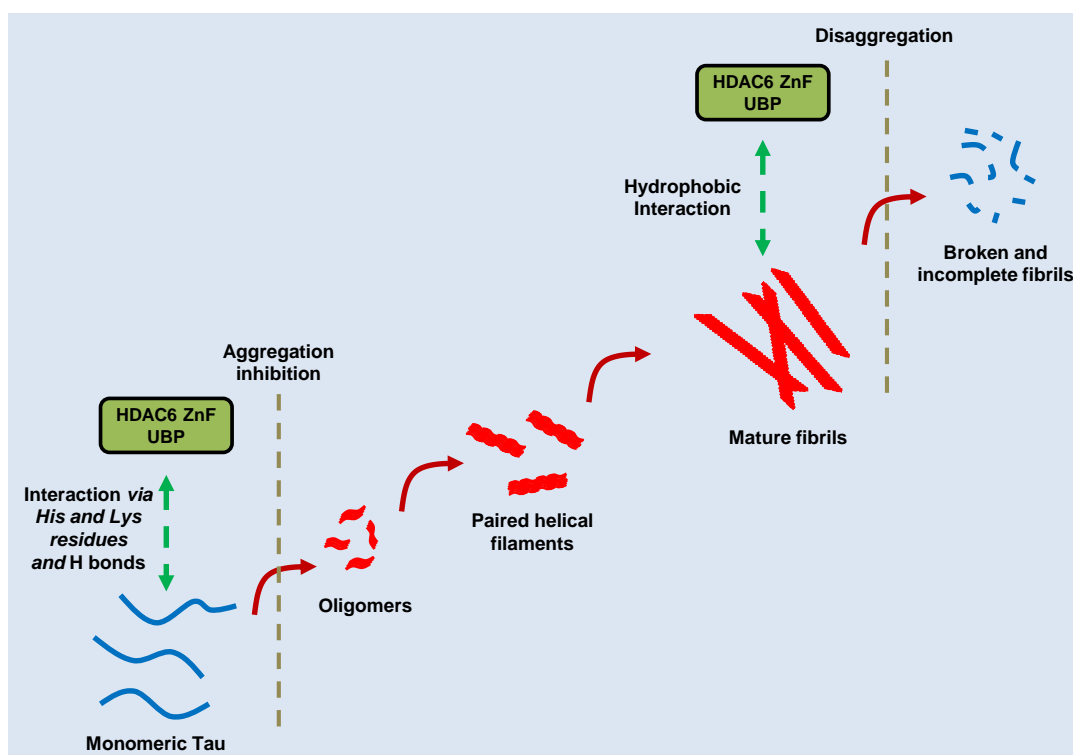


Fig. 6.1. HDAC6 ZnF UBP-mediated Tau aggregation inhibition and disaggregation. The efficacy of HDAC6 ZnF UBP in aggregation inhibition and disaggregation of pre-formed Tau aggregates was studied by *in vitro* assays. HDAC6 ZnF UBP interacts with Tau *via* hydrophobic interactions as well as through His and Lys residue majorly through its repeat domain. The interaction leads to weakening of intermolecular Tau interactions resulting in aggregation inhibition and disaggregation.

cysteine mutations. Tau has been reported to have intrinsic proteolytic function which leads to its autoprolysis. We hypothesize that interaction of HDAC6 ZnF UBP with Tau can catalyze the autoprolysis activity of Tau and bring about its degradation. Increased degradation of Tau over time was observed when Tau was incubated with HDAC6 ZnF UBP. In-silico data analysis also clearly suggest that the arginine (R1155) - aspartic acid (D283) interaction of HDAC6 ZnF UBP and repeat-Tau respectively could play a possible role in this protein-protein interaction supported by other interacting residues of Tau such as V275, Q276, I277 and N279 from the hexapeptide region and N286. Interaction through hydrophobic forces may be involved in Tau-

HDAC6 association as indicated by involvement of V300 and V363 revealed by 1H-15N HSQC NMR. Histidine residues H268, H299, H329, H330 and H362 showed chemical shift perturbations upon titration with HDAC6 ZnF UBP; of which H299 and H329 were found to interact hydrophobically indicated by interpreting the simulation data. The RMSF data from in-silico analysis also stated that the residues around 320-332 were highly unstable during the interaction. The change in the chemical shift of residues such as H329, H330 and K331 may be due to its structural instability during the interaction that may lead to change in structural conformation. The change in the chemical shift of residues may be indicative of a direct interaction between Tau and HDAC6 ZnF UBP or conformational changes in Tau brought about by its transient interact with HDAC6 ZnF UBP. The involvement of these residues in interaction with Tau may have a mechanistic role where it exerts a catalytic function. However, whether this effect originates from HDAC6 ZnF UBP or it is due to enhanced auto-proteolysis of Tau need to be explored further. Tau upon aggregation exposes hydrophobic patches which get buried in the core of the aggregate structure. HDAC6 ZnF UBP may associate with Tau involving hydrophobic residues and thus hindering aggregates formation or destabilizing the aggregate structure. However, the underlying mechanism leading to the degradation of Tau need to be further elucidated. Here, we hypothesize that interaction of HDAC6 ZnF UBP with Tau result in its degradation either due to enhancement of its auto-proteolysis function or inherent proteolytic activity of HDAC6 ZnF UBP domain (**Fig. 6.2**). We suggest that the association of HDAC6 ZnF UBP with Tau may enhance auto-proteolytic function of Tau or HDAC6 ZnF UBP itself has intrinsic proteolytic function similar to the other members of ZnF UBP containing proteins such as ubiquitin specific proteases (USPs) (**Fig. 6.3**) [199, 218]. Further study is required in this case to fully understand the process of HDAC6 ZnF UBP-mediated Tau degradation.

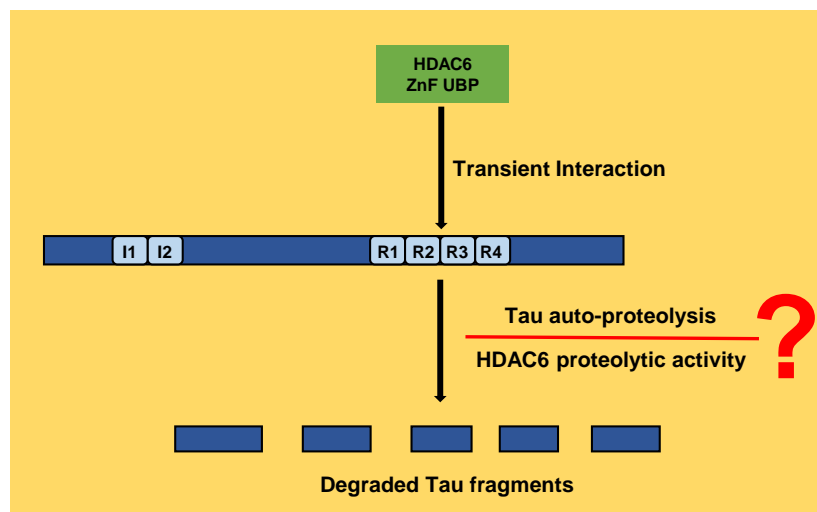


Fig. 6.2. HDAC6 ZnF UBP interacts transiently with Tau enhancing its degradation. Degradation of Tau in the presence of HDAC6 ZnF UBP can be attributed to either modulation of Tau stability by augmenting its auto-proteolysis or HDAC6 ZnF UBP itself exhibiting proteolytic function.

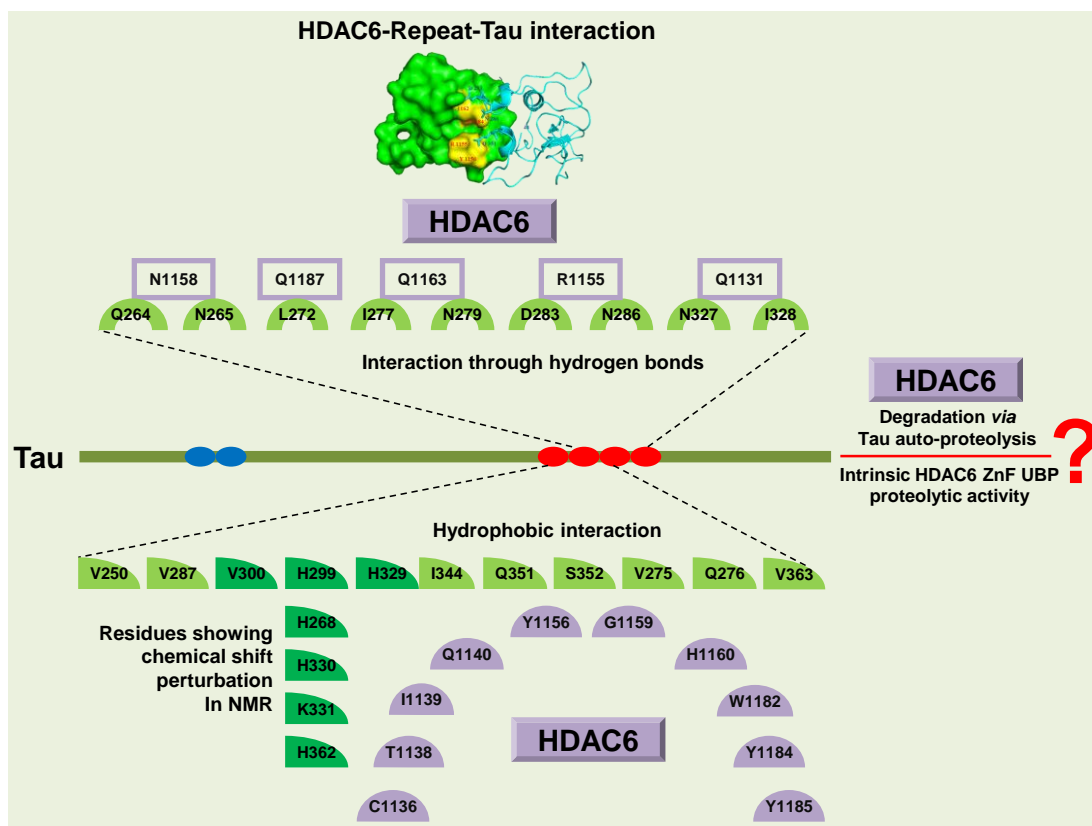


Fig. 6.3. HDAC6 ZnF UBP modulates stability and aggregation of Tau. HDAC6 ZnF UBP interacts transiently with microtubule-associated protein Tau mainly through its repeat region. Molecular dynamics and simulation suggested residues important for Tau-HDAC6 association and revealed the involvement of hydrogen bonds and hydrophobic forces. NMR analysis suggested five histidines, a lysine (K331) and a valine (V300) may be involved in ionic and hydrophobic interactions. Interaction of HDAC6 ZnF UBP with repeat region of Tau may destabilize Tau aggregates leading to their disruption and aggregation inhibition. Their interaction also results in degradation of Tau which may involve either Tau auto-proteolysis or possible proteolytic activity of HDAC6. The aggregation properties of Tau are also modulated by HDAC6 ZnF UBP as Tau aggregation inhibition as well as disaggregation of Tau aggregates was observed in the presence of HDAC6 ZnF UBP.

6.4 HDAC6 ZnF UBP plays an important role in diverse neuronal functions

The pathological attributes of AD are shown in the alteration of several neuronal functions. The progression of AD is marked by numerous losses of physiological functions. These include hindered cargo transport across the neurons; especially, the anterograde transport is affected due to defective microtubule dynamics [306]. Also, there is a depletion of myelin sheath leading to axonal damage and neurotransmission deficits [76]. The actin cytoskeleton is also affected resulting in overall morphology of neuronal cells. Neuron extensions form the intricate neuronal network, which are important for signal transduction [307]. Actin re-organization in a directional manner forms the basis of neuronal extensions. In AD, the actin regulation is impeded causing loss of neuronal extensions. Apart from these, aberrant signalling cascades presume during the disease progression due to over-activity or under-activity of regulatory proteins *viz.* kinases, phosphatases and others enzymes. Tau hyperphosphorylation is one of the key markers in AD

and disease-specific phosphoepitopes of Tau have been identified in the AD brain [308]. Notably, in Braak staging to characterize the progression of AD, phosphorylation at AT8 phospho-epitope (Ser202/Thr205) is considered as an important disease-associated phosphorylation [309]. Similarly, pT181 is another important phosphorylation site of Tau which is known to be associated with nuclear Tau dysfunction and also linked to the development of Amyloid- β pathology and development of AD in early stages [310-312]. There are other cellular factors which plays an important role in the etiology of AD. ApoE is a protein involved in lipid metabolism by mediating the mobilization of lipids by packaging and carrying them at different sites in the body through bloodstream [313]. Astrocytes produce ApoE in the central nervous system which facilitates cholesterol transport to neurons through its receptors on neuronal cells [313, 314]. It is known genetic risk factor in AD since one of its isoform named ApoE4 is involved in pathological processing of APP generating toxic Amyloid- β peptides [315].

HDAC6 levels are found to be elevated in the AD patients following increase in the aggregate burden in cells [111]. This suggests the possibility of involvement of this domain in tackling aggregates in a deacetylase-independent manner. We have investigated the involvement of HDAC6 ZnF UBP domain in neuronal functions that are critical with respect to AD. Neuro2a cells treated with various concentrations of HDAC6 ZnF UBP to assess their viability upon treatment using MTT assay and LDH assay. Phosphorylations at AT8 and pT181 phosphoepitopes of Tau are implicated in AD. The levels of phosphorylation at both these sites reduced when neuronal cells were treated with HDAC6 ZnF UBP at 50 nM concentration. Neuro2a showed no toxicity in the presence of HDAC6 ZnF UBP. pT181 and AT8 (pS202/pT205) are two pathological phosphorylation events of Tau implicated in AD [131]. Okadaic acid treatment increases the level of these two epitopes by inhibition of PP2a activity. Treatment with HDAC6 ZnF UBP decreased the levels of both pT181 and AT8. The effect possibly arises from replenishing the PP2a activity upon inhibition by OA rather than inhibition of phosphorylation [316]. Class II HDACs - HDAC1, HDAC6 and HDAC10 can form molecular complexes with phosphatases (PP1 or PP2a). However, HDAC6 was shown to interact only with the catalytic subunit of PP1 to form a complex retaining both phosphatase and deacetylase catalytic activity [317]. The binding of HDAC6 to PP1 was mapped to the second catalytic domain and C-terminal domain of HDAC6, which corresponds to ZnF UBP domain [316]. In order to understand the effect of HDAC6 ZnF UBP on phosphorylation, the levels of total GSK-3 β and its down-regulated form *i.e.* GSK-3 β phosphorylated at Ser9 (pGSK-3 β) were analyzed after HDAC6 ZnF UBP exposure. GSK-3 β is a versatile protein kinase with more than hundred substrates [243]. GSK-3 β acts on Tau in two different manners *i.e.* on pre-phosphorylated primed Tau and unprimed Tau [318]. In order for GSK-3 β to work on primed substrate, the N-terminal primed substrate binding domain provides binding-site for primed substrates upregulating the kinase activity of GSK-3 β . Phosphorylation at Serine 9 is the regulatory mechanism to down regulate GSK-3 β activity [230]. N-terminal domain with pSer9 acts as a pseudosubstrate for the primed substrate binding-domain of GSK-3 β restricting the binding of other primed substrates-like Tau [319]. HDAC6 ZnF UBP was found to increase the level of pSer9 phosphorylation on

GSK-3 β indicative of down-regulated GSK-3 β activity with HDAC6 treatment in neuro2a cells. Modulation of GSK-3 β by HDAC6 ZnF UBP may involve regulation of Akt *via* PP1. PP1 dephosphorylates Akt, which is a negative regulator of GSK-3 β in its phosphorylated state [320]. HDAC6 is known to associate with PP1 through its C-terminal region, which corresponds to ZnF UBP domain [316]. HDAC6 ZnF UBP addition to cells increases PP1-HDAC6 association rendering Akt in its active phosphorylated state, which in turn phosphorylates Ser9 on GSK-3 β down regulating its activity (**Fig 6.4**).

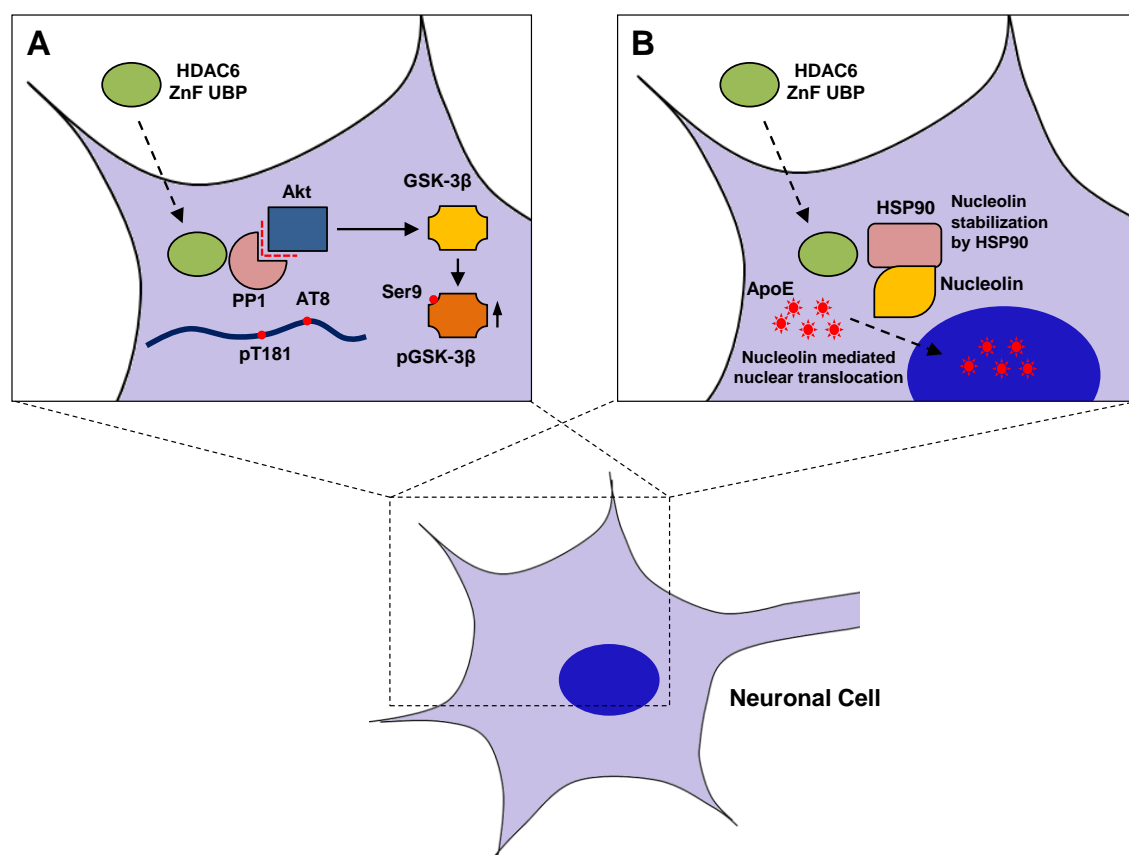


Fig. 6.4. Effect of HDAC6 ZnF UBP on Tau phosphorylation and ApoE localization. HDAC6 ZnF UBP is proposed to be involved in GSK-3 β regulation in Akt and PP1 dependent manner. GSK-3 β activity is negatively regulated by Akt kinase, which phosphorylates GSK-3 β at Ser9. Akt is active in its phosphorylated state which in turn is regulated by PP1. HDAC6 ZnF UBP associates with PP1 restricting it from dephosphorylating Akt, hence resulting in its active phosphorylated state. Enhanced ApoE localization upon HDAC6 ZnF UBP treatment may be mediated by nucleolin dependent transport of ApoE. ApoE requires an active transport system as it contains weak NLS signal. Nucleolin may serve this function as it is a known interacting partner of apolipoproteins and is stabilized by HSP90 whose activity is regulated by HDAC6.

The enhanced nuclear localization of ApoE may indicate in improved neuronal health [321]. ApoE can get translocated to the nucleus through a nuclear targeting chaperone nucleolin [254]. ApoE consists of weak nuclear localizing sequence, which indicates that there must be other mechanism involved in ApoE nuclear transport. Nucleolin is known to associate with apolipoproteins facilitating their translocation [322]. HDAC6 may mediate ApoE translocation

through HSP90 as it is known to stabilize nucleolin during mitosis (**Fig. 6.4**) [323]. However, the exact mechanism needs to be further elucidated.

HDAC6 is a known modulator of microtubule dynamics as well as actin re-organization and acts as an interacting partner for both cytoskeletal assemblies [324]. The formation of F-actin is required for cellular migration, attachment to extracellular matrix (ECM) and structural organization like neuronal extensions to form neurites [325-327]. Neuronal extensions are important to sense their environment and cell to cell communication. The loss of neuronal extensions in AD ultimately leads to neuronal cell death. We studied the effect of HDAC6 ZnF UBP, on cytoskeletal organization and found the ability of this domain to restructure cytoskeletal network. HDAC6 ZnF UBP treatment to neuronal cells resulted in enhancement of neuronal extensions suggesting that actin re-organization by HDAC6 may involve mechanisms other than deacetylation.

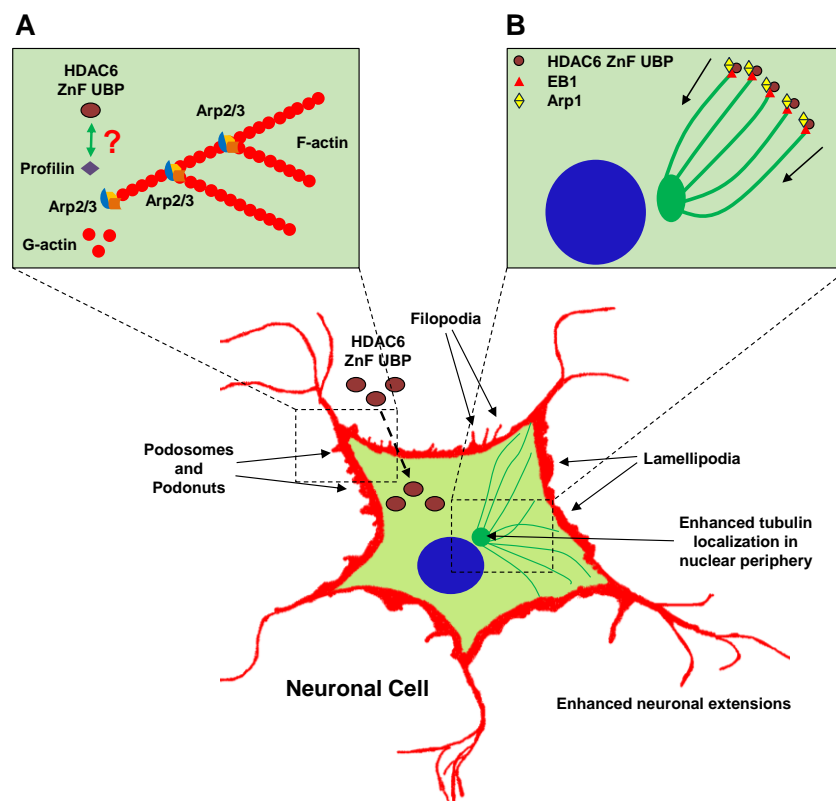


Fig. 6.5. Effect of HDAC6 ZnF UBP on cytoskeletal organization. HDAC6 ZnF UBP modulated the Actin polymerization and tubulin organization in neuro2a cells. It associates with profilin and Arp2/3, one of the actin polymerization factor to promote F-actin formation resulting in enhanced neuronal extensions and actin rich structure *viz.* podosomes, podonuts, lamellipodia and filopodia. Similarly, HDAC6 ZnF UBP promoted tubulin localization in nuclear periphery by associating with microtubule end-associated proteins EB1 and Arp1.

We observed the co-localization of actin and HDAC6 in the neurite extensions and the formation of other actin rich structure like podosomes, lamellipodia and filopodia further strengthen this concept. Podosomes are membranes invaginations formed in cells-like macrophages, dendritic,

smooth muscle, invasive cancer cells and in post-synaptic apparatus [328]. The association of HDAC6 ZnF UBP with the elements of actin polymerization in order to form F-actin may provide a clue about its role in actin assembly. HDAC6 ZnF UBP interacts with F-actin polymerizing factor profilin and branching factor Arp2/3, to mediate F-actin assembly which forms the basis of neuronal outgrowths including enhanced extensions, podosomes, lamellipodia and filopodia (**Fig. 6.5, Panel A**) [105]. Further, localization of tubulin in the nuclear periphery was observed upon HDAC6 ZnF UBP treatment. Growth and shrinkage rate of microtubules are affected by HDAC6 in a deacetylase independent manner. HDAC6 associates physically with end-binding protein1 (EB1) and a core component of Dynactin called Arp1 through its N and C terminal region but not with its catalytic domain [114]. Thus, the ZnF UBP domain of HDAC6 may be involved in binding with EB1 and Arp1, which in turn regulates microtubule growth and shrinkage as both these proteins are associated with the tip of growing microtubule (**Fig. 6.5, Panel B**). We hypothesize that HDAC6 ZnF UBP may regulate microtubule growth and shrinkage by associating with the proteins involved in tubulin polymerization. However, to deduce the exact mechanism of regulation, further studies are required.

6.5 Current status of therapeutic approaches against AD

The etiology of AD involves a variety of factors governing the onset and progression of disease. Thus, the therapeutic approach against AD incorporates multiple potential targets. This includes designing drugs to inhibit or dissolve the proteinaceous aggregates of Tau and Amyloid- β , targeting different protein kinases involved in the hyper-phosphorylation of Tau, using therapies to reduce the oxidative stress, which promotes neurodegeneration and ameliorating toxic effects like aberrant neurotransmission and neuro-inflammation. The therapeutic approaches against AD have limited success due to various reasons [329]. For example, acetylcholinesterase inhibitors used to prolong acetylcholine retention to improve neurotransmission, have modest effect, brief period of effectiveness and significant side-effects [330]. NMDA antagonists are used in the treatment of AD to reduce excito-toxicity of glutamate receptors [331]. These are substantially neurotoxic and can produce psychotic episodes in patients. Anti-inflammatory drugs have a mild and limited effect in improving the cognitive impairment associated with AD [332]. In order to ameliorate Amyloid- β toxicity, β and γ -secretase inhibitors are used. Secretase inhibitors reduce Amyloid- β burden and even inhibit Tau hyperphosphorylation but with mild to moderate side effects [333]. Similarly, immunotherapy against Amyloid- β or Tau aggregates provides a limited benefit as the symptoms of cognitive decline does not get reduced effectively. Aggregation inhibition and clearance of pre-formed aggregates also presents as an approach with limited benefits. Many natural and synthetic small molecules have been designed to target the aggregates but their effect is limited mainly due to less bioavailability or poor ability to cross the blood-brain barrier. The limitations of current therapeutic approaches show that the prevention of AD requires a multi-targeted approach to effectively salvage the neurodegenerative conditions. Thus, a combination of effective drugs or therapeutic agents having multi-faceted roles may provide desirable effects.

6.6 Therapeutic approaches against AD based on action of small molecules

Several classes of compounds have been screened and studied for their effectiveness against AD. Of the various kinds of small molecules under study as the therapeutics against AD, natural occurring molecules have the advantage of having no or less side effects. Melatonin, a neurohormone, has drawn attention as a therapeutic molecule for AD treatment and prevention due to its multiple roles as a neuroprotective agent [334]. Melatonin functions as an endocrine hormone to regulate circadian rhythms, anti-oxidant, anti-inflammatory agent, free radical scavenger, regulator of anti-oxidant enzymes and other key proteins like kinases. Various studies have been carried out on the efficacy of Melatonin against neurodegenerative conditions including AD and PD. It is found to be highly effective in preventing neurodegeneration and promotes neuronal health and survival.

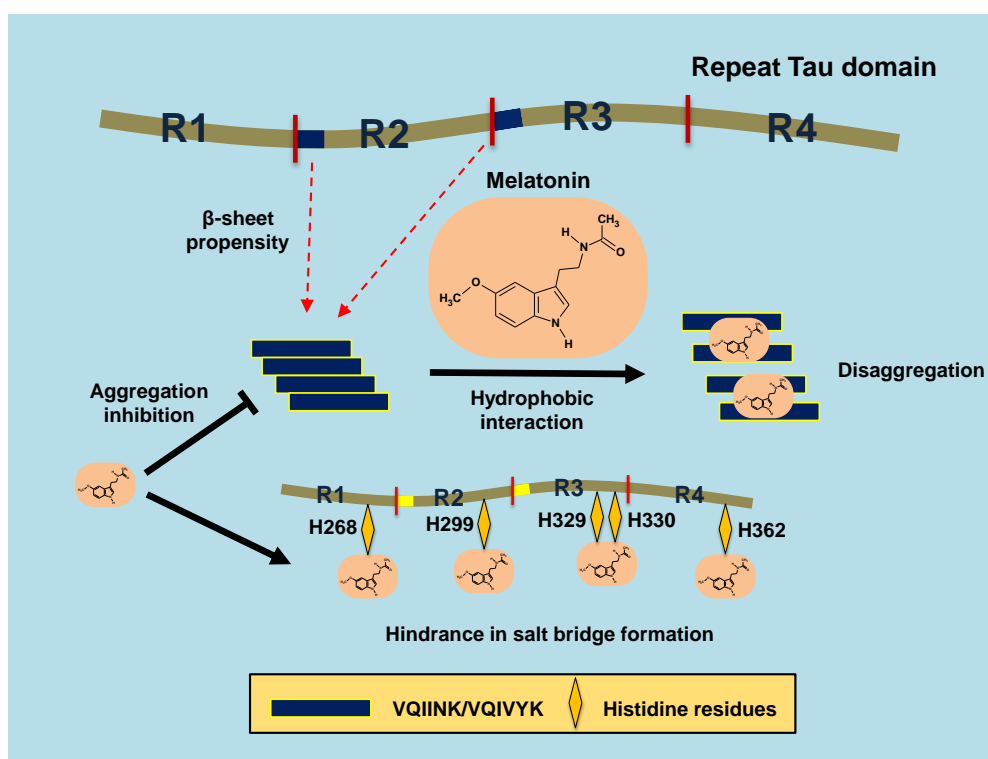


Fig. 6.6. Disaggregation of Tau aggregates by Melatonin. Melatonin showed its potency as an aggregation inhibitor as well as in disaggregation of repeat Tau aggregates. Salt bridges are formed between repeat Tau molecules, which strengthen the core of PHF during aggregation. Melatonin can bind to repeat Tau by associating with the Histidine residues and hindering the formation of salt bridges between two repeat molecules, thus inhibiting their aggregation. Melatonin can also interact with repeat Tau through hydrophobic interaction once the aggregation is established. Hydrophobic interaction with Melatonin weakens the Tau interaction in PHF assembly resulting in their disaggregation.

Melatonin has been studied for its role as an aggregation inhibitor against Amyloid- β and α -Synuclein aggregates and found to be effective against both amyloid aggregates. Melatonin interacts with A β 40 and A β 42 and inhibits the progressive formation of β -sheet structures and fibrillar aggregates [335, 336]. The aggregation effect is hypothesized to involve salt bridge

disruption between Asp and His residues through which Melatonin interacts. Similarly, in case of α -Synuclein, Melatonin inhibited both its oligomerization as well as fibrils formation *in vitro*. α -Synuclein showed reduction in the β -sheet content in the presence of Melatonin [275, 337]. We explored the potency of Melatonin against Tau aggregation and found it to be effective against pre-formed Tau fibrils at higher Melatonin concentration. Melatonin interacts with repeat region of Tau through histidine moieties which suggest mechanism similar to Amyloid- β aggregate disruption (**Fig. 6.6**). The interaction of Melatonin with repeat Tau was found to be highly dynamic and attains equilibrium having constant association and dissociation. NMR studies for the interaction of repeat Tau and Melatonin suggests that Melatonin binds to all five Histidine residues (H268, H299, H329, H330 and H362) in repeat Tau along with V300, K331 and V363. We propose a mechanism by which Melatonin exerts its disaggregation effect through its interaction with histidine residues and thus results in destabilization of aggregates assembly. Melatonin can hinder the salt bridge formation between two Tau molecules, which in turn hinders the strengthening of PHF assembly. Also, it weakens the PHF assembly through its hydrophobic interaction with the pre-formed aggregates. However, the concentration required to show its effect is high since the interaction between repeat Tau and Melatonin is weak as revealed by NMR and ITC. Also, it did not showed any significant effect on retention of cell-viability upon repeat Tau aggregates treatment. Thus, it is suggested to incorporate Melatonin along with other potent drugs to enhance the effect of therapeutics [338]. Melatonin serves a wide array of function as anti-oxidant, anti-inflammatory agent and modulator of other functions-like phosphorylation and gene regulation. In this aspect, the combination of Melatonin with other potent molecule, which allows the optimum activity of both, can be a helpful measure. Furthermore, we have found potency of Melatonin in modulating cell surface morphology and full-length Tau aggregation in another study [339]. The high bioavailability as well as pleiotropic functions of Melatonin makes it a good candidate for therapeutics in Alzheimer's disease. Melatonin administration at high doses (1 g/day) to human subjects has been shown to induce no toxic effect. The effectiveness of Melatonin against protein aggregation along with its beneficial properties in neuronal protection presents Melatonin as a potent neuroprotective drug which can be further improved.

Baicalein (5, 6, 7 trihydroxyflavone) is the major bioactive ingredient of Chinese herb *Scutellaria baicalensis*. The herb has been used in traditional medicine for the treatment of various ailments like neurological disorders, inflammatory conditions, cancer *etc.* Baicalein exhibit neuroprotective functions such as anti-inflammation, anti-oxidant, anti-apoptotic, aggregation inhibition *etc.*, which makes it a suitable candidate as a therapeutic molecule against neurodegenerative disease [340-342]. Baicalein is a natural flavonoid, which gets oxidized to quinone form and work as a covalent inhibitor as the reaction progresses.

Tau pathology undergoes a formation of series of intermittent species and the feasibility of their formation depends on both physiological concentration of free Tau and ability to form aggregation competent conformations [343]. The soluble oligomers of Tau are more toxic than

the Tau fibrils [344] and hence the Tau oligomers are gaining more attention as therapeutic targets in AD [345]. Baicalein has been widely studied for its aggregation inhibition and disaggregation properties against Amyloid- β and α -Synuclein aggregates. Baicalein has been found to be effective in inhibiting α -Synuclein aggregation in SH-SY5Y and Hela cells after inducing aggregation by using α -Synuclein oligomers [164, 342]. It is also capable of dissolving α -Synuclein fibrils as reported in an *in vitro* study [162]. Baicalein interacts with α -Synuclein and forms stable non-toxic oligomers resulting in the attenuation of further aggregation. Similarly, it is effective in Amyloid- β aggregation inhibition and alleviation of Amyloid- β induced toxicity [346]. Tau aggregation inhibitors either act to weaken the cross beta structures by inserting their rings between the beta sheet stacks or modify the protein or its intermediate aggregates, thus decreasing its aggregation potency [347]. We propose Baicalein belongs to the latter class of inhibitors as it binds and stabilizes the high molecular weight Tau oligomers, which are not capable of fibrillization. The ANS fluorescence clearly suggest the increased hydrophobicity of these sequestered molecules [196, 348]. In our studies, we tested the potency of Baicalein in disaggregation of repeat Tau aggregates and found it to significantly dissolve preformed Tau oligomers and fibrils (**Fig. 6.7**). Baicalein interacts weakly with repeat Tau and forms off-pathway stable oligomers. The size-exclusion chromatography results also support this hypothesis, as the Baicalein treated samples showed the disappearance of a peak corresponding to tetramer. Interestingly, there is an appearance of oligomeric species of higher order in the sample incubated with Baicalein. These findings strongly suggest that Baicalein exhibit inhibition activity by sequestration of Tau into oligomers of different nature and taking it off the pathway of aggregation. Although effective against inhibiting fibrillization, Baicalein also worked as a potent molecule for disaggregation of preformed Tau fibrils as well as oligomers. The ANS fluorescence studies clearly depict the decrease in fluorescence intensity in the initial stages after Baicalein addition, but are found to increase after 12-24 hours at higher concentrations. This behavior of ANS fluorescence can be attributed to the fact that increase in ANS fluorescence depends on binding with hydrophobic residues as well as with cationic amino acids like arginine and lysine [349]. Thus, the Baicalein stabilized oligomer interacts through their cationic residues even though the overall surface hydrophobicity is greatly reduced. The disaggregation potential of Baicalein upon treatment of Tau aggregates signifies that the interaction between these two involves rearrangement of bonds and change in binding energies. If the oligomers formed are stable enough that they do not further interact with other protein species, (either soluble Tau or other oligomers) it can lead to attenuation of further fibrillization of Tau. The Baicalein stabilized oligomers are non-toxic and results in dissolution of Tau fibrils. The aggregation inhibition property of Baicalein along with its other beneficial functions makes it a strong candidate for therapeutic molecule against AD.

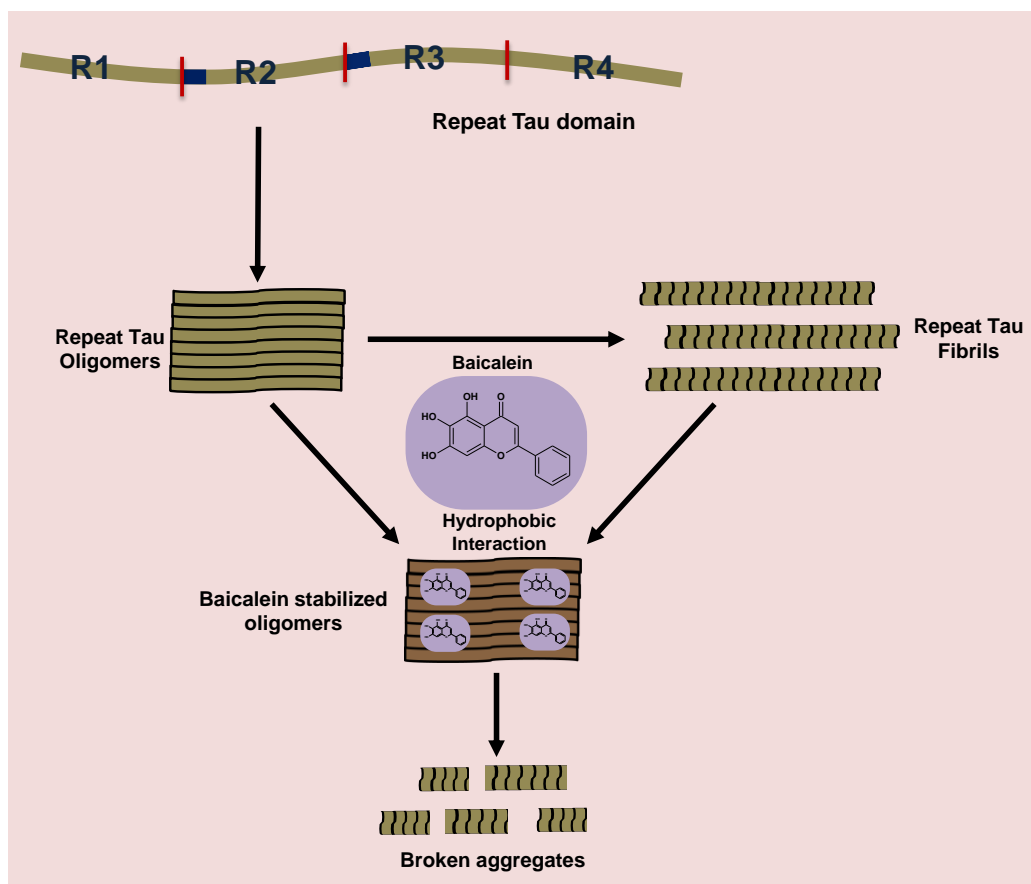


Fig. 6.7. Tau aggregation inhibition and disaggregation modulated by Baicalein. Baicalein is able to interact with soluble repeat Tau, Tau oligomers and mature Tau fibrils. It showed enhancement in the oligomeric population which are stabilized by Baicalein and do not aggregate further. Baicalein enables disaggregation of both Tau oligomers and fibrils through hydrophobic interaction leading to the formation of smaller non-amyloidogenic species.

Conclusion and Future directions

Conclusion

The modification of Tau into pathological form develops several toxic gain of function as well as result in loss of normal Tau functions. The formation of toxic Tau species in the form of insoluble oligomers and NFTs elicit responses which interfere with the normal functioning of neuronal cells. The formation of NFTs hinders with the organelle location and transport mechanism within the cell. Due to molecular crowding, cytoplasmic organelles are known to get displaced along with decrease in their numbers in the presence of NFTs. Cytoplasmic transport is also affected by the formation of NFT, which results in cellular homeostasis as important functions like proteasomal activity. Tau fibrils result in aberrant anterograde transport by dissociation of kinesin-1 from its vesicular cargo while the retrograde transport is retained. Further, microtubule assembly remains intact even in the presence of mature Tau aggregates *i.e.* NFTs. Thus, Tau toxicity does not initiate completely from NFTs but also involves intermediate species of aggregation *viz.* oligomers and protofilaments. Also, in an rTg4510 mice model with P301L Tau over-expression, later suppression of mutant Tau attenuated neuronal damage even NFTs continue to form. The oligomeric Tau species are reactive and promotes further aggregation of soluble Tau and elicit inflammatory response and damage to cell membrane. Thus, in order to effectively curb down the ill effect of Tau aggregates, therapeutic strategies need to be focused on targeting both mature fibrils as well as intermediate species. In our work, we have addressed the significance of HDAC6 ZnF UBP in Tau pathology and neuronal functions as well as potentiality of small molecules Melatonin and Baicalein against Tau aggregates. The findings of our study can be concluded as-

A. In order to study the dynamics and biophysical properties of Tau aggregates, *in vitro* aggregation assays proved to be a valuable tool and provide an important tool for screening of aggregation inhibitors. *In vitro* aggregation assays are designed to mimic the Tau aggregation in physiological conditions.

The molecular mechanisms involved in the aggregation of Tau protein involve interplay of various proteins. Tau interacts with various enzymes as well as non-enzymes, which regulates its function. Alterations in the interaction and function of these proteins may dispose Tau towards pathological form. We have studied and explored the role of HDAC6 ZnF UBP domain in modulation of Tau protein aggregation and other functions associated with neuronal health. HDAC6 ZnF UBP is an important protein involved in neurodegenerative diseases, which performs a protective function by mediating the clearance of aggregates through aggresome formation. Our studies have shown that HDAC6 ZnF UBP domain can interact directly with Tau protein resulting in its degradation. Further, it inhibits Tau aggregation and dissolves pre-formed aggregates reflecting its possible direct role in Tauopathies.

B. Earlier studies have shown that HDAC6 may have a dual role in AD depending upon the domain involved. The enzymatic activity through its catalytic domain renders deleterious effects leading to neuronal loss while ZnF UBP domain has been shown to have a protective function.

Our studies on HDAC6 ZnF UBP domain suggest the same as it showed protective functions when neuronal cells are exposed to HDAC6 ZnF UBP. HDAC6 ZnF UBP upon internalization in neurons resulted in decreased levels of Tau phosphorylation upon simultaneous OA treatment, enhanced pGSK-3 β (Ser9) levels indicating its downregulation and increased ApoE localization to nucleus. All these functions are indicative of improved neuronal health and survival. Further, in AD, cytoskeletal regulation gets adversely affected due to Tau loss of function and aberrant signaling cascades. HDAC6 ZnF UBP treatment resulted in enhanced neuritic extensions and formation of actin rich structures suggesting its role in actin dynamics. Also, tubulin was found to be localized in the nuclear periphery indicating HDAC6 ZnF UBP involvement in tubulin dynamics in deacetylase-independent manner. Overall, exploring the functions of HDAC6 ZnF UBP in neuroprotection provides an important therapeutic aspect in AD by promoting the domain function while keeping the deacetylase activity under control.

C. Both the small molecules (Melatonin and Baicalein) used in our study against Tau aggregation exhibit multiple neuroprotective function. Melatonin has a weak interaction with repeat Tau and mediates disaggregation of repeat Tau. It has been widely studied with respect to neurodegenerative diseases and has a great potential in therapeutics against AD owing to its multifaceted roles. We studied the potency of flavonoid Baicalein against preformed aggregates of repeat Tau in different stages of maturation and found that Baicalein can interact with the repeat region of Tau and direct them to form stable oligomers which are non-toxic in nature. Baicalein was found to interact both with early oligomers and mature fibrils to disaggregate the preformed aggregates.

Future directions

The underlying mechanisms of Tau protein aggregation and its stability involve interplay of many PTMs and Tau interacting partners. The modulation of Tau to acquire pathological form provides an opportunity to identify the key factors involved in the process. In this regard, HDAC6 ZnF UBP is proposed to have a novel function in direct Tau modulation in terms of its aggregation and stability. Further, it functions in diverse cellular pathways, which reflect its role in neuronal health. Augmenting the functions of HDAC6 ZnF UBP and understanding the mechanisms through which these functions are mediated can help in designing therapeutics targeting the specific neuronal deficits in AD.

The therapeutics against Tau aggregation in AD requires involvement of molecules capable of altering different aspects of neurodegeneration in a beneficial way. In this regard, Melatonin and Baicalein are the two important drug candidates, which we have studied with respect to Tau fibril disaggregation. Both these molecules have multiple protective functions like anti-oxidant, free-radical scavenger, down-regulator of inflammatory conditions and modulators of proteins involved in neurodegeneration. Their protective functions have been extensively studied with respect to pathological conditions involving Amyloid- β and α -Synuclein. We explored their role in the modulation of Tau aggregates. Both the molecules interact with Tau and were found to

dissolve Tau aggregates through different mechanisms. Melatonin interact with Tau either hydrophobically weakening Tau-Tau interaction or through His residues resulting in salt-bridge disruption in aggregates. Baicalein forms stable oligomeric species with Tau inhibiting their further aggregation.

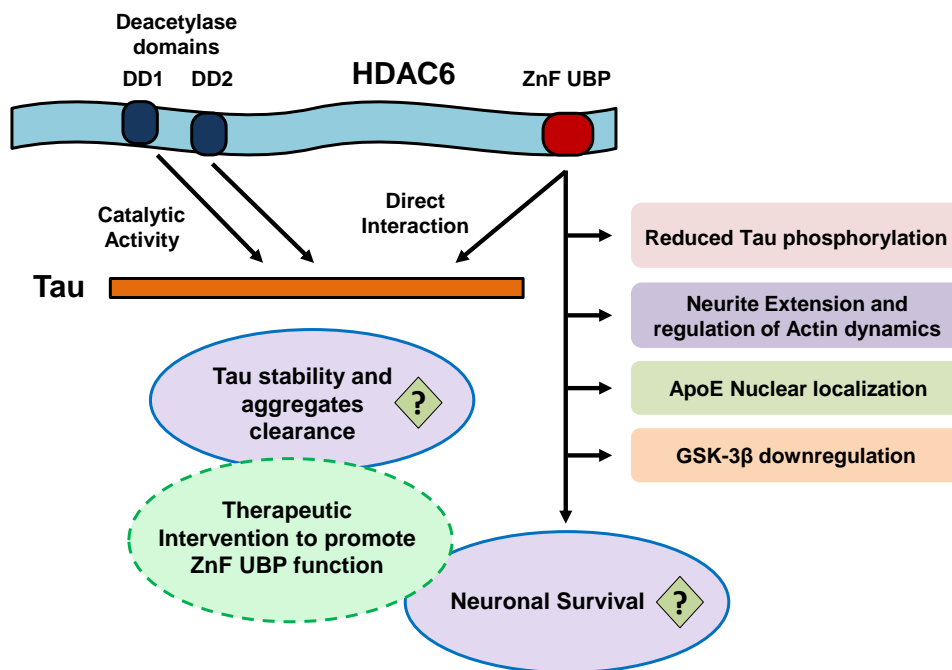


Figure I. Proposed effects of HDAC6 ZnF UBP on Tau stability and neuronal health. The neuronal loss in Alzheimer’s disease involves a myriad of factors, which are either ‘cause or effect’ of pathological cascade. The therapeutic approach for the prevention and cure of AD would require a multifactorial approach on various levels, which can promote neuronal survival as well as Tau clearance. Augmentation of HDAC6 ZnF UBP function can have a potential to develop a beneficial therapeutic advancement.

The prevention and treatment of AD requires a multi-targeted approach in order to modulate various pathological aspects (**Fig. I**). By intervening the function of HDAC6 to promote ZnF UBP domain may provide a suitable direction to promote the restoration of Tau homeostasis in Tauopathies while the small molecule therapy involving Melatonin and Baicalein in combination of other potent drugs can help in preventing the progression of Tau aggregation and provide neuronal protection.

Bibliography

1. Frydman, J., *Folding of newly translated proteins in vivo: the role of molecular chaperones*. Annual review of biochemistry, 2001. **70**(1): p. 603-647.
2. Eder, J. and A.R. Fersht, *Pro-sequence-assisted protein folding*. Molecular microbiology, 1995. **16**(4): p. 609-614.
3. Onuchic, J.N., Z. Luthey-Schulten, and P.G. Wolynes, *Theory of protein folding: the energy landscape perspective*. Annual review of physical chemistry, 1997. **48**(1): p. 545-600.
4. Brockwell, D.J. and S.E. Radford, *Intermediates: ubiquitous species on folding energy landscapes?* Current opinion in structural biology, 2007. **17**(1): p. 30-37.
5. Roder, H. and W. Colón, *Kinetic role of early intermediates in protein folding*. Current opinion in structural biology, 1997. **7**(1): p. 15-28.
6. Soto, C., *Unfolding the role of protein misfolding in neurodegenerative diseases*. Nature Reviews Neuroscience, 2003. **4**(1): p. 49-60.
7. Mandelkow, E.-M. and E. Mandelkow, *Tau in Alzheimer's disease*. Trends in cell biology, 1998. **8**(11): p. 425-427.
8. Baba, M., et al., *Aggregation of alpha-synuclein in Lewy bodies of sporadic Parkinson's disease and dementia with Lewy bodies*. The American journal of pathology, 1998. **152**(4): p. 879.
9. Irwin, D.J., V.M.-Y. Lee, and J.Q. Trojanowski, *Parkinson's disease dementia: convergence of α -synuclein, tau and amyloid- β pathologies*. Nature Reviews Neuroscience, 2013. **14**(9): p. 626-636.
10. Creighton, T.E., N.J. Darby, and J. Kemmink, *The roles of partly folded intermediates in protein folding*. The FASEB journal, 1996. **10**(1): p. 110-118.
11. Lasagna-Reeves, C.A., et al., *Tau oligomers impair memory and induce synaptic and mitochondrial dysfunction in wild-type mice*. Molecular neurodegeneration, 2011. **6**(1): p. 39.
12. Mandelkow, E.-M. and E. Mandelkow, *Biochemistry and cell biology of tau protein in neurofibrillary degeneration*. Cold Spring Harbor perspectives in medicine, 2012. **2**(7): p. a006247.
13. Wang, Y. and E. Mandelkow, *Tau in physiology and pathology*. Nature reviews neuroscience, 2016. **17**(1): p. 22.
14. Kadavath, H., et al., *Tau stabilizes microtubules by binding at the interface between tubulin heterodimers*. Proceedings of the National Academy of Sciences, 2015. **112**(24): p. 7501-7506.
15. Brandt, R. and G. Lee, *Functional organization of microtubule-associated protein tau. Identification of regions which affect microtubule growth, nucleation, and bundle formation in vitro*. Journal of Biological Chemistry, 1993. **268**(5): p. 3414-3419.
16. Sobów, T., M. Flirski, and P.P. Liberski, *Amyloid-beta and tau proteins as biochemical markers of Alzheimer's*. Acta Neurobiol Exp, 2004. **64**: p. 53-70.
17. Chiti, F. and C.M. Dobson, *Protein misfolding, amyloid formation, and human disease: a summary of progress over the last decade*. Annual review of biochemistry, 2017. **86**: p. 27-68.
18. Mann, D., et al., *Predominant deposition of amyloid-beta 42 (43) in plaques in cases of Alzheimer's disease and hereditary cerebral hemorrhage associated with mutations in the amyloid precursor protein gene*. The American journal of pathology, 1996. **148**(4): p. 1257.
19. Hartmann, T., *Intracellular biology of Alzheimer's disease amyloid beta peptide*. European archives of psychiatry and clinical neuroscience, 1999. **249**(6): p. 291-298.
20. Selkoe, D.J., *The molecular pathology of Alzheimer's disease*. Neuron, 1991. **6**(4): p. 487-498.

21. Mukrasch, M.D., et al., *Sites of tau important for aggregation populate β -structure and bind to microtubules and polyanions*. Journal of Biological Chemistry, 2005. **280**(26): p. 24978-24986.
22. Von Bergen, M., et al., *Tau aggregation is driven by a transition from random coil to beta sheet structure*. Biochimica et Biophysica Acta (BBA)-Molecular Basis of Disease, 2005. **1739**(2-3): p. 158-166.
23. Zabik, N.L., M.M. Imhof, and S. Martic-Milne, *Structural evaluations of tau protein conformation: Methodologies and approaches*. Biochemistry and Cell Biology, 2017. **95**(3): p. 338-349.
24. Zhu, H.-L., et al., *Quantitative characterization of heparin binding to tau protein implication for inducer-mediated tau filament formation*. Journal of Biological Chemistry, 2010. **285**(6): p. 3592-3599.
25. Wagner, U., et al., *Cellular phosphorylation of tau by GSK-3 beta influences tau binding to microtubules and microtubule organisation*. Journal of cell science, 1996. **109**(6): p. 1537-1543.
26. Ferrer, I., et al., *Current advances on different kinases involved in tau phosphorylation, and implications in Alzheimer's disease and tauopathies*. Current Alzheimer Research, 2005. **2**(1): p. 3-18.
27. Martin, L., et al., *Tau protein phosphatases in Alzheimer's disease: the leading role of PP2A*. Ageing research reviews, 2013. **12**(1): p. 39-49.
28. Sevcik, J., et al., *X-ray structure of the PHF core C-terminus: insight into the folding of the intrinsically disordered protein tau in Alzheimer's disease*. FEBS letters, 2007. **581**(30): p. 5872-5878.
29. Johnson, G.V. and W.H. Stoothoff, *Tau phosphorylation in neuronal cell function and dysfunction*. Journal of cell science, 2004. **117**(24): p. 5721-5729.
30. Buée, L., et al., *Tau protein isoforms, phosphorylation and role in neurodegenerative disorders*. Brain Research Reviews, 2000. **33**(1): p. 95-130.
31. Martin, L., X. Latypova, and F. Terro, *Post-translational modifications of tau protein: implications for Alzheimer's disease*. Neurochemistry international, 2011. **58**(4): p. 458-471.
32. Gong, C.-X., et al., *Phosphorylation of microtubule-associated protein tau is regulated by protein phosphatase 2A in mammalian brain implications for neurofibrillary degeneration in Alzheimer's disease*. Journal of Biological Chemistry, 2000. **275**(8): p. 5535-5544.
33. Liu, F., et al., *Contributions of protein phosphatases PP1, PP2A, PP2B and PP5 to the regulation of tau phosphorylation*. European Journal of Neuroscience, 2005. **22**(8): p. 1942-1950.
34. Chen, S., et al., *PP2A 1 affects Tau phosphorylation via association with the catalytic subunit of protein phosphatase 2A*. Journal of Biological Chemistry, 2008. **283**(16): p. 10513-10521.
35. Kontaxi, C., P. Piccardo, and A.C. Gill, *Lysine-directed post-translational modifications of tau protein in Alzheimer's disease and related Tauopathies*. Frontiers in molecular biosciences, 2017. **4**: p. 56.
36. Yan, S., et al., *Glycated tau protein in Alzheimer disease: a mechanism for induction of oxidant stress*. Proceedings of the National Academy of Sciences, 1994. **91**(16): p. 7787-7791.
37. Li, J., et al., *Advanced glycation end products and neurodegenerative diseases: mechanisms and perspective*. Journal of the neurological sciences, 2012. **317**(1-2): p. 1-5.
38. Necula, M. and J. Kuret, *Pseudophosphorylation and glycation of tau protein enhance but do not trigger fibrillization in vitro*. Journal of Biological Chemistry, 2004. **279**(48): p. 49694-49703.
39. Kuhla, B., et al., *Effect of pseudophosphorylation and cross-linking by lipid peroxidation and advanced glycation end product precursors on tau aggregation and filament formation*. Journal of Biological Chemistry, 2007. **282**(10): p. 6984-6991.
40. Morishima-Kawashima, M., et al., *Ubiquitin is conjugated with amino-terminally processed tau in paired helical filaments*. Neuron, 1993. **10**(6): p. 1151-1160.

41. Kim, H.T., et al., *Certain pairs of ubiquitin-conjugating enzymes (E2s) and ubiquitin-protein ligases (E3s) synthesize nondegradable forked ubiquitin chains containing all possible isopeptide linkages*. Journal of biological chemistry, 2007. **282**(24): p. 17375-17386.
42. Zhang, Y.-J., et al., *Carboxyl terminus of heat-shock cognate 70-interacting protein degrades tau regardless its phosphorylation status without affecting the spatial memory of the rats*. Journal of Neural Transmission, 2008. **115**(3): p. 483-491.
43. Dorval, V. and P.E. Fraser, *Small ubiquitin-like modifier (SUMO) modification of natively unfolded proteins tau and α -synuclein*. Journal of Biological Chemistry, 2006. **281**(15): p. 9919-9924.
44. Takahashi, K., et al., *SUMO-1 immunoreactivity co-localizes with phospho-Tau in APP transgenic mice but not in mutant Tau transgenic mice*. Neuroscience letters, 2008. **441**(1): p. 90-93.
45. Luo, H.-B., et al., *SUMOylation at K340 inhibits tau degradation through deregulating its phosphorylation and ubiquitination*. Proceedings of the National Academy of Sciences, 2014. **111**(46): p. 16586-16591.
46. Webb, K.J., et al., *Identification of protein N-terminal methyltransferases in yeast and humans*. Biochemistry, 2010. **49**(25): p. 5225-5235.
47. Thomas, S.N., et al., *Dual modification of Alzheimer's disease PHF-tau protein by lysine methylation and ubiquitylation: a mass spectrometry approach*. Acta neuropathologica, 2012. **123**(1): p. 105-117.
48. Funk, K.E., et al., *Lysine methylation is an endogenous post-translational modification of tau protein in human brain and a modulator of aggregation propensity*. Biochemical Journal, 2014. **462**(1): p. 77-88.
49. Min, S.-W., et al., *Critical role of acetylation in tau-mediated neurodegeneration and cognitive deficits*. Nature medicine, 2015. **21**(10): p. 1154.
50. Cohen, T.J., et al., *Intrinsic tau acetylation is coupled to auto-proteolytic tau fragmentation*. PloS one, 2016. **11**(7).
51. Gorsky, M.K., et al., *Acetylation mimic of lysine 280 exacerbates human Tau neurotoxicity in vivo*. Scientific reports, 2016. **6**(1): p. 1-12.
52. Cook, C., et al., *Acetylation: a new key to unlock tau's role in neurodegeneration*. Alzheimer's research & therapy, 2014. **6**(3): p. 29.
53. Cook, C., et al., *Loss of HDAC6, a novel CHIP substrate, alleviates abnormal tau accumulation*. Human molecular genetics, 2012. **21**(13): p. 2936-2945.
54. Ding, H., P.J. Dolan, and G.V. Johnson, *Histone deacetylase 6 interacts with the microtubule-associated protein tau*. Journal of neurochemistry, 2008. **106**(5): p. 2119-2130.
55. Wang, Y., et al., *Proteolytic processing of tau*. 2010, Portland Press Ltd.
56. Gamblin, T.C., et al., *Caspase cleavage of tau: linking amyloid and neurofibrillary tangles in Alzheimer's disease*. Proceedings of the national academy of sciences, 2003. **100**(17): p. 10032-10037.
57. Rohn, T.T., et al., *Caspase-9 activation and caspase cleavage of tau in the Alzheimer's disease brain*. Neurobiology of disease, 2002. **11**(2): p. 341-354.
58. Yang, L.S. and H. Ksiezak-Reding, *Calpain-induced proteolysis of normal human tau and tau associated with paired helical filaments*. European journal of biochemistry, 1995. **233**(1): p. 9-17.
59. Goll, D.E., et al., *Is calpain activity regulated by membranes and autolysis or by calcium and calpastatin?* Bioessays, 1992. **14**(8): p. 549-556.
60. Steiner, B., et al., *Phosphorylation of microtubule-associated protein tau: identification of the site for Ca²⁺ (+)-calmodulin dependent kinase and relationship with tau phosphorylation in Alzheimer tangles*. The EMBO journal, 1990. **9**(11): p. 3539-3544.

61. Watanabe, A., et al., *Molecular aging of tau: disulfide-independent aggregation and non-enzymatic degradation in vitro and in vivo*. Journal of neurochemistry, 2004. **90**(6): p. 1302-1311.
62. Poepsel, S., et al., *Determinants of amyloid fibril degradation by the PDZ protease HTRA1*. Nature chemical biology, 2015. **11**(11): p. 862-869.
63. Chu, Q., et al., *Htra1 proteolysis of ApoE in vitro is allele selective*. Journal of the American Chemical Society, 2016. **138**(30): p. 9473-9478.
64. Ding, W.-X. and X.-M. Yin, *Sorting, recognition and activation of the misfolded protein degradation pathways through macroautophagy and the proteasome*. Autophagy, 2008. **4**(2): p. 141-150.
65. David, D.C., et al., *Proteasomal degradation of tau protein*. Journal of neurochemistry, 2002. **83**(1): p. 176-185.
66. Duennwald, M.L., *Cellular stress responses in protein misfolding diseases*. Future science OA, 2015. **1**(2).
67. Ruijter, A.J.d., et al., *Histone deacetylases (HDACs): characterization of the classical HDAC family*. Biochemical Journal, 2003. **370**(3): p. 737-749.
68. Yao, Y.-L. and W.-M. Yang, *Beyond histone and deacetylase: an overview of cytoplasmic histone deacetylases and their nonhistone substrates*. BioMed Research International, 2010. **2011**.
69. Ouyang, H., et al., *Protein aggregates are recruited to aggresome by histone deacetylase 6 via unanchored ubiquitin C termini*. Journal of Biological Chemistry, 2012. **287**(4): p. 2317-2327.
70. Kawaguchi, Y., et al., *The deacetylase HDAC6 regulates aggresome formation and cell viability in response to misfolded protein stress*. Cell, 2003. **115**(6): p. 727-738.
71. Pandey, U.B., et al., *HDAC6 rescues neurodegeneration and provides an essential link between autophagy and the UPS*. Nature, 2007. **447**(7146): p. 860-864.
72. Borza, L.R., *A review on the cause-effect relationship between oxidative stress and toxic proteins in the pathogenesis of neurodegenerative diseases*. The Medical-Surgical Journal, 2014. **118**(1): p. 19-27.
73. Eckert, A., et al., *Convergence of amyloid- β and tau pathologies on mitochondria in vivo*. Molecular neurobiology, 2010. **41**(2-3): p. 107-114.
74. Haque, M., et al., *Crosstalk between Oxidative Stress and Tauopathy*. International Journal of Molecular Sciences, 2019. **20**(8): p. 1959.
75. Liu, Z., et al., *The ambiguous relationship of oxidative stress, tau hyperphosphorylation, and autophagy dysfunction in Alzheimer's disease*. Oxidative medicine and cellular longevity, 2015. **2015**.
76. Dong, Y.-X., et al., *Association between Alzheimer's disease pathogenesis and early demyelination and oligodendrocyte dysfunction*. Neural regeneration research, 2018. **13**(5): p. 908.
77. Das, R. and S. Chinnathambi, *Microglial priming of antigen presentation and adaptive stimulation in Alzheimer's disease*. Cellular and Molecular Life Sciences, 2019: p. 1-14.
78. Ingelsson, M., et al., *Early A β accumulation and progressive synaptic loss, gliosis, and tangle formation in AD brain*. Neurology, 2004. **62**(6): p. 925-931.
79. Shen, J., *Impaired neurotransmitter release in Alzheimer's and Parkinson's diseases*. Neurodegenerative Diseases, 2010. **7**(1-3): p. 80-83.
80. Zhou, L., et al., *Tau association with synaptic vesicles causes presynaptic dysfunction*. Nature communications, 2017. **8**(1): p. 1-13.
81. Rush, T., et al., *Synaptotoxicity in Alzheimer's disease involved a dysregulation of actin cytoskeleton dynamics through cofilin 1 phosphorylation*. Journal of Neuroscience, 2018. **38**(48): p. 10349-10361.

82. Cho, Y. and V. Cavalli, *HDAC signaling in neuronal development and axon regeneration*. Current opinion in neurobiology, 2014. **27**: p. 118-126.
83. Yang, X.-J. and S. Grégoire, *Class II histone deacetylases: from sequence to function, regulation, and clinical implication*. Molecular and cellular biology, 2005. **25**(8): p. 2873-2884.
84. Bertos, N.R., A.H. Wang, and X.-J. Yang, *Class II histone deacetylases: structure, function, and regulation*. Biochemistry and cell biology, 2001. **79**(3): p. 243-252.
85. Seto, E. and M. Yoshida, *Erasers of histone acetylation: the histone deacetylase enzymes*. Cold Spring Harbor perspectives in biology, 2014. **6**(4): p. a018713.
86. Donmez, G. and T.F. Outeiro, *SIRT1 and SIRT2: emerging targets in neurodegeneration*. EMBO molecular medicine, 2013. **5**(3): p. 344-352.
87. Outeiro, T.F., O. Marques, and A. Kazantsev, *Therapeutic role of sirtuins in neurodegenerative disease*. Biochimica et Biophysica Acta (BBA)-Molecular Basis of Disease, 2008. **1782**(6): p. 363-369.
88. Morrison, B.E., et al., *Neuroprotection by histone deacetylase-related protein*. Molecular and cellular biology, 2006. **26**(9): p. 3550-3564.
89. Dobbin, M.M., et al., *SIRT1 collaborates with ATM and HDAC1 to maintain genomic stability in neurons*. Nature neuroscience, 2013. **16**(8): p. 1008.
90. Contreras, P.S., et al., *Neuronal gene repression in Niemann–Pick type C models is mediated by the c-Abl/HDAC2 signaling pathway*. Biochimica et Biophysica Acta (BBA)-Gene Regulatory Mechanisms, 2016. **1859**(2): p. 269-279.
91. Guan, J.-S., et al., *HDAC2 negatively regulates memory formation and synaptic plasticity*. Nature, 2009. **459**(7243): p. 55-60.
92. Bhaskara, S., et al., *Hdac3 is essential for the maintenance of chromatin structure and genome stability*. Cancer cell, 2010. **18**(5): p. 436-447.
93. Broide, R.S., et al., *Distribution of histone deacetylases 1–11 in the rat brain*. Journal of Molecular Neuroscience, 2007. **31**(1): p. 47-58.
94. Bardai, F.H. and S.R. D'Mello, *Selective toxicity by HDAC3 in neurons: regulation by Akt and GSK3 β* . Journal of Neuroscience, 2011. **31**(5): p. 1746-1751.
95. McKinsey, T.A., et al., *Signal-dependent nuclear export of a histone deacetylase regulates muscle differentiation*. Nature, 2000. **408**(6808): p. 106-111.
96. Majdzadeh, N., et al., *HDAC4 inhibits cell-cycle progression and protects neurons from cell death*. Developmental neurobiology, 2008. **68**(8): p. 1076-1092.
97. Chen, B. and C.L. Cepko, *HDAC4 regulates neuronal survival in normal and diseased retinas*. Science, 2009. **323**(5911): p. 256-259.
98. Hageman, J., et al., *A DNAJB chaperone subfamily with HDAC-dependent activities suppresses toxic protein aggregation*. Molecular cell, 2010. **37**(3): p. 355-369.
99. Herrup, K., J. Li, and J. Chen, *The role of ATM and DNA damage in neurons: upstream and downstream connections*. DNA repair, 2013. **12**(8): p. 600-604.
100. Mielcarek, M., et al., *SAHA decreases HDAC 2 and 4 levels in vivo and improves molecular phenotypes in the R6/2 mouse model of Huntington's disease*. PloS one, 2011. **6**(11).
101. Cho, Y., et al., *Injury-induced HDAC5 nuclear export is essential for axon regeneration*. Cell, 2013. **155**(4): p. 894-908.
102. Thomas, E.A., *Focal nature of neurological disorders necessitates isotype-selective histone deacetylase (HDAC) inhibitors*. Molecular neurobiology, 2009. **40**(1): p. 33-45.
103. Boyault, C., et al., *HDAC6 controls major cell response pathways to cytotoxic accumulation of protein aggregates*. Genes & development, 2007. **21**(17): p. 2172-2181.

104. Dompierre, J.P., et al., *Histone deacetylase 6 inhibition compensates for the transport deficit in Huntington's disease by increasing tubulin acetylation*. Journal of Neuroscience, 2007. **27**(13): p. 3571-3583.
105. Valenzuela-Fernandez, A., et al., *HDAC6: a key regulator of cytoskeleton, cell migration and cell-cell interactions*. Trends in cell biology, 2008. **18**(6): p. 291-297.
106. Jung, H.-Y., et al., *RASSF1A suppresses cell migration through inactivation of HDAC6 and increase of acetylated α -tubulin*. Cancer research and treatment: official journal of Korean Cancer Association, 2013. **45**(2): p. 134.
107. Yan, Y. and R. Jiao, *HDAC6: A MoleCule with Multiple FunCtions in neuroDegenerAtive DiseAses*. The Functions, Disease-Related Dysfunctions, and Therapeutic Targeting of Neuronal Mitochondria, 2015: p. 146.
108. Watabe, M. and T. Nakaki, *Protein kinase CK2 regulates the formation and clearance of aggresomes in response to stress*. Journal of cell science, 2011. **124**(9): p. 1519-1532.
109. Han, Y., et al., *Acetylation of histone deacetylase 6 by p300 attenuates its deacetylase activity*. Biochemical and biophysical research communications, 2009. **383**(1): p. 88-92.
110. Di Fulvio, S., et al., *Dysferlin interacts with histone deacetylase 6 and increases alpha-tubulin acetylation*. PloS one, 2011. **6**(12): p. e28563.
111. Zhang, L., S. Sheng, and C. Qin, *The role of HDAC6 in Alzheimer's disease*. Journal of Alzheimer's Disease, 2013. **33**(2): p. 283-295.
112. Yan, J., *Interplay between HDAC6 and its interacting partners: essential roles in the aggresome-autophagy pathway and neurodegenerative diseases*. DNA and cell biology, 2014. **33**(9): p. 567-580.
113. Zhang, Y., et al., *HDAC-6 interacts with and deacetylates tubulin and microtubules in vivo*. The EMBO journal, 2003. **22**(5): p. 1168-1179.
114. Zilberman, Y., et al., *Regulation of microtubule dynamics by inhibition of the tubulin deacetylase HDAC6*. Journal of cell science, 2009. **122**(19): p. 3531-3541.
115. Miyake, Y., et al., *Structural insights into HDAC6 tubulin deacetylation and its selective inhibition*. Nature chemical biology, 2016. **12**(9): p. 748.
116. Zhou, D., Y.-J. Choi, and J.-H. Kim, *Histone deacetylase 6 (HDAC6) is an essential factor for oocyte maturation and asymmetric division in mice*. Scientific reports, 2017. **7**(1): p. 1-8.
117. d'Ydewalle, C., E. Bogaert, and L. Van Den Bosch, *HDAC 6 at the Intersection of Neuroprotection and Neurodegeneration*. Traffic, 2012. **13**(6): p. 771-779.
118. Albiges-Rizo, C., et al., *Actin machinery and mechanosensitivity in invadopodia, podosomes and focal adhesions*. Journal of cell science, 2009. **122**(17): p. 3037-3049.
119. Perez, M., et al., *Tau—an inhibitor of deacetylase HDAC6 function*. Journal of neurochemistry, 2009. **109**(6): p. 1756-1766.
120. Balmik, A.A., S.K. Sonawane, and S. Chinnathambi, *Modulation of Actin network and Tau phosphorylation by HDAC6 ZnF UBP domain*. BioRxiv, 2019: p. 702571.
121. Forman, M.S., J.Q. Trojanowski, and V.M. Lee, *Neurodegenerative diseases: a decade of discoveries paves the way for therapeutic breakthroughs*. Nature medicine, 2004. **10**(10): p. 1055-1063.
122. Sochocka, M., K. Zwolinska, and J. Leszek, *The infectious etiology of Alzheimer's disease*. Current neuropharmacology, 2017. **15**(7): p. 996-1009.
123. Wang, W.-Y., et al., *Role of pro-inflammatory cytokines released from microglia in Alzheimer's disease*. Annals of translational medicine, 2015. **3**(10).
124. Kowalska, A., *The beta-amyloid cascade hypothesis: a sequence of events leading to neurodegeneration in Alzheimer's disease*. Neurologia i neurochirurgia polska, 2004. **38**(5): p. 405-411.

125. Haass, C. and B. De Strooper, *The presenilins in Alzheimer's disease--proteolysis holds the key*. Science, 1999. **286**(5441): p. 916-919.
126. De Strooper, B., *Aph-1, Pen-2, and nicastrin with presenilin generate an active γ -secretase complex*. Neuron, 2003. **38**(1): p. 9-12.
127. Zhou, X., et al., *An overview on therapeutics attenuating amyloid β level in Alzheimer's disease: Targeting neurotransmission, inflammation, oxidative stress and enhanced cholesterol levels*. American journal of translational research, 2016. **8**(2): p. 246.
128. Cehlar, O., et al., *Structural aspects of Alzheimer's disease immunotherapy targeted against amyloid-beta peptide*. Bratislavske lekarske listy, 2018. **119**(4): p. 201-204.
129. Chowdhury, S.R., et al., *Small-Molecule Amyloid Beta-Aggregation Inhibitors in Alzheimer's Disease Drug Development*. Pharmaceutical Fronts, 2019. **1**(01): p. e22-e32.
130. Hasegawa, M., *Molecular mechanisms in the pathogenesis of Alzheimer's disease and tauopathies-prion-like seeded aggregation and phosphorylation*. Biomolecules, 2016. **6**(2): p. 24.
131. Šimić, G., et al., *Tau protein hyperphosphorylation and aggregation in Alzheimer's disease and other tauopathies, and possible neuroprotective strategies*. Biomolecules, 2016. **6**(1): p. 6.
132. Dubey, T., et al., *Photoexcited Toluidine Blue Inhibits Tau Aggregation in Alzheimer's Disease*. ACS omega, 2019. **4**(20): p. 18793-18802.
133. Gorantla, N.V., et al., *Neem derivatives inhibits tau aggregation*. Journal of Alzheimer's disease reports, 2019. **3**(1): p. 169-178.
134. Gorantla, N.V., et al., *Molecular cobalt (II) complexes for tau polymerization in Alzheimer's disease*. ACS omega, 2019. **4**(16): p. 16702-16714.
135. Zemek, F., et al., *Outcomes of Alzheimer's disease therapy with acetylcholinesterase inhibitors and memantine*. Expert opinion on drug safety, 2014. **13**(6): p. 759-774.
136. Claustrat, B., J. Brun, and G. Chazot, *The basic physiology and pathophysiology of melatonin*. Sleep medicine reviews, 2005. **9**(1): p. 11-24.
137. Hardeland, R. and B. Poeggeler, *Melatonin beyond its classical functions*. 2008.
138. Kim, M.J., et al., *Melatonin increases cell proliferation in the dentate gyrus of maternally separated rats*. Journal of pineal research, 2004. **37**(3): p. 193-197.
139. Wang, J.-z. and Z.-f. Wang, *Role of melatonin in Alzheimer-like neurodegeneration*. Acta Pharmacologica Sinica, 2006. **27**(1): p. 41-49.
140. Reiter, R.J., *Oxidative processes and antioxidative defense mechanisms in the aging brain*. The FASEB journal, 1995. **9**(7): p. 526-533.
141. Tomás-Zapico, C. and A. Coto-Montes, *A proposed mechanism to explain the stimulatory effect of melatonin on antioxidative enzymes*. Journal of pineal research, 2005. **39**(2): p. 99-104.
142. Lin, L., et al., *Melatonin in Alzheimer's disease*. International journal of molecular sciences, 2013. **14**(7): p. 14575-14593.
143. Ling, Z.-Q., et al., *Constant illumination induces Alzheimer-like damages with endoplasmic reticulum involvement and the protection of melatonin*. Journal of Alzheimer's Disease, 2009. **16**(2): p. 287-300.
144. Quinn, J., et al., *Chronic melatonin therapy fails to alter amyloid burden or oxidative damage in old Tg2576 mice: implications for clinical trials*. Brain Research, 2005. **1037**(1): p. 209-213.
145. Matsubara, E., et al., *Melatonin increases survival and inhibits oxidative and amyloid pathology in a transgenic model of Alzheimer's disease*. Journal of Neurochemistry, 2003. **85**(5): p. 1101-1108.
146. Klongpanichapak, S., et al., *Melatonin inhibits amphetamine-induced increase in α -synuclein and decrease in phosphorylated tyrosine hydroxylase in SK-N-BE cells*. Neuroscience letters, 2008. **436**(3): p. 309-313.

147. Sae-Ung, K., et al., *Melatonin reduces the expression of alpha-synuclein in the dopamine containing neuronal regions of amphetamine-treated postnatal rats*. Journal of pineal research. **52**(1): p. 128-137.
148. Ono, K., et al., *Effect of melatonin on $\hat{\pm}$ -synuclein self-assembly and cytotoxicity*. Neurobiology of aging. **33**(9): p. 2172-2185.
149. Rong-Xiu, L., et al., *Distribution patterns of the contents of five biologically activate ingredients in the root of Scutellaria baicalensis*. Chinese journal of natural medicines, 2017. **15**(2): p. 152-160.
150. Dinda, B., et al., *Therapeutic potentials of baicalin and its aglycone, baicalein against inflammatory disorders*. European journal of medicinal chemistry, 2017. **131**: p. 68-80.
151. Wang, C.-x., et al., *Baicalin alleviates early brain injury after experimental subarachnoid hemorrhage in rats: Possible involvement of TLR4/NF- κ B-mediated inflammatory pathway*. Brain Research, 2015. **1594**: p. 245-255.
152. Tsai, T., et al., *The effects of the cyclosporin A, a P-glycoprotein inhibitor, on the pharmacokinetics of baicalein in the rat: a microdialysis study*. British journal of pharmacology, 2002. **137**(8): p. 1314-1320.
153. Lee, H.J., et al., *Baicalein attenuates 6-hydroxydopamine-induced neurotoxicity in SH-SY5Y cells*. European Journal of Cell Biology, 2005. **84**(11): p. 897-905.
154. Mu, X., et al., *Baicalein exerts neuroprotective effects in 6-hydroxydopamine-induced experimental parkinsonism in vivo and in vitro*. Pharmacology Biochemistry and Behavior, 2009. **92**(4): p. 642-648.
155. Gao, L., et al., *In silico target fishing for the potential targets and molecular mechanisms of baicalein as an antiparkinsonian agent: discovery of the protective effects on NMDA receptor-mediated neurotoxicity*. Chemical biology & drug design, 2013. **81**(6): p. 675-687.
156. Lee, E., et al., *Baicalein attenuates astroglial activation in the 1-methyl-4-phenyl-1, 2, 3, 4-tetrahydropyridine-induced Parkinson's disease model by downregulating the activations of nuclear factor- κ B, ERK, and JNK*. Journal of Neuroscience Research, 2014. **92**(1): p. 130-139.
157. Oh, S.B., et al., *Baicalein attenuates impaired hippocampal neurogenesis and the neurocognitive deficits induced by γ -ray radiation*. British journal of pharmacology, 2013. **168**(2): p. 421-431.
158. Im, H.-I., et al., *Baicalein prevents 6-hydroxydopamine-induced dopaminergic dysfunction and lipid peroxidation in mice*. Journal of pharmacological sciences, 2005. **98**(2): p. 185-189.
159. Yu, X., et al., *Assessment of the treatment effect of baicalein on a model of Parkinsonian tremor and elucidation of the mechanism*. Life Sciences, 2012. **91**(1-2): p. 5-13.
160. Zhang, X., et al., *Baicalein exerts anti-neuroinflammatory effects to protect against rotenone-induced brain injury in rats*. International Immunopharmacology, 2017. **50**: p. 38-47.
161. Gao, L., et al., *Ameliorative effects of baicalein in MPTP-induced mouse model of Parkinson's disease: A microarray study*. Pharmacology Biochemistry and Behavior, 2015. **133**: p. 155-163.
162. Zhu, M., et al., *The flavonoid baicalein inhibits fibrillation of α -synuclein and disaggregates existing fibrils*. Journal of Biological Chemistry, 2004. **279**(26): p. 26846-26857.
163. Hu, Q., et al., *Baicalein inhibits α -synuclein oligomer formation and prevents progression of α -synuclein accumulation in a rotenone mouse model of Parkinson's disease*. Biochimica et Biophysica Acta (BBA)-Molecular Basis of Disease, 2016. **1862**(10): p. 1883-1890.
164. Lu, J.H., et al., *Baicalein Inhibits Formation of α -Synuclein Oligomers within Living Cells and Prevents A β Peptide Fibrillation and Oligomerisation*. Chembiochem, 2011. **12**(4): p. 615-624.
165. Caruana, M., et al., *Polyphenolic compounds are novel protective agents against lipid membrane damage by α -synuclein aggregates in vitro*. Biochimica et Biophysica Acta (BBA)-Biomembranes, 2012. **1818**(11): p. 2502-2510.

166. Zhang, S.Q., et al., *Baicalein reduces β -amyloid and promotes nonamyloidogenic amyloid precursor protein processing in an Alzheimer's disease transgenic mouse model*. Journal of neuroscience research, 2013. **91**(9): p. 1239-1246.
167. Balmik, A.A., et al., *Melatonin interacts with repeat domain of Tau to mediate disaggregation of paired helical filaments*. Biochimica et Biophysica Acta (BBA)-General Subjects, 2020. **1864**(3): p. 129467.
168. Sonawane, S.K., et al., *Baicalein suppresses Repeat Tau fibrillization by sequestering oligomers*. Archives of biochemistry and biophysics, 2019. **675**: p. 108119.
169. Sonawane, S.K., et al., *EGCG impedes human Tau aggregation and interacts with Tau*. Scientific reports, 2020. **10**(1): p. 1-17.
170. Walker, J.M., *The bicinchoninic acid (BCA) assay for protein quantitation*, in *The protein protocols handbook*. 2009, Springer. p. 11-15.
171. Kruger, N.J., *The Bradford method for protein quantitation*, in *The protein protocols handbook*. 2009, Springer. p. 17-24.
172. Das, R., A.A. Balmik, and S. Chinnathambi, *Melatonin reduces GSK3 β expression and tau phosphorylation via Nrf2 nuclear translocation*. bioRxiv, 2019: p. 861229.
173. Das, R., A.A. Balmik, and S. Chinnathambi, *Phagocytosis of full-length Tau oligomers by Actin-remodeling of activated microglia*. Journal of neuroinflammation, 2020. **17**(1): p. 1-15.
174. Gorantla, N.V., A.V. Shkumatov, and S. Chinnathambi, *Conformational dynamics of intracellular tau protein revealed by CD and SAXS*, in *Tau Protein*. 2017, Springer. p. 3-20.
175. Lee, W., M. Tonelli, and J.L. Markley, *NMRFAM-SPARKY: enhanced software for biomolecular NMR spectroscopy*. Bioinformatics, 2014. **31**(8): p. 1325-1327.
176. Freire, E., O.L. Mayorga, and M. Straume, *Isothermal titration calorimetry*. Analytical chemistry, 1990. **62**(18): p. 950A-959A.
177. Berman, H.M., et al., *The protein data bank*. Nucleic acids research, 2000. **28**(1): p. 235-242.
178. Dong, A., et al., *Crystal structure of human HDAC6 zinc finger domain*. J Mol Biol, 2008. **370**(2): p. 290-302.
179. Duhovny, D., R. Nussinov, and H.J. Wolfson. *Efficient unbound docking of rigid molecules*. in *International workshop on algorithms in bioinformatics*. 2002. Springer.
180. Schneidman-Duhovny, D., et al., *PatchDock and SymmDock: servers for rigid and symmetric docking*. Nucleic acids research, 2005. **33**(suppl_2): p. W363-W367.
181. Berendsen, H.J., D. van der Spoel, and R. van Drunen, *GROMACS: a message-passing parallel molecular dynamics implementation*. Computer physics communications, 1995. **91**(1-3): p. 43-56.
182. Duan, Y., et al., *A point-charge force field for molecular mechanics simulations of proteins based on condensed-phase quantum mechanical calculations*. Journal of computational chemistry, 2003. **24**(16): p. 1999-2012.
183. Van Der Spoel, D., et al., *GROMACS: fast, flexible, and free*. Journal of computational chemistry, 2005. **26**(16): p. 1701-1718.
184. Laskowski, R.A. and M.B. Swindells, *LigPlot+: multiple ligand-protein interaction diagrams for drug discovery*. 2011, ACS Publications.
185. Williams, D., *Tauopathies: classification and clinical update on neurodegenerative diseases associated with microtubule-associated protein tau*. Internal medicine journal, 2006. **36**(10): p. 652-660.
186. Drubin, D.G. and M.W. Kirschner, *Tau protein function in living cells*. The Journal of cell biology, 1986. **103**(6): p. 2739-2746.
187. Boutajangout, A., E. M Sigurdsson, and P. K Krishnamurthy, *Tau as a therapeutic target for Alzheimer's disease*. Current Alzheimer Research, 2011. **8**(6): p. 666-677.

188. Seidler, P., et al., *Structure-based inhibitors of tau aggregation*. Nature chemistry, 2018. **10**(2): p. 170.
189. Hilgeroth, A.P. and V. Tell, *Recent developments of protein kinase inhibitors as potential AD therapeutics*. Frontiers in cellular neuroscience, 2013. **7**: p. 189.
190. Fabbro, D., *25 years of small molecular weight kinase inhibitors: potentials and limitations*. Molecular pharmacology, 2015. **87**(5): p. 766-775.
191. Desai, B.S., et al., *Blood-brain barrier pathology in Alzheimer's and Parkinson's disease: implications for drug therapy*. Cell transplantation, 2007. **16**(3): p. 285-299.
192. Mietelska-Porowska, A., et al., *Tau protein modifications and interactions: their role in function and dysfunction*. International journal of molecular sciences, 2014. **15**(3): p. 4671-4713.
193. Sergeant, N., et al., *Biochemistry of Tau in Alzheimer's disease and related neurological disorders*. Expert review of proteomics, 2008. **5**(2): p. 207-224.
194. Sahara, N., S. Maeda, and A. Takashima, *Tau oligomerization: a role for tau aggregation intermediates linked to neurodegeneration*. Current Alzheimer Research, 2008. **5**(6): p. 591-598.
195. De Strooper, B., *Proteases and proteolysis in Alzheimer disease: a multifactorial view on the disease process*. Physiological reviews, 2010. **90**(2): p. 465-494.
196. Kumar, S., et al., *Stages and conformations of the Tau repeat domain during aggregation and its effect on neuronal toxicity*. Journal of biological chemistry, 2014. **289**(29): p. 20318-20332.
197. Lafarga, V., et al., *A novel GRK2/HDAC6 interaction modulates cell spreading and motility*. The EMBO journal, 2012. **31**(4): p. 856-869.
198. Zhang, X., et al., *HDAC6 modulates cell motility by altering the acetylation level of cortactin*. Molecular cell, 2007. **27**(2): p. 197-213.
199. Hard, R.L., et al., *HDAC6 and Ubp-M BUZ domains recognize specific C-terminal sequences of proteins*. Biochemistry, 2010. **49**(50): p. 10737-10746.
200. Aldana-Masangkay, G.I. and K.M. Sakamoto, *The role of HDAC6 in cancer*. BioMed Research International, 2010. **2011**.
201. Zhang, L., et al., *Proteomic identification and functional characterization of MYH9, Hsc70, and DNAJA1 as novel substrates of HDAC6 deacetylase activity*. Protein & cell, 2015. **6**(1): p. 42-54.
202. Kovacs, J.J., C. Hubbert, and T.-P. Yao. *The HDAC complex and cytoskeleton*. in *Novartis Foundation symposium*. 2004. Wiley Online Library.
203. Yan, J., et al., *SQSTM1/p62 interacts with HDAC6 and regulates deacetylase activity*. PloS one, 2013. **8**(9).
204. Hebron, M.L., et al., *Parkin ubiquitinates Tar-DNA binding protein-43 (TDP-43) and promotes its cytosolic accumulation via interaction with histone deacetylase 6 (HDAC6)*. Journal of Biological Chemistry, 2013. **288**(6): p. 4103-4115.
205. Avvakumov, G.V., et al., *Two ZnF-UBP domains in isopeptidase T (USP5)*. Biochemistry, 2012. **51**(6): p. 1188-1198.
206. Nizynski, B., W. Dzwolak, and K. Nieznanski, *Amyloidogenesis of Tau protein*. Protein Science, 2017. **26**(11): p. 2126-2150.
207. Köpke, E., et al., *Microtubule-associated protein tau. Abnormal phosphorylation of a non-paired helical filament pool in Alzheimer disease*. Journal of Biological Chemistry, 1993. **268**(32): p. 24374-24384.
208. Martin, L., et al., *Tau protein kinases: involvement in Alzheimer's disease*. Ageing research reviews, 2013. **12**(1): p. 289-309.
209. Kovacech, B. and M. Novak, *Tau truncation is a productive posttranslational modification of neurofibrillary degeneration in Alzheimer's disease*. Current Alzheimer Research, 2010. **7**(8): p. 708-716.

210. Wang, Y., et al., *Stepwise proteolysis liberates tau fragments that nucleate the Alzheimer-like aggregation of full-length tau in a neuronal cell model*. Proceedings of the National Academy of Sciences, 2007. **104**(24): p. 10252-10257.
211. Rissman, R.A., et al., *Caspase-cleavage of tau is an early event in Alzheimer disease tangle pathology*. The Journal of clinical investigation, 2004. **114**(1): p. 121-130.
212. Corsetti, V., et al., *Identification of a caspase-derived N-terminal tau fragment in cellular and animal Alzheimer's disease models*. Molecular and Cellular Neuroscience, 2008. **38**(3): p. 381-392.
213. Horowitz, P.M., et al., *N-terminal fragments of tau inhibit full-length tau polymerization in vitro*. Biochemistry, 2006. **45**(42): p. 12859-12866.
214. Matsumoto, S.-E., et al., *The twenty-four kDa C-terminal tau fragment increases with aging in tauopathy mice: implications of prion-like properties*. Human molecular genetics, 2015. **24**(22): p. 6403-6416.
215. Park, S.-Y. and A. Ferreira, *The generation of a 17 kDa neurotoxic fragment: an alternative mechanism by which tau mediates β -amyloid-induced neurodegeneration*. Journal of Neuroscience, 2005. **25**(22): p. 5365-5375.
216. Wang, Y. and E. Mandelkow, *Degradation of tau protein by autophagy and proteasomal pathways*. 2012, Portland Press Ltd.
217. Barré, P. and D. Eliezer, *Structural transitions in tau k18 on micelle binding suggest a hierarchy in the efficacy of individual microtubule-binding repeats in filament nucleation*. Protein Science, 2013. **22**(8): p. 1037-1048.
218. dos Santos Passos, C., et al., *Molecular dynamics of zinc-finger ubiquitin binding domains: a comparative study of histone deacetylase 6 and ubiquitin-specific protease 5*. Journal of Biomolecular Structure and Dynamics, 2016. **34**(12): p. 2581-2598.
219. Cohen, T.J., et al., *Intrinsic tau acetylation is coupled to auto-proteolytic tau fragmentation*. PloS one, 2016. **11**(7): p. e0158470.
220. Coppola, G., et al., *Evidence for a role of the rare p. A152T variant in MAPT in increasing the risk for FTD-spectrum and Alzheimer's diseases*. Human molecular genetics, 2012. **21**(15): p. 3500-3512.
221. Ciechanover, A. and Y.T. Kwon, *Degradation of misfolded proteins in neurodegenerative diseases: therapeutic targets and strategies*. Experimental & molecular medicine, 2015. **47**(3): p. e147.
222. Gorantla, N.V. and S. Chinnathambi, *Tau protein squired by molecular chaperones during Alzheimer's disease*. Journal of Molecular Neuroscience, 2018. **66**(3): p. 356-368.
223. Casadei, N., et al., *Overexpression of synphilin-1 promotes clearance of soluble and misfolded alpha-synuclein without restoring the motor phenotype in aged A30P transgenic mice*. Human molecular genetics, 2013. **23**(3): p. 767-781.
224. Simões-Pires, C., et al., *HDAC6 as a target for neurodegenerative diseases: what makes it different from the other HDACs?* Molecular neurodegeneration, 2013. **8**(1): p. 7.
225. Pandey, U.B., et al., *HDAC6 at the intersection of autophagy, the ubiquitin-proteasome system, and neurodegeneration*. Autophagy, 2007. **3**(6): p. 643-645.
226. Hao, R., et al., *Proteasomes activate aggresome disassembly and clearance by producing unanchored ubiquitin chains*. Molecular cell, 2013. **51**(6): p. 819-828.
227. Iwata, A., et al., *HDAC6 and microtubules are required for autophagic degradation of aggregated huntingtin*. Journal of Biological Chemistry, 2005. **280**(48): p. 40282-40292.
228. Drewes, G., et al., *MARK, a novel family of protein kinases that phosphorylate microtubule-associated proteins and trigger microtubule disruption*. Cell, 1997. **89**(2): p. 297-308.

229. Lucas, J.J., et al., *Decreased nuclear β -catenin, tau hyperphosphorylation and neurodegeneration in GSK-3 β conditional transgenic mice*. The EMBO journal, 2001. **20**(1-2): p. 27-39.
230. Cho, J.H. and G.V. Johnson, *Primed phosphorylation of tau at Thr231 by glycogen synthase kinase 3 β (GSK3 β) plays a critical role in regulating tau's ability to bind and stabilize microtubules*. Journal of neurochemistry, 2004. **88**(2): p. 349-358.
231. Šimić, G., A. Diana, and P.R. Hof, *Phosphorylation pattern of tau associated with distinct changes of the growth cone cytoskeleton*, in *Guidance Cues in the Developing Brain*. 2003, Springer. p. 33-48.
232. Arendt, T., et al., *Paired helical filament-like phosphorylation of tau, deposition of β /A4-amyloid and memory impairment in rat induced by chronic inhibition of phosphatase 1 and 2A*. Neuroscience, 1995. **69**(3): p. 691-698.
233. Sontag, E., et al., *Downregulation of protein phosphatase 2A carboxyl methylation and methyltransferase may contribute to Alzheimer disease pathogenesis*. Journal of Neuropathology & Experimental Neurology, 2004. **63**(10): p. 1080-1091.
234. Vintém, A.P.B., et al., *PP1 inhibition by A β peptide as a potential pathological mechanism in Alzheimer's disease*. Neurotoxicology and teratology, 2009. **31**(2): p. 85-88.
235. Li, B., et al., *Disruption of microtubule network by Alzheimer abnormally hyperphosphorylated tau*. Acta neuropathologica, 2007. **113**(5): p. 501-511.
236. Penzes, P. and J.-E. VanLeeuwen, *Impaired regulation of synaptic actin cytoskeleton in Alzheimer's disease*. Brain research reviews, 2011. **67**(1-2): p. 184-192.
237. Fiala, J.C., J. Spacek, and K.M. Harris, *Dendritic spine pathology: cause or consequence of neurological disorders?* Brain research reviews, 2002. **39**(1): p. 29-54.
238. Selkoe, D.J., *Alzheimer's disease is a synaptic failure*. Science, 2002. **298**(5594): p. 789-791.
239. Boyault, C., et al., *HDAC6, at the crossroads between cytoskeleton and cell signaling by acetylation and ubiquitination*. Oncogene, 2007. **26**(37): p. 5468.
240. Li, J. and J. Yuan, *Caspases in apoptosis and beyond*. Oncogene, 2008. **27**(48): p. 6194-6206.
241. D'amelio, M., V. Cavallucci, and F. Cecconi, *Neuronal caspase-3 signaling: not only cell death*. Cell Death & Differentiation, 2010. **17**(7): p. 1104-1114.
242. Beurel, E., *HDAC6 regulates LPS-tolerance in astrocytes*. PLoS One, 2011. **6**(10): p. e25804.
243. Beurel, E., S.F. Grieco, and R.S. Jope, *Glycogen synthase kinase-3 (GSK3): regulation, actions, and diseases*. Pharmacology & therapeutics, 2015. **148**: p. 114-131.
244. Avila, J., *Tau kinases and phosphatases*. Journal of cellular and molecular medicine, 2008. **12**(1): p. 258-259.
245. Boban, M., et al., *Human neuroblastoma SH-SY5Y cells treated with okadaic acid express phosphorylated high molecular weight tau-immunoreactive protein species*. Journal of neuroscience methods, 2018.
246. Oda, T., et al., *The nature of the globular-to fibrous-actin transition*. Nature, 2009. **457**(7228): p. 441.
247. Lee, S.H. and R. Dominguez, *Regulation of actin cytoskeleton dynamics in cells*. Molecules and cells, 2010. **29**(4): p. 311-325.
248. Moghaddam, H.S. and M.H. Aarabi, *A β -Mediated Dysregulation of F-Actin Nanoarchitecture Leads to Loss of Dendritic Spines and Alzheimer's Disease-Related Cognitive Impairments*. Journal of Neuroscience, 2018. **38**(26): p. 5840-5842.
249. Biswas, S. and K. Kalil, *The microtubule-associated protein tau mediates the organization of microtubules and their dynamic exploration of actin-rich lamellipodia and filopodia of cortical growth cones*. Journal of Neuroscience, 2018. **38**(2): p. 291-307.
250. Gimona, M., et al., *Assembly and biological role of podosomes and invadopodia*. Current opinion in cell biology, 2008. **20**(2): p. 235-241.

251. Siddiqui, T.A., et al., *Regulation of podosome formation, microglial migration and invasion by Ca²⁺-signaling molecules expressed in podosomes*. Journal of neuroinflammation, 2012. **9**(1): p. 250.
252. Sen, A., T.J. Nelson, and D.L. Alkon, *ApoE4 and A β oligomers reduce BDNF expression via HDAC nuclear translocation*. Journal of Neuroscience, 2015. **35**(19): p. 7538-7551.
253. Jiang, Q., et al., *ApoE promotes the proteolytic degradation of A β* . Neuron, 2008. **58**(5): p. 681-693.
254. Kim, W.S., et al., *Analysis of apolipoprotein E nuclear localization using green fluorescent protein and biotinylation approaches*. Biochemical Journal, 2008. **409**(3): p. 701-709.
255. Sancho, D., et al., *Regulation of microtubule-organizing center orientation and actomyosin cytoskeleton rearrangement during immune interactions*. Immunological reviews, 2002. **189**(1): p. 84-97.
256. Palazzo, A.F., et al., *Cdc42, dynein, and dynactin regulate MTOC reorientation independent of Rho-regulated microtubule stabilization*. Current Biology, 2001. **11**(19): p. 1536-1541.
257. Götz, J., A. Ittner, and L.M. Ittner, *Tau targeted treatment strategies in Alzheimer's disease*. British journal of pharmacology, 2012. **165**(5): p. 1246-1259.
258. Congdon, E.E. and E.M. Sigurdsson, *Tau-targeting therapies for Alzheimer disease*. Nature Reviews Neurology, 2018: p. 1.
259. Bulic, B., et al., *Tau protein and tau aggregation inhibitors*. Neuropharmacology, 2010. **59**(4): p. 276-289.
260. Lawatscheck, C., et al., *Generalizing the Concept of Specific Compound Formulation Additives towards Non-Fluorescent Drugs: A Solubilization Study on Potential Anti-Alzheimer-Active Small-Molecule Compounds*. Angewandte Chemie International Edition, 2016. **55**(30): p. 8752-8756.
261. Holtzman, D.M., et al., *Tau: From research to clinical development*. Alzheimer's & Dementia, 2016. **12**(10): p. 1033-1039.
262. Pandi-Perumal, S.R., et al., *Physiological effects of melatonin: role of melatonin receptors and signal transduction pathways*. Progress in neurobiology, 2008. **85**(3): p. 335-353.
263. Cajochen, C., K. Kräuchi, and A. Wirz-Justice, *Role of melatonin in the regulation of human circadian rhythms and sleep*. Journal of neuroendocrinology, 2003. **15**(4): p. 432-437.
264. Reiter, R.J. and D.-X. Tan, *What constitutes a physiological concentration of melatonin?* Journal of Pineal Research, 2003. **34**(1): p. 79-80.
265. Yu, H., et al., *High membrane permeability for melatonin*. The Journal of general physiology, 2016. **147**(1): p. 63-76.
266. Wang, X., *The antiapoptotic activity of melatonin in neurodegenerative diseases*. CNS neuroscience & therapeutics, 2009. **15**(4): p. 345-357.
267. Tomas-Zapico, C. and A. Coto-Montes, *A proposed mechanism to explain the stimulatory effect of melatonin on antioxidative enzymes*. Journal of pineal research, 2005. **39**(2): p. 99-104.
268. Tan, D.-X., et al., *Melatonin directly scavenges hydrogen peroxide: a potentially new metabolic pathway of melatonin biotransformation*. Free Radical Biology and Medicine, 2000. **29**(11): p. 1177-1185.
269. Zempel, H., et al., *A β oligomers cause localized Ca²⁺ elevation, missorting of endogenous Tau into dendrites, Tau phosphorylation, and destruction of microtubules and spines*. Journal of Neuroscience, 2010. **30**(36): p. 11938-11950.
270. Wang, D.L., et al., *Melatonin attenuates isoproterenol-induced protein kinase A overactivation and tau hyperphosphorylation in rat brain*. Journal of pineal research, 2004. **37**(1): p. 11-16.
271. Planel, E., et al., *Inhibition of protein phosphatase 2A overrides Tau protein kinase I/glycogen synthase kinase 3 β and cyclin-dependant kinase 5 inhibition and results in tau*

- hyperphosphorylation in the hippocampus of starved mouse*. Journal of Biological Chemistry, 2001.
272. Lin, L., et al., *Melatonin in Alzheimer's disease*. International journal of molecular sciences, 2013. **14**(7): p. 14575-14593.
273. Balmik, A.A. and S. Chinnathambi, *Multi-Faceted Role of Melatonin in Neuroprotection and Amelioration of Tau Aggregates in Alzheimer's Disease*. Journal of Alzheimer's Disease, 2018(Preprint): p. 1-13.
274. Quinn, J., et al., *Chronic melatonin therapy fails to alter amyloid burden or oxidative damage in old Tg2576 mice: implications for clinical trials*. Brain Research, 2005. **1037**(1-2): p. 209-213.
275. Ono, K., et al., *Effect of melatonin on α -synuclein self-assembly and cytotoxicity*. Neurobiology of aging, 2012. **33**(9): p. 2172-2185.
276. Pappolla, M., et al., *Inhibition of Alzheimer β -fibrillogenesis by melatonin*. Journal of Biological Chemistry, 1998. **273**(13): p. 7185-7188.
277. Sae-Ung, K., et al., *Melatonin reduces the expression of alpha-synuclein in the dopamine containing neuronal regions of amphetamine-treated postnatal rats*. Journal of pineal research, 2012. **52**(1): p. 128-137.
278. Hornedo-Ortega, R., et al., *In Vitro Effects of Serotonin, Melatonin, and Other Related Indole Compounds on Amyloid- β Kinetics and Neuroprotection*. Molecular nutrition & food research, 2018. **62**(3): p. 1700383.
279. Amor, S., et al., *Inflammation in neurodegenerative diseases*. Immunology, 2010. **129**(2): p. 154-169.
280. Costantino, G., et al., *Protective effects of melatonin in zymosan-activated plasma-induced paw inflammation*. European journal of pharmacology, 1998. **363**(1): p. 57-63.
281. Vauzour, D., et al., *The neuroprotective potential of flavonoids: a multiplicity of effects*. Genes & nutrition, 2008. **3**(3-4): p. 115-126.
282. Xiong, Y., et al., *HDAC6 mutations rescue human tau-induced microtubule defects in Drosophila*. Proceedings of the National Academy of Sciences, 2013. **110**(12): p. 4604-4609.
283. Barré, P. and D. Eliezer, *Structural transitions in tau k18 on micelle binding suggest a hierarchy in the efficacy of individual microtubule-binding repeats in filament nucleation*. Protein Science, 2013. **22**(8): p. 1037-1048.
284. Luo, J., et al., *Cellular polyamines promote amyloid-beta ($A\beta$) peptide fibrillation and modulate the aggregation pathways*. ACS chemical neuroscience, 2013. **4**(3): p. 454-462.
285. Jeganathan, S., et al., *Global hairpin folding of tau in solution*. Biochemistry, 2006. **45**(7): p. 2283-2293.
286. Chenprakhon, P., et al., *Measuring Binding Affinity of Protein– Ligand Interaction Using Spectrophotometry: Binding of Neutral Red to Riboflavin-Binding Protein*. Journal of chemical education, 2010. **87**(8): p. 829-831.
287. Wei, Y., et al., *Binding to the minor groove of the double-strand, tau protein prevents DNA from damage by peroxidation*. PloS one, 2008. **3**(7): p. e2600.
288. Brandt, R., J. Léger, and G. Lee, *Interaction of tau with the neural plasma membrane mediated by tau's amino-terminal projection domain*. The Journal of cell biology, 1995. **131**(5): p. 1327-1340.
289. Terwel, D., I. Dewachter, and F. Van Leuven, *Axonal transport, tau protein, and neurodegeneration in Alzheimer's disease*. Neuromolecular medicine, 2002. **2**(2): p. 151-165.
290. Marciniak, E., et al., *Tau deletion promotes brain insulin resistance*. Journal of Experimental Medicine, 2017. **214**(8): p. 2257-2269.
291. Sotiropoulos, I., et al., *Selective impact of tau loss on nociceptive primary afferents and pain sensation*. Experimental neurology, 2014. **261**: p. 486-493.

292. Guillozet-Bongaarts, A.L., et al., *Pseudophosphorylation of tau at serine 422 inhibits caspase cleavage: in vitro evidence and implications for tangle formation in vivo*. Journal of neurochemistry, 2006. **97**(4): p. 1005-1014.
293. Goedert, M., et al., *Tau proteins of Alzheimer paired helical filaments: abnormal phosphorylation of all six brain isoforms*. Neuron, 1992. **8**(1): p. 159-168.
294. Trojanowski, J.Q. and V. Lee, *Paired helical filament tau in Alzheimer's disease. The kinase connection*. The American journal of pathology, 1994. **144**(3): p. 449.
295. Monteiro, K.L., et al., *Tau Protein Aggregation in Alzheimer's Disease: Recent Advances in the Development of Novel Therapeutic Agents*. Current Pharmaceutical Design, 2020. **26**(15): p. 1682-1692.
296. Dajas-Bailador, F., E.V. Jones, and A.J. Whitmarsh, *The JIP1 scaffold protein regulates axonal development in cortical neurons*. Current Biology, 2008. **18**(3): p. 221-226.
297. Cheng, Y. and F. Bai, *The association of tau with mitochondrial dysfunction in alzheimer's disease*. Frontiers in neuroscience, 2018. **12**: p. 163.
298. Shafiei, S.S., M.J. Guerrero-Muñoz, and D.L. Castillo-Carranza, *Tau oligomers: cytotoxicity, propagation, and mitochondrial damage*. Frontiers in aging neuroscience, 2017. **9**: p. 83.
299. Sonawane, S.K., A. Ahmad, and S. Chinnathambi, *Protein-capped metal nanoparticles inhibit tau aggregation in Alzheimer's disease*. ACS omega, 2019. **4**(7): p. 12833-12840.
300. Medina, M., *An overview on the clinical development of tau-based therapeutics*. International Journal of Molecular Sciences, 2018. **19**(4): p. 1160.
301. Sinsky, J., et al., *Physiological tau interactome in brain and its link to tauopathies*. Journal of Proteome Research, 2020.
302. Li, Y., D. Shin, and S.H. Kwon, *Histone deacetylase 6 plays a role as a distinct regulator of diverse cellular processes*. The FEBS journal, 2013. **280**(3): p. 775-793.
303. Seidel, C., et al., *Histone deacetylase 6 in health and disease*. Epigenomics, 2015. **7**(1): p. 103-118.
304. Gorantla, N.V., et al., *Global conformation of tau protein mapped by Raman spectroscopy*, in *Tau Protein*. 2017, Springer. p. 21-31.
305. Patterson, K.R., et al., *Characterization of prefibrillar Tau oligomers in vitro and in Alzheimer disease*. Journal of Biological Chemistry, 2011. **286**(26): p. 23063-23076.
306. Calkins, M.J. and P.H. Reddy, *Amyloid beta impairs mitochondrial anterograde transport and degenerates synapses in Alzheimer's disease neurons*. Biochimica et Biophysica Acta (BBA)-Molecular Basis of Disease, 2011. **1812**(4): p. 507-513.
307. Luo, L., *Actin cytoskeleton regulation in neuronal morphogenesis and structural plasticity*. Annual review of cell and developmental biology, 2002. **18**(1): p. 601-635.
308. Goedert, M., et al., *Epitope mapping of monoclonal antibodies to the paired helical filaments of Alzheimer's disease: identification of phosphorylation sites in tau protein*. Biochemical Journal, 1994. **301**(3): p. 871-877.
309. Braak, H., et al., *Staging of Alzheimer disease-associated neurofibrillary pathology using paraffin sections and immunocytochemistry*. Acta neuropathologica, 2006. **112**(4): p. 389-404.
310. Barthélemy, N.R., et al., *A soluble phosphorylated tau signature links tau, amyloid and the evolution of stages of dominantly inherited Alzheimer's disease*. Nature Medicine, 2020. **26**(3): p. 398-407.
311. Eftekharzadeh, B., et al., *Tau protein disrupts nucleocytoplasmic transport in Alzheimer's disease*. Neuron, 2018. **99**(5): p. 925-940. e7.
312. Ulrich, G., et al., *Phosphorylation of nuclear Tau is modulated by distinct cellular pathways*. Scientific reports, 2018. **8**(1): p. 1-14.

313. Huang, Y. and R.W. Mahley, *Apolipoprotein E: structure and function in lipid metabolism, neurobiology, and Alzheimer's diseases*. Neurobiology of disease, 2014. **72**: p. 3-12.
314. Han, X., *The role of apolipoprotein E in lipid metabolism in the central nervous system*. Cellular and molecular life sciences, 2004. **61**(15): p. 1896-1906.
315. Urosevic, N. and R.N. Martins, *Infection and Alzheimer's disease: the APOE ϵ 4 connection and lipid metabolism*. Journal of Alzheimer's disease, 2008. **13**(4): p. 421-435.
316. Brush, M.H., et al., *Deacetylase inhibitors disrupt cellular complexes containing protein phosphatases and deacetylases*. Journal of Biological Chemistry, 2004. **279**(9): p. 7685-7691.
317. Esteves, S.L., et al., *Protein phosphatase 1 α interacting proteins in the human brain*. Omics: a journal of integrative biology, 2012. **16**(1-2): p. 3-17.
318. Cho, J.-H. and G.V. Johnson, *Glycogen Synthase Kinase 3 β Phosphorylates tau at both primed and unprimed sites differential impact on microtubule binding*. Journal of Biological Chemistry, 2003. **278**(1): p. 187-193.
319. Fang, X., et al., *Phosphorylation and inactivation of glycogen synthase kinase 3 by protein kinase A*. Proceedings of the National Academy of Sciences, 2000. **97**(22): p. 11960-11965.
320. Alao, J.P., et al., *Role of glycogen synthase kinase 3 beta (GSK3 β) in mediating the cytotoxic effects of the histone deacetylase inhibitor trichostatin A (TSA) in MCF-7 breast cancer cells*. Molecular cancer, 2006. **5**(1): p. 40.
321. Rohn, T.T. and Z.D. Moore, *Nuclear localization of apolipoprotein E4: a new trick for an old protein*. International journal of neurology and neurotherapy, 2017. **4**(2).
322. Semenkovich, C.F., et al., *A protein partially expressed on the surface of HepG2 cells that binds lipoproteins specifically is nucleolin*. Biochemistry, 1990. **29**(41): p. 9708-9713.
323. Wang, S.-A., et al., *Heat shock protein 90 stabilizes nucleolin to increase mRNA stability in mitosis*. Journal of Biological Chemistry, 2011. **286**(51): p. 43816-43829.
324. Elie, A., et al., *Tau co-organizes dynamic microtubule and actin networks*. Scientific reports, 2015. **5**: p. 9964.
325. Gardel, M.L., et al., *Mechanical integration of actin and adhesion dynamics in cell migration*. Annual review of cell and developmental biology, 2010. **26**: p. 315-333.
326. Bradke, F. and C.G. Dotti, *Establishment of neuronal polarity: lessons from cultured hippocampal neurons*. Current opinion in neurobiology, 2000. **10**(5): p. 574-581.
327. Small, J.V., et al., *Assembling an actin cytoskeleton for cell attachment and movement*. Biochimica Et Biophysica Acta (BBA)-Molecular Cell Research, 1998. **1404**(3): p. 271-281.
328. Vincent, C., T.A. Siddiqui, and L.C. Schlichter, *Podosomes in migrating microglia: components and matrix degradation*. Journal of neuroinflammation, 2012. **9**(1): p. 190.
329. Giacobini, E. and G. Gold, *Alzheimer disease therapy—moving from amyloid- β to tau*. Nature Reviews Neurology, 2013. **9**(12): p. 677-686.
330. Colovic, M.B., et al., *Acetylcholinesterase inhibitors: pharmacology and toxicology*. Current neuropharmacology, 2013. **11**(3): p. 315-335.
331. Tanović, A. and V. Alfaro, *Glutamate-related excitotoxicity neuroprotection with memantine, an uncompetitive antagonist of NMDA-glutamate receptor, in Alzheimer's disease and vascular dementia*. Revista de neurologia, 2006. **42**(10): p. 607-616.
332. Townsend, K.P. and D. Praticò, *Novel therapeutic opportunities for Alzheimer's disease: focus on nonsteroidal anti-inflammatory drugs*. The FASEB Journal, 2005. **19**(12): p. 1592-1601.
333. Ghosh, A.K., M. Brindisi, and J. Tang, *Developing β -secretase inhibitors for treatment of Alzheimer's disease*. Journal of neurochemistry, 2012. **120**: p. 71-83.
334. Balmik, A.A. and S. Chinnathambi, *Multi-faceted role of melatonin in neuroprotection and amelioration of Tau aggregates in Alzheimer's disease*. Journal of Alzheimer's Disease, 2018. **62**(4): p. 1481-1493.

335. He, H., W. Dong, and F. Huang, *Anti-amyloidogenic and anti-apoptotic role of melatonin in Alzheimer disease*. *Current neuropharmacology*, 2010. **8**(3): p. 211-217.
336. Skribanek, Z., L. Balásperi, and M. Mák, *Interaction between synthetic amyloid- β -peptide (1–40) and its aggregation inhibitors studied by electrospray ionization mass spectrometry*. *Journal of mass spectrometry*, 2001. **36**(11): p. 1226-1229.
337. Ishido, M., *Melatonin inhibits maneb-induced aggregation of α -synuclein in rat pheochromocytoma cells*. *Journal of pineal research*, 2007. **42**(2): p. 125-130.
338. Papagiannidou, E., D.J. Skene, and C. Ioannides, *Potential drug interactions with melatonin*. *Physiology & behavior*, 2014. **131**: p. 17-24.
339. Das, R., A.A. Balmik, and S. Chinnathambi, *Effect of Melatonin on Tau aggregation and Tau-mediated cell surface morphology*. *International Journal of Biological Macromolecules*, 2020. **152**: p. 30-39.
340. Sowndhararajan, K., et al., *Baicalein as a potent neuroprotective agent: A review*. *Biomedicine & Pharmacotherapy*, 2017. **95**: p. 1021-1032.
341. Zhu, Q., X. Zhuang, and J. Lu, *Neuroprotective effects of baicalein in animal models of Parkinson's disease: A systematic review of experimental studies*. *Phytomedicine*, 2019. **55**: p. 302-309.
342. Li, Y., J. Zhao, and C. Hölscher, *Therapeutic potential of baicalein in Alzheimer's disease and Parkinson's disease*. *CNS drugs*, 2017. **31**(8): p. 639-652.
343. Congdon, E.E., et al., *Nucleation-dependent tau filament formation the importance of dimerization and an estimation of elementary rate constants*. *Journal of Biological Chemistry*, 2008. **283**(20): p. 13806-13816.
344. Flach, K., et al., *Tau oligomers impair artificial membrane integrity and cellular viability*. *Journal of Biological Chemistry*, 2012. **287**(52): p. 43223-43233.
345. Guzmán-Martinez, L., G.A. Farías, and R.B. Maccioni, *Tau oligomers as potential targets for Alzheimer's diagnosis and novel drugs*. *Tau oligomers*, 2014. **3**(14): p. 35.
346. Song, S.-m., et al., *Interaction between baicalein and amyloid- β fibrils studied by fluorescence spectroscopy*. *Chemical Research in Chinese Universities*, 2013. **29**(1): p. 20-25.
347. Margittai, M. and R. Langen, *Template-assisted filament growth by parallel stacking of tau*. *Proceedings of the National Academy of Sciences of the United States of America*, 2004. **101**(28): p. 10278-10283.
348. Semisotnov, G., et al., *Study of the "molten globule" intermediate state in protein folding by a hydrophobic fluorescent probe*. *Biopolymers*, 1991. **31**(1): p. 119-128.
349. Gasymov, O.K. and B.J. Glasgow, *ANS fluorescence: Potential to augment the identification of the external binding sites of proteins*. *Biochimica et Biophysica Acta (BBA)-Proteins and Proteomics*, 2007. **1774**(3): p. 403-411.

ABSTRACT

Name of the Student: Abhishek Balmik

Faculty of Study: Biological Science

AcSIR academic Centre/CSIR Lab: CSIR-NCL, Pune

Registration No. : 10BB15J26039

Year of Submission: 2020

Name of the Supervisor(s):

Dr. Subashchandrabose Chinnathambi

Title of the thesis: Histone Deacetylase-6 ZnF UBP as a regulator of Tau stability and neuronal functions

Alzheimer's disease (AD) is an age associated Neurodegenerative disease, which have two key players involved in its pathogenesis-Amyloid- β peptide and microtubule-associated protein Tau (MAPT). The aggregates consisting of these two are found in the brains of AD patient. Amyloid- β peptides form extracellular plaques while Tau forms intracellular neurofibrillary tangles (NFT). HDAC6 is a class II histone deacetylase majorly present in the cytoplasm. It plays an important role in aggresome formation by recruiting polyubiquitinated aggregates to the motor protein dynein. Here, we have studied the effect of HDAC6 ZnF UBP domain as a modifier of Tau aggregation by its direct interaction with the polyproline region/ repeat region of Tau. Interaction of HDAC6 ZnF UBP with Tau was found to reduce the propensity of Tau to self-aggregate as well as to disaggregate pre-formed aggregates. Additionally, conformational changes in Tau protein and its accelerated degradation with HDAC6 ZnF UBP suggest a mechanism by which it either acts on Tau to degrade or enhance its auto-proteolysis. Immunocytochemistry revealed that HDAC6 ZnF UBP can modulate Tau phosphorylation and actin cytoskeleton organization when the cells are exposed to the domain. HDAC6 ZnF UBP treatment to cells resulted in enhanced neurite extension and formation of structures similar to podosomes, lamellipodia-like structures and podonuts suggesting its role in actin re-organization. Also, HDAC6 treatment showed increased nuclear localization of ApoE and tubulin localization in MTOC. All these findings suggest the regulatory role of this domain in different aspects apart from its well-known function in aggresome formation. We also explored the potency of two small molecules – Melatonin and Baicalein in the disaggregation of Tau aggregates. Both these molecules have a pleiotropic role with respect to neuronal health. In our studies, we found that both Melatonin and Baicalein can interact with Tau to bring about dissolution of Tau aggregates. We hypothesized for the mechanism of action of Melatonin and Baicalein and proposed these molecules to be developed as potential therapeutic agents in treatment of Alzheimer's disease.

Details of the publications emanating from the thesis work

List of publication(s) in SCI Journal(s) (published & accepted) emanating from the thesis work:

1. **Balmik, A. A.**, Sonawane, S. K., & Chinnathambi, S.* (2019). Modulation of Actin network and Tau phosphorylation by HDAC6 ZnF UBP domain. **bioRxiv**, 702571.
2. **Balmik, A. A.***, Das, R., Dangi, A., Gorantla, N. V., Marelli, U. K., & Chinnathambi, S.* (2019). Melatonin interacts with repeat domain of Tau to mediate disaggregation of paired helical filaments. **Biochimica et Biophysica Acta (BBA)-General Subjects**, 129467.
3. Sonawane, S. K., **Balmik, A. A.**, Boral, D., Ramasamy, S., & Chinnathambi, S.* (2019). Baicalein suppresses Repeat Tau fibrillization by sequestering oligomers. **Archives of Biochemistry and Biophysics**, 675, 108119.
4. Das, R., **Balmik, A. A.**, & Chinnathambi, S.*. Effect of Melatonin on Tau aggregation and Tau-mediated cell surface morphology. **International Journal of Biological Macromolecules**, 152, 30-39.

List of papers with abstract presented (oral/poster) at national/international conferences/seminars:

1. **Abhishek Ankur Balmik** and Subashchandrabose Chinnathambi*. HDAC6 functions as the modifier of Tau aggregation and cytoskeletal organization. **National Science day poster, 2019 (CSIR-NCL (Pune)).**

Abstract: Microtubule-associated protein Tau undergoes aggregation in Alzheimer's disease and a group of related diseases collectively known as Tauopathies. The misfolded proteins and aggregates are cleared by different mechanisms, which include ubiquitin proteasomal system (UPS), cell mediated autophagy (CMA) and macroautophagy through aggresome formation. HDAC6 is a class II histone deacetylase majorly present in the cytoplasm. It plays an important role in aggresome formation by recruiting polyubiquitinated aggregates to the motor protein dynein. Apart from its catalytic activity, HDAC6 interacts with other proteins either through SE14 domain or ZnF UBP domain to modulate their functions. Here, we have studied the role of HDAC6 ZnF UBP as a modifier of Tau aggregation and stability. Interaction of HDAC6 with Tau reduces its propensity to self-aggregate and also bring about the conformational changes. Immunocytochemistry and western blot analysis reveals that HDAC6 ZnF UBP can modulate Tau phosphorylation and actin cytoskeleton organization in neuronal cells. Our studies suggested the regulatory role of this domain in different aspects of neurodegenerative diseases apart from its well-known function in aggresome formation.

2. **Abhishek Ankur Balmik** and Subashchandrabose Chinnathambi*. HDACs as the modifier of Microtubule Associated Protein Tau's structure and function. **The XXXV Annual Meet of Indian Academy of Neuroscience & International Conference on Translational Neurosciences and its Application in Protection of Mental Health, 2017 (Ravenshaw University, Cuttack).**

Abstract: Intracellular Neurofibrillary Tangles are one of the major hallmarks of Alzheimer's disease, which contains aggregated microtubule-associated protein Tau as its main component. The aggregated form of Tau has signature of post-translational modifications, which are either the cause, or effect of Tauopathies. Acetylation and methylation are such modifications of Tau which regulate its function and structure. There are two classes of enzymes involved in regulation of acetylation – Acetyl transferases and deacetylases. HDAC6, cytoplasmic deacetylase, apart from removing acetyl groups from lysine is also involved in the clearance of aggregates load in cells by formation of aggresomes. Aggresome formation is mediated by its interaction with polyubiquitinated protein aggregates, but we are trying to find out whether its direct interaction has any effect on Tau aggregation propensity. If HDAC6 is able to interact directly with protein either in aggregated or soluble form, then what is the nature of this interaction and what are its implications. Also, the competition between ubiquitination, acetylation and methylation for available lysine can drive the protein to different fates. Acetylation and methylation contribute to Tauopathies either by causing hindrance to the normal clearance of aggregated proteins or by having cross talks with other PTMs

affecting their normal role. We are also interested in studying the cross talk between these modifications and how it regulates the function of Tau protein in Alzheimer's disease.

3. **Abhishek Ankur Balmik**, Tushar Dubey and Subashchandrabose Chinnathambi*. Signaling Cascades and Post-translational modifications of Tau. **EMBO- Meeting, Indo-French Conference, 2015 (IISER-Pune)**.

Abstract: Intracellular Neurofibrillary Tangles (NFTs) are one of the major hallmarks of Alzheimer's disease, with Microtubule Associated Protein Tau (MAPT) as its main component. Pathological form of Tau loses its ability to bind and stabilize microtubules and tend to self-associate and form Paired Helical Filaments (PHFs) which further leads to the formation of NFTs. Familial mutations as well as imbalance in post translational modifications (PTMs) can drive the conversion of Tau from normal to pathological form which has a high propensity for aggregation. Aggregated Tau in NFTs are found to be hyper phosphorylated signifying the role of phosphorylation as one of the PTMs responsible for Tauopathies. But the events which lead to Tau hyper phosphorylation are not clear. There are other PTMs like acetylation and methylation which are found to contribute in Tauopathies either by causing hindrance to the normal clearance of aggregated proteins or by having cross talks with other PTMs, affecting their normal role. It has been found that the acetylation of Tau at certain sites can prevent the degradation of hyper phosphorylated Tau which leads to the stability of Tau aggregates. However, it is known that the propensity of Tau aggregation decreases in case of acetylation at KXGS motifs in the repeat region. As the location of these acetylation sites interferes with the phosphorylation at sites known to be responsible for enhancing aggregation, indicating that there may be a protective role imparted by acetylation. In this regard, it would be interesting to study the role of enzymes involved in these modifications. There are two classes of enzymes involved in regulation of acetylation – Acetyl transferases and deacetylases. The best known acetyl transferases are CBP (CREB Binding Protein) and p300 while there are eleven protein deacetylases bearing the names HDACs and seven SIRT (Sirtuins) proteins homologous to yeast Sir2 (Sirtuin2). There may be interplay of different enzymes involved in acetylation and de-acetylation such that they act on different lysine residues of Tau in different conditions. The effect of Tau methylation with respect to its function is varied. Both phosphorylation and methylation are seen in Tau associated with microtubules in physiological condition and the balance between these two PTMs is important for its normal function. The direct role of methylation in Tauopathies is not clear. However, the competition between ubiquitination, acetylation and methylation for the available lysine can drive the protein to different fates. The motivation behind studying these PTMs is to derive the regulatory mechanisms which decide the state of protein.



Contents lists available at ScienceDirect

BBA - General Subjects

journal homepage: www.elsevier.com/locate/bbagen

Melatonin interacts with repeat domain of Tau to mediate disaggregation of paired helical filaments



Abhishek Ankur Balmik^{a,c,*}, Rashmi Das^{a,c,1}, Abha Dangi^{b,c}, Nalini Vijay Gorantla^{a,c},
Udaya Kiran Marelli^{b,c}, Subashchandrabose Chinnathambi^{a,c,*}

^a Neurobiology Group, Division of Biochemical Sciences, CSIR-National Chemical Laboratory, Dr. Homi Bhabha Road, 411008 Pune, India

^b Central NMR Facility and Division of Organic Chemistry, CSIR-National Chemical Laboratory, Dr. Homi Bhabha Road, 411008 Pune, India

^c Academy of Scientific and Innovative Research (AcSIR), 411008 Pune, India

ARTICLE INFO

Keywords:

Alzheimer's disease
Tau protein
Paired helical filaments
Tauopathies
Melatonin
Disaggregation

ABSTRACT

Tau is the major neuronal protein involved in the stabilization of microtubule assembly. In Alzheimer's disease, Tau self-assembles to form intracellular protein aggregates which are toxic to cells. Various methods have been tried and tested to restrain the aggregation of Tau. Most of the agents tested for this purpose have limitations in their effectiveness and availability to neuronal cells. We have tested melatonin, a neurohormone secreted by pineal gland and a well-known anti-oxidant, for its ability to interact with the repeat domain of Tau using ITC and NMR. In aggregation inhibition and disaggregation studies of repeat Tau, melatonin was found to modulate the aggregation propensity of repeat Tau at a concentration of 5000 μ M and was more effective in dissolving preformed aggregates rather than acting as an aggregation inhibitor. However, there were no major conformational changes in Tau in presence of melatonin as observed by CD spectroscopy. On the basis of our findings, we are proposing a mechanism by which melatonin can interact with the repeat domain of Tau and exhibit its disaggregation effect.

1. Introduction

Microtubule-associated protein Tau has been implicated in a series of neurological diseases called Tauopathies. Its main function in the neurons is to stabilize the microtubule structure by associating with them through its four repeat domains [1,2]. However, in Tauopathies, the repeat domains lose their function by self-associating to form intracellular protein aggregates called neurofibrillary tangles. Alzheimer's disease (AD) is associated with these intracellular NFTs along with deposition of extracellular Amyloid- β plaques, which results in progressive neurodegeneration [3]. The etiology of Alzheimer's disease is explained by two hypothesis *i.e.* Amyloid cascade hypothesis and Tau hypothesis [4,5]. However, Amyloid cascade hypothesis alone seems to be insufficient in explaining the etiology of AD since Amyloid- β is found to be deposited in adult brains without any pathological implication [6]. Also, Tauopathies include diseases that progress without any role of Amyloid- β plaques [7]. Thus, Tau mediated neurotoxicity draws

major attention as a potential therapeutic target [8,9]. Current therapies against Tau-mediated neuropathology target in various aspects [10]. One of the therapeutic approaches focus on the hyperphosphorylated state of Tau by targeting various kinases [11,12]. GSK3- β is one such important target which is involved in both Tau and Amyloid- β mediated pathology. Similarly, inhibitors for several other kinases like CDK5/p25, ERK, JNK are extensively studied for their phosphorylation on Tau and some of them are in clinical trials [1,13,14]. The other therapeutic strategies involves development of small molecules are able to inhibit Tau aggregation or dissolve the pre-existing aggregates, phosphatase activators, immunotherapy, acetylation inhibitors, microtubule stabilizers and deglycosylation inhibitors [1]. The progression of Alzheimer's disease is a multi-factorial process dependent on events like protein aggregation, neuro-inflammation and oxidative stress, which in turn are dependent on each other as cause or effect. However, the exact mechanism for the etiology of AD so far is not clearly understood.

Melatonin is an endocrine hormone secreted mainly from pineal

Abbreviations: NFTs, neurofibrillary tangles; PHF, paired helical filaments; A β , amyloid β ; CDK5/p25, cyclin dependent kinase 5/p25; GSK3- β , Glycogen synthase kinase 3- β ; ERK, extra-cellular signal regulated kinase; JNK, c-jun N-terminal kinase; PKA, protein kinase A; TNF- α , tumour necrosis factor - α ; IL, interleukins.

* Corresponding authors at: Neurobiology group, Division of Biochemical Sciences, CSIR-National Chemical Laboratory (CSIR-NCL), Dr. Homi Bhabha Road, 411008 Pune, India.

E-mail addresses: a.balmik@ncl.res.in (A.A. Balmik), s.chinnathambi@ncl.res.in (S. Chinnathambi).

¹ The authors wish it to be known that, in their opinion, the first two authors should be regarded as joint First Authors.

<https://doi.org/10.1016/j.bbagen.2019.129467>

Received 22 August 2019; Received in revised form 18 October 2019; Accepted 31 October 2019

Available online 09 November 2019

0304-4165/© 2019 Elsevier B.V. All rights reserved.

gland and functions as a regulator of circadian rhythm [15,16]. Melatonin is mainly known for its role in maintenance of circadian rhythm via regulation of transcription factor CLOCK and its homologs [17,18]. In conditions of depression and sleep disorders, exogenous melatonin administration is known to relieve the symptoms without any side-effects. Melatonin is rapidly metabolized in the liver through hydroxylation at C6 [19,20]. It can also be synthesized by other tissues in variable quantities as the enzymes for melatonin biosynthesis are ubiquitously expressed [21,22]. Melatonin is an amphipathic molecule, which can cross all biological membranes [23,24]. The role of melatonin in neuroprotection has been studied in terms of its various functions. It is well known that melatonin has potent anti-oxidant properties as well as regulator of other enzymes involved in protection against oxidative stress [25–28]. Anti-oxidant properties of melatonin and its metabolites have been well-studied. Mitochondria are the major source for the generation of free radicals during electron transport chain. Melatonin has been reported to cross mitochondrial membrane and ameliorate oxidative stress-induced mitochondrial dysfunction [29]. It also scavenges H₂O₂ and forms N 1-acetyl-N 2-formyl-5-methoxykynuramine which further gets converted to N 1-acetyl-5-methoxykynuramine, both of which are potent free radical scavengers themselves [30]. Melatonin also regulates the function of kinases like GSK3- β and PKA which are known to play a major role in Tau hyperphosphorylation [31,32]. Upon melatonin treatment, GSK3- β and PKA activity get reduced leading to decreased phosphorylation of Tau [32–34]. Due to its pleiotropic properties, high bioavailability and low toxicity, melatonin has drawn attention as a potent therapeutic molecule. Administration of melatonin in age-associated neurological disorders was found to improve the cognitive function and sleep patterns [35,36]. The effect of melatonin is most extensively studied with respect to Amyloid- β but its role in Tau pathology needs to be explored in terms of its multiple functions [37]. When melatonin is administered in Tg2576 mouse model for Amyloid- β pathology, it was found to ameliorate the A β induced oxidative stress and toxicity in early stages of disease development. However, it proved to be less effective in later stages of disease as A β burden increased [38,39]. The effect of melatonin as an aggregation inhibitor has been studied for A β and α -Synuclein [40,41]. It is also found to decrease the expression level of α -Synuclein in 4 day post-natal rats [42]. A recent study shows that melatonin and its close analogues inhibit and destabilize the aggregation of A β thereby acting as neuroprotective agents [43]. The binding of these agents to A β has been characterized in a residue specific manner by using NMR spectroscopy. Neurodegenerative diseases are often associated with inflammatory response, which further causes neuronal damage [44]. Melatonin inhibits the production of pro-inflammatory cytokines such as IL-6, IL-8 and TNF- α , hence, suppressing inflammation [45,46].

In the current studies, we explored the role of melatonin in interaction with repeat domain of Tau and modulation of its aggregation properties. We found that melatonin interacts with repeat Tau with a weak interaction. It is effective in repeat Tau aggregation inhibition and disaggregation at a high concentration. The current scenario suggests that melatonin can affect Tau aggregation but its potency as a drug need to be explored further in combination with other potent drugs.

2. Materials and methods

2.1. Materials

Melatonin, BES, MES, Glycine, SDS, ThT, Protease inhibitor cocktail and ANS were purchased from Sigma-Aldrich. Other biochemical or molecular biology grade chemicals used were - DTT and IPTG (Calbiochem), APS, NaCl, PMSF, Sodium Azide, Ampicillin (MP Biomedicals), Luria-Bertani broth (Himedia), Acrylamide, EGTA, TEMED, DMSO (Invitrogen). Cell culture media and reagents like DMEM, FBS, PBS and Penstrep were purchased from Invitrogen. BCA assay reagents used for protein estimation were purchased from Sigma-

Aldrich, ¹⁵N – Ammonium Chloride (Cambridge Isotopes Laboratories). Filtration devices were used from Merck and Pall Life sciences.

2.2. Protein expression and purification

Repeat domain Tau (K18wt) cloned in pT7C was transformed and induced for expression by 0.5 mM IPTG in BL21* cells [47,48]. Both proteins were purified in two steps using cation exchange chromatography and gel filtration chromatography. The cells expressing these proteins after transformation were scaled up and harvested. The cells were lysed by homogenization at 15 KPSI (using Constant cell disruption system). The lysate was supplied with 0.5 M NaCl and 5 mM DTT and kept at 90 °C for 20 min to denature all the structured protein. The resulting sample was centrifuged at 40000 rpm for 45 min. The supernatant was kept for overnight dialysis in 20 mM MES pH 6.8. The dialyzed sample was centrifuged again at 40000 rpm for 45 min and the supernatant was filtered and loaded onto Sepharose fast flow (SPFF) column (GE17–0729-01) pre-equilibrated with 20 mM MES pH 6.8, 50 mM NaCl. Elution was carried out using 20 mM MES pH 6.8, 1 M NaCl. The fractions collected from cation exchange chromatography containing Tau protein were pooled, concentrated and subjected to Gel filtration chromatography using 1 × PBS, 2 mM DTT using Superdex 75 Hi-load 16/600 column (GE28–9893-33). Protein concentrations were determined by using BCA assay.

2.3. ¹⁵N repeat Tau labelling and production

¹⁵N Repeat Tau protein was labelled by growing transformed BL21* E.coli cells first in LB broth (Unlabelled media) to obtain high cell density and then transferring the cells to minimal media containing ¹⁵N labelled ammonium chloride [49]. The pT7C repeat Tau transformed BL21* cells were initially grown in LB (6 L) with 100 μ g/mL Ampicillin at 37 °C till the OD reaches 0.6 at 600 nm. The cells were pelleted down and washed with 1 × M9 salts, after which they are re-suspended in minimal media containing ¹⁵N labelled ammonium chloride. In order to clear unlabelled metabolites, the cells were grown at 37 °C for 1 h prior to induction with 0.5 mM IPTG and harvesting after 4–5 h. The labelled protein was prepared similarly as previously described method for unlabelled Tau protein.

2.4. Tau aggregation inhibition assay

Aggregates of repeat Tau were prepared in 20 mM BES, pH 7.4 by supplementing heparin as an aggregation inducer in 1:4 ratio with protein (Heparin: protein). The assembly buffer also consisted of 25 mM NaCl, 1 mM DTT and 0.01% Sodium azide. The reactions were set up as 20 μ M Tau in microcentrifuge amber tubes and incubated at 37 °C for 24 h and 96 h for repeat Tau. Melatonin prepared in 10% DMSO was added in reaction tubes for repeat Tau (50, 100, 200, 500 and 1000 μ M). Aliquots of repeat Tau aggregates were taken at different time intervals to measure ThT or ANS fluorescence. All the measurements were taken in triplicates. ThT fluorescence was measured by excitation at 450 nm and emission at 475 nm while ANS was measured at 375 nm as excitation and 490 nm as emission. The ratio of protein and ThT was taken as 1:1. For ANS fluorescence, the ratio between the protein and ANS was taken as 1:20. ThT and ANS fluorescence for BES buffer was measured for blank subtraction.

2.5. Disaggregation of matured Tau aggregates

Repeat Tau aggregates were prepared as mentioned above for inhibition assay in a concentration of 100 μ M incubated with 25 μ M of heparin. After 6 days of incubation at 37 °C, the protein was diluted to 20 μ M in a series of reaction tubes with 20 mM BES, pH 7.4 in which various concentrations of melatonin prepared in 10% DMSO (100, 200, 1000 and 5000 μ M) were added and again kept at 37 °C. The reaction

tubes also contained 25 mM NaCl, 1 mM DTT and 0.01% Sodium azide. ThT fluorescence was measured at 450 nm excitation and 475 nm emission in 30 min interval for 4 h.

For continuous measurement mode, the reaction was set-up in 20 mM BES, pH 7.4 in 96 well black flat bottom plates in a total volume of 200 μ L without any additives. The measuring concentration of Tau was taken as 5 μ M while melatonin was added in 500, 1000, 2000 and 5000 μ M concentrations. ThT fluorescence of BES buffer was measured as blank while 5 μ M Tau with BES was measured as aggregate control. A control measurement for 10% DMSO was taken to rule out the effect of DMSO. ThT fluorescence was measured continuously at 450 nm excitation and 475 nm emission wavelength at an interval of 1 min with a shaking time of 30 s in a Tecan M200pro spectrophotometer. A total of 20 such measurements were taken over the time of \sim 30 min. Two sets of disaggregation assay in continuous mode were performed.

2.6. NMR spectroscopy

A 200 μ M solution of 15 N labelled repeat Tau protein in 50 mM phosphate buffer (10:90 D₂O:H₂O) containing 1 mM DTT was used for NMR spectroscopic experiments. All NMR studies were carried out at 278 K on Bruker Avance III HD 700 MHz spectrometer equipped with a TXI probe. 1 H- 15 N HSQC experiments were acquired with 512 increments (16 scans per increment) in the indirect dimension and 2 k complex points were collected in the direct dimension. All the data was analyzed using Sparky program [50] after processing by Bruker toppsin 3.2 software.

2.7. Far-UV CD spectroscopy

Far-UV CD spectrum was acquired for soluble Tau, Tau aggregates and melatonin treated samples using Jasco J-815 CD spectrometer in a cuvette with a path length of 1 mm under nitrogen atmosphere. The scans were carried out at a scan speed of 100 nm/min and bandwidth 1 nm with a scan range from 190 to 250 nm. The final spectra were taken as an average of 5 acquisitions. In each experiment, measurements were done at 25 $^{\circ}$ C. The buffer baseline was set with 50 mM sodium phosphate buffer, pH 6.8 and subtracted from the measured spectra for each sample. Tau concentration was maintained as 5 μ M for all CD measurements. The final subtracted values were plotted using SigmaPlot 10.0 (Systat software).

2.8. Transmission electron microscopy

For TEM imaging, 2 μ M of Tau samples were applied on 400 mesh carbon coated copper grids, washed twice with filtered milliQ water and negatively stained with 2% aqueous uranyl acetate for 2 min. The samples were visualized by using TECNAI T20 Transmission Electron Microscope at 120 KV.

2.9. Isothermal titration calorimetry

Isothermal titration Calorimetry experiments were carried out by using Malvern PEAQ-ITC instrument (Microcal). Final concentration of repeat Tau and melatonin used for titration was adjusted by 20 mM BES buffer pH 7.4. Stock solution of melatonin (3000 μ M) was made in the same buffer to minimize buffer mismatch during titration. Both repeat Tau and melatonin were filtered prior to titration. Reverse titration was performed at 25 $^{\circ}$ C by using melatonin in the sample cell while repeat Tau in the syringe. Different ratio of repeat Tau and melatonin was used so as to reach the equimolar ratio of repeat Tau and melatonin. Each titration comprises of 19 injections of 2 μ L for 5 s at an interval of 180 s between each injection. An initial injection of 0.4 μ L was given for stabilization. The data obtained was analyzed by PEAQ-ITC software and fitted using one set of sites model. The values of Δ G, Δ H and Δ S were used to calculate the binding constant or the association constant.

$$-RT \ln K = \Delta G = \Delta H - T \Delta S$$

2.10. Cytotoxicity assay for repeat Tau aggregates

Repeat Tau aggregates were tested for their effect on viability of Neuro2A cells. Neuro2A cell line was cultured in Dulbecco modified eagle's media (DMEM) with 10% FBS and 100 μ g/mL of penicillin and streptomycin. Neuro2A cells were seeded in 96 well plates (10,000 cells/well) and incubated at 37 $^{\circ}$ C for 12 h at 5% CO₂. Cells were treated with 1–40 μ M repeat Tau aggregates in reduced serum media (DMEM with 0.5% FBS) in each well and incubated for 24 h. MTT assay was performed to check the cell viability. MTT was added in 0.5 mg/mL concentration in each well and incubated for 3 h. The formazan end product solubilized by adding absolute DMSO. The spectrophotometric absorbance was measured at 570 nm in triplicate (Tecan Infinite 200 Pro).

2.11. Statistical analysis

All the experimental analyses were carried out in triplicate. The statistical analysis of control and treated samples were carried out by SigmaPlot 10.0 (Systat software). One way ANOVA was conducted for the analysis of results. Tukey's HSD (Honest significant difference) post-hoc analysis was performed to compare the significance within groups (Significant at mean difference between groups > Tukey's criterion; T).

3. Results

3.1. Melatonin in higher concentrations inhibits repeat Tau aggregation

We investigated the potential of melatonin as an inhibitor of Tau protein aggregation by subjecting melatonin at a concentration range of 100–5000 μ M. Repeat domain of Tau (Fig. 1A-I) was subjected to aggregation in presence of melatonin (Fig. 1A-II). The aggregation kinetics of repeat Tau was monitored by ThT and ANS fluorescence. It was observed that melatonin was able to inhibit repeat Tau aggregation at a concentration as high as 1000 μ M (Fig. 1B) without affecting the hydrophobicity of Tau protein as indicated by ANS fluorescence (Fig. 1C). Transmission electron microscopy images for repeat Tau samples subjected to aggregation in presence of 1000 μ M of melatonin showed distinct morphology of small, broken Tau aggregates while control aggregates showed mature Tau fibrils (Fig. 1E).

3.2. Melatonin has no effect on structural conformation of Tau

Tau in its soluble form exists in a random coil conformation which changes to β -sheet form when it aggregates. We studied the effect of melatonin using circular dichroism spectroscopy for its ability to alter the structure of repeat and found that it does not affect the conformation of Tau during interaction. CD spectroscopy for soluble repeat Tau shows a negative band at \sim 198 nm while upon aggregation in the presence of heparin, the spectrum shifts towards β -sheet structure with a signature negative band at 208 nm (Fig. 1D). However, there was no change in the spectra indicating that the β -sheet conformation was retained even in the presence of melatonin.

3.3. Melatonin disaggregates pre-formed repeat Tau aggregates

Tau protein upon aggregation forms well defined fibrillar protein aggregates through a series of intermediate species. We prepared repeat Tau aggregates and incubated them with various concentrations of melatonin. Treatment of aggregates with 100 μ M of melatonin shows little or insignificant disaggregation effect while at higher concentrations (200, 1000 and 5000 μ M) of melatonin, there was effective disaggregation of repeat Tau fibrils (Fig. 2A). There was 54%

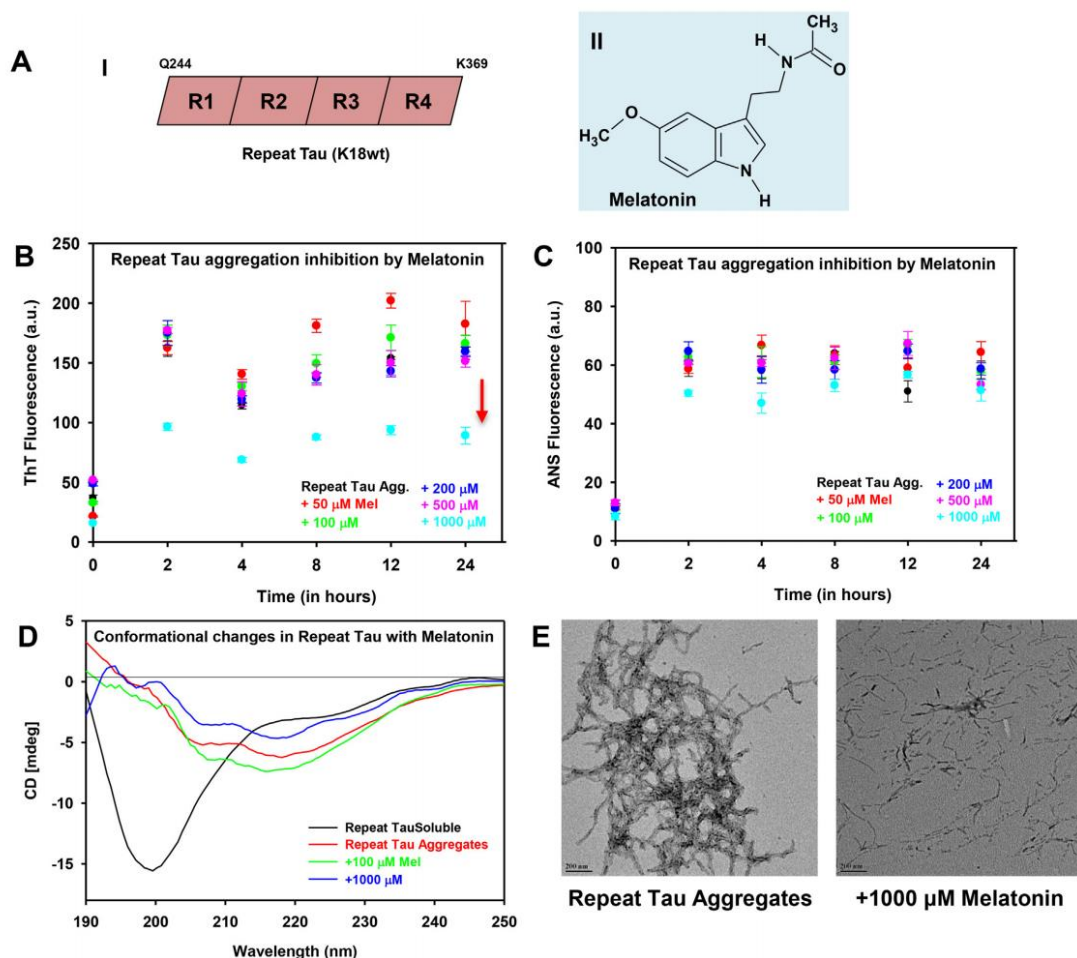


Fig. 1. Effect of melatonin on repeat Tau aggregation. A) Domain organization of repeat Tau. The four repeat domains hold importance as the microtubule-binding domain of Tau as well as the core of the pathological PHF assembly. The polyproline domain plays an important role in the phosphorylation of Tau via proline directed kinases. (II) Chemical structure of melatonin. B) ThT fluorescence assay for repeat Tau aggregation inhibition by melatonin. Melatonin inhibited repeat Tau aggregation at the concentration of 1000 µM (Data represented as SD ± Mean of triplicate values). C) ANS fluorescence assay for repeat Tau aggregation with different concentration of melatonin. Melatonin does not cause any change in hydrophobicity of repeat Tau (Data represented as SD ± Mean of triplicate values). D) CD spectroscopy for repeat Tau aggregation samples with or without melatonin. For melatonin treated samples, no difference was observed as compared to control aggregates samples. E) Electron micrographs for repeat Tau control aggregates and repeat Tau incubated with 1000 µM of melatonin. Broken aggregates were observed in the melatonin treated sample while control shows mature repeat Tau aggregates.

disaggregation observed with 5000 µM melatonin while 100 µM melatonin gives only around 14% disaggregation (Fig. 2B). Statistical significance was calculated with respect to Tukey's criterion where the groups having difference of means greater than Tukey's criterion are statistically significant. In order to study the time course of disaggregation, continuous fluorescence measurement was taken which showed similar results for the same range of melatonin concentrations (Fig. 2C). The samples at the end-point of the assay were observed under TEM which revealed fewer and shorter fibrils in samples with 1000 and 5000 µM melatonin distinct from mature Tau fibrils in control aggregates (Fig. 2D–F).

3.4. Melatonin interacts weakly with the repeat Tau

Being an amphipathic molecule, melatonin can interact with a wide variety of molecules. Melatonin exhibited the property as modifier of repeat Tau aggregation, both as an inhibitor and in disaggregation. We studied their interaction using ITC as a function of its activity with repeat Tau. In ITC, the non-specific heat change was ruled out by titrating melatonin with titration buffer (Fig. S1A). At lower concentrations of titrants, there was no significant heat change (Fig. S1B). We performed reverse titration in ITC with ratios of melatonin to repeat Tau as 1:1, 1:2 and 1:10 (Fig. 3A–C). There was significant heat change for the interaction of repeat Tau and melatonin at these concentrations. As the concentration of repeat Tau is increased with respect to

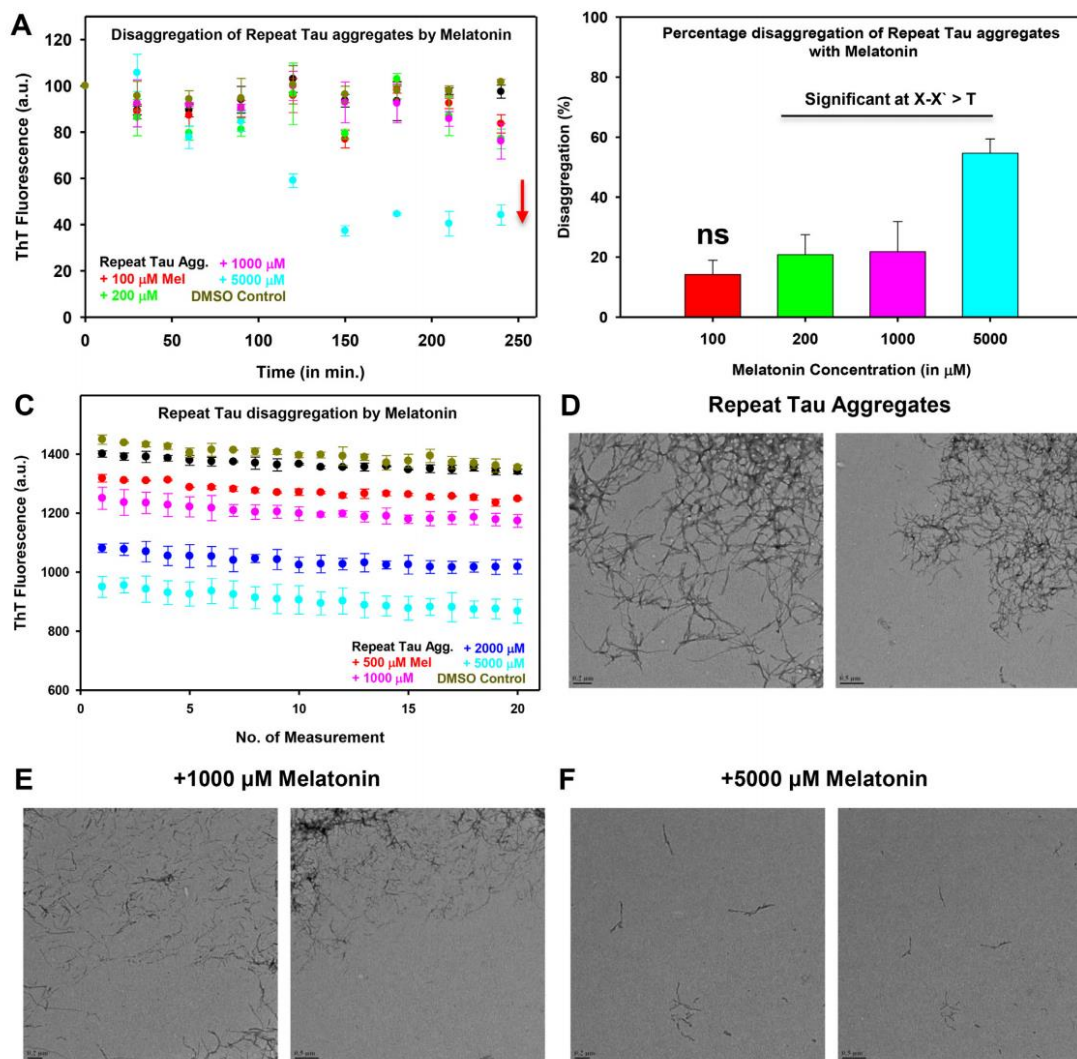


Fig. 2. Disaggregation of repeat Tau fibrils by melatonin. **A)** ThT fluorescence assay for repeat Tau disaggregation with different melatonin concentration. Disaggregation of preformed repeat Tau aggregates observed for 1000 and 5000 μM of melatonin. **B)** Melatonin shows nearly 60% disaggregation of repeat Tau aggregates at 5000 μM as compared to the end-point fluorescence value of repeat Tau aggregates (Significant at mean difference $> T = 16.589$). **C)** Repeat Tau disaggregation assay in continuous mode. Disaggregation assay for pre-formed repeat Tau aggregates was monitored in a continuous mode using ThT fluorescence. Melatonin was used in the concentration range from 500 to 5000 μM . Melatonin showed disaggregation effect only at higher concentrations range. **D,E,F)** TEM images repeat Tau aggregates treated with 1000 and 5000 μM melatonin shows morphology of broken fibrils as compared to the control aggregates sample (Scale bars – 0.2 and 0.5 μm).

melatonin, the molar ratio approaches unity (Fig. 3D–F). However, this result in the equilibrium shift towards dissociation before the saturation can be attained in the system. These results shows the interaction between melatonin and repeat Tau without attaining the saturation and melatonin can bind to repeat Tau with a weak affinity.

3.5. Characterization of residue specific interaction of melatonin and repeat Tau using NMR spectroscopy

NMR spectroscopic studies were carried out to characterize the interaction of melatonin with repeat Tau. 200 μM solution of repeat Tau in phosphate buffer was titrated against stoichiometric ratios (1:0, 1:5, 1:10, 1:25, 1:50 ratios of repeat Tau to melatonin) of melatonin and the residue specific chemical shift perturbations were monitored by ^1H – ^{15}N HSQC experiments (Fig. 4). NMR data revealed considerable

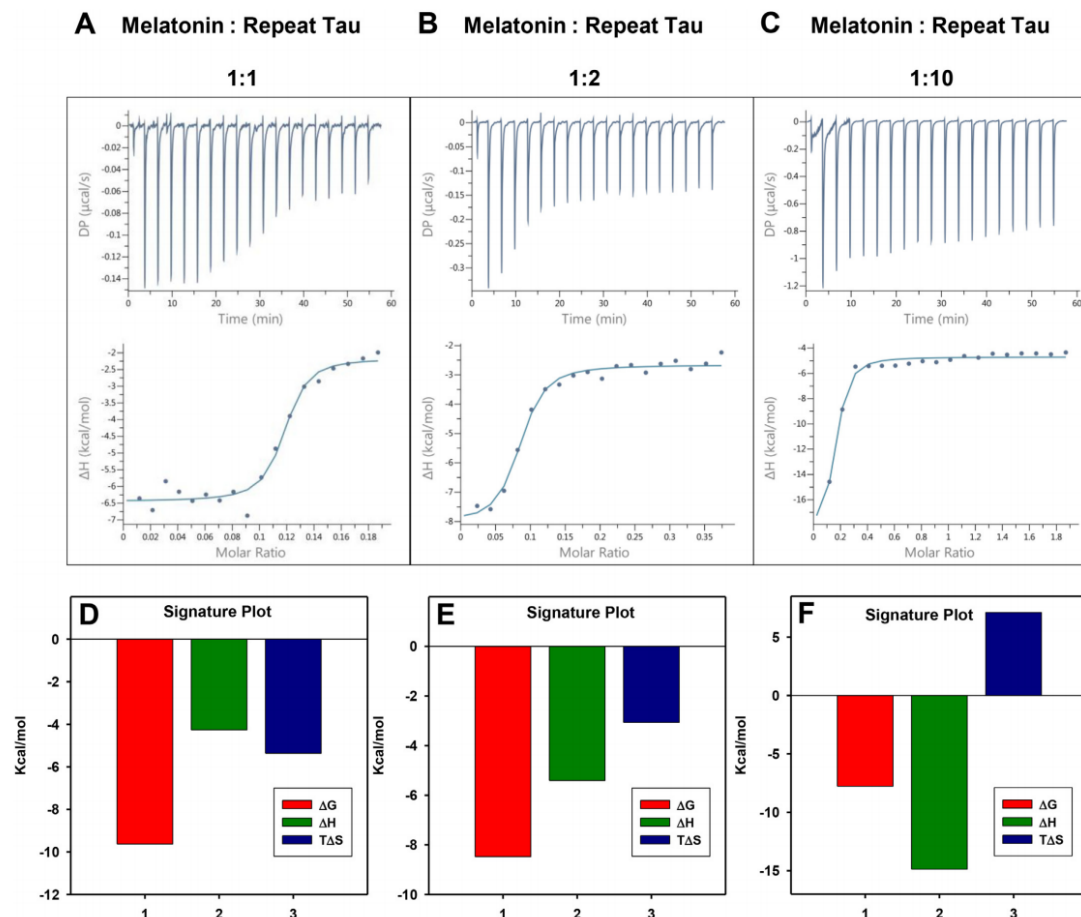


Fig. 3. Repeat Tau-melatonin interaction by ITC A) Isothermal titration Calorimetry thermographs for the reverse titration of repeat Tau (titrant) and melatonin (titrand) at 1:1 ratio shows the association between the two although without attaining saturation. B) Reverse titration at 1:2 ratio produce a near exponential heat plot indicative of concentration dependent association of repeat Tau and melatonin. C) At 1:10 ratio, rapid heat change was observed with each injection along with exponential heat plot, but saturation was not observed due to dynamic nature of Tau-melatonin binding. D, E, F) Signature plots for repeat Tau-melatonin reverse titration at 1:1, 1:2 and 1:10 ratios showing highly negative free energy change indicating the spontaneity of association.

perturbation of all the five histidine residues in repeat Tau H268, H299, H329, H330, H362 and the other residues such as V300, K331 and V363, which are adjacent to histidines. Apparently, the interaction of melatonin with repeat Tau is similar to the interaction by polyamines such as spermine and spermidine, which also bind at the histidine sites of repeat Tau or A β [51]. However, melatonin is weakly binding and requires millimolar concentration for observable effects. Furthermore titration with melatonin has slowly populated a new HSQC cross peak at $\delta(^1\text{H}, ^{15}\text{N}) = (7.933, 127.178)$ (bottom right corner of Fig. 4), whose intensity rose with increasing concentration of melatonin, which otherwise was completely absent in the native conditions. Hence, this cross peak could not be traced to any residue due to the lack of an appropriate backbone chemical shift assignment. We speculate that the cross peak might be resulting from a residue which was flexible and broadened beyond observation in the absence of melatonin.

3.6. Effect of melatonin on repeat Tau aggregates-mediated toxicity

Melatonin showed inhibitory effect on repeat Tau aggregation which prompted us to check whether it can revert the aggregates-mediated cytotoxicity. Firstly, neuro2a cells were treated with repeat Tau aggregates in 0–40 μM concentrations to determine its minimal toxicity on neuro2a cells (Fig. 5A and S2). It was observed that 5 μM repeat Tau aggregates induced 50% cytotoxicity. 0–100 μM of melatonin along with 5 μM of repeat Tau aggregates were given to neuro2a cells. Melatonin treatment showed no significant rescuing effect from aggregates mediated toxicity (Fig. 5B). Tau aggregates used for treatment were also measured by SDS-PAGE, ThT fluorescence and CD spectroscopy (Fig. S3A–C). Statistical significance was determined by single factor ANOVA followed by Tukey's post-hoc analysis. The significant groups are represented by assigning different letters while for non-significant results same letters have been assigned.

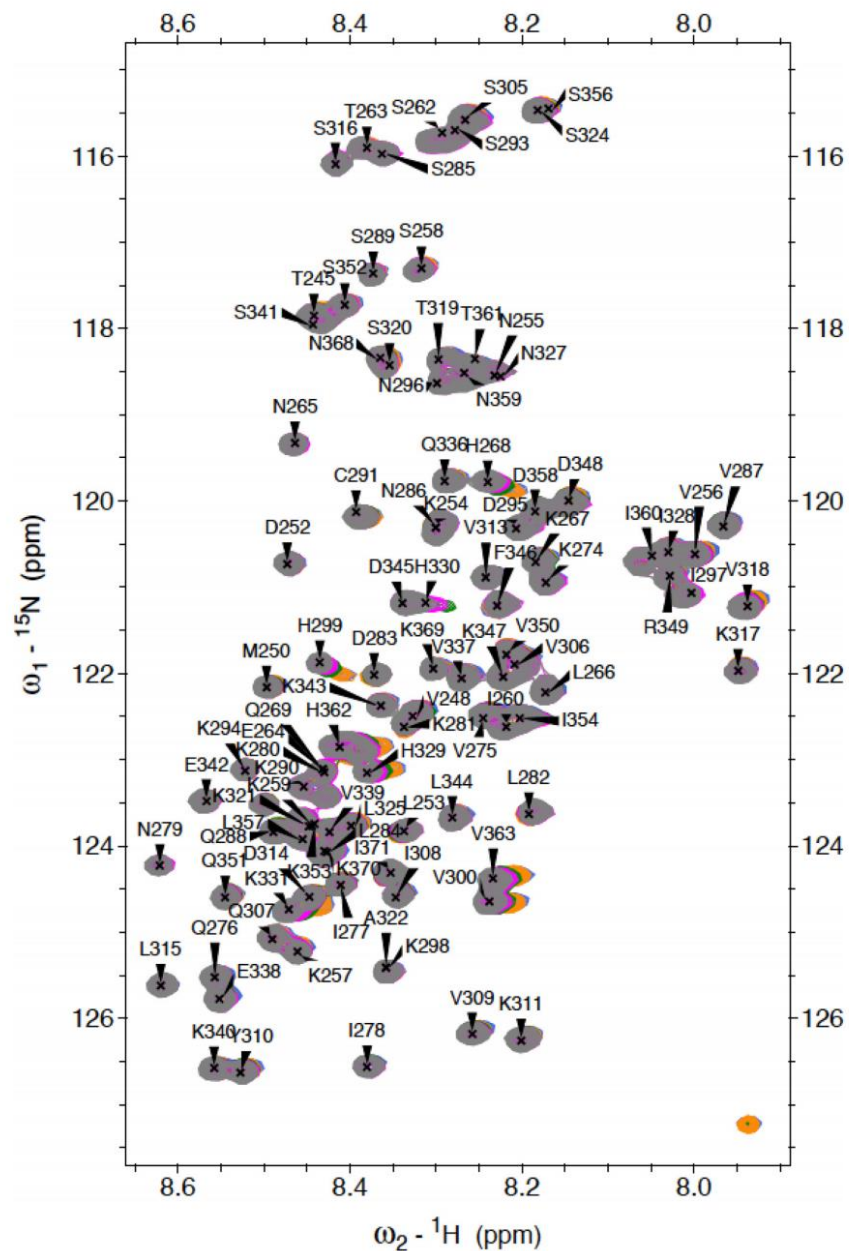


Fig. 4. ^1H - ^{15}N HSQC NMR for repeat Tau and melatonin. ^1H - ^{15}N HSQC chemical shift perturbation plot for the titration of 200 μM solution of repeat Tau with melatonin in concentration ratios 1:0 (gray), 1:5 (magenta), 1:10 (green), 1:25 (dark orange), 1:50 (dark blue) of repeat Tau to melatonin. Almost all the cross peaks in ^1H - ^{15}N HSQC have been labelled with the names of the respective residues from repeat Tau [61]. Residues from repeat Tau that are involved in interaction with melatonin can be identified based on the shifting position of their corresponding cross peaks with increasing concentration of melatonin.

A.A. Balmik, et al.

BBA - General Subjects 1864 (2020) 129467

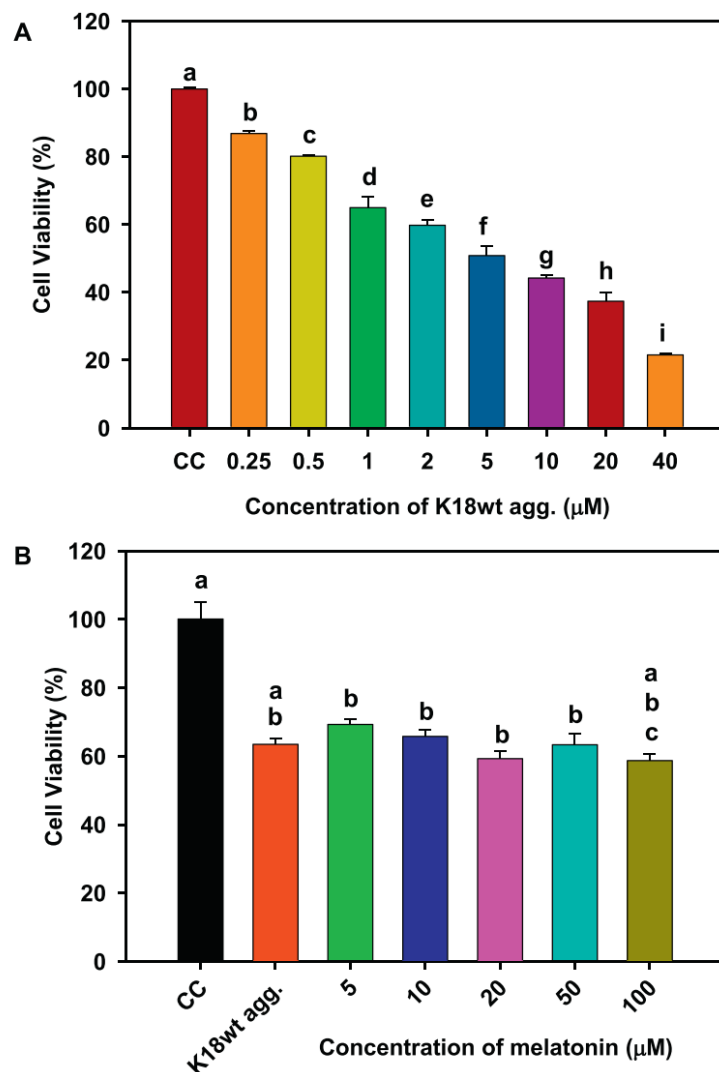


Fig. 5. Cytotoxicity of repeat Tau aggregates on neuro2a and effect of melatonin on Tau aggregates mediated toxicity. A) Neuro2a cells were treated with repeat Tau aggregates prepared *in vitro* with heparin as an inducer. Treatment with repeat Tau aggregates shows reduced cell viability in a concentration dependent manner. 50% viability was obtained with 5 μM aggregates treatment while the highest concentration of aggregates used in the study (40 μM) showed 20% cell viability. (Significant at mean difference $> T = 5.0716$, Groups with the same letters are not significantly different). B) 5 μM of repeat Tau aggregates were used to induce cyto-toxicity in neuro2a. Melatonin treatment (0–100 μM) along with aggregates did not show significant rescue. (Significant at mean difference $> T = 9.245$, Groups with the same letters are not significantly different, Data represented as SD \pm Mean of triplicate values).

4. Discussion

Microtubule-associated protein Tau undergoes loss of physiological function in Alzheimer's disease where the repeat domain of Tau plays an important role as they form the core of the aggregated Tau fibrils. The approaches for designing potent inhibitors of Tau aggregation are based on various properties of Tau aggregates. Inhibitors may function as electrophiles to compensate the charge imbalance in Tau or may interact covalently to modify the binding properties of Tau [52,53]. For example, cinnamaldehyde functions as an electrophile attacking cysteine residues while oleocanthal, a natural phenolic compound interacts covalently with Lysine residues of Tau [54,55]. Some other inhibitors can change their course of action as the reaction environment changes. Baicalein is a natural flavonoid which gets oxidized to quinone form and work as a covalent inhibitor as the reaction progresses [56].

Melatonin has been studied with respect to its action on Amyloid- β and alpha synuclein aggregates. Melatonin interacts with Amyloid- β peptides through Histidine and Aspartate residues which disrupts the His-Asp salt bridge leading to aggregation inhibition [41]. In another study on middle aged mice, Amyloid- β_{25-35} induced oxidative damage was found to be alleviated. Injecting melatonin to the brain of affected mice reduced lipid peroxidation as well as enhanced the activity of antioxidant enzymes like superoxide dismutase and glutathione peroxidase [57]. Similar observations have been reported in the studies with α -synuclein, where melatonin was found to inhibit as well as dissolves α -synuclein fibrils [40]. It is also found to reduce the expression of α -synuclein and ameliorate amphetamine induced α -synuclein toxicity [58]. In our studies, we explored the role of melatonin in terms of its interaction with the repeat domain and its ability to inhibit aggregation or dissolve pre-formed aggregates. Melatonin is known to interact with

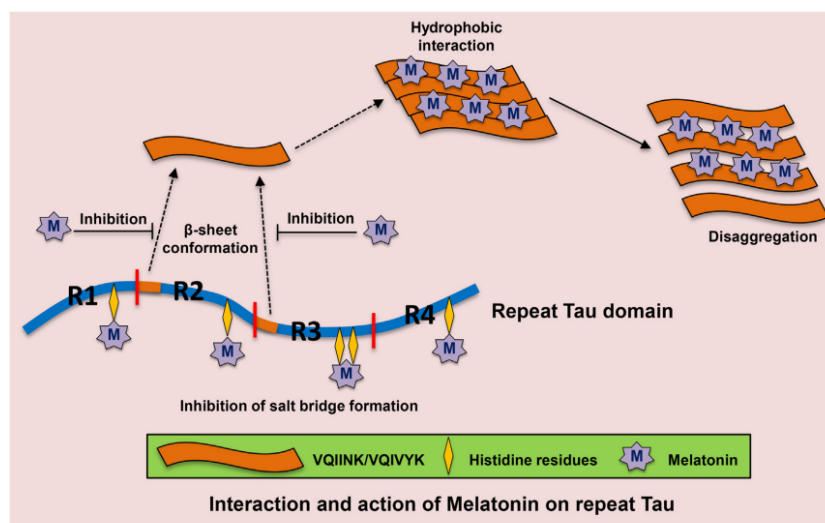


Fig. 6. Mode of interaction and action of Melatonin on repeat Tau. Figure shows the possible model for the mode of action of Melatonin as an aggregation inhibitor as well as disaggregation of repeat Tau aggregates. Salt bridges are formed between repeat Tau molecules which strengthen the core of PHF during aggregation. Melatonin can bind to repeat Tau by associating with the Histidine residues and hindering the formation of salt bridges between two repeat molecules, thus inhibiting their aggregation. Melatonin can also interact with repeat Tau through hydrophobic interaction once the aggregation is established. Hydrophobic interaction with Melatonin weakens the Tau interaction in PHF assembly resulting in their disaggregation.

Histidine residues and hydrophobic patches in amyloid- β aggregates through which it either disrupts His-Asp salt-bridge formation or diminishes hydrophobic interaction that impairs fibril assembly [41,59]. In TEM analysis of aggregation assay samples, there was observable effect in melatonin treated samples as compared to control aggregates. NMR studies for the interaction of repeat Tau and melatonin suggests that melatonin binds to all five Histidine residues (H268, H299, H329, H330 and H362) in repeat Tau along with V300, K331 and V363. We propose a mechanism by which melatonin exerts its disaggregation effect through its interaction with histidine residues and thus results in destabilization of aggregates assembly. Melatonin can hinder the salt bridge formation between two Tau molecules which in turn hinders the strengthening of PHF assembly. Also, it weakens the PHF assembly through its hydrophobic interaction with the pre-formed aggregates (Fig. 6). However, the concentration required to show its effect is high since the interaction between repeat Tau and melatonin is weak as revealed by NMR and ITC. Also, it did not showed any significant effect on retention of cell-viability upon repeat Tau aggregates treatment. Thus, it is suggested to incorporate melatonin along with other potent drugs to enhance the effect of therapeutics [60].

Melatonin serves a wide array of function as anti-oxidant, anti-inflammatory agent and modulator of other functions like phosphorylation and gene regulation. In this aspect, the combination of melatonin with other potent molecule, which allows the optimum activity of both, can be a helpful measure. The high bioavailability as well as pleiotropic functions of melatonin makes it a good candidate for therapeutics in Alzheimer's disease.

5. Conclusion

Melatonin is a neuro-modulatory hormone which serves multiple functions as free radical scavenger, anti-oxidant, transcriptional and functional regulator of various proteins. All these functions have been linked to its function as cytoprotective agent in general. The ability of melatonin to cross blood-brain barrier makes it a potent

neuroprotective agent. Our results showed that melatonin interacts with the repeat domain of Tau weakly. In spite of its weak interaction and slow kinetics, it was apt enough to dissolve Tau fibrils. The inhibition and disaggregation effects of melatonin on repeat Tau were mediated by its interaction with the histidine sites on the protein. It required high concentration of melatonin to exert its effect on aggregation of Tau, but it is known to be non-toxic even at higher concentrations. Melatonin is a potent biomolecule whose therapeutic action has been well studied in neurodegenerative diseases. However, its low half-life period in biological system limits its therapeutic use. Thus, we suggest enhancing its ameliorating effects either by conjugation in order to stabilize the molecule or in combination with other potent drugs to complement their action.

Author contributions

A.B, R.D. and S.C. designed and carried out the experiments. A.D. and U.M. carried out the NMR experiments, analyzed and wrote the NMR part. A.B and S.C. analyzed the data and wrote the article. S.C. conceived the idea of the project, supervised the project, provided resources and wrote the manuscript. All authors contributed to the discussions and manuscript review.

Funding

This project is supported in part by grant from the in-house CSIR-National Chemical Laboratory grant MLP029526.

Notes

The authors declare no competing financial interest.

Acknowledgements

Abhishek Ankur Balmik acknowledges the Shyama Prasad

Mukherjee fellowship (SPMF) from Council of Scientific Industrial Research (CSIR), India. Rashmi Das and Nalini Vijay Gorantla acknowledges the fellowship from University Grant Commission (UGC) India. Abha Dangi acknowledges the fellowship from Council of Scientific Industrial Research (CSIR). Tau constructs were kindly gifted by Prof. Roland Brandt from University of Osnabruck, Germany.

Appendix A. Supplementary data

Supplementary data to this article can be found online at <https://doi.org/10.1016/j.bbagen.2019.129467>.

References

- [1] E.E. Congdon, E.M. Sigurdsson, Tau-targeting therapies for Alzheimer disease, *Nat. Rev. Neurol.* (2018) 1.
- [2] E.-M. Mandelkow, E. Mandelkow, Biochemistry and cell biology of tau protein in neurofibrillary degeneration, *Cold Spring Harbor Perspect. Med.* 2 (2012) a006247.
- [3] D.W. Dickson, S.-H.C. Yen, Beta-amyloid deposition and paired helical filament formation: which histopathological feature is more significant in Alzheimer's disease? *Neurobiol. Aging* 10 (1989) 402–404.
- [4] J.A. Hardy, G.A. Higgins, Alzheimer's disease: the amyloid cascade hypothesis, *Science* 256 (1992) 184.
- [5] A.d.C. Alonso, I. Grundke-Iqbal, K. Iqbal, Alzheimer's disease hyperphosphorylated tau sequesters normal tau into tangles of filaments and disassembles microtubules, *Nat. Med.* 2 (1996) 783–787.
- [6] D.W. Dickson, H.A. Crystal, L.A. Mattiace, D.M. Masur, A.D. Blau, P. Davies, S.-H. Yen, M.K. Aronson, Identification of normal and pathological aging in prospectively studied nondemented elderly humans, *Neurobiol. Aging* 13 (1992) 179–189.
- [7] M. Tolnay, A. Probst, The neuropathological spectrum of neurodegenerative tauopathies, *IUBMB Life* 55 (2003) 299–305.
- [8] S. Mondragón-Rodríguez, G. Perry, X. Zhu, J. Boehm, Amyloid beta and tau proteins as therapeutic targets for Alzheimer's disease treatment: rethinking the current strategy, *Int. J. Alzheimers Dis.* 2012 (2012).
- [9] E. Giacomini, G. Gold, Alzheimer disease therapy—moving from amyloid- β to tau, *Nat. Rev. Neurol.* 9 (2013) 677.
- [10] J. Götz, A. Ittner, L.M. Ittner, Tau targeted treatment strategies in Alzheimer's disease, *Br. J. Pharmacol.* 165 (2012) 1246–1259.
- [11] V.M.Y. Lee, K.R. Brunden, M. Hutton, J.Q. Trojanowski, Developing therapeutic approaches to tau, selected kinases, and related neuronal protein targets, *Cold Spring Harbor Perspect. Med.* 1 (2011) a006437.
- [12] T. Li, L.E. Chalifour, H.K. Paudel, Phosphorylation of protein phosphatase 1 by cyclin-dependent protein kinase 5 during nerve growth factor-induced PC12 cell differentiation, *J. Biol. Chem.* 282 (2007) 6619–6628.
- [13] C.X. Gong, K. Iqbal, Hyperphosphorylation of microtubule-associated protein tau: a promising therapeutic target for Alzheimer disease, *Curr. Med. Chem.* 15 (2008) 2321–2328.
- [14] A.P.D. Hilgeroth, V. Tell, Recent developments of protein kinase inhibitors as potential AD therapeutics, *Front. Cell. Neurosci.* 7 (2013) 189.
- [15] B. Claustrat, J. Brun, G. Chazot, The basic physiology and pathophysiology of melatonin, *Sleep Med. Rev.* 9 (2005) 11–24.
- [16] S.R. Pandi-Perumal, I. Trakht, V. Srinivasan, D.W. Spence, G.J.M. Maestroni, N. Zisapel, D.P. Cardinali, Physiological effects of melatonin: role of melatonin receptors and signal transduction pathways, *Prog. Neurobiol.* 85 (2008) 335–353.
- [17] M.H. Vitaterna, D.P. King, A.-M. Chang, J.M. Kornhauser, P.L. Lowrey, J.D. McDonald, W.F. Dove, L.H. Pinto, F.W. Turek, J.S. Takahashi, Mutagenesis and mapping of a mouse gene, clock, essential for circadian behavior, *Science* 264 (1994) 719–725.
- [18] G. Asher, U. Schibler, A CLOCK-less clock, *Trends Cell Biol.* 16 (2006) 547–549.
- [19] C. Cajochen, K. Kräuchi, A. Wirz-Justice, Role of melatonin in the regulation of human circadian rhythms and sleep, *J. Neuroendocrinol.* 15 (2003) 432–437.
- [20] D.P. CARDINALI, H.J. LYNCH, R.J. WURTMAN, Binding of melatonin to human and rat plasma proteins, *Endocrinology* 91 (1972) 1213–1218.
- [21] J. Stefulj, M. Hörtnner, M. Ghosh, K. Schauenstein, I. Rinner, A. Wölfler, J. Semmler, P.M. Liebmann, Gene expression of the key enzymes of melatonin synthesis in extrapineal tissues of the rat, *J. Pineal Res.* 30 (2001) 243–247.
- [22] R.J. Reiter, D.-X. Tan, What constitutes a physiological concentration of melatonin? *J. Pineal Res.* 34 (2003) 79–80.
- [23] F.D.J.L. Anton-Tay, J.L. Diaz, A. Fernandez-Guardiola, On the effect of melatonin upon human brain. Its possible therapeutic implications, *Life Sci.* 10 (1971) 841–850.
- [24] H. Yu, E.J. Dickson, S.-R. Jung, D.-S. Koh, B. Hille, High membrane permeability for melatonin, *J. General Physiol.* 147 (2016) 63–76.
- [25] C. Tomas-Zapico, A. Coto-Montes, A proposed mechanism to explain the stimulatory effect of melatonin on antioxidative enzymes, *J. Pineal Res.* 39 (2005) 99–104.
- [26] X. Wang, The antiapoptotic activity of melatonin in neurodegenerative diseases, *CNS Neurosci. Ther.* 15 (2009) 345–357.
- [27] J.Z. Wang, Z.F. Wang, Role of melatonin in Alzheimer-like neurodegeneration, *Acta Pharmacol. Sin.* 27 (2006) 41–49.
- [28] D.X. Tan, R.J. Reiter, L.C. Manchester, M.T. Yan, M. El-Sawi, R.M. Sainz, J.C. Mayo, R. Kohen, M.C. Allegra, R. Hardeland, Chemical and physical properties and potential mechanisms: melatonin as a broad spectrum antioxidant and free radical scavenger, *Curr. Top. Med. Chem.* 2 (2002) 181–197.
- [29] M.J. Jou, T.I. Peng, R.J. Reiter, S.B. Jou, H.Y. Wu, S.T. Wen, Visualization of the antioxidative effects of melatonin at the mitochondrial level during oxidative stress-induced apoptosis of rat brain astrocytes, *J. Pineal Res.* 37 (2004) 55–70.
- [30] D.-X. Tan, L.C. Manchester, R.J. Reiter, B.F. Plummer, J. Limson, S.T. Weintraub, W. Qi, Melatonin directly scavenges hydrogen peroxide: a potentially new metabolic pathway of melatonin biotransformation, *Free Radic. Biol. Med.* 29 (2000) 1177–1185.
- [31] H. Zempel, E. Thies, E. Mandelkow, E.-M. Mandelkow, A β oligomers cause localized Ca $^{2+}$ elevation, misrouting of endogenous tau into dendrites, tau phosphorylation, and destruction of microtubules and spines, *J. Neurosci.* 30 (2010) 11938–11950.
- [32] D.L. Wang, Z.Q. Ling, F.Y. Cao, L.Q. Zhu, J.Z. Wang, Melatonin attenuates isoproterenol-induced protein kinase A overactivation and tau hyperphosphorylation in rat brain, *J. Pineal Res.* 37 (2004) 11–16.
- [33] E. Planel, K. Yasutake, S.C. Fujita, K. Ishiguro, Inhibition of protein phosphatase 2A overrides tau protein kinase 1/glycogen synthase kinase 3 β and cyclin-dependent kinase 5 inhibition and results in tau hyperphosphorylation in the hippocampus of starved mouse, *J. Biol. Chem.* 276 (36) (Sep 7 2001) 34298–34306.
- [34] J.-z. Wang, Q. Wu, A. Smith, I. Grundke-Iqbal, K. Iqbal, τ is phosphorylated by GSK-3 at several sites found in Alzheimer disease and its biological activity markedly inhibited only after it is prephosphorylated by A-kinase, *FEBS Lett.* 436 (1998) 28–34.
- [35] L. Lin, Q.-X. Huang, S.-S. Yang, J. Chu, J.-Z. Wang, Q. Tian, Melatonin in Alzheimer's disease, *Int. J. Mol. Sci.* 14 (2013) 14575–14593.
- [36] J.N. Zhou, R.Y. Liu, W. Kamphorst, M.A. Hofman, D.F. Swaab, Early neuropathological Alzheimer's changes in aged individuals are accompanied by decreased cerebrospinal fluid melatonin levels, *J. Pineal Res.* 35 (2003) 125–130.
- [37] A.A. Balmik, S. Chinnathambi, Multi-faceted role of melatonin in neuroprotection and amelioration of tau aggregates in Alzheimer's disease, *J. Alzheimers Dis.* 62 (2018) 1481–1493.
- [38] J. Quinn, D. Kulhanek, J. Nowlin, R. Jones, D. Praticò, J. Rokach, R. Stackman, Chronic melatonin therapy fails to alter amyloid burden or oxidative damage in old Tg2576 mice: implications for clinical trials, *Brain Res.* 1037 (2005) 209–213.
- [39] E. Matsubara, T. Bryant-Thomas, J. Pacheco Quinto, T.L. Henry, B. Poegeeler, D. Herbert, F. Cruz-Sanchez, Y.-J. Chyan, M.A. Smith, G. Perry, Melatonin increases survival and inhibits oxidative and amyloid pathology in a transgenic model of Alzheimer's disease, *J. Neurochem.* 85 (2003) 1101–1108.
- [40] K. Ono, H. Mochizuki, T. Ikeda, T. Nihira, J.-i. Takasaki, D.B. Teplow, M. Yamada, Effect of melatonin on α -synuclein self-assembly and cytotoxicity, *Neurobiol. Aging* 33 (2012) 2172–2185.
- [41] M. Pappolla, P. Bozner, C. Soto, H. Shao, N.K. Robakis, M. Zagorski, B. Frangione, J. Ghiso, Inhibition of Alzheimer β -fibrillogenesis by melatonin, *J. Biol. Chem.* 273 (1998) 7185–7188.
- [42] K. Sae-Ung, K. Ueda, P. Govitrapong, P. Phansuwan-Pujito, Melatonin reduces the expression of alpha-synuclein in the dopamine containing neuronal regions of amphetamine-treated postnatal rats, *J. Pineal Res.* 52 (2012) 128–137.
- [43] R. Hornedo-Ortega, G. Da Costa, A.B. Cerezo, A.M. Troncoso, T. Richard, M.C. Garcia-Parrilla, In vitro effects of serotonin, melatonin, and other related indole compounds on amyloid- β kinetics and neuroprotection, *Mol. Nutr. Food Res.* 62 (2018) 1700383.
- [44] S. Amor, F. Puentes, D. Baker, P. Van Der Valk, Inflammation in neurodegenerative diseases, *Immunology* 129 (2010) 154–169.
- [45] D. Pozo, R.J. Reiter, J.R. Calvo, J.M. Guerrero, Inhibition of cerebellar nitric oxide synthase and cyclic GMP production by melatonin via complex formation with calmodulin, *J. Cell. Biochem.* 65 (1997) 430–442.
- [46] G. Costantino, S. Cuzzocrea, E. Mazzon, A.P. Caputi, Protective effects of melatonin in zymosan-activated plasma-induced paw inflammation, *Eur. J. Pharmacol.* 363 (1998) 57–63.
- [47] N.V. Gorantla, A.V. Shkumatov, S. Chinnathambi, Conformational dynamics of intracellular tau protein revealed by CD and SAXS, *Tau Protein*, Springer, 2017, pp. 3–20.
- [48] N.V. Gorantla, P. Khandelwal, P. Poddar, S. Chinnathambi, Global conformation of tau protein mapped by Raman spectroscopy, *Tau Protein*, Springer, Humana Press, 2017, pp. 21–31.
- [49] J. Marley, M. Lu, C. Bracken, A method for efficient isotopic labeling of recombinant proteins, *J. Biomol. NMR* 20 (2001) 71–75.
- [50] W. Lee, M. Tonelli, J.L. Markley, NMR-FAM-SPARKY: enhanced software for biomolecular NMR spectroscopy, *Bioinformatics* 31 (2014) 1325–1327.
- [51] J. Luo, C.-H. Yu, H. Yu, R. Borstnar, S.C.L. Kamerlin, A. Grafslund, J.P. Abrahams, S.K.T.S. Wal'mlal'nder, Cellular polyamines promote amyloid-beta (A β) peptide fibrillation and modulate the aggregation pathways, *ACS Chem. Neurosci.* 4 (2013) 454–462.
- [52] K. Cisek, G.L. Cooper, C.J. Huseby, J. Kuret, Structure and mechanism of action of tau aggregation inhibitors, *Curr. Alzheimer Res.* 11 (2014) 918–927.
- [53] L.J. Lapidus, Understanding protein aggregation from the view of monomer dynamics, *Mol. Biosyst.* 9 (2013) 29–35.
- [54] R.C. George, J. Lew, D.J. Graves, Interaction of cinnamaldehyde and epicatechin with tau: implications of beneficial effects in modulating Alzheimer's disease pathogenesis, *J. Alzheimers Dis.* 36 (2013) 21–40.
- [55] M.C. Monti, L. Margarucci, R. Riccio, A. Casapulo, Modulation of tau protein fibrillation by oleoanthal, *J. Nat. Prod.* 75 (2012) 1584–1588.
- [56] M. Zhu, S. Rajamani, J. Kaylor, S. Han, F. Zhou, A.L. Fink, The flavonoid baicalin inhibits fibrillation of α -synuclein and disaggregates existing fibrils, *J. Biol. Chem.* 279 (26) (Jun 25 2004) 26846–26857.

A.A. Balmik, et al.

BBA - General Subjects 1864 (2020) 129467

- [57] Y. Shen, S. Xu, W. Wei, X. Sun, L. Liu, J. Yang, C. Dong, The protective effects of melatonin from oxidative damage induced by amyloid beta-peptide 25–35 in middle-aged rats, *J. Pineal Res.* 32 (2002) 85–89.
- [58] S. Klongpanichapak, P. Phansuwan-Pujito, M. Ebadi, P. Govitrapong, Melatonin inhibits amphetamine-induced increase in α -synuclein and decrease in phosphorylated tyrosine hydroxylase in SK-N-SH cells, *Neurosci. Lett.* 436 (2008) 309–313.
- [59] Z. Skribanek, L. Balásperi, M. Mák, Interaction between synthetic amyloid- β -peptide (1–40) and its aggregation inhibitors studied by electrospray ionization mass spectrometry, *J. Mass Spectrom.* 36 (2001) 1226–1229.
- [60] E. Papagiannidou, D.J. Skene, C. Ioannides, Potential drug interactions with melatonin, *Physiol. Behav.* 131 (2014) 17–24.
- [61] P. Barré, D. Eliezer, Structural transitions in tau k18 on micelle binding suggest a hierarchy in the efficacy of individual microtubule-binding repeats in filament nucleation, *Protein Sci.* 22 (2013) 1037–1048.



Contents lists available at ScienceDirect

Archives of Biochemistry and Biophysics

journal homepage: www.elsevier.com/locate/yabbi

Baicalein suppresses Repeat Tau fibrillization by sequestering oligomers

Shweta Kishor Sonawane^{a,c,1}, Abhishek Ankur Balmik^{a,c,1}, Debjyoti Boral^{b,c},
Sureshkumar Ramasamy^{b,c}, Subashchandrabose Chinnathambi^{a,c,*}^a Neurobiology Group, Division of Biochemical Sciences, CSIR-National Chemical Laboratory, Dr. Homi Bhabha Road, 411008, Pune, India^b Structural Biology Group, Division of Biochemical Sciences, CSIR-National Chemical Laboratory, Dr. Homi Bhabha Road, 411008, Pune, India^c Academy of Scientific and Innovative Research (AcSIR), 411008, Pune, India

ARTICLE INFO

Keywords:
Alzheimer disease
Tau protein
Protein aggregation
Paired helical filaments
Microtubule assembly
Baicalein

ABSTRACT

Alzheimer's disease (AD) is a neurodegenerative disorder caused by protein misfolding, aggregation and accumulation in the brain. A large number of molecules are being screened against these pathogenic proteins but the focus for therapeutics is shifting towards the natural compounds as aggregation inhibitors, mainly due to their minimum adverse effects. Baicalein is a natural compound belonging to the class of flavonoids isolated from the Chinese herb *Scutellaria baicalensis*. Here we applied fluorescence, absorbance, microscopy, MALDI-TOF spectrophotometry and other biochemical techniques to investigate the interaction between Tau and Baicalein *in vitro*. We found the aggregation inhibitory properties of Baicalein for the repeat Tau. Overall, the potential of Baicalein in dissolving the preformed Tau oligomers as well as mature fibrils can be of utmost importance in therapeutics for Alzheimer's disease.

1. Introduction

Alzheimer's Disease is a neurodegenerative disorder characterized by memory loss and progressive dementia. The cytosolic Tau aggregates and the extracellular amyloid beta plaques are the typical traits of AD [1–3]. The therapeutics for AD is being designed to act on both the targets in a discreet as well as integrated manner. The efficacy of the drugs designed seems to reduce as the level of trial increases [4,5]. The accumulation of cytosolic neurofibrillary tangles mainly composed of Tau PHFs (paired helical filaments) [6] leads to neuronal degeneration. Along with microtubule stabilization Tau has varied roles such as neurite outgrowth, intracellular trafficking etc. that are hampered in AD due to elevated Tau levels [7,8]. All these neuronal abnormalities and degeneration due to Tau dysfunction and aggregation necessitates screening for molecules to inhibit Tau aggregation as well as to dissolve the preformed aggregates.

Tau aggregation in AD succeeds via several intermediates like oligomers, proto-fibrils, paired helical filaments formation, which when untreated forms neurofibrillary tangles [9–11]. Hence, these intermediates are being targeted for therapeutics in AD. The oligomer species are found to be more toxic than the filamentous aggregates [12] and hence Tau oligomers are gaining much attention as a therapeutic

target in AD. Several molecules belonging to different classes like synthetic molecules, natural compounds, peptide inhibitors etc. have found to be potent against Tau aggregation [13–17]. In recent time, methylene blue was found to be a potent molecule in AD [18–20] but failed to show effects on cognitive abilities in a transgenic mouse model of AD [21]. On the other hand, the methylene blue derivatives MTC methylthioninium chloride (MTC); and its reduced form leuco-methylthioninium salts (LMTX) has shown positive effects on Tau aggregation inhibition [22] by modifying the cysteine residues to the oxidized forms [23]. Other approaches to inhibit Tau aggregation include targeting PTMs (post-translational modifications) of Tau. Accordingly, kinase inhibitors or phosphatase activators have been screened for these molecules but failed to show potency due to low specificity and less efficiency. Since the ultimate effect of Tau aggregation is microtubule destabilization, an alternative strategy for designing of therapeutics in AD is to screen or synthesize the microtubule stabilizing compounds [24–26]. The natural compounds having varied targets in AD have also shown to have a potential as therapeutics in AD like curcumin, paclitaxel, geldanamycin etc. [27]. Azaphilones, a class of fungal metabolites have shown the aggregation inhibition as well as disaggregation activity for Tau aggregates [28]. The secondary metabolites of *Aspergillus nidulans* like 2,ω-Dihydroxyemodin,

* Corresponding author. Neurobiology group, Division of Biochemical Sciences, CSIR-National Chemical Laboratory (CSIR-NCL), Dr. Homi Bhabha Road, 411008, Pune, India.

E-mail address: s.chinnathambi@ncl.res.in (S. Chinnathambi).

¹ Equal contribution.

<https://doi.org/10.1016/j.abbi.2019.108119>

Received 1 August 2019; Received in revised form 5 September 2019; Accepted 24 September 2019

Available online 27 September 2019

0003-9861/ © 2019 Published by Elsevier Inc.

Asperthecin, and Asperbenzaldehyde having aromatic rings are potent Tau aggregation inhibitors [29]. Oleocanthal, derived from extra virgin olive oil have shown inhibition of Tau aggregation by covalently modifying the protein at its lysine residues [30]. EGCG is an active component of green tea and has been shown to interfere with the aggregation of amyloid beta, α -synuclein as well as Tau in *in vitro* studies [31,32]. Baicalein is a polyphenol compound belonging to the class of flavonoids isolated from the Chinese herb *Scutellaria baicalensis*. Flavonoids are a rich source of anti-oxidants and are known to play a neuroprotective role [33]. Baicalein has been known to exert anti-allergic, anti-carcinogenic anti-inflammatory as well as cardio protective properties. It has also shown a potential for inhibiting aggregation of proteins involved in neurodegenerative diseases. Baicalein not only prevents fibrillization of α -synuclein but also disaggregates the pre-formed fibrils involved in Parkinson's disease [34]. In AD transgenic mouse model, Baicalein has shown to reduce the amyloid- β accumulation and enhance the processing of amyloid precursor protein via α -secretases thus leading to non-amyloidogenic processing of APP [35]. In this study, we report that Baicalein shows a dual property of inhibiting aggregation as well as dissolving the pre-formed fibrils of repeat domain of Tau in *in vitro* conditions at sub micro-molar concentrations. To explore the putative binding site and mode of Baicalein binding with Tau, the molecular docking and simulations were studied with the hexapeptide repeat region. Only this region is amenable to predict the reliable model from the presently available structure information. The dynamics simulation on Tau filament reported previously showed the aggregation mechanism due to hyperphosphorylation [36]. This study would reveal nature of interaction and mechanism of Baicalein in inhibition of Tau aggregates formation.

2. Experimental procedures

2.1. Chemicals and reagents

Baicalein, ThS, ANS, BES, sinapinic acid, BCA reagent and MTT were purchased from Sigma. Heparin, NaCl and sodium azide were purchased from MP Biomedicals. DTT and protease inhibitor cocktail were purchased from Calbiochem and Roche respectively. ECL reagent (32132) and antibodies anti-oligomer A11 rabbit polyclonal (AHB0052) and goat anti-rabbit HRP conjugated (A16110) were purchased from Thermo Fisher Scientific. The cell culture reagents DMEM F12, Fetal Bovine Serum (FBS), Penicillin-Streptomycin (Penstrep), L-glutamine, trypsin-EDTA, 1X phosphate buffered saline (PBS) were purchased from Invitrogen. 10 mM and 1 mM stock of Baicalein was prepared in ethanol. 12.5 mM mother stock of ThS was prepared in 1:1 ethanol:miliQ water, which was further, diluted to 200 μ M stock in filtered miliQ water. ANS was prepared as 10 mM stock in filtered miliQ.

2.2. Tau purification

The protein purification was carried out as previously described [37]. In brief, the cell pellets obtained after induction of protein expression were homogenized under high pressure (15,000 psi) in a microfluidics device for 15 min. The obtained lysate was heated at 90 °C for 15 min after addition of 0.5 M NaCl and 5 mM DTT. The heated lysate was then cooled and centrifuged at 40,000 rpm for 50 min. The supernatant was collected and dialyzed in Sepharose A buffer overnight. The obtained dialyzed sample was then subjected to a second round of ultracentrifugation and the supernatant was loaded onto the cation exchange column (Sepharose fast flow GE healthcare) for further purification. The bound protein was eluted using an ionic gradient. The eluted proteins were pooled and concentrated for size exclusion chromatography (16/600 Superdex 75 pg GE healthcare). The Tau concentration was measured using BCA method.

2.3. Molecular modeling

To identify templates for homology model building, a similarity search using Basic Local Alignment Search Tool (BLAST) [38] algorithm was performed against the Protein Data Bank (PDB), to identify high-resolution crystal structures of homologous proteins 63, 64. The sequence identity cut off was set to $\geq 30\%$ (E-value cut off = 1). Homology modeling of Tau K18 was then carried out using Modeller 9.16 [39] by taking structures homologous to the target proteins as templates, in order to study their structural features, binding mode and affinity with the substrates.

2.4. Model validation and refinement

The initial models obtained, were evaluated for the stereochemical quality of the protein backbone and side chains using PROCHECK and RAMPAGE [40,41]. ERRAT server checked the environments of the atoms in the protein model [42]. Errors in the model structures were also checked with ProSA server [43]. After model validation, initial models were refined using impref minimization of protein preparation wizard and Impact 5.8 minimization [44]. These energy minimized final models were further used for the binding studies with Baicalein.

2.5. Ligand-protein preparation and docking studies

The ligand molecules considered in the present study were downloaded from ZINC compound database in the mol2 format. The protein and ligands were prepared first before proceeding with the docking studies. The water molecules and other hetero atom groups were removed from the protein structures using protein preparation utility of Maestro. Hydrogens were added subsequently to carry out restrained minimization of the models. The minimization was done using impref utility of Maestro in which the heavy atoms were restrained such that the strains generated upon protonation could be relieved. The root mean square deviation (RMSD) of the atomic displacement for terminating the minimization was set as 0.3 Å. Similarly, ligands were refined with the help of LigPrep 2.5 to define their charged state and enumerate their stereoisomers. The processed receptors and ligands were further used for the docking studies using Glide 5.8 [45]. Results from fluorescence microscopy and MALDI-TOF spectrophotometry, indicated that certain flavonoids interact with the Tau protein, influencing their aggregation and disaggregation propensities. Thereby one such flavonoid originally isolated from the roots of *Scutellaria baicalensis* and *Scutellaria lateriflora*, believed to enhance liver health, Baicalein was docked in the binding site cavity of the prepared receptor molecule, aka the protein. A Sitemap analysis [46] was performed on the prepared receptor molecule, to identify the probable binding sites for our ligands of interest, since no prior information was available regarding the same. Next, grids were generated by selecting any of the Sitemap points obtained above. Flexible ligand docking was carried out using the standard precision option.

A total of 6 poses with the respective ligand and different sites were generated and scored on the basis of their docking score, glide score and E-model values. The hydrogen bond interactions between the protein and ligands were visualized using PyMOL.

2.6. Molecular dynamics simulations

The docked complexes were prepared first using protein preparation wizard and then subjected to molecular dynamics simulations for a time scale of 15 ns (ns) using Desmond 3.1 of Maestro [47]. OPLS2005 force field was applied on docked complexes placed in the center of the orthorhombic box solvated in water. Protein was immersed in orthorhombic water box of SPC water model. Total negative charges on the docked structures were balanced by suitable number of counter-ions to make the whole system neutral (10 Cl-ions). The system was initially

energy minimized for maximum 2000 iterations of the steepest descent (500 steps) and the limited memory Broyden–Fletcher–Goldfarb–Shanno (BFGS) algorithm with a convergence threshold of 1.0 kcal/mol/Å. The short and long-range Coulombic interactions were handled by Cutoff and Smooth particle mesh Ewald method with a cut off radius of 9.0 Å and Ewald tolerance of 1e_09. Periodic boundary conditions were applied in all three directions. The relaxed system was simulated for 10ns with a time step of 2.0 fs (fs), NPT ensemble using a Berendsen thermostat at 300K temperature and atmospheric pressure of 1 bar. The energies and trajectories were recorded after every 2.0 ps (ps). The energies and RMSD of the complex in each trajectory were monitored with respect to simulation time. The C-alpha atom root mean square fluctuation (RMSF) of each residue was analyzed. The intermolecular interactions between the target and substrate were assessed to check the stability of the complexes.

2.7. Tau aggregation inhibition assay

Tau aggregation inhibition assay was performed with a few modifications in the already described protocol [73]. In brief, the soluble Tau protein was centrifuged at 60,000 rpm for 1 h (Optima Max XP Beckman Coulter) to remove aggregates present if any and 20 μM of soluble Tau protein was incubated in 20 mM BES buffer pH 7.4 with 5 μM of Heparin 17,500 Da in presence of 25 mM NaCl, 1 mM DTT, protease inhibitor cocktail, 0.01% sodium azide, and different concentrations of Baicalein ranging from 0 to 500 μM. The reaction mixtures were incubated at 37 °C.

2.8. Soluble protein assay

The soluble protein of repeat Tau was centrifuged as mentioned above prior setting up the reaction. 20 μM of each protein was incubated with 25 and 100 μM of Baicalein in absence of heparin. The other reaction mixture composition was maintained as mentioned above. A positive and negative control was kept with and without addition of heparin respectively. The reaction mixtures were incubated at 37 °C.

2.9. UV-visible spectroscopy

50 μM Baicalein in 20 mM BES buffer was placed in a cuvette and an absorption spectrum was recorded in 230–450 nm range using Jasco V-530 spectrophotometer. Aliquots of repeat Tau were added to the cuvette in 3.5, 7, 14, 28, 42, 56, 70, 84, 98 μM concentration and respective spectra were recorded for each addition. The total volume of repeat Tau added was less than 100 μl to avoid the dilution effect.

2.10. Repeat Tau disaggregation assay (oligomers and fibrils)

The effect of Baicalein on the dissolution of Tau aggregates was studied by incubating the preformed PHFs with different concentrations of Baicalein at 37 °C. Aggregation of 20 μM repeat Tau was carried out and induced by 5 μM heparin in 20 mM BES, pH 7.4. Repeat Tau oligomers and mature fibrils were prepared prior to the addition of Baicalein by incubating Tau in aggregation conditions for 4 h and 60 h respectively. Baicalein was added in 50–500 μM concentration after 4 h for repeat Tau oligomer disaggregation and after 60 h for fibril disaggregation. ThS and ANS fluorescence assays were employed for monitoring the disaggregation kinetics. 20 μl samples from different time points during the course of assay were loaded onto 17% SDS-PAGE and analyzed using Bio-Rad Image Lab software.

2.11. ThS fluorescence assay

ThS fluorescence assay monitored Tau aggregates formation as described. The 5 μl of 20 μM reaction mixtures were diluted in 50 mM

ammonium acetate pH 7.0 containing 8 μM of ThS to a final volume of 50 μl. The ratio of protein to ThS was maintained as 1:4 for the fluorescence measurement. Fluorescence measurements were carried out using Tecan Infinite 200 Pro series plate reader. The excitation and emission wavelengths were set at 440 nm and 521 nm respectively. The plate was given a quick shaking for 10 s before the measurement. The readings were carried out in triplicates for each sample at 25 °C. Initial readings were taken within an interval of 1 h till 6 h and later readings were continued at an interval of 12 h each. The fluorescence was normalized for background by subtracting the buffer blank fluorescence.

2.12. ANS fluorescence assay

The level of protein hydrophobicity was measured by ANS fluorescence. The 5 μl of 20 μM reaction mixtures were diluted in 50 mM ammonium acetate pH 7.0 containing 40 μM of ANS to a final volume of 50 μl. The ratio of protein to ANS was maintained as 1:20 for the fluorescence measurement. The excitation was carried out at 390 nm and the emission data was collected at 475 nm. Each sample was read in triplicate and subtracting from respective blanks eliminated the background fluorescence. All measurements were carried out in Tecan Infinite 200 Pro series plate reader at 25 °C. The time points were followed in a similar way as ThS fluorescence.

2.13. SDS-PAGE analysis

Samples left after fluorescence assay were collected and analyzed by SDS-PAGE for visual detection of aggregation inhibition on 17% polyacrylamide gels with different time points. The SDS-PAGE gel quantification was carried out using Image Lab software (Bio-Rad). The quantification for complete individual lanes was carried out using the software and the obtained intensities were plotted in the form of the bar graphs.

2.14. Filter trap assay

The detection of repeat Tau oligomers induced by Baicalein and separated by SEC was carried out by filter trap assay using A11 anti-oligomers rabbit polyclonal antibody. The fractions obtained after SEC were blotted onto Protran 0.45 μm membrane (Amersham Biosciences) using Minifold Dot-Blot System (Amersham Biosciences). The membrane was blocked with 10% milk in PBST (0.01% Tween 20) for 1 h at room temperature. The primary antibody A11 was diluted to 1:2000 and the blot was incubated with it overnight at 4 °C. After washing the unbound antibody thrice with PBST, the blot was incubated with secondary goat anti-rabbit antibody conjugated to HRP for 1 h at room temperature in 1:10000 dilutions. The unbound antibody was washed thrice with PBST. The blot was developed using ECL-Plus reagent and the chemiluminescence was detected on Amersham Imager 600 and quantified using Image Quant TL software.

2.15. Circular dichroism spectroscopy

CD spectroscopy was performed for determination of conformational changes occurring during the aggregation inhibition process using Jasco J-815 CD spectrometer in a cuvette with a path length of 1 mm under nitrogen atmosphere. The scan was carried out with bandwidth 1 nm, scan speed 100 nm/min; scan range 190–250 nm, and an average of 5 acquisitions were taken. In each experiment, measurements were done at 25 °C. The buffer baseline was set with sodium phosphate buffer, pH 6.8. The concentration was maintained 1 μM for repeat Tau for all CD measurements.

2.16. Electron microscopy

Transmission electron microscopy was carried out to qualitatively

determine the Tau filaments formation in presence and absence of Baicalein. 2 μ M of the reaction mixtures were applied to 400 mesh carbon coated copper grids for 45 s followed by 2 washes with filtered MilliQ water for 45 s each. The samples were negatively stained for 1 min using 2% uranyl acetate. The dried grids were analyzed using Tecnai G2 20 S-Twin transmission electron microscope.

2.17. Size exclusion chromatography for Tau oligomers

Size-exclusion chromatography was carried out for repeat Tau in presence of Baicalein at different time points in order to characterize the effect of Baicalein on the tendency of oligomerization. Repeat Tau samples were prepared by incubating the protein in 20 μ M concentration in 20 mM BES buffer, pH 7.4 with or without Baicalein in 200 μ M final concentration. Heparin was added in 1:4 ratios as an inducer of aggregation. Baicalein was added to the reaction mixture after 4 h of incubation at 37 °C. The initial incubation was provided for the preparation of lower order oligomers. The time point of Baicalein addition was considered as 0 h. The protein sample was filtered prior to loading on to Superdex 75 10/300 GL column (GE). BSA and Lysozyme were loaded as standards in 3 mg/ml concentration and soluble repeat Tau was loaded as a control. The separation was carried out in PBS buffer. Samples at 0, 6, 12, 24 and 60 h of incubation were subjected to size-exclusion chromatography.

2.18. MALDI-TOF analysis of Baicalein modified Tau

Repeat Tau protein (1 mg/ml) was incubated with different concentrations of Baicalein (5, 10, 25, 50, 100, 200, 500 μ M) for 1 h and 12 h at 37 °C respectively. The samples were then diluted 1:20 in Sinapic acid and spotted on the MALDI plate and analyzed using ABSCIEX 4800 MALDI-TOF analyzer.

2.19. Cell culture and toxicity assays

The neuroblastoma N2a cells were seeded in 96 well culture plates at the cell density of 25,000 cells/well. The cells were grown in DMEM F12 media containing 0.5% FBS and antibiotic (Penstrep) for 24 h. For studying the toxicity of Baicalein induced oligomers 10 μ l from the SEC fractions was added to cells/well and incubated for 24 h 10 μ l of 5 mg/ml MTT (Methylthiazolyl-diphenyl-tetrazolium bromide) was added to each well and incubated for 4 h at 37 °C. The formazan crystals formed after reduction of MTT by viable cells enzymes were dissolved in 100 μ l of 100% DMSO. The purple colour developed was read at 570 nm in Tecan plate reader.

2.20. Statistical analysis

SigmaPlot 10.2 carried all the statistical analyses out using unpaired T-test. The error bars represent mean \pm SD values. 95% confidence intervals were maintained for the analyses.

3. Results

3.1. Baicalein binds to Tau in vitro

Tau protein is one of the major microtubule-associated proteins in neuronal axons that mainly functions to stabilize and assemble microtubules. Tau is highly soluble protein and adopts a natively unfolded structure in solution [48]. The repeat domain of Tau plus the proline rich flanking regions confer the property of microtubule binding and assembly (Fig. 1A), where the repeat domain of Tau represents the core of the PHFs. The chemical structure of Baicalein is depicted in (Fig. 1B). Baicalein shows characteristic λ_{max} at two wavelengths 270 nm and 362 nm (Figs. S1B and C). Upon titrating with repeat Tau from 0 to 98 μ M, the peak at 362 nm was found to decrease in intensity indicating

the binding of Baicalein (Figs. 1D and S1C). The maxima at 362 nm plotted against increasing Tau concentration (0–98 μ M) shows a gradual decrease in absorbance intensity (Fig. 1E). The dissociation constant (K_d) for the binding of Tau with Baicalein was found to be 3.5 μ M by using the following formula:

$$[C_{\text{Tau}C_{\text{Baicalein}}}] = \frac{[C_{\text{Tau}}] \times [C_{\text{Baicalein}}]}{K_d + [C_{\text{Baicalein}}]}$$

Where $[C_{\text{Tau}}]$ is the initial Tau concentration, $[C_{\text{Baicalein}}]$ is the free Baicalein concentration, $[C_{\text{Tau}C_{\text{Baicalein}}}]$ is the concentration of Tau-Baicalein complex and K_d is the dissociation constant [49–51].

3.2. Molecular models of Tau protein

The molecular structures of repeat Tau were modeled, in order to ascertain the putative binding site of Baicalein and the role of the conserved hexapeptide repeat regions ²⁷⁵VQIINK²⁸¹ and ³⁰⁶VQIVYK³¹¹ in the interactions with Baicalein (Fig. 1C). It is very challenging to predict the full-length Tau model due to its disordered nature of the regions in both N- and C-terminal. But the hexapeptide repeat region forms the stable secondary structure as reported by many biochemical studies and structural information [52–54]. A BLAST search against PDB identified homologous structures, to be used as templates to build the homology models of this region. Structures of Tau (267–312) bound to microtubules (2MZ7) and shared an identity of 100% and query coverage of 92% with the target sequence, and were thus used for modeling studies.

The initial models were evaluated for their stereochemical parameters. More than 98% of all residues were in the allowed regions of Ramachandran plot. The model refinement phase involved preprocessing the initial models by adding hydrogen's, assigning bond order, and filling missing loops and side chains. Next, the models were subjected to restrained minimization by applying the constraint to converge the non-hydrogen atoms to an RMSD of 0.3 using OPLS 2005 force field. Subsequently, the models were subjected to 500 steps of steepest descent energy minimization followed by 1000 steps of conjugate gradient energy minimization using the same force field. These energy-minimized models were used for docking and molecular dynamics studies.

3.3. Molecular docking of repeat Tau and Baicalein

The docking studies of Baicalein with repeat Tau model generated the best pose with glide score and E-model values of - 5.06 and - 44.365 respectively. The O₁ atom of Baicalein interacts with the NH₂ group of Asn 265 and the NH group of the imidazole ring of His 268. The OH groups involving O₃ and O₄ atoms of Baicalein, interacts with the carboxyl O⁻ atom of Glu 338, forming hydrogen bonds in the process (Fig. 2A). While the two -OH groups (O₃ and O₄) have an interaction distance of 2.70 Å, 2.0 Å and 1.80 Å respectively, the interactions with the amine group stand at a distance of 2.30 Å for Asn 265. Further hydrophobic interaction was observed with residues Tyr 310 and Val 313, of which one (Tyr 310), interestingly, belongs to the hexapeptide repeat ³⁰⁶VQIVYK³¹¹ and the other (Val 313) is a flanking residue to the same repeat, a prime area of interest in our study. Another crucial residue His 299 is predicted to have an important interaction with Baicalein via water bridges, which may be involved in the probable mechanism of Tau disaggregation in presence of Baicalein.

3.4. Molecular dynamics simulation of repeat Tau and Baicalein

The Baicalein docked complex was subjected to a simulation of 15ns time duration to analyze the stability of the interaction and other structural changes. The RMSD graph was plotted by assigning time in ns on the X-axis and RMSD values of the C α atoms of the protein and ligand in/Å on the left and right Y-axes respectively (Fig. S2). The graph and the snapshots at different time intervals of simulation indicated

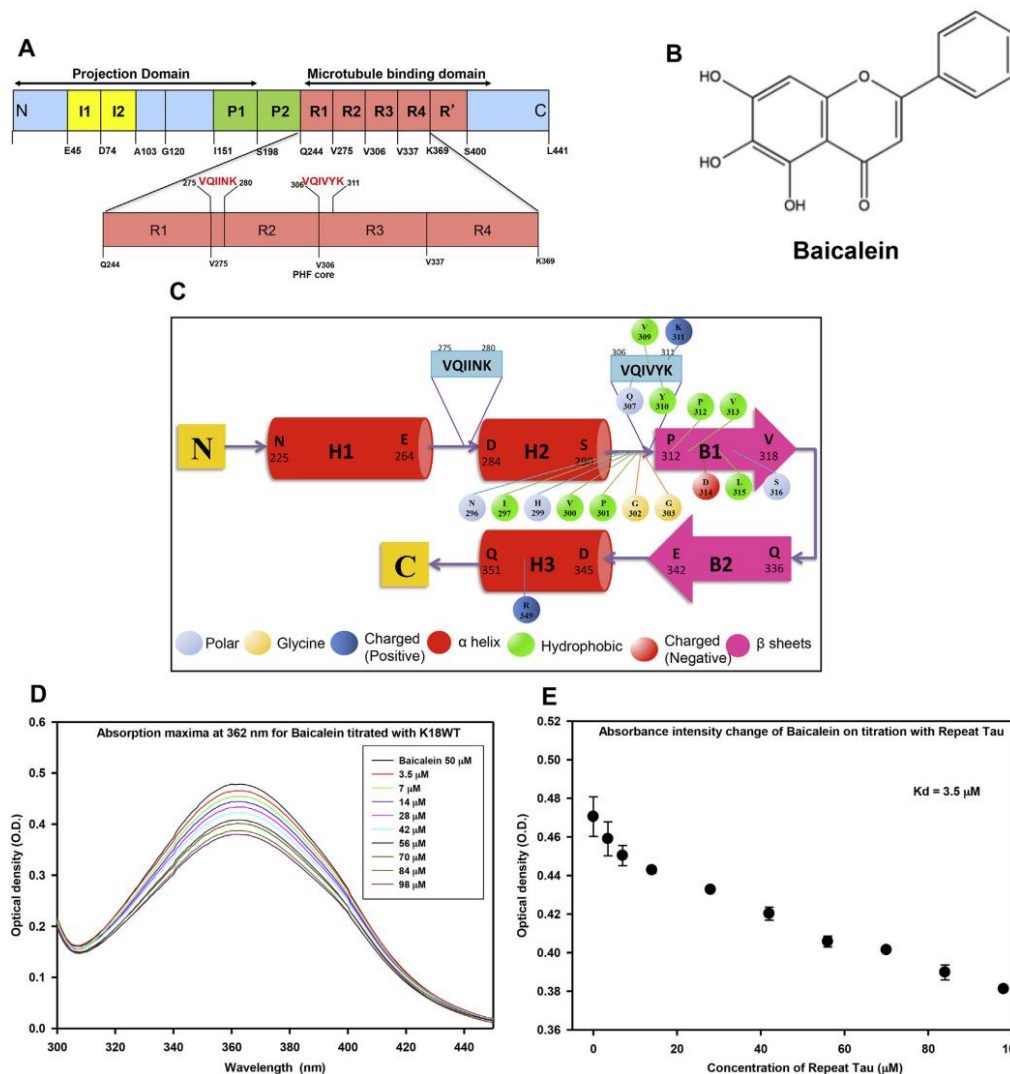


Fig. 1. The interaction of Tau with Baicalein. A) Bar diagram showing full-length and repeat Tau. The figure shows longest isoform of human Tau with 441 amino acids. The yellow blocks represent two inserts of 29 amino acids each at the N-terminal region followed by the polyproline rich region, which gives a transient helix structure. The 4 red boxes represent the four repeats of 30 amino acids each. The K18 construct comprises of only the repeat domain of Tau, which forms the core of Paired Helical Filaments. B) Chemical structure of the flavonoid Baicalein. C) A schematic diagram of the repeat Tau model secondary structure depicting three predicted α helices (H1, H2, and H3) and two predicted β sheets (B1, B2) with two distinct and characteristic hexa-peptide regions ²⁷⁵VQIINK²⁸⁰ and ³⁰⁶VQIVYK³¹¹. The predicted ligand interacting residues, color coded according to their type of interaction is also shown. D) Figure shows decrease in the absorbance intensity at 362 nm upon increasing the protein concentration against Baicalein. E) The absorbance intensity at 362 nm obtained for different titrations when plotted against respective concentrations gives a plot representing the binding affinity of Tau with Baicalein. (For interpretation of the references to colour in this figure legend, the reader is referred to the Web version of this article.)

that the RMSD of $C\alpha$ atoms of the generated structures over the complete trajectory is quite stable with minor repositioning of Baicalein with respect to the hexapeptide repeat region ³⁰⁶VQIVYK³¹¹. The $C\alpha$ RMSD between the initial and final conformation after the simulation of docked complex was $\sim 10 \text{ \AA}$ indicated the considerable conformational change upon binding. During the course of the simulation, a few residues namely Asn 296, Ile 297, His 299, Gln 307, Tyr 310, Lys 311, Val

313 and Leu 315 out of which three residues belong to the hexapeptide region mentioned above, were found to form an increasingly high number of interactions with Baicalein, indicating that these may be crucial residues to stabilize the complex (Figs. 2B and S3).

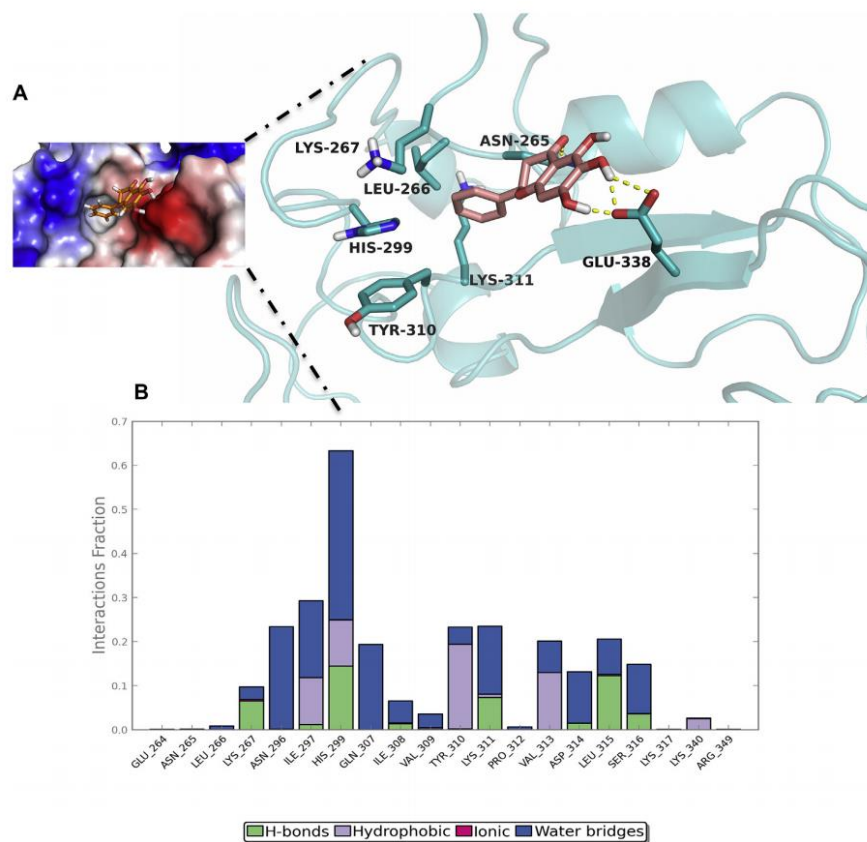


Fig. 2. Docking and Simulation of Tau with Baicalein. A) A detailed snapshot of the ligand-binding pocket of Baicalein in our proposed model of repeat Tau including the interacting residues as indicated and the corresponding surface represented in terms of electrostatic potential. B) A bar diagram depicting the extent of interaction over the course of 15 ns simulation using the same docked structure which indicates that the residues mentioned are majorly involved in the binding and probable biochemistry of the ligand binding to Tau. The protein-ligand interactions or contacts are categorized into four types: Hydrogen Bonds, Hydrophobic, Ionic and Water Bridges.

3.5. Baicalein inhibits Tau aggregation *in vitro*

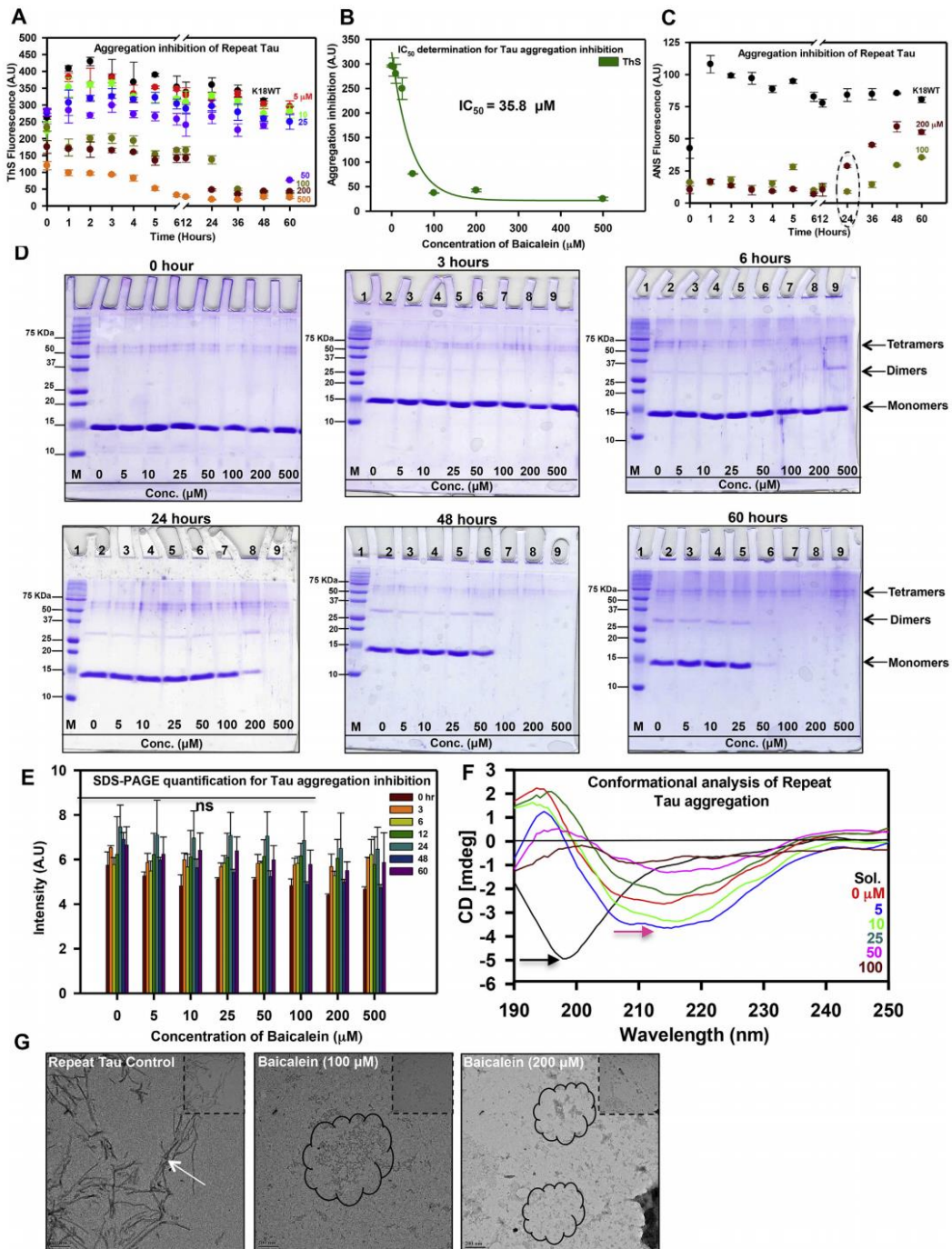
Tau is a natively unfolded protein with an overall positive charge. This property makes it possible to aggregate Tau *in vitro* by using polyanionic co-factors like heparin. Heparin is a polymer of glycosaminoglycan monomers, which has a negative charge and induces aggregation of Tau *in vitro* [55,56]. This approach has been widely used to screen for the Tau aggregation inhibitors [18,30,57]. The aggregation inhibition of the repeat Tau by Baicalein was determined using 0, 5, 25, 50, 100, 200, and 500 μ M concentrations. The rate of Tau fibril formation was monitored by ThS fluorescence. The ThS fluorescence intensity decreased with increasing concentrations of Baicalein in the treated samples. The ThS fluorescence showed an initial increase in control as well as treated samples till 4 h of incubation (Fig. 3A). As the time progressed, the treated samples showed decrease in fluorescence intensity but the control showed stagnant saturated fluorescence suggesting a concentration dependent inhibition of aggregation. The inhibition was observed to occur at an early time point and the IC_{50} value for repeat Tau aggregation inhibition was found to be 35.8 μ M of Baicalein (Fig. 3). The pattern of rise and fall in fluorescence intensity for the treated samples suggest that Baicalein might be inducing initial

oligomerization of Tau protein and inhibiting the further fibrillization by sequestering these oligomers.

3.6. Baicalein enhances Tau oligomerization in presence of heparin

The *in vitro* formation of PHFs in presence of heparin undergoes various intermittent stages [58], which results in changes in hydrophobicity of the Tau protein [59]. One of the intermittent stages in PHFs formation is the formation of oligomeric species, which acts as a nucleation step to further enhance fibrillization. The primary studies with ThS indicated that Baicalein prevents Tau fibril formation. We further investigated the role of Baicalein in Tau oligomerization. As an intermediate in Tau fibrillization, Tau oligomers show enhanced hydrophobicity due to their partially folded characteristics. ANS is a dye, which emits enhanced fluorescence on interaction with partially, folded or exposed hydrophobic micro domains of the proteins.

Thus, to study the effect of Baicalein on Tau oligomerization and accompanied hydrophobicity changes, we monitored ANS fluorescence for the control as well as treated samples. ANS showed an initial decrease in fluorescence and then the rapid increase before becoming stagnant (Fig. S4). This effect was evident at the earlier time points in



(caption on next page)

Fig. 3. Tau aggregation inhibition by Baicalein. A) The ThS fluorescence show a concentration dependent decrease in intensity suggesting inhibition of repeat Tau aggregation by increasing dose of Baicalein. B) The IC_{50} value for repeat Tau aggregation inhibition was found to be 35.8 μ M of Baicalein. C) The ANS fluorescence for the higher concentrations of Baicalein showing initial decrease and further rapid increase in fluorescence at 24 h (dotted circle). D) The SDS-PAGE analysis at zero time point control as well as treated samples does not show presence of any higher order aggregates. With an increase in time there is an increase in higher order oligomers observed especially after 6 h of incubation. At 24 h, the 500 μ M of Baicalein (lane 9) shows the presence of dimer as well as tetramer. With increase in incubation time (48 and 60 h), the oligomers are seen in all treated samples with differential intensity. The further incubation reveals the disappearance of these oligomers in concentration dependent manner. E) Quantification for the SDS-PAGE at different time points and different Baicalein concentrations shows decrease in the aggregates at higher concentrations of Baicalein. F) The CD analysis of the repeat Tau aggregation shows a shift in the spectra (pink arrow) in control as well as treated samples as compared to soluble protein (black arrow) indicating a shift towards β -sheet structure. The Sol. represents for soluble protein. G) The electron micrographs show the presence of filamentous aggregates (white arrow) in control as opposed to amorphous aggregates (encircled black) in the Baicalein treated samples. (For interpretation of the references to colour in this figure legend, the reader is referred to the Web version of this article.)

the higher concentrations of Baicalein (Fig. 3C). This behavior of ANS suggests that Baicalein might be involved in initial Tau oligomer formation and sequestration.

3.7. SDS-PAGE analysis reveals the enhanced Tau oligomerization and sequestration by Baicalein

In order to confirm our hypothesis, we carried out SDS-PAGE analysis of the control as well as Baicalein treated samples at different time intervals. We examined 10 μ l of all the reaction mixtures at zero time point to rule out the presence of any preformed higher order aggregates (Fig. 3D). At 6 h of incubation, we observed the dimers and tetramers in the highest concentration of Baicalein (Fig. 3D and E) and these oligomers appear in all the concentrations of Baicalein treated samples in a time dependent manner. We observed a complete clearance of dimer and monomers in 500 μ M Baicalein treatment after 12 h of incubation but the band for tetramers still remains. At 24 h, 200 μ M of Baicalein treated Tau show complete conversion from soluble to higher order oligomers. It is to be noted that this is the exact time point when we see stable decrease in ThS fluorescence and an increase in ANS fluorescence (Fig. 3A, C). This seems to be the point where Baicalein sequesters the oligomers formed and inhibits further fibril formation. These results indicate that Baicalein enhances the oligomerization of Tau and blocks them at an oligomeric stage without further leading to fibril formation.

3.8. Baicalein binds and stabilizes partially folded Tau oligomers

Since Baicalein demonstrated the enhancement of Tau oligomerization and their sequestration, we proceeded further to elucidate the conformation of these oligomers by Circular dichroism spectroscopy. The soluble Tau protein is natively unfolded and showed CD spectra of typical random coil at 198 nm (Fig. 3F). Tau on aggregation shows the structural transition from typical random coil to the β -sheet structure [54]. Tau protein treated with Baicalein showed shift in the wavelength towards a partial β -structure (Fig. 3F) suggesting that Baicalein is able to bind and stabilize the partially folded Tau oligomers.

3.9. Electron microscopy visualization of Baicalein induced Tau aggregation inhibition

The time dependent effect of Baicalein on Tau oligomerization and aggregation inhibition was observed by electron micrographs. The untreated sample showed the presence of long fibrillar structures, which are characteristics of Tau filamentous aggregates (Fig. 3G). On the contrary, the 100 μ M Baicalein treated Tau showed presence of only pieces of Tau filaments (Fig. 3G). The electron micrograph observation supports our previous observations that Baicalein prevents Tau fibrillization.

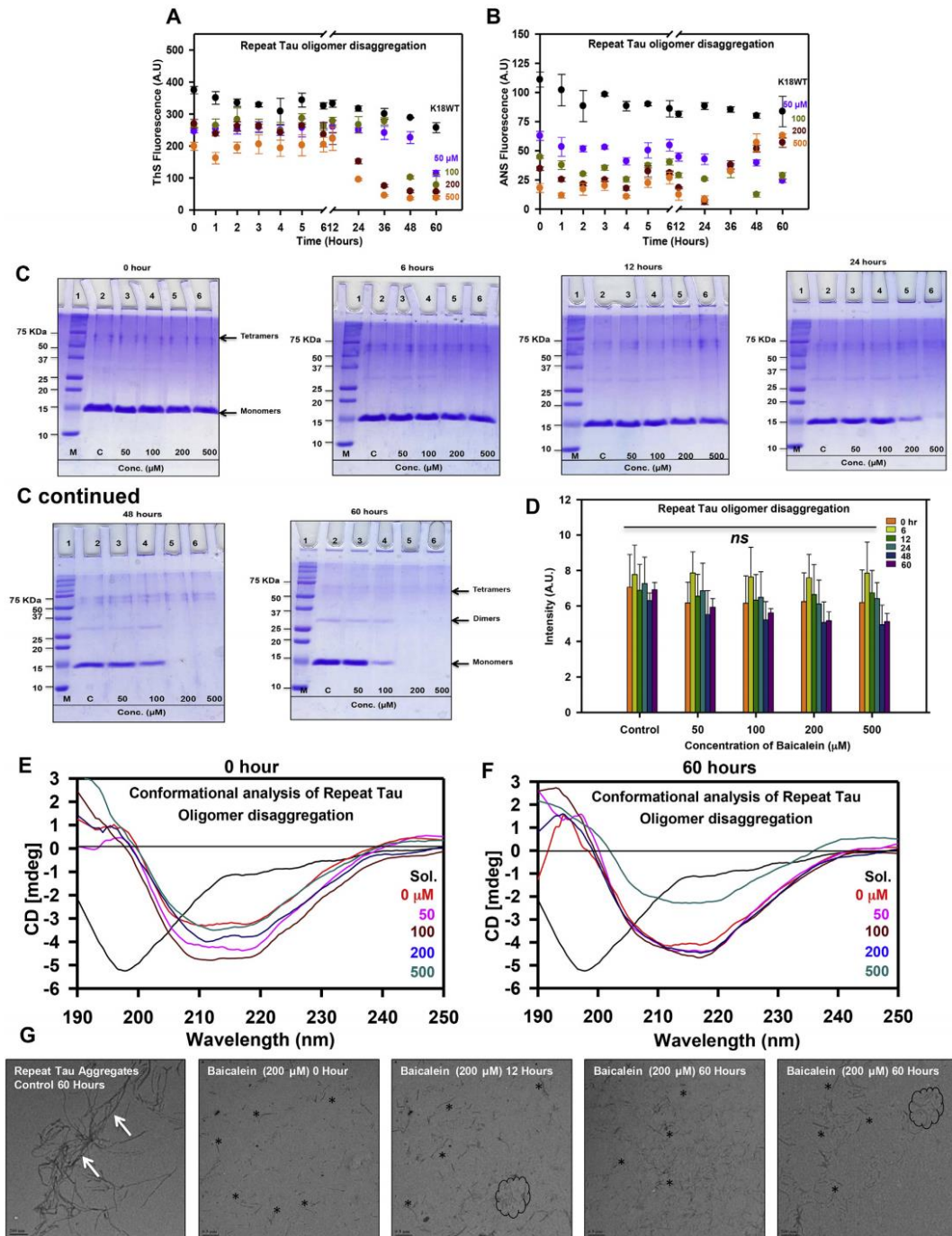
3.10. Baicalein does not cause Tau conformational change

As our results suggested that Baicalein could stabilize Tau oligomers having partial β -sheet structure, it was necessary to understand whether, Baicalein alone can cause the random coil to β -sheet transition of

Tau protein. For this, we incubated repeat Tau with Baicalein in absence of heparin. We maintained a positive control (with heparin) and negative control (without heparin) for standard aggregation kinetics. The kinetics for both ThS and ANS did not show any increase in fluorescence for negative control as well as Baicalein treated samples (Figs. S6A and B). The positive control showed an increase in ThS and ANS fluorescence as expected. The SDS-PAGE analysis showed the presence of higher order structures in the positive control from 24 h onwards (Fig. S6C). The sample treated with higher concentration of Baicalein (100 μ M) showed presence of very faint higher order bands at a later time point for both the proteins (Fig. S6D). The fluorescence kinetics and the SDS-PAGE analysis clearly suggest that Baicalein might be able to induce Tau oligomerization but at a much slower pace. The structural analysis of these oligomers revealed that they do not show transition to β -sheet structure (Fig. S6E) and do not form Tau fibrils (Fig. S6F). These results clearly suggest that Baicalein might be able to induce soluble Tau oligomers at a slower rate without causing any structural changes.

3.11. Disaggregation and sequestration of repeat Tau oligomers by Baicalein

Oligomers of repeat Tau were prepared by incubating Tau in aggregation conditions for 4 h and then subjected to various concentrations of Baicalein to study the disaggregation of repeat Tau oligomers. ThS fluorescence assay suggested that Baicalein is able to disaggregate preformed oligomers in a concentration dependent manner (Fig. 4A). Baicalein was found to enhance and moderately induce oligomerization as well as sequester oligomers into an aggregation incompetent form. The underlying mechanism of disaggregation may involve the breaking of aggregates into smaller fragments and then inhibiting the reformation of higher order aggregates. It was observed that both ThS and ANS fluorescence was decreased upon addition of Baicalein in 4 h (Fig. 4A and B) incubated samples suggesting disaggregation and decreased hydrophobicity respectively. However, the ANS fluorescence increased after 12 h in all the incubated samples. The SDS-PAGE analysis showed that Baicalein could bind to the preformed oligomers and sequester them at this stage. The presence of a tetramer band in all the concentrations of Baicalein can be observed but the dimer as well as the monomer completely disappears (Fig. 4C). We observed the formation of oligomers on the SDS-PAGE and increase in ANS fluorescence but a complete decrease in ThS fluorescence for the Baicalein treated oligomers. This strongly suggests the role of Baicalein in sequestering the Tau oligomers. The SDS-PAGE quantification for repeat Tau oligomer disaggregation (Fig. 4D) shows a gradual decrease in soluble repeat Tau in a concentration dependent manner. Further, CD spectra analysis for repeat Tau samples treated with a varying range of Baicalein concentrations shows a shift towards the β -sheet structure in all concentrations (Fig. 4E and F). Electron micrographs for disaggregation assay samples shows fragility of Tau aggregates and absence of mature Tau filaments (Fig. 4G). Formation of Baicalein induced oligomers was also evident in size exclusion chromatography (SEC). Repeat Tau incubated with Baicalein leads to formation of oligomers as seen in the SEC profiles for samples at 0, 6, 12, 24, 48 and 60 h (Fig. 5A) as compared to soluble repeat Tau. Further, the repeat Tau was incubated



(caption on next page)

Fig. 4. Disaggregation of repeat Tau oligomers by Baicalein. A) Formation of repeat Tau aggregates was monitored by ThS fluorescence after addition of Baicalein at different concentrations after 4 h of incubation. ThS fluorescence shows a marked decrease in a concentration dependent manner. B) ANS fluorescence assay for repeat Tau oligomers disaggregation on addition of different concentrations of Baicalein at 4 h of incubation shows a prominent decrease in fluorescence after Baicalein addition in all the concentrations. There is an increase in fluorescence from 24 h onwards indicating that at higher concentrations Baicalein can increase the hydrophobicity of protein aggregates. C) SDS-PAGE analysis shows a marked decrease in the monomeric form of repeat Tau, which are mostly entrapped as dimeric and tetrameric forms in presence of all different concentrations of Baicalein. D) Quantification of SDS-PAGE showing concentration dependent decrease in intensity for repeat Tau oligomers. E, F) The CD spectra for repeat Tau oligomer disaggregation samples at 0, and 60 h of incubation with different Baicalein concentrations. In all the treated samples, the shift in the spectrum towards β -sheet structure can be observed (shown by pink arrow) as compared to soluble repeat Tau. The Sol. represents for soluble protein. G) Electron micrographs for repeat Tau at 0, 12 and 60 h of incubation with 200 μ M Baicalein show smaller broken filaments (black asterisks and encircled area) as compared to untreated control (white arrow). (For interpretation of the references to colour in this figure legend, the reader is referred to the Web version of this article.)

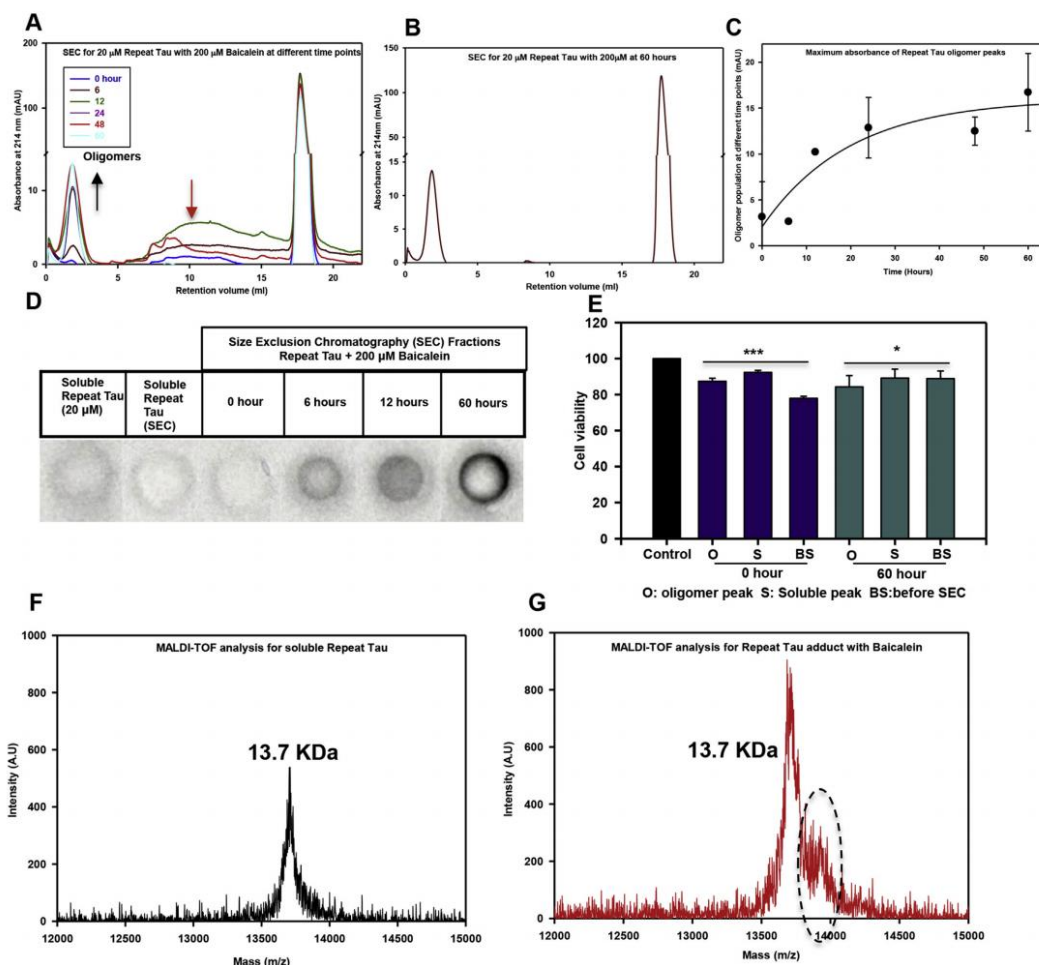


Fig. 5. Size-exclusion chromatography for repeat Tau aggregates. A) Comparison of the chromatograms for repeat Tau incubated with Baicalein at different time points. Figure shows a decrease in dimeric population of repeat Tau (pink arrow) with subsequent increase in the Baicalein stabilized oligomers (black arrow). B) Chromatogram for repeat Tau incubated with Baicalein for 60 h shows increase in oligomer population. C) Maximum absorbance obtained for the peaks for oligomers at different time points shows a gradual increase in Baicalein stabilized oligomers with time. D) The Baicalein induced repeat Tau oligomerization observed by SEC was confirmed by filter trap assay using A11 (anti-oligomers antibody). No significant signal was observed for the soluble repeat Tau before and after SEC confirming absence of oligomers in untreated sample. E) The oligomer as well as the soluble fractions obtained after the SEC of Baicalein treated repeat Tau did not show toxicity on N2a cells. F) The MALDI-TOF analysis of soluble repeat Tau showing 13.7 KDa molecular weight. G) The Baicalein modified Tau showing an adjacent peak of 13.9 KDa in addition to 13.7 KDa peak suggesting covalent modification of repeat Tau by Baicalein. (For interpretation of the references to colour in this figure legend, the reader is referred to the Web version of this article.)

with Baicalein at 1:10 ratio showed presence oligomers while it was absent in the control aggregation sample at 60 h (Fig. 5B), suggesting enhancement of oligomerization in presence of Baicalein. There is an increase in the intensity of peak corresponding to repeat Tau oligomers with respect to time (Fig. 5C). This increase in the population of oligomers as confirmed by probing the obtained fractions with A11 anti-oligomer antibody by filter trap assay (Fig. 5D). An increase in oligomeric population was observed with increase in incubation time, which is in conjunction with the prior results reiterating the role of Baicalein in inducing Tau oligomerization. To further elucidate the nature of these oligomers, we treated the neuro2a cells with the oligomer as well as soluble fractions obtained after SEC. The preformed oligomers treated with Baicalein at 0 h were found to be more toxic as compared to 60 h treated oligomers. The toxicity was reduced in presence of Baicalein though not 100% rescuing the viability of the cells (Fig. 5E).

3.12. Baicalein covalently modifies Tau protein as observed by MALDI-TOF

Baicalein showed oligomer inducing property for Tau in presence of heparin and sequestering these oligomers from further fibrillization. To understand the mechanism by which this occurs, MALDI-TOF analysis was carried out to study whether Baicalein can lead to covalent modification of Tau. The repeat Tau having a theoretical molecular weight of 13.7 kDa was incubated with a range of concentrations of Baicalein for 1 h and 12 h respectively. The samples incubated for 1 h showed an additional peak of 13.9 kDa at higher concentration of Baicalein (Figs. 5F and S5D), which was not observed in untreated samples (Figs. 5G and S5A) as well as in lower concentrations of Baicalein (Figs. S5B and C). But after 12 h of incubation, all Baicalein treated samples showed a peak adjacent to the peak given by soluble Tau (13.7 kDa) of 13.9 kDa suggesting the covalent modification of repeat Tau by Baicalein (270 Da) (Figs. S5F, G, H) as opposed to untreated (Fig. S5E). Thus, Baicalein could be involved in covalently modifying Tau protein, thus, preventing it from aggregation.

3.13. Baicalein disaggregate mature fibrils of repeat Tau

Disaggregation of repeat Tau fibrils was carried out using different concentrations of Baicalein and monitored by ThS and ANS fluorescence assay. Repeat Tau fibrils were prepared by subjecting the protein to aggregation conditions for 60 h. Initially, after addition of Baicalein, there was decrease in the ThS fluorescence within 12 h in all concentrations of Baicalein suggesting disaggregation of Tau fibrils (Fig. 6A). However, ANS fluorescence decreased initially for 12 h and increased afterwards indicating the formation of oligomers (Fig. 6B). In SDS-PAGE analysis, Baicalein treated samples showed decrease in the population of oligomeric species at different time points (Fig. 6C). The SDS-PAGE quantification for fibril disaggregation (Fig. 6D) shows a gradual decrease in soluble repeat Tau in a concentration dependent manner. This is also supported by the electron micrographs (Fig. 6G), which shows fragility of Tau and absence of mature Tau filaments. Further, CD spectra analysis for repeat Tau samples treated with a varying range of Baicalein concentrations shows a shift towards the β -sheet structure in all concentrations (Fig. 6E and F).

4. Discussion

Aggregation of Tau into insoluble aggregates inside the neuronal cells contributes to the pathogenesis of Alzheimer's disease. The screening of compounds against Tau neurofibrillary tangles has yielded variety of potent molecules [60–62]. Tau pathology undergoes a formation of series of intermittent species and the feasibility of their formation depends on both physiological concentration of free Tau and ability to form aggregation competent conformations [63]. The soluble oligomers of Tau are more toxic than the Tau fibrils [64] and hence the Tau oligomers are gaining more attention as therapeutic targets in AD

[65].

The screening for Tau aggregation inhibitors has generally yielded compounds with ring structures, which might have differential interactions with the Tau monomer, Tau aggregates and their intermediates [14,57]. Our current study elucidates that the herbal compound Baicalein binds to specific hydrophobic patches of the repeat domain of Tau and inhibits the Tau aggregation by targeting Tau into soluble oligomers. Similar results have been observed for the structurally similar polyphenol altemusin wherein *in vitro* Tau pathology is inhibited by the polyphenol but the *in vivo* pathology in transgenic mice could not be rescued [66]. The progress of Tau aggregation leads to formation of β -sheet rich structure [54], which provides the stability to these aggregates. Tau aggregation inhibitors either act to weaken the cross beta structures by inserting their rings between the beta sheet stacks or modify the protein or its intermediate aggregates, thus decreasing its aggregation potency [67]. We propose Baicalein belongs to the latter class of inhibitors as it binds and stabilizes the high molecular weight Tau oligomers, which are not capable of fibrillization. The ANS fluorescence clearly suggest the increased hydrophobicity of these sequestered molecules [59,68]. The MALDI analysis reveals the modification of Tau by Baicalein as it forms adduct with repeat Tau as evidenced by an increase in molecular weight of Tau with Baicalein.

In order to shed light on the binding site and the molecular nature of Baicalein interaction with the Tau monomer, we have performed the docking and simulation studies. As the full-length Tau model is impossible to predict due to the disordered nature of the protein, we could get reliable model for the structured regions of Tau only, which is hexapeptide repeat region (244–373). Our results demonstrated that the Baicalein binds to this region. The MD simulation demonstrated that the structure was stable and the nature of interaction is primarily mediated by hydrophobic interaction and later stabilized by the water-mediated hydrogen bonds. Also, the trajectory of complex simulation suggests the observable conformational change of this aggregation prone region of Tau after Baicalein binding. This conformational dynamicity may be due to the relatively flexible bond between C7-C4 of the Baicalein. This observation is in agreement with the structure of Baicalein as it has two adjacent –OH groups that might have the ability to modify the Tau oligomers and form high molecular weight aggregates, which are visible on SDS-PAGE. Similar mechanism has been postulated for Tau aggregation inhibition with respect to other flavonoids having adjacent –OH groups [69]. Hence, it can be conceived that Baicalein belongs to the class of covalent inhibitor of aggregation. The other potent inhibitors of this class include Oleocanthal, an aldehyde by nature, which reacts with the epsilon amino group of lysine residues to form imines [70]. The mechanism of other covalent inhibitors like cinnamaldehyde and asperbenzaldehyde [29], which are α , β unsaturated aldehydes, involves nucleophilic attack by the cysteine residues of Tau. In contrast, Baicalein a polyalcohol flavonoid can undergo oxidation to quinone form, which is involved in electrophilic attack [71]. The previous studies with aggregation inhibition of α -synuclein have also revealed the similar mechanism of inhibition wherein the oligomers of α -synuclein are prevented to undergo fibril formation in presence of Baicalein [34]. Thus, any inhibitor, which can serve the function of targeting these nucleating species, can be of great therapeutic importance. The effect of Baicalein must be prior to the nucleation as its inhibitory effect on Tau aggregation can be observed early in the course of *in vitro* aggregation. The size-exclusion chromatography results also support this hypothesis, as the Baicalein treated samples showed the disappearance of a peak corresponding to tetramer. Interestingly, there is an appearance of oligomeric species of higher order in the sample incubated with Baicalein. These findings strongly suggest that Baicalein exhibit inhibition activity by sequestration of Tau into oligomers of different nature and taking it off the pathway of aggregation. Although effective against inhibiting fibrillization, Baicalein also worked as a potent molecule for disaggregation of preformed Tau fibrils as well as oligomers (Fig. 7). The ANS fluorescence studies

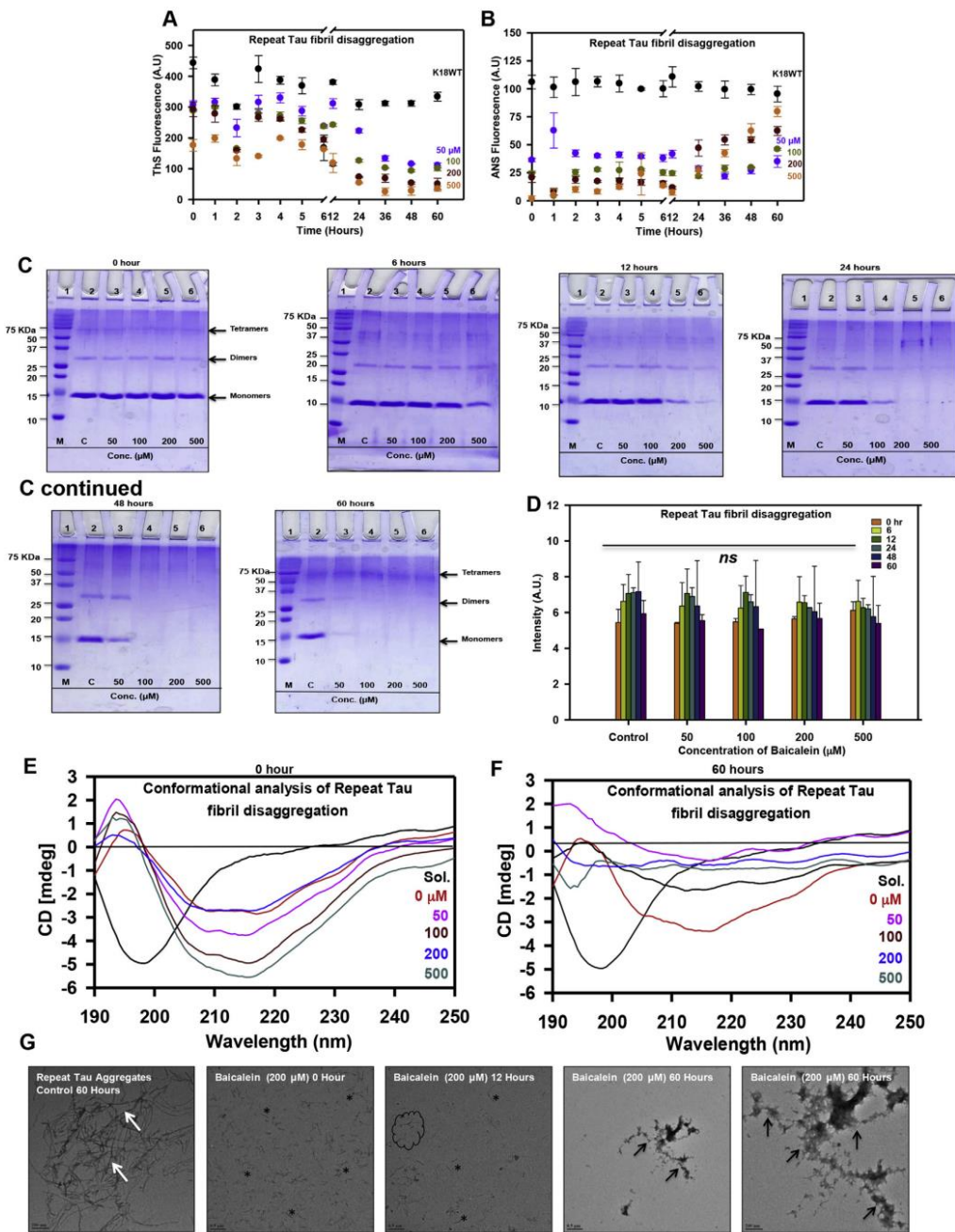


Fig. 6. Disaggregation of repeat Tau fibrils by Baicalein. A) ThS fluorescence for repeat Tau fibril disaggregation shows a decrease with increase in Baicalein concentration and the time of incubation. B) The ANS fluorescence assay for repeat Tau fibrils disaggregation shows more prominent decrease in all concentrations of Baicalein. Furthermore, there is similar increase in ANS fluorescence after 12.

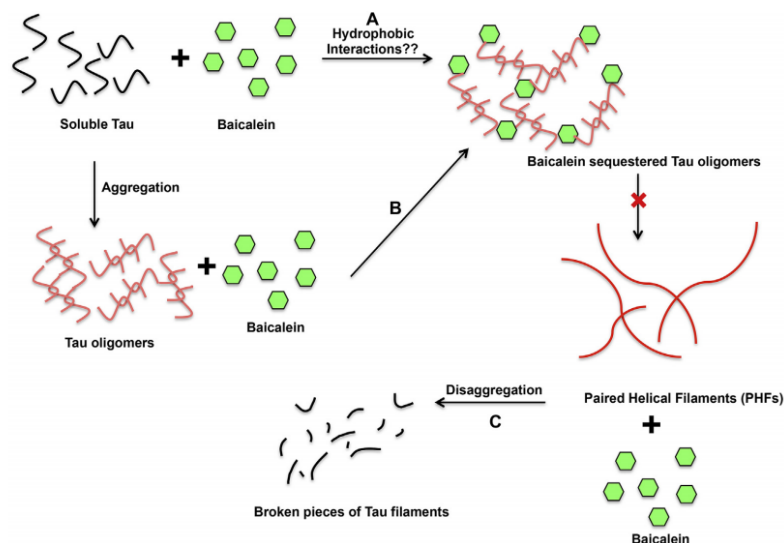


Fig. 7. Model for Baicalein mediated Tau aggregation inhibition and disaggregation. Baicalein may show interaction with various intermittent species of Tau aggregates. A) Baicalein may interact at first step with soluble Tau to induce Tau oligomerization and sequester them based on hydrophobic interactions and prevent their further participation in fibril formation. B) Baicalein might enhance the Tau oligomerization in presence of heparin and further bind these oligomers and inhibit fibril formation. C) Baicalein might also interact with Tau fibrils and lead to their disaggregation leading to formation of small pieces of Tau aggregates.

clearly depict the decrease in fluorescence intensity in the initial stages after Baicalein addition, but are found to increase after 12–24 h at higher concentrations. This behavior of ANS fluorescence can be attributed to the fact that increase in ANS fluorescence depends on binding with hydrophobic residues as well as with cationic amino acids like arginine and lysine [72]. Thus, the Baicalein stabilized oligomer interacts through their cationic residues even though the overall surface hydrophobicity is greatly reduced. The disaggregation potential of Baicalein upon treatment of Tau aggregates signifies that the interaction between these two involves rearrangement of bonds and change in binding energies. If the oligomers formed are stable enough that they do not further interact with other protein species, (either soluble Tau or other oligomers) it can lead to attenuation of further fibrillization of Tau.

Altogether, Baicalein plays a dual role of preventing Tau aggregation as well as dissolving the preformed aggregates and can be further considered for the therapeutic screening.

5. Conclusions

The potency of Baicalein in inhibiting the aggregation of proteins like α -synuclein, amyloid beta and amylin has made this molecule important for screening against the other amyloidogenic proteins. Our current investigation demonstrates the ability of Baicalein to inhibit the Tau aggregation by covalent modification. The simulation and docking studies revealed the interaction of 2 adjacent –OH groups of Baicalein with Leucine 266 of the repeat Tau. These adjacent hydroxyl groups might also be involved in the covalent modification of Tau as observed by MALDI-TOF analysis. Along with hydrogen bonding, the hydrophobic interactions were found to play a role in Tau-Baicalein binding. In summary, Baicalein inhibits the Tau aggregation by inducing the off-pathway oligomer formation and preventing the filamentous aggregate formation thus highlighting its potential to be developed as a future therapeutic agent in AD.

Acknowledgement

This work was supported in part by grants from the Department of Science and Technology-Science and Engineering Research Board DST-

SERB/EMR000306 and in-house CSIR-National Chemical Laboratory grant MLP029526. Shweta Kishor Sonawane acknowledges the fellowship from Department of Biotechnology (DBT), India. Abhishek Ankur Balmik acknowledges the Shyama Prasad Mukherjee fellowship (SPMF) from Council of Scientific Industrial Research (CSIR), India. Tau constructs were kindly gifted by Prof. Roland Brandt from University of Osnabruck, Germany and Prof. Jeff Kuret from Ohio State University College of Medicine, USA. We thank Mr. Yugendra R. Patil, Dr. Santhakumari and Dr. Mahesh J Kulkarni for their fruitful discussion on MALDI-TOF.

Appendix A. Supplementary data

Supplementary data to this article can be found online at <https://doi.org/10.1016/j.abb.2019.108119>.

References

- [1] L.M. Ittner, J. Götz, Amyloid- β and tau—a toxic pas de deux in Alzheimer's disease, *Nat. Rev. Neurosci.* 12 (2011) 67–72.
- [2] J. Hardy, Alzheimer's disease: the amyloid cascade hypothesis: an update and re-appraisal, *J. Alzheimer's Dis.* 9 (2006) 151–153.
- [3] Y. Wang, E. Mandelkow, Tau in physiology and pathology, *Nat. Rev. Neurosci.* 17 (1) (2015) 5–21.
- [4] S. Lovestone, M. Boada, B. Dubois, M. Hüll, J.O. Rinne, H.-J. Huppertz, M. Calero, M.V. Andrés, B. Gómez-Carrillo, T. León, A phase II trial of tideglusib in Alzheimer's disease, *J. Alzheimer's Dis.* 45 (2015) 75–88.
- [5] B.H. Morimoto, D. Schmechel, J. Hirman, A. Blackwell, J. Keith, M. Gold, A... S. Investigators, A double-blind, placebo-controlled, ascending-dose, randomized study to evaluate the safety, tolerability and effects on cognition of AL-108 after 12 weeks of intranasal administration in subjects with mild cognitive impairment, *Dement. Geriatr. Cognit. Disord.* 35 (2013) 325–339.
- [6] K.S. Kosik, C.L. Joachim, D.J. Selkoe, Microtubule-associated protein tau (tau) is a major antigenic component of paired helical filaments in Alzheimer disease, *Proc. Natl. Acad. Sci.* 83 (1986) 4044–4048.
- [7] K.S. Kosik, L. McConlogue, Microtubule-associated protein function: lessons from expression in *spodoptera frugiperda* cells, *Cell Motil. Cytoskeleton.* 28 (1994) 195–198.
- [8] A. Ebneth, R. Godemann, K. Stamer, S. Illenberger, B. Trinczek, E.-M. Mandelkow, E. Mandelkow, Overexpression of tau protein inhibits kinesin-dependent trafficking of vesicles, mitochondria, and endoplasmic reticulum: implications for Alzheimer's disease, *The Journal of cell biology* 143 (1998) 777–794.
- [9] E.-M. Mandelkow, E. Mandelkow, Biochemistry and cell biology of tau protein in neurofibrillary degeneration, *Cold Spring Harbor perspectives in medicine* 2 (2012) a006247.
- [10] K. Iqbal, F. Liu, C.-X. Gong, A.d.C. Alonso, I. Grundke-Iqbal, Mechanisms of tau-

- induced neurodegeneration, *Acta Neuropathol.* 118 (2009) 53–69.
- [11] E.-M. Mandelkow, E. Mandelkow, Tau in Alzheimer's disease, *Trends Cell Biol.* 8 (1998) 425–427.
- [12] C.M. Cowan, S. Quraishe, A. Mudher, What is the pathological significance of tau oligomers? *Biochem. Soc. Trans.* 40 (2012) 693–697.
- [13] B. Bulic, M. Pickhardt, B. Schmidt, E.M. Mandelkow, H. Waldmann, E. Mandelkow, Development of tau aggregation inhibitors for Alzheimer's disease, *Angew. Chem. Int. Ed.* 48 (2009) 1740–1752.
- [14] B. Bulic, M. Pickhardt, E.-M. Mandelkow, E. Mandelkow, Tau protein and tau aggregation inhibitors, *Neuropharmacology* 59 (2010) 276–289.
- [15] C. Lawatschek, M. Pickhardt, S. Wiczorek, A. Grafmüller, E. Mandelkow, H.G. Börner, Generalizing the concept of specific compound formulation additives towards non-fluorescent drugs: a solubilization study on potential anti-alzheimer-active small-molecule compounds, *Angew. Chem. Int. Ed.* 55 (2016) 8752–8756.
- [16] D.M. Holtzman, M.C. Carrillo, J.A. Hendrix, L.J. Bain, A.M. Catafau, L.M. Gault, M. Goedert, E. Mandelkow, E.-M. Mandelkow, D.S. Miller, Tau: from research to clinical development, *Alzheimer's Dementia* 12 (2016) 1033–1039.
- [17] V.M. Lee, K.R. Brunden, M. Hutton, J.Q. Trojanowski, Developing therapeutic approaches to tau, selected kinases, and related neuronal protein targets, *Cold Spring Harbor perspectives in medicine* 1 (2011) a006437.
- [18] A. Crowe, M.J. James, V.M.-Y. Lee, A.B. Smith, J.Q. Trojanowski, C. Ballatore, K.R. Brunden, Aminothienopyridazines and methylene blue affect Tau fibrillization via cysteine oxidation, *J. Biol. Chem.* 288 (2013) 11024–11037.
- [19] C. Wischik, P. Edwards, R. Lai, M. Roth, C. Harrington, Selective inhibition of Alzheimer disease-like tau aggregation by phenothiazines, *Proc. Natl. Acad. Sci.* 93 (1996) 11213–11218.
- [20] R.H. Schirmer, H. Adler, M. Pickhardt, E. Mandelkow, ... , Let us forget you—methylene blue, *Neurobiol. Aging* 32 (2011) 2325. e2327–2325. e2316.
- [21] J.C. O'Leary, Q. Li, P. Marinac, L.J. Blair, E.E. Congdon, A.G. Johnson, U.K. Jinwal, J. Koren, J.R. Jones, C. Kraft, Phenothiazine-mediated rescue of cognition in tau transgenic mice requires neuroprotection and reduced soluble tau burden, *Mol. Neurodegener.* 5 (2010) 1.
- [22] C.M. Wischik, C.R. Harrington, J.M. Storey, Tau-aggregation inhibitor therapy for Alzheimer's disease, *Biochem. Pharmacol.* 88 (2014) 529–539.
- [23] E. Akoury, M. Pickhardt, M. Gajda, J. Biernat, E. Mandelkow, M. Zweckstetter, Mechanistic basis of phenothiazine-driven inhibition of tau aggregation, *Angew. Chem. Int. Ed.* 52 (2013) 3511–3515.
- [24] C. Ballatore, K.R. Brunden, D.M. Hurny, J.Q. Trojanowski, V.M.-Y. Lee, A.B. Smith III, Microtubule stabilizing agents as potential treatment for Alzheimer's disease and related neurodegenerative tauopathies, *J. Med. Chem.* 55 (2012) 8979–8996.
- [25] B. Zhang, J. Carroll, J.Q. Trojanowski, Y. Yao, M. Iba, J.S. Potuzak, A.-M.L. Hogan, S.X. Xie, C. Ballatore, A.B. Smith, The microtubule-stabilizing agent, epothilone D, reduces axonal dysfunction, neurotoxicity, cognitive deficits, and Alzheimer-like pathology in an interventional study with aged tau transgenic mice, *J. Neurosci.* 32 (2012) 3601–3611.
- [26] K.R. Brunden, B. Zhang, J. Carroll, Y. Yao, J.S. Potuzak, A.-M.L. Hogan, M. Iba, M.J. James, S.X. Xie, C. Ballatore, Epothilone D improves microtubule density, axonal integrity, and cognition in a transgenic mouse model of tauopathy, *J. Neurosci.* 30 (2010) 13861–13866.
- [27] L. Calcul, B. Zhang, U.K. Jinwal, C.A. Dickey, B.J. Baker, Natural products as a rich source of tau-targeting drugs for Alzheimer's disease, *Future Med. Chem.* 4 (2012) 1751–1761.
- [28] S.R. Paranjape, A.P. Riley, A.D. Somoza, C.E. Oakley, C.C. Wang, T.E. Prinszano, B.R. Oakley, T.C. Gambin, Azaphilones inhibit tau aggregation and dissolve tau aggregates in vitro, *ACS Chem. Neurosci.* 6 (2015) 751–760.
- [29] S.R. Paranjape, Y.-M. Chiang, J.F. Sanchez, R. Entwistle, C.C. Wang, B.R. Oakley, T.C. Gambin, Inhibition of Tau aggregation by three *Aspergillus nidulans* secondary metabolites: 2, ω -dihydroxyemodin, asperthecin, and asperbenzaldehyde, *Planta Med.* 80 (2014) 77–85.
- [30] W. Li, J.B. Sperry, A. Crowe, J.Q. Trojanowski, A.B. Smith III, V.M.Y. Lee, Inhibition of tau fibrillization by oleochemical via reaction with the amino groups of tau, *J. Neurochem.* 110 (2009) 1339–1351.
- [31] J. Bieschke, J. Russ, R.P. Friedrich, D.E. Ehrnhoefer, H. Wobst, K. Neugebauer, E.E. Wanker, EGGC remodels mature α -synuclein and amyloid- β fibrils and reduces cellular toxicity, *Proc. Natl. Acad. Sci.* 107 (2010) 7710–7715.
- [32] H.J. Wobst, A. Sharma, M.I. Diamond, E.E. Wanker, J. Bieschke, The green tea polyphenol (–)-epigallocatechin gallate prevents the aggregation of tau protein into toxic oligomers at substoichiometric ratios, *FEBS Lett.* 589 (2015) 77–83.
- [33] D. Vauzour, K. Vafeiadou, A. Rodriguez-Mateos, C. Rendeiro, J.P. Spencer, The neuroprotective potential of flavonoids: a multiplicity of effects, *Genes & nutrition* 3 (2008) 115–126.
- [34] M. Zhu, S. Rajamani, J. Kaylor, S. Han, F. Zhou, A.L. Fink, The flavonoid baicalin inhibits fibrillation of α -synuclein and disaggregates existing fibrils, *J. Biol. Chem.* 279 (2004) 26846–26857.
- [35] S.Q. Zhang, D. Obregon, J. Ehrhart, J. Deng, J. Tian, H. Hou, B. Giunta, D. Sawmiller, J. Tan, Baicalin reduces β -amyloid and promotes nonamyloidogenic amyloid precursor protein processing in an Alzheimer's disease transgenic mouse model, *J. Neurosci.* 91 (2013) 1239–1246.
- [36] P.D.Q. Huy, Q.V. Vuong, G. La Penna, P. Fallor, M.S. Li, Impact of Cu (II) binding on structures and dynamics of A β 42 monomer and dimer: molecular dynamics study, *ACS Chem. Neurosci.* 7 (2016) 1348–1363.
- [37] S. Barghorn, J. Biernat, E. Mandelkow, Purification of recombinant tau protein and preparation of Alzheimer-paired helical filaments in vitro, *Amyloid Proteins: Methods and Protocols* (2005) 35–51.
- [38] S.F. Altschul, W. Gish, W. Miller, E.W. Myers, D.J. Lipman, Basic local alignment search tool, *J. Mol. Biol.* 215 (1990) 403–410.
- [39] B. Webb, A. Sali, Protein structure modeling with MODELLER, *Protein Structure Prediction*, Springer, 2014, pp. 1–15.
- [40] R.A. Laskowski, M.W. MacArthur, D.S. Moss, J.M. Thornton, PROCHECK: a program to check the stereochemical quality of protein structures, *J. Appl. Crystallogr.* 26 (1993) 283–291.
- [41] S.C. Lovell, I.W. Davis, W.B. Arendall III, P.L. De Bakker, J.M. Word, M.G. Prisant, J.S. Richardson, D.C. Richardson, Structure validation by Ca geometry: ϕ , ψ and C β deviation, *Proteins: Structure, Function, and Bioinformatics* 50 (2003) 437–450.
- [42] C. Colovos, T.O. Yeates, Verification of protein structures: patterns of nonbonded atomic interactions, *Protein Sci.* 2 (1993) 1511–1519.
- [43] M. Wiederstein, M.J. Sippl, ProSA-web: interactive web service for the recognition of errors in three-dimensional structures of proteins, *Nucleic Acids Res.* 35 (2007) W407–W410.
- [44] G.M. Sastry, M. Adzhigirey, T. Day, R. Annabhimou, W. Sherman, Protein and ligand preparation: parameters, protocols, and influence on virtual screening enrichments, *J. Comput. Aided Mol. Des.* 27 (2013) 221–234.
- [45] R.A. Friesner, J.L. Banks, R.B. Murphy, T.A. Halgren, J.J. Klicic, D.T. Mainz, M.P. Repasky, E.H. Knoll, M. Shelley, J.K. Perry, Glide: a new approach for rapid, accurate docking and scoring. 1. Method and assessment of docking accuracy, *J. Med. Chem.* 47 (2004) 1739–1749.
- [46] T.A. Halgren, Identifying and characterizing binding sites and assessing drug-ability, *J. Chem. Inf. Model.* 49 (2009) 377–389.
- [47] K.J. Bowers, D.E. Chow, H. Xu, R.O. Dror, M.P. Eastwood, B.A. Gregersen, J.L. Klepeis, I. Kolossvary, M.A. Moraes, F.D. Sacerdoti, Scalable algorithms for molecular dynamics simulations on commodity clusters, SC06: Proceedings of the 2006 ACM/IEEE Conference on Supercomputing, IEEE, 2006:43–43.
- [48] S. Jeganathan, M. von Bergen, H. Bruch, H.-J. Steinhoff, E. Mandelkow, Global hairpin folding of tau in solution, *Biochemistry* 45 (2006) 2283–2293.
- [49] P. Chenprakhon, J. Sucharitakul, B. Panijpan, P. Chaiyen, Measuring binding affinity of Protein–ligand interaction using spectrophotometry: binding of neutral red to flavin-binding protein, *J. Chem. Educ.* 87 (2010) 829–831.
- [50] Y.-J. Hu, Y. Liu, J.-B. Wang, X.-H. Xiao, S.-S. Qu, Study of the interaction between monoammonium glycyrrhizinate and bovine serum albumin, *J. Pharm. Biomed. Anal.* 36 (2004) 915–919.
- [51] F. Zsila, Z. Bikádi, M. Simonyi, Probing the binding of the flavonoid, quercetin to human serum albumin by circular dichroism, electronic absorption spectroscopy and molecular modelling methods, *Biochem. Pharmacol.* 65 (2003) 447–456.
- [52] V. Daebl, S. Chinnambhi, J. Biernat, M. Schwalbe, B. Habenstein, A. Loquet, E. Akoury, K. Tepper, H. Müller, M. Baldus, β -Sheet core of tau paired helical filaments revealed by solid-state NMR, *J. Am. Chem. Soc.* 134 (2012) 13982–13989.
- [53] M.D. Mukrasch, J. Biernat, M. von Bergen, C. Griesinger, E. Mandelkow, M. Zweckstetter, Sites of tau important for aggregation populate β (tau)-structure and bind to microtubules and polyanions, *J. Biol. Chem.* 280 (2005) 24978–24986.
- [54] M. Von Bergen, S. Barghorn, J. Biernat, E.-M. Mandelkow, E. Mandelkow, Tau aggregation is driven by a transition from random coil to beta sheet structure, *Biochim. Biophys. Acta (BBA) - Mol. Basis Dis.* 1739 (2005) 158–166.
- [55] P. Friedhoff, M. Von Bergen, E.-M. Mandelkow, P. Davies, E. Mandelkow, A nucleated assembly mechanism of Alzheimer paired helical filaments, *Proc. Natl. Acad. Sci.* 95 (1998) 15712–15717.
- [56] M. Goedert, R. Jakes, M. Spillantini, M. Hasegawa, M. Smith, R. Crowther, Assembly of Microtubule-Associated Protein Tau into Alzheimer-like Filaments Induced by Sulphated Glycosaminoglycans, (1996).
- [57] M. Pickhardt, Z. Gazova, M. von Bergen, I. Khlistunova, Y. Wang, A. Hascher, E.-M. Mandelkow, J. Biernat, E. Mandelkow, Anthraquinones inhibit tau aggregation and dissolve Alzheimer's paired helical filaments in vitro and in cells, *J. Biol. Chem.* 280 (2005) 3628–3635.
- [58] G. Ramachandran, J.B. Udgaonkar, Understanding the kinetic roles of the inducer heparin and of rod-like protofibrils during amyloid fibril formation by Tau protein, *J. Biol. Chem.* 286 (2011) 38948–38959.
- [59] S. Kumar, K. Tepper, S. Kaniyappan, J. Biernat, S. Wegmann, E.-M. Mandelkow, D.J. Müller, E. Mandelkow, Stages and conformations of the Tau repeat domain during aggregation and its effect on neuronal toxicity, *J. Biol. Chem.* 289 (2014) 20318–20332.
- [60] A. Crowe, C. Ballatore, E. Hyde, J.Q. Trojanowski, V.M.-Y. Lee, High throughput screening for small molecule inhibitors of heparin-induced tau fibril formation, *Biochem. Biophys. Res. Commun.* 358 (2007) 1–6.
- [61] K.R. Brunden, J.Q. Trojanowski, V.M.-Y. Lee, Advances in tau-focused drug discovery for Alzheimer's disease and related tauopathies, *Nat. Rev. Drug Discov.* 8 (2009) 783–793.
- [62] B. Bulic, M. Pickhardt, E. Mandelkow, Progress and developments in tau aggregation inhibitors for Alzheimer disease, *J. Med. Chem.* 56 (2013) 4135–4155.
- [63] E.E. Congdon, S. Kim, J. Bonchak, T. Songrug, A. Matzavinos, J. Kureu, Nucleation-dependent tau filament formation: the importance of dimerization and an estimation of elementary rate constants, *J. Biol. Chem.* 283 (2008) 13806–13816.
- [64] K. Flach, I. Hilbrich, A. Schiffmann, U. Gärtner, M. Krüger, M. Leonhardt, H. Waschpky, L. Wick, T. Arendt, M. Holzer, Tau oligomers impair artificial membrane integrity and cellular viability, *J. Biol. Chem.* 287 (2012) 43223–43233.
- [65] L. Guzmán-Martínez, G.A. Farías, R.B. Maccioni, Tau oligomers as potential targets for Alzheimer's diagnosis and novel drugs, *Tau oligomers* 3 (2014) 35.
- [66] S.W. Chua, A. Cornejo, J. van Eersel, C.H. Stevens, I. Vaca, M. Cueto, M. Kassou, A. Gladbach, A. Macmillan, L. Lewis, The polyphenol altemusin inhibits in vitro fibrillization of tau and reduces induced tau pathology in primary neurons, *ACS Chem. Neurosci.* 8 (2017) 743–751.
- [67] M. Margittai, R. Langen, Template-assisted filament growth by parallel stacking of tau, *Proc. Natl. Acad. Sci. U.S.A.* 101 (2004) 10278–10283.

S.K. Sonawane, et al.

Archives of Biochemistry and Biophysics 675 (2019) 108119

- [68] G. Semisotnov, N. Rodionova, O. Razgulyaev, V. Uversky, A. Gripas, R. Gilmanshin, Study of the "molten globule" intermediate state in protein folding by a hydrophobic fluorescent probe, *Biopolymers* 31 (1991) 119–128.
- [69] S. Taniguchi, N. Suzuki, M. Masuda, S.-i. Hisanaga, T. Iwatsubo, M. Goedert, M. Hasegawa, Inhibition of heparin-induced tau filament formation by phenothiazines, polyphenols, and porphyrins, *J. Biol. Chem.* 280 (2005) 7614–7623.
- [70] M.C. Monti, L. Margarucci, R. Riccio, A. Casapullo, Modulation of tau protein fibrillization by oleocanthal, *J. Nat. Prod.* 75 (2012) 1584–1588.
- [71] K. Cisek, G.L. Cooper, C.J. Hulseby, J. Kuret, Structure and mechanism of action of tau aggregation inhibitors, *Curr. Alzheimer Res.* 11 (2014) 918–927.
- [72] O.K. Gasmov, B.J. Glasgow, ANS fluorescence: potential to augment the identification of the external binding sites of proteins, *Biochim. Biophys. Acta Protein Proteomics* 1774 (2007) 403–411.
- [73] S. Sonawane, et al., Protein-Capped Metal Nanoparticles Inhibit Tau Aggregation in Alzheimer's Disease, *ACS Omega* (2019) 12833–12840, <https://doi.org/10.1021/acsomega.9b01411>.



Contents lists available at ScienceDirect

International Journal of Biological Macromolecules

journal homepage: <http://www.elsevier.com/locate/ijbiomac>

Effect of Melatonin on Tau aggregation and Tau-mediated cell surface morphology

Rashmi Das^{a,b,1}, Abhishek Ankur Balmik^{a,b,1}, Subashchandra Bose Chinnathambi^{a,b,*}^a Neurobiology Group, Division of Biochemical Sciences, CSIR-National Chemical Laboratory, Dr. Homi Bhabha Road, 411008 Pune, India^b Academy of Scientific and Innovative Research (AcSIR), 110025 New Delhi, India

ARTICLE INFO

Article history:

Received 28 November 2019

Received in revised form 23 January 2020

Accepted 30 January 2020

Available online 07 February 2020

Keywords:

Alzheimer's disease

Tau protein

Paired helical filaments

Tauopathies

Melatonin

Cell surface morphology

ABSTRACT

Aggregation of Microtubule-associated protein Tau and its deposition in the form of neurofibrillary tangles (NFTs) is one of the pathological hallmarks of Alzheimer's disease (AD). Tau aggregation inhibition has been targeted in various studies including natural compounds and synthetic small molecules. Here, we have studied neurohormone- Melatonin against *in vitro* Tau aggregation and observed its effect on membrane topology, tubulin network and Tau phosphorylation in Neuro2A and N9 cell lines. The aggregation and conformation of Tau was determined by ThT fluorescence and CD spectroscopy respectively. The morphology of Tau aggregates in presence and absence of Melatonin was studied by transmission electron microscopy. Melatonin was found to reduce the formation of higher order oligomeric structures without affecting the overall aggregation kinetics of Tau. Melatonin also modulates and helps to maintain membrane morphology, independent on tubulin network as evidenced by FE-SEM and immunofluorescence analysis. Overall, Melatonin administration shows mild anti-aggregation and cytoprotective effects.

© 2018 Elsevier B.V. All rights reserved.

1. Introduction

Microtubule-associated protein Tau undergoes misfolding and forms intracellular aggregates in Alzheimer's disease (AD) and related Tauopathies [1]. Deposition of extracellular fibrillar aggregates of amyloid- β also has deleterious effects on neuronal functions [2,3]. Both the proteinaceous aggregates have been widely studied with respect to their pathological consequences in AD and form the basis of two hypotheses known as 'Tau' and 'amyloid- β ' hypothesis. Tau hypothesis has attained more attention in last decade since only amyloid- β deposition is found in brain without any pathological effect [4]. The main physiological functions of Tau include the stabilization of microtubule, axonal growth and cargo trafficking etc. Under pathological condition, a series of signalling cascade leads to phosphorylation of Tau by various kinases. Tau is hyperphosphorylated upon upregulation of several kinases like CDK5 and GSK-3 β . Therapeutic strategies have

been employed involving the use of specific kinase inhibitors [5–7]. CDK5 complexed with p25 increases its activation state and induces the phosphorylation of Tau at the following amino acids Ser202, Thr205, Ser235 and Ser404. Additionally, the amyloidogenic protein aggregates accumulate around the phospho-lipid bilayer which leads to the formation of membrane pore in cholesterol-rich domain [8,9]. AD is associated with a multiple factors, which ultimately lead to neurodegeneration. Thus, multi-targeted approach is required for the effective amelioration of Tau-mediated neuropathology [10]. Therapeutic strategies have been studied involving different aspects of neurodegeneration. A wide range of small molecules with multiple targets like-aggregation inhibition, kinase inhibition or phosphatase activation are under study [7]. Melatonin is a neurohormone, which is derived from pineal gland and involved in the maintenance of circadian rhythm [11,12]. Melatonin is also produced in non-pineal sites and its receptors are present in most cell types [13,14]. It is rapidly metabolized in liver and converted to secondary metabolites called kynuramines [15–17]. It is well known that Melatonin is an anti-oxidant molecule, which can cross all biological membranes and also functions in the upregulation of other enzymes involved in protection against oxidative damage [18–23]. Melatonin is a pleiotropic molecule with a high bioavailability and low toxicity. It is considered as a potent candidate against neurodegenerative diseases due to its wide range of functions. The role of Melatonin in kinase function has been studied where it was found to

Abbreviations: NFTs, neurofibrillary tangles; PHF, paired helical filaments; A β , amyloid- β ; CDK5/p25, cyclin dependent kinase 5/p25; GSK-3 β , glycogen synthase kinase-3 β .

* Corresponding author at: Division of Biochemical Sciences, CSIR-National Chemical Laboratory (CSIR-NCL), Dr. Homi Bhabha Road, 411008 Pune, India.

E-mail address: s.chinnathambi@ncl.res.in (S. Chinnathambi).

¹ The authors wish it to be known that, in their opinion, the first two authors should be regarded as joint First Authors.

<https://doi.org/10.1016/j.ijbiomac.2020.01.296>

0141-8130/© 2018 Elsevier B.V. All rights reserved.

downregulate kinases like GSK-3 β and PKA, which in turn affects the phosphorylation status of Tau [24–27]. Melatonin is found to be effective in amelioration of neurological defects and restoration of cognitive functions [28,29]. Melatonin has also been studied with respect to inhibition of amyloid- β and α -synuclein aggregation [30,31]. Hence, The multi-faceted role of Melatonin makes it a potent lead for therapeutic approach [32].

Here, we have studied the potential role of Melatonin in inhibition of full-length Tau (4R2N) aggregates and its effect on cell viability. We have also performed the function of Melatonin in CDK5-mediated phosphorylation of Tau at Ser202/Thr205 sites. Melatonin reduces the membrane roughness induced by Tau aggregates in Neuro2A and N9 microglial cells while the tubulin network remain unaltered by Melatonin and Tau aggregates.

2. Materials and methods

2.1. Materials

Melatonin, BES, MES, Glycine, SDS, ThT, Protease inhibitor cocktail and ANS were purchased from Sigma-Aldrich. Other biochemical or molecular biology grade chemicals used were - DTT and IPTG (Calbiochem), APS, NaCl, PMSF, Sodium Azide, Ampicillin (MP Biomedicals), Luria-Bertani broth (Himedia), Acrylamide, EGTA, TEMED, DMSO (Invitrogen). BCA assay reagents used for protein estimation were purchased from Sigma-Aldrich. Filtration devices were used from Merck and Pall Life sciences. Ethanol (Mol Bio grade), Chloroform, Isopropanol (Mol Bio grade) were purchased from MP Biomedicals; For cell culture studies, Dulbecco modified eagle's media (DMEM), Fetal bovine Serum (FBS), Horse serum, Phosphate buffer saline (PBS, cell biology grade), trypsin-EDTA, Penicillin-streptomycin, RIPA buffer were also purchased from Invitrogen. MTT reagent, Okadaic acid, Paraformaldehyde (16%), and TritonX-100 were purchased from Sigma. The coverslip of 0.17 mm was purchased from blue star for immunofluorescence and SEM study. In immunofluorescence and western blot study we used the following antibodies: mouse Beta Tubulin loading control (BT7R) (Thermo fisher, cat no MA516308), mouse monoclonal CDK5 antibody (Invitrogen, Cat no AHZ0492) and total Tau antibody K9JA (Dako, Cat no A0024), AT8 (Thermo fisher, Cat no MN1020), Goat anti-Rabbit IgG (H + L) Cross-Adsorbed Secondary Antibody HRP (Invitrogen, A16110), anti-mouse secondary antibody conjugated with Alexa flour-488 (Invitrogen, Cat no A-11001), Goat anti-Rabbit IgG (H + L) Cross-Adsorbed Secondary Antibody with Alexa Fluor 555 (A-21428), DAPI (Invitrogen). For real-time quantification of cytokine expression profile, Trizol reagent, First strand cDNA synthesis kit (Cat no K1612), Maxima SYBR Green/Fluorescein qPCR Master Mix (2 \times) (Cat no K0241) were used from Thermo.

2.2. Protein expression and purification

pT7C full-length Tau (hTau40wt) were expressed in *E. coli* BL21* upon induction by 0.5 mM IPTG and purified as previously described [33–35]. Cell homogenization was carried out at 15 KPSI using Constant cell disruption system. 0.5 M NaCl and 5 mM DTT were added to the resulting lysate and kept in water bath at 90 °C for 20 min. The lysate was cooled, centrifuged at 40,000 rpm for 45 min and dialyzed overnight. After a second round of centrifugation, the supernatant was filtered and subject to cation exchange chromatography using Sepharose fast flow (SPFF) column pre-equilibrated with 20 mM MES pH 6.8, 50 mM NaCl. For eluting Tau protein, 20 mM MES pH 6.8 with 1 M NaCl was used. The fractions containing Tau protein were pooled, concentrated and subjected to size-exclusion chromatography using 1 \times PBS buffer with 2 mM DTT in Superdex 75 Hi-load 16/600 column. The final concentration of Tau was obtained by performing Bicinchoninic acid assay.

2.3. Aggregation inhibition assay

Full-length Tau aggregates were prepared in 20 mM BES pH 7.4 as assembly buffer, in the presence of heparin as an inducer (Tau:heparin = 4:1) [36]. The reaction was set-up in microcentrifuge amber tubes and incubated at 37 °C for 96 h. Aggregation reaction tubes with 200–5000 μ M of Melatonin in 10% DMSO were also prepared. ThT fluorescence for all reactions at various time-points (0–96 h) was measured at 450 nm excitation and 475 nm emission wavelengths. The measurements for all time-points were taken in triplicates with Tau and ThT ratio of 1:2. Fluorescence of assembly buffer was measured for blank subtraction.

2.4. CD spectroscopy

CD spectra for 3 μ M soluble Tau and Tau aggregates with or without Melatonin were recorded in Jasco J-815 CD spectrometer in 1 mm cuvette under nitrogen atmosphere. The spectra were recorded at 100 nm/min scan speed at 1 nm bandwidth in 190–250 nm scan range. The baseline was recorded for 50 mM sodium phosphate buffer pH -6.8 and subtracted for each spectrum. The final spectra were obtained as an average of five CD acquisitions.

2.5. Transmission electron microscopy

Morphology of Tau aggregates with or without Melatonin was visualized by transmission electron microscopy. 2 μ M of Tau aggregates were placed on 400 mesh carbon coated copper grids, washed twice with filtered milliQ water for 30 s and stained with 2% uranyl acetate for 2 min. The samples were dried and scanned using TECNAI T20 Transmission Electron Microscope at 120 KV.

2.6. Size-exclusion chromatography

Full-length Tau aggregates were prepared in 20 μ M BES, pH 7.4 in 4:1 (Tau:heparin) ratio with heparin in the presence of 1000 μ M Melatonin and additives as mentioned earlier. A control experiment was performed with only full-length Tau aggregates. Size-exclusion chromatography was performed at 0 h after 24 h using 1 \times PBS buffer for elution. The respective samples were loaded onto Superdex Increase 10/300 GL column in 100 μ l sample volume after filtration through 0.45 μ m centrifugal filters. The peak fractions of 0.25 ml were collected for each run.

2.7. Cytotoxicity assay for SEC fractions

The fractions obtained from size-exclusion chromatography of full-length Tau aggregates in presence or absence of 1000 μ M Melatonin were tested for their effect on viability of Neuro2A cells (Fractions F7-F10 corresponds to Tau with Melatonin, Fractions F11-F14 corresponds to Tau only from SEC). Neuro2A cells were cultured in DMEM with 10% FBS and 100 μ g/mL of penicillin and streptomycin. Neuro2A cells were seeded in 96 well plates (10,000 cells/well) and incubated at 37 °C for 12 h at 5% CO₂. Peak fractions (F7-F10) were obtained from SEC of full length Tau with Melatonin and fractions (F11-F14) were obtained from SEC of Tau aggregates. Cells were treated with 30 μ l of fractions and 70 μ l of reduced serum media (DMEM with 0.5% FBS) in each well and incubated for 24 h. MTT assay was performed to check the cell viability. MTT was added at 0.5 mg/ml concentration in each well and incubated for 3 h. The formazan end product solubilized by adding absolute DMSO. The spectrophotometric absorbance was measured at 570 nm in triplicate (Tecan Infinite 200 Pro).

2.8. Real-time PCR

Neuro2A cells were treated with Melatonin (50 μ M) and okadaic acid (25 nM) for 6 h. Okadaic acid is used widely for the global cellular

phosphorylation by inhibiting protein phosphatases and then induces Tau hyperphosphorylation. Then the cells were washed in PBS and total RNA were isolated by the conventional TRIZOL, chloroform and isopropanol procedure. The RNA pellets were proceeded for cDNA synthesis (First-strand cDNA synthesis kit) with oligo-dT primer. The expression level of CDK5 was checked by quantitative PCR. The fold change was calculated by $\Delta\Delta CT$ method with respect to house-keeping GAPDH control.

2.9. Western blot

Neuro2A cells with okadaic acid (25 nM) and Melatonin (50 μM) separately and together for 24 h. The cells were washed with PBS, lysed with RIPA buffer and cell lysate were subjected to western blot with anti-CDK5 monoclonal antibody (1:1500) with β -tubulin

(1:5000). Then, the bands intensity was quantified by using BIORAD Quality one 4.6.6 software. The band-density of the treated groups was compared with its corresponding untreated control group and the relative fold changes were plotted with respective proteins and treated group.

2.10. Immunofluorescence microscopy

Misfolded Tau becomes hyperphosphorylated in case of AD due to over-activation of various protein kinases. Phosphorylated Tau tends to aggregate inside the cells and subsequently secreted outside which lead to improper functioning. To study the over-activation of one of the cellular kinases- CDK5 and intracellular Tau phosphorylation, we treated the Neuro2A cells with okadaic acid (25 nM) and Melatonin (50 μM) separately and together for 24 h. The cells were washed with

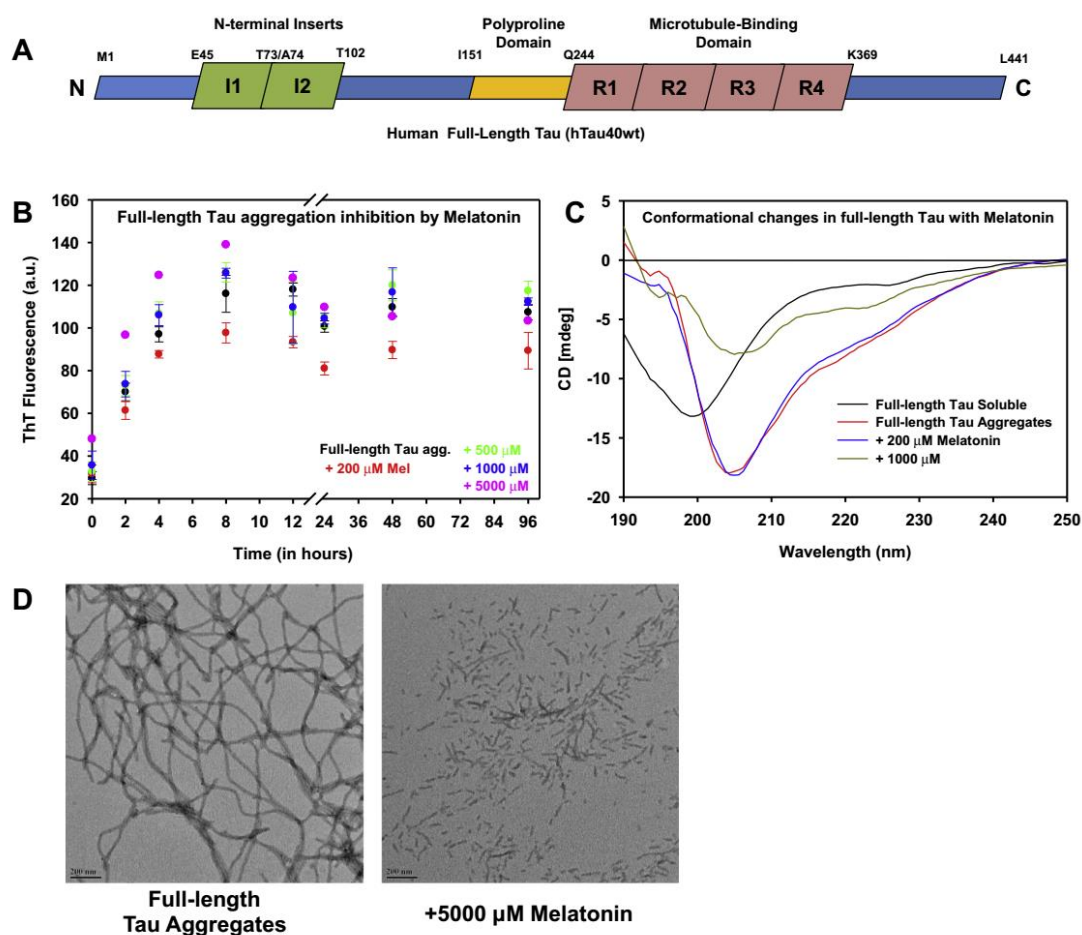


Fig. 1. Effect of Melatonin on full-length Tau aggregation. A) Full-length Tau (hTau40wt) in CNS consists of two N-terminal inserts and four repeat domains. Functionally, the C-terminal region of Tau corresponds to microtubule binding domain while the N-terminal region comprises projection domain facilitating the spatial arrangement of microtubules. The repeat region is preceded by polyproline domain important in Tau phosphorylation by providing docking site for proline directed kinases. B) Aggregation inhibition assay for full-length Tau monitored by ThT fluorescence. There was no change in ThT fluorescence in samples incubated with Melatonin in as high concentration as 5000 μM . C) CD spectroscopy for full-length Tau incubated with Melatonin at 200 and 1000 μM concentration. CD spectrum for Tau control aggregates was also measured. At higher concentrations of Melatonin, spectra shift towards random coil. There are no conformational changes in full-length Tau sample with 200 μM of Melatonin as compared to control Tau aggregates. D) TEM images for full-length Tau control aggregates showed mature fibrils while in Melatonin treated sample (5000 μM) broken aggregates were observed.

PBS thrice and fixed with 4% paraformaldehyde for 15 min and permeabilized with 0.2% TritonX-100. The cells were stained with AT8 (1:100), K9JA (1:500), CDK5 (1:50) and mouse anti-tubulin antibody (1:100) for overnight in 2% horse serum-PBS. Then, Alexa flour conjugated secondary antibody was allowed to bind p-Tau, CDK5 specific primary antibody (anti-mouse Alexa flour 555, 1:500) and K9JA (anti-rabbit Alexa flour 488, 1:1000) for 1 h along with nuclear staining DAPI (300 nM) for 5 min. The images and 3D localization (orthogonal view) were observed in Zeiss Axio observer with Apotome2 fluorescence microscope at 63× oil immersion and analyzed by ZEN2 software.

2.11. Surface morphology by field-emission scanning electron microscopy (FE-SEM)

To study the cell surface morphology of Neuro2A and microglia (N9) cells by Melatonin and Tau aggregates treatment, the cells were grown onto coverslip for 16 h at 37 °C, 5% CO₂. Then the cells were washed with PBS twice and treated individually and in combination with 10 μM of Tau aggregates and 50 μM of Melatonin for 6 h. After the treatment, cells were fixed with 2.5% glutaraldehyde for 1 h at 4 °C, followed by step-wise dehydration with 10, 25, 50, 75, 95 and 100% ethanol. The

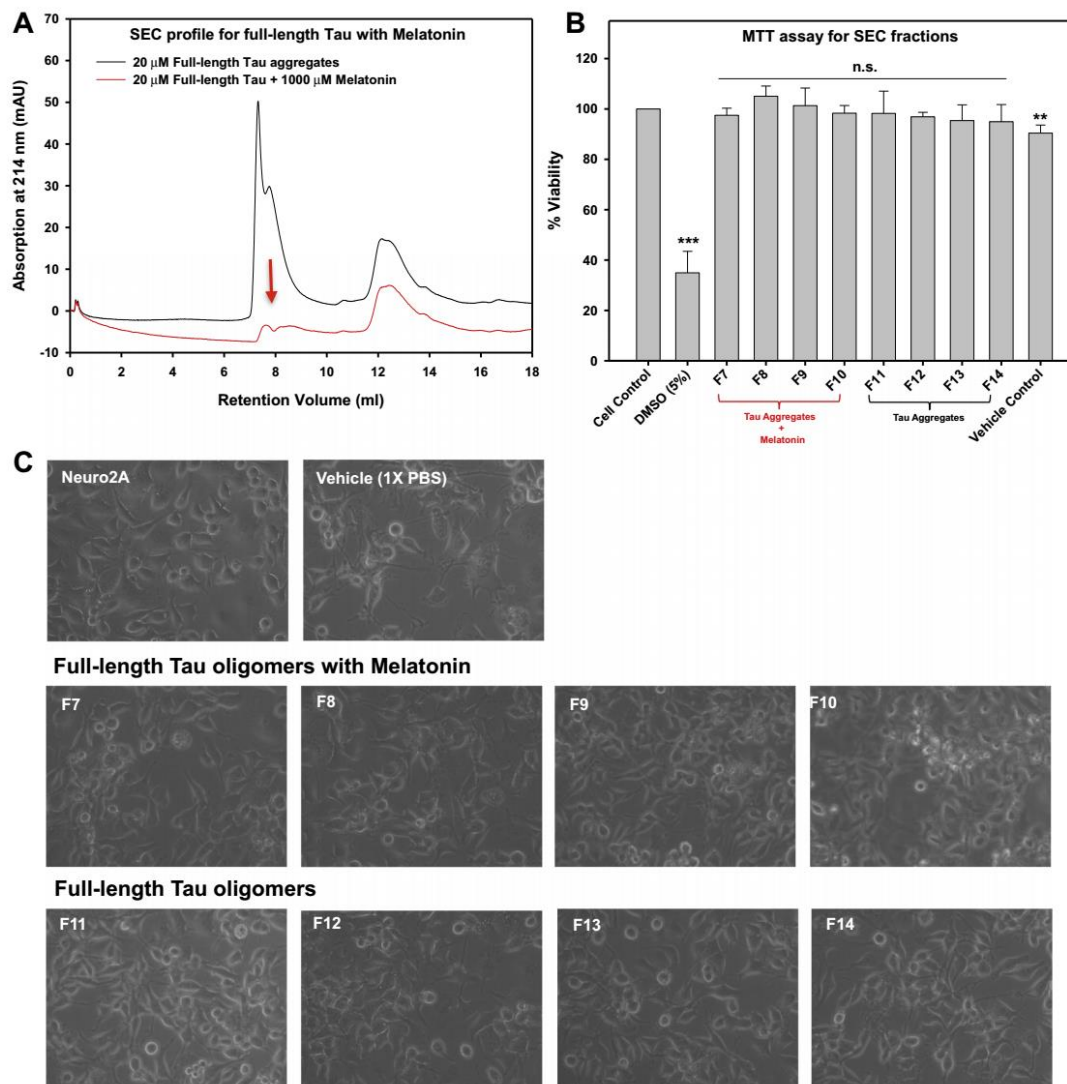


Fig. 2. Size-exclusion chromatography for full-length Tau upon Melatonin treatment. A) Size-exclusion chromatography for 20 μM hTau40wt aggregates with 1000 μM Melatonin as compared to hTau40wt aggregates control after 24 h of incubation. The higher order oligomer peak for Tau disappears in the sample incubated with Melatonin. B) Cell viability assay for the fractions obtained from SEC runs for hTau40wt aggregates control and hTau40wt aggregates with Melatonin. No toxicity was observed from the fractions obtained from either SEC (n.s.-non-significant, * indicates $P \leq 0.05$, ** indicates $P \leq 0.01$, *** indicates $P \leq 0.001$). C) Bright field images for neuronal cells treated with SEC fractions showed morphology similar to untreated cells (Scale bar – 100 μm). (For interpretation of the references to color in this figure, the reader is referred to the web version of this article.)

cells were kept overnight in vacuumed desiccator in presence of anhydrous calcium carbonate for complete drying. The complete coverslips were coated with gold nanoparticle and scanned in FE-SEM (FEI-NOVA NANOSEM 450) at 8000 or 10,000 \times magnification with 18 KV electron beam.

2.12. Statistical analysis

All the experimental analyses were carried out in triplicate. The statistical analysis of control and treated samples were carried out by SigmaPlot 10.0 (Systat software). Two-tailed student unpaired *t*-test was performed to show the significance. (n.s.-non-significant, * indicates $P \leq 0.05$, ** indicates $P \leq 0.01$, *** indicates $P \leq 0.001$).

3. Results and discussion

3.1. Melatonin shows no effect on aggregation of full-length Tau

The effect of Melatonin in the inhibition of full-length Tau protein (Fig. 1A) aggregation was studied using ThT fluorescence assay. Our previous studies suggested that the Melatonin can inhibit Tau aggregation by interacting with repeat domain through histidine residues [37].

Melatonin was used against Tau aggregation at a concentration range of 200–5000 μ M. Surprisingly, it did not show any significant effect on the aggregation of full-length Tau protein in ThT fluorescence, even with higher concentration (5000 μ M) of Melatonin (Fig. 2A). Also, CD spectroscopy revealed that Melatonin treatment does not bring about significant structural change. Tau aggregates shows the signature for β -sheet structure, which remained unchanged with Melatonin treatment (Fig. 1C). However, the electron microscopy images for full-length Tau aggregation samples in presence of Melatonin at 5000 μ M showed distinct morphology of Tau fibrils where mostly broken filaments were observed (Fig. 1D). Melatonin has been studied earlier in the inhibition of amyloid- β and α -synuclein aggregates [30]. The mode of action of Melatonin involves the disruption of salt-bridge formation or reducing the hydrophobic interaction between proteins [31,38]. For Tau aggregation inhibition, Melatonin may employ the same mechanism but it is required in higher concentration to disrupt the fibril formation.

3.2. Melatonin reduces the formation of higher order oligomeric species of Tau

The aggregation of Tau protein forms intermediate toxic oligomers, which also act like seeding species for further aggregation

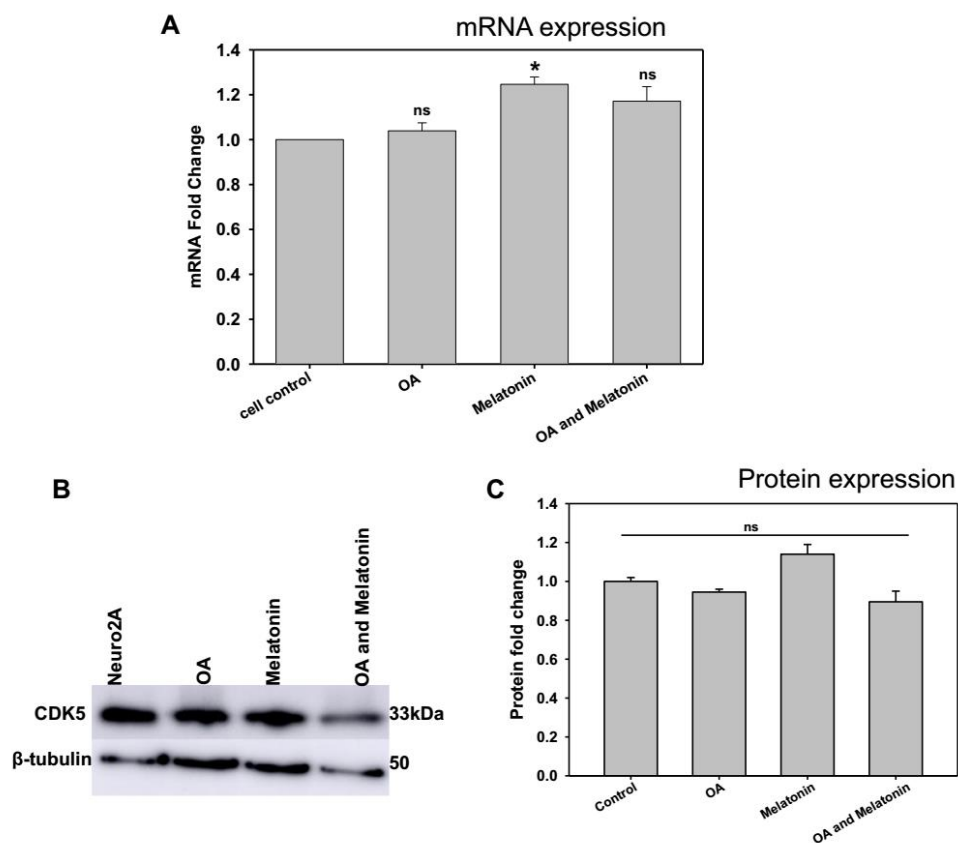


Fig. 3. Cellular level of CDK5 and Tau upon OA and Melatonin exposure (A, B, C) CDK5 mRNA expression level and protein level remain constant in Neuro2A cells upon the exposure of Melatonin and OA treatment. (n.s.-non-significant, * indicates $P \leq 0.05$, ** indicates $P \leq 0.01$, *** indicates $P \leq 0.001$).

[39]. We prepared Tau aggregates in the presence or absence of Melatonin and carried out SEC for the separation of oligomeric species [40]. For the preparation of oligomers, full-length Tau was incubated at 37 °C in the presence of heparin with or without Melatonin. Size-exclusion chromatography (SEC) was performed after 24 h to separate these oligomers and to see its effect on viability of Neuro2A cells upon exposure. When the aggregates were prepared in presence of Melatonin, the higher order oligomer were not observed in SEC. In

SEC experiment, the peak fractions for full-length Tau oligomeric species of lower order were obtained as suggested by the retention volume. These oligomeric species were absent in SEC of full-length Tau aggregates in the presence of Melatonin (indicated by downward red arrow) (Fig. 2A). The fractions collected from SEC for full-length Tau aggregates and corresponding fractions from SEC for Tau aggregates with Melatonin showed no cytotoxicity when treated to Neuro2A cells. It also had no effect on morphology of cells after

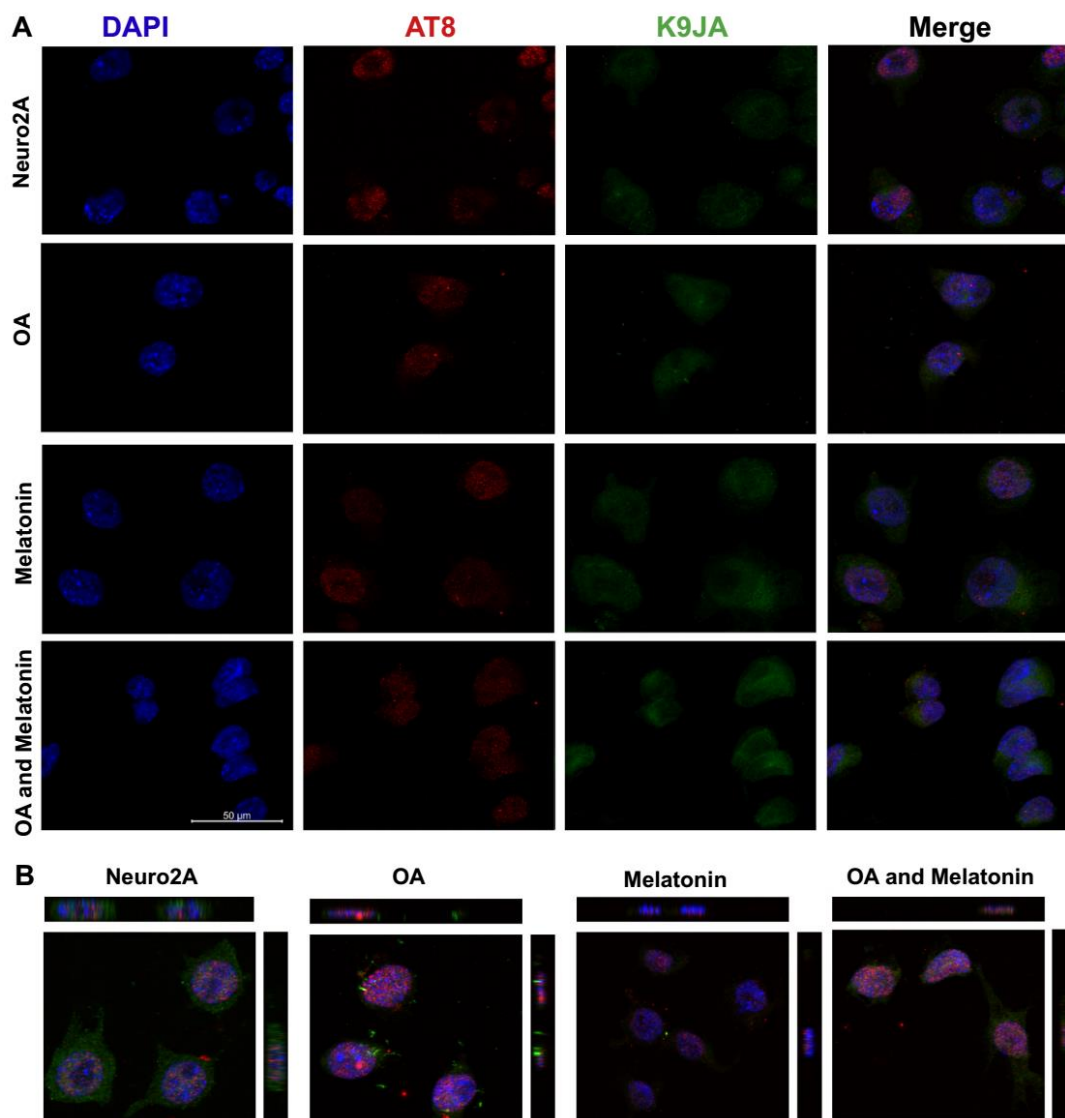


Fig. 4. Level of phospho-Tau (AT8) and total Tau (K9JA) in OA and Melatonin treatment by immunofluorescence study. (A) OA treatment did not alter the level of Tau phosphorylation (AT8: S202/T205) on Neuro2A cells while Melatonin also did not alter the level of AT8 immunostaining, localized mainly in nucleus. (B) Orthogonal projection for 3D localization of AT8-Tau inside the nucleus while unmodified Tau was dispersed throughout the cytosol.

treatment for 24 h (Fig. 2C) probably due to the lower oligomer concentration or non-toxic forms of oligomer species. The results showed that Melatonin can effectively inhibit the formation of these intermediate oligomeric species.

3.3. Phospho-Tau (AT8) and CDK5 levels remained unaltered by Melatonin

Misfolded Tau can undergo several post-translational modifications, among which phosphorylation is the most frequent (80 possible serine,

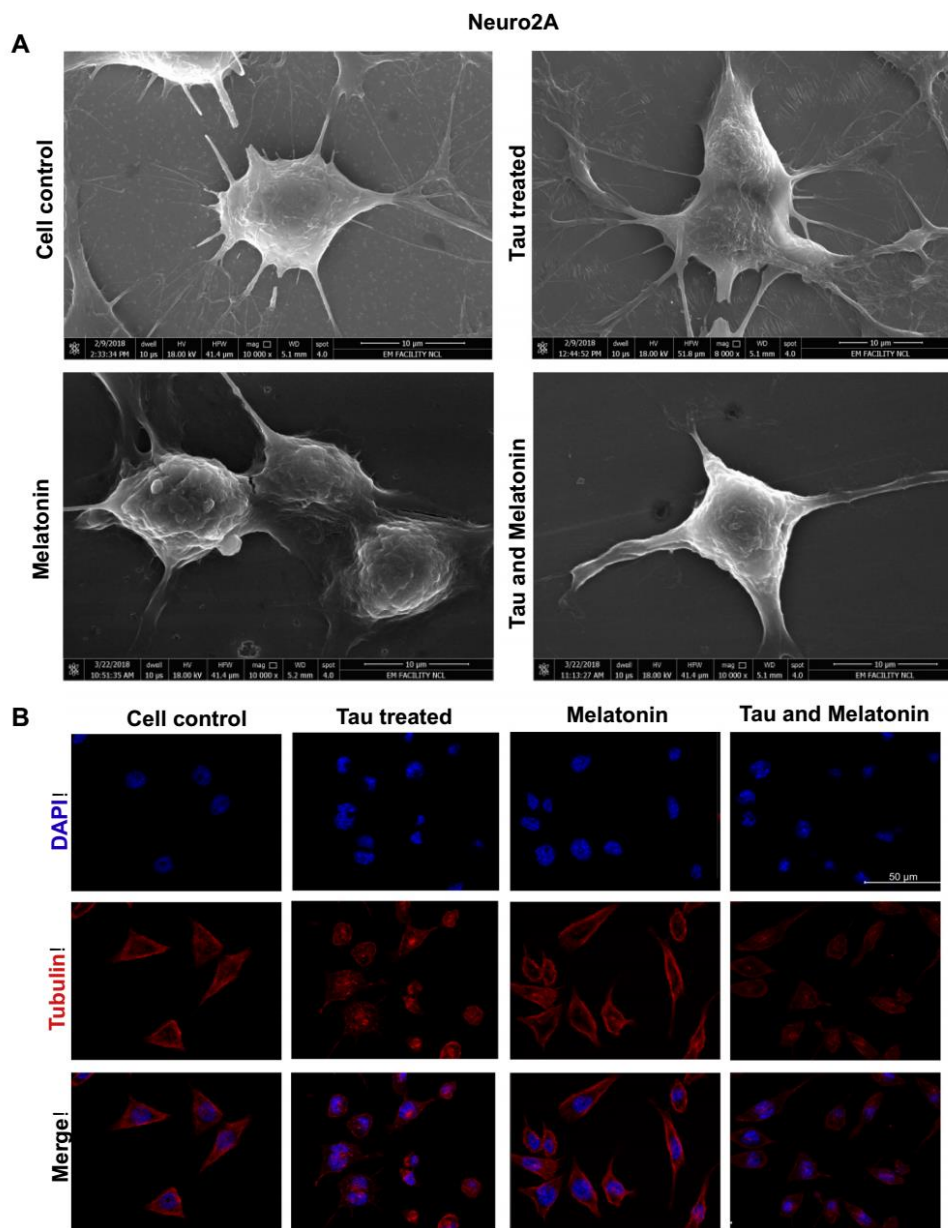


Fig. 5. Alteration of membrane morphology of Neuro2A and tubulin network by FE-SEM and immunofluorescence study. (A) Untreated control revealed smooth membrane morphology of Neuro2A. Tau aggregates treatment showed membrane roughness on N9 cells Melatonin treatment restored the membrane stiffness completely on Neuro2A cells Melatonin showed unaltered membrane morphology on Neuro2A (B) Tau aggregates treatment did not alter any intracellular tubulin network into the cytosol of neurons as compared to untreated control.

threonine, tyrosine residues), [1] which consecutively induces Tau aggregation [41]. CDK5 complexed with p25 (CDK5-p25), with enhanced kinase activity which induces hyperphosphorylation of Tau in AD (at Threonine 231, Serine 202/Threonine 205, Serine 262, Serine 396) [42].

Melatonin and OA maintained the basal level expression of CDK5 level on Neuro2A cells as observed by qRT-PCR and western blot (Fig. 3A, B, C).

To confirm the localization of p-Tau into the Neuro2A cells upon same treatment, cells were immuno-stained with AT8 antibody along

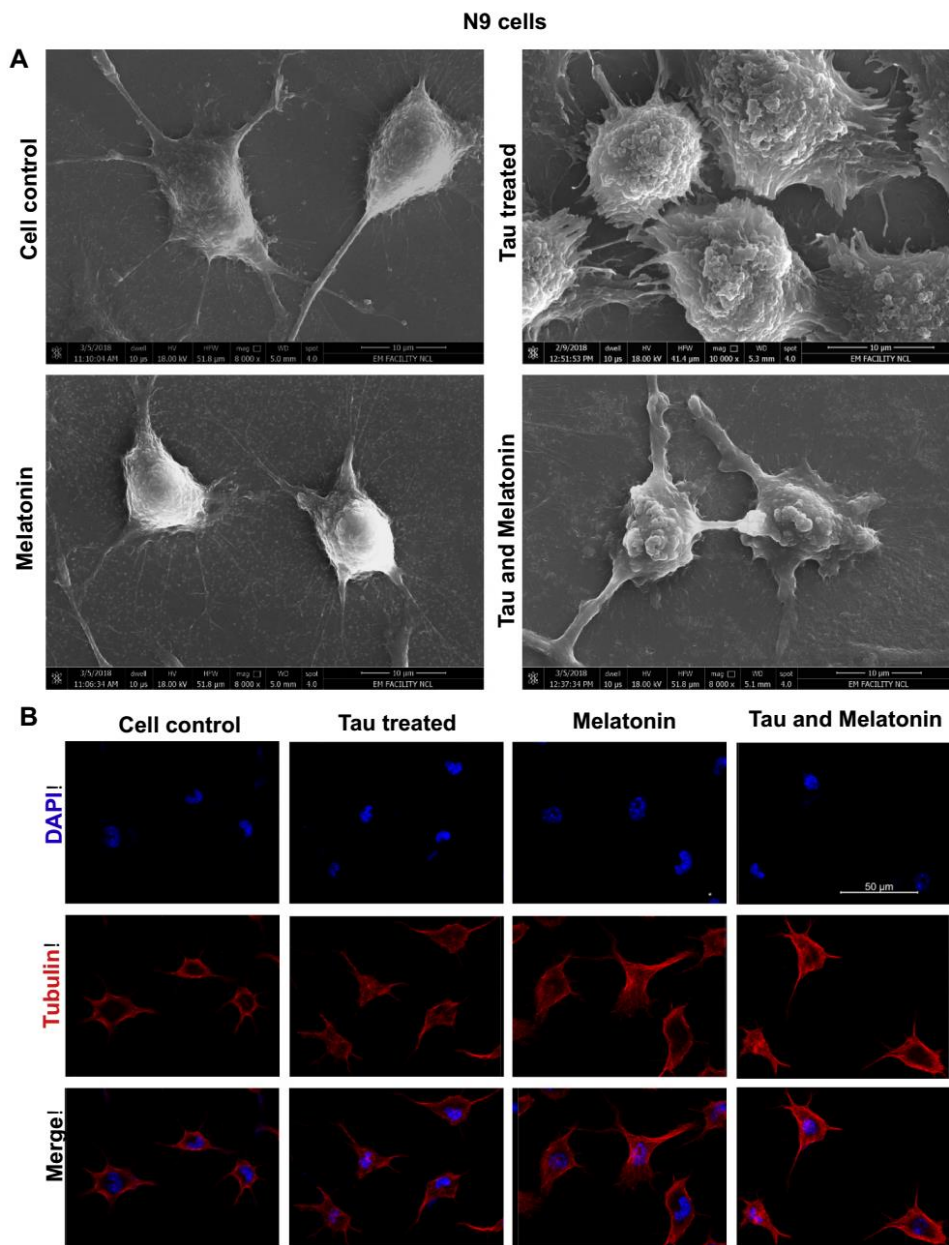


Fig. 6. Missorting of tubulin network and membrane morphology in Tau aggregates and Melatonin-treated glial cell (N9). (A) Tau aggregates treatment showed membrane blebbing on N9 cells while Melatonin treatment showed restored membrane morphology. (B) Tau aggregates treated N9 cells showed extended morphology and Melatonin treatment rearranged the tubulin throughout the cell.

with total-Tau K9JA antibody as a control. Neuroblastoma cells have expressed a constant level of intracellular AT8 epitope of Tau (Fig. 4A) whereas; OA and Melatonin treatment did not alter basal level phospho-Tau expression inside the nucleus (Fig. 4B). In our study, we have showed the constant level of CDK5 and AT8-Tau throughout the groups. This signifies that okadaic acid as well as Melatonin did not involve in CDK5-mediated Tau phosphorylation.

3.4. Alteration of membrane morphology and tubulin network by Tau aggregates and Melatonin

The plasma membrane topography is a determinant of either physiological or pathological state of neuro-glial cells. The alteration of membrane structure occurs either due to changes in raft region or the variation of cytoskeleton configuration. The membrane topography can be broadly two types: roughness and stiffness. A β which is one of the key protein responsible for AD, increases membrane stiffness [43] whereas; Taxol reduces membrane roughness by stabilizing microtubules [44]. Neuro-glial cells when treated with Tau aggregates, it induced membrane roughness as compared to cell control group (Fig. 5A, B). The membrane roughness was more in case of Neuro2A cells (Fig. 5C) whereas; bulging-type structures were more prominent in N9 cells (Fig. 5D). As it is well proved that Tau is a microtubule stabilizing protein and Tau aggregation leads to microtubule disorganization during AD, extracellular Tau aggregates may influence the cytoskeleton mis-orientation. Similarly, microglia are important in spreading of Tau by exosomal release [45] and astrocytes become reactivated by microglial cross-talk [46]. Tau is reported to be associated with membrane through annexin A2 and A6 in axonal membrane via N-terminal of Tau [47]. Annexin anchors Tau to axons and thus ensure Tau enrichment in axons and stabilization of axonal microtubules [48,49]. However, the rates of slow and fast axonal transport in neurons are not significantly affected by Tau deletion or overexpression [50]. External Tau aggregates may induce microtubule disorganization, or membrane raft dislodging and improper vesicular release in this immune cell and neuronal cells. Melatonin reduced the degree of membrane roughness after Tau aggregates treatment, which may have a role in cytoskeleton stabilization or membrane raft organization (Fig. 6A).

Microtubules stabilize the cell shape, structure and facilitate several plasmalemma events like- migration, exosomal release, endocytosis, induction of signalling cascade etc. To study the effect of Tau aggregates and Melatonin on cytoskeletal network, cellular tubulin was immunostained after the same treatments as mentioned above. Extracellular Tau aggregates and Melatonin did not altered tubulin network in the Neuro2A cells. Tau aggregates treatment might activate the microglia with more extended cell bodies compared to untreated control. Melatonin treatment did not alter the microtubule network in microglia (Fig. 6B). In our study, we evidenced the initiation of membrane roughness and unaltered tubulin network on neurons and microglial cells upon Tau fibrils exposure. But the event was reinstated by Melatonin which might signify its role in remodelling of membrane dynamics and cell-to-cell communication in neurodegenerative diseases.

4. Conclusion

Melatonin is a neurohormone, which serves a wide variety of function apart from maintenance of circadian rhythm. It mediates its cytoprotective action as an anti-oxidant itself as well as regulator of other proteins involved in anti-oxidant and anti-inflammatory function. Our studies shows *in vitro* administration of Melatonin does not affect the aggregation of full-length Tau but it does reduce higher order oligomers. Melatonin also affected Tau phosphorylation and helps to maintain tubulin network and membrane topology in Neuro2A and N9 cells.

Author contributions

R.D., A.B. and S.C. designed the experiments. R.D. and A.B. carried out the experiments. R.D., A.B. and S.C. analyzed the data and wrote the article. S.C. conceived the idea of the project. All authors contributed to the discussions and manuscript review.

Funding

This project is supported by grant from in-house CSIR-National Chemical Laboratory grant MLP029526.

Declaration of competing interest

The authors declare no competing financial interest.

Acknowledgements

Rashmi Das acknowledges the fellowship from University Grant Commission (UGC) India. Abhishek Ankur Balmik acknowledges the Shyama Prasad Mukherjee fellowship (SPMF) from Council of Scientific Industrial Research (CSIR), India.

References

- [1] E.-M. Mandelkow, E. Mandelkow, Biochemistry and cell biology of tau protein in neurofibrillary degeneration, *Cold Spring Harb. Perspect. Med.* 2 (7) (2012) a006247.
- [2] D.W. Dickson, S.-H.C. Yen, Beta-amyloid deposition and paired helical filament formation: which histopathological feature is more significant in Alzheimer's disease? *Neurobiol. Aging* 10 (5) (1989) 402–404.
- [3] J.A. Hardy, G.A. Higgins, Alzheimer's disease: the amyloid cascade hypothesis, *Science* 256 (5054) (1992) 184.
- [4] D.W. Dickson, H.A. Crystal, L.A. Mattiace, D.M. Masur, A.D. Blau, P. Davies, S.-H. Yen, M.K. Aronson, Identification of normal and pathological aging in prospectively studied nondemented elderly humans, *Neurobiol. Aging* 13 (1) (1992) 179–189.
- [5] C.X. Gong, K. Iqbal, Hyperphosphorylation of microtubule-associated protein tau: a promising therapeutic target for Alzheimer disease, *Curr. Med. Chem.* 15 (23) (2008) 2321–2328.
- [6] A.P.D. Hilgeroth, V. Tell, Recent developments of protein kinase inhibitors as potential AD therapeutics, *Front. Cell. Neurosci.* 7 (2013) 189.
- [7] E.E. Congdon, E.M. Sigurdsson, Tau-targeting therapies for Alzheimer disease, *Nat. Rev. Neurol.* (2018) 1.
- [8] G. Künze, P. Barré, H.A. Scheidt, L. Thomas, D. Eliezer, D. Huster, Binding of the three-repeat domain of tau to phospholipid membranes induces an aggregated-like state of the protein, *Biochim. Biophys. Acta Biomembr.* 1818 (9) (2012) 2302–2313.
- [9] J. McLaurin, A. Chakrabarty, Characterization of the interactions of Alzheimer β -amyloid peptides with phospholipid membranes, *Eur. J. Biochem.* 245 (2) (1997) 355–363.
- [10] J. Götz, A. Ittner, L.M. Ittner, Tau targeted treatment strategies in Alzheimer's disease, *Br. J. Pharmacol.* 165 (5) (2012) 1246–1259.
- [11] B. Claustrat, J. Brun, G. Chazot, The basic physiology and pathophysiology of melatonin, *Sleep Med. Rev.* 9 (1) (2005) 11–24.
- [12] S.R. Pandi-Perumal, I. Trakht, V. Srinivasan, D.W. Spence, G.J.M. Maestroni, N. Zisapel, D.P. Cardinali, Physiological effects of melatonin: role of melatonin receptors and signal transduction pathways, *Prog. Neurobiol.* 85 (3) (2008) 335–353.
- [13] J. Stefulj, M. Hörtner, M. Ghosh, K. Schauenstein, I. Rinner, A. Wölfler, J. Semmler, P.M. Liebmann, Gene expression of the key enzymes of melatonin synthesis in extrapineal tissues of the rat, *J. Pineal Res.* 30 (4) (2001) 243–247.
- [14] R.J. Reiter, D.-X. Tan, What constitutes a physiological concentration of melatonin? *J. Pineal Res.* 34 (1) (2003) 79–80.
- [15] C. Cajochen, K. Kräuchi, A. Wirz-Justice, Role of melatonin in the regulation of human circadian rhythms and sleep, *J. Neuroendocrinol.* 15 (4) (2003) 432–437.
- [16] D.P. Cardinali, H.J. Lynch, R.J. Wurtman, Binding of melatonin to human and rat plasma proteins, *Endocrinology* 91 (5) (1972) 1213–1218.
- [17] R. Hardeland, D.X. Tan, R.J. Reiter, Kynuramines, metabolites of melatonin and other indoles: the resurrection of an almost forgotten class of biogenic amines, *J. Pineal Res.* 47 (2) (2009) 109–126.
- [18] F.D.J.L. Anton-Tay, J.L. Diaz, A. Fernandez-Guardiola, On the effect of melatonin upon human brain. Its possible therapeutic implications, *Life Sci.* 10 (15) (1971) 841–850.
- [19] H. Yu, E.J. Dickson, S.-R. Jung, D.-S. Koh, B. Hille, High membrane permeability for melatonin, *J. Gen. Physiol.* 147 (1) (2016) 63–76.
- [20] C. Tomas-Zapico, A. Coto-Montes, A proposed mechanism to explain the stimulatory effect of melatonin on antioxidative enzymes, *J. Pineal Res.* 39 (2) (2005) 99–104.
- [21] X. Wang, The antiapoptotic activity of melatonin in neurodegenerative diseases, *CNS Neurosci. Ther.* 15 (4) (2009) 345–357.
- [22] J.Z. Wang, Z.F. Wang, Role of melatonin in Alzheimer-like neurodegeneration, *Acta Pharmacol. Sin.* 27 (1) (2006) 41–49.

- [23] D.X. Tan, R.J. Reiter, L.C. Manchester, M.T. Yan, M. El-Sawi, R.M. Sainz, J.C. Mayo, R. Kohen, M.C. Allegra, R. Hardeland, Chemical and physical properties and potential mechanisms: melatonin as a broad spectrum antioxidant and free radical scavenger, *Curr. Top. Med. Chem.* 2 (2) (2002) 181–197.
- [24] H. Zempel, E. Thies, E. Mandelkow, E.-M. Mandelkow, A β oligomers cause localized Ca $^{2+}$ elevation, misrouting of endogenous tau into dendrites, tau phosphorylation, and destruction of microtubules and spines, *J. Neurosci.* 30 (36) (2010) 11938–11950.
- [25] D.L. Wang, Z.Q. Ling, F.Y. Cao, L.Q. Zhu, J.Z. Wang, Melatonin attenuates isoproterenol-induced protein kinase A overactivation and tau hyperphosphorylation in rat brain, *J. Pineal Res.* 37 (1) (2004) 11–16.
- [26] E. Planel, K. Yasutake, S.C. Fujita, K. Ishiguro, Inhibition of protein phosphatase 2A overrides tau protein kinase I/glycogen synthase kinase 3b and cyclin-dependant kinase 5 inhibition and results in tau hyperphosphorylation in the hippocampus of starved mouse, *J. Biol. Chem.* (2001).
- [27] J. Wang, Q. Wu, A. Smith, I. Grundke-Iqbal, K. Iqbal, τ is phosphorylated by GSK-3 at several sites found in Alzheimer disease and its biological activity markedly inhibited only after it is prephosphorylated by A-kinase, *FEBS Lett.* 436 (1) (1998) 28–34.
- [28] L. Lin, Q.-X. Huang, S.-S. Yang, J. Chu, J.-Z. Wang, Q. Tian, Melatonin in Alzheimer's disease, *Int. J. Mol. Sci.* 14 (7) (2013) 14575–14593.
- [29] J.N. Zhou, R.Y. Liu, W. Kamphorst, M.A. Hofman, D.F. Swaab, Early neuropathological Alzheimer's changes in aged individuals are accompanied by decreased cerebrospinal fluid melatonin levels, *J. Pineal Res.* 35 (2) (2003) 125–130.
- [30] K. Ono, H. Mochizuki, T. Ikeda, T. Nihira, J. Takasaki, D.B. Teplow, M. Yamada, Effect of melatonin on α -synuclein self-assembly and cytotoxicity, *Neurobiol. Aging* 33 (9) (2012) 2172–2185.
- [31] M. Pappolla, P. Bozner, C. Soto, H. Shao, N.K. Robakis, M. Zagorski, B. Frangione, J. Chiso, Inhibition of Alzheimer β -fibrillogenesis by melatonin, *J. Biol. Chem.* 273 (13) (1998) 7185–7188.
- [32] A.A. Balmik, S. Chinnathambi, Multi-faceted role of melatonin in neuroprotection and amelioration of tau aggregates in Alzheimer's disease, *J. Alzheimers Dis.* 62 (4) (2018) 1481–1493.
- [33] N.V. Gorantla, A.V. Shkumatov, S. Chinnathambi, Conformational Dynamics of Intracellular Tau Protein Revealed by CD and SAXS, *Tau Protein*, Springer, 2017 3–20.
- [34] N.V. Gorantla, P. Khandelwal, P. Poddar, S. Chinnathambi, Global Conformation of Tau Protein Mapped by Raman Spectroscopy, *Tau Protein*, Springer, Humana Press, 2017 21–31.
- [35] S.K. Sonawane, A. Ahmad, S. Chinnathambi, Protein-capped metal nanoparticles inhibit tau aggregation in Alzheimer's disease, *ACS Omega* 4 (7) (2019) 12833–12840.
- [36] N.V. Gorantla, R. Das, F.A. Mulani, H.V. Thulasiram, S. Chinnathambi, Neem derivatives inhibits tau aggregation, *J. Alzheimer Dis. Rep.* 3 (1) (2019) 169–178.
- [37] A.A. Balmik, R. Das, A. Dangi, N.V. Gorantla, U.K. Marelli, S. Chinnathambi, Melatonin interacts with repeat domain of tau to mediate disaggregation of paired helical filaments, *Biochim. Biophys. Acta Gen. Subj.* (2019) 129467.
- [38] Z. Skribanek, L. Balásperi, M. Mák, Interaction between synthetic amyloid- β -peptide (1–40) and its aggregation inhibitors studied by electrospray ionization mass spectrometry, *J. Mass Spectrom.* 36 (11) (2001) 1226–1229.
- [39] S.M. Ward, D.S. Himmelstein, J.K. Lancia, L.I. Binder, *Tau Oligomers and Tau Toxicity in Neurodegenerative Disease*, Portland Press Limited, 2012.
- [40] K. Flach, I. Hilbrich, A. Schifffmann, U. Gärtner, M. Krüger, M. Leonhardt, H. Waschipky, L. Wick, T. Arendt, M. Holzer, Tau oligomers impair artificial membrane integrity and cellular viability, *J. Biol. Chem.* 287 (52) (2012) 43223–43233.
- [41] J. Avila, Tau phosphorylation and aggregation in Alzheimer's disease pathology, *FEBS Lett.* 580 (12) (2006) 2922–2927.
- [42] L.-H. Sun, T. Ban, C.-D. Liu, Q.-X. Chen, X. Wang, M.-L. Yan, X.-L. Hu, X.-L. Su, Y.-N. Bao, L.-L. Sun, L.-J. Zhao, S.-C. Pei, X.-M. Jiang, D.-K. Zong, J. Ai, Activation of Cdk5/p25 and tau phosphorylation following chronic brain hypoperfusion in rats involves microRNA-195 down-regulation, *J. Neurochem.* 134 (6) (2015) 1139–1151.
- [43] H.-J. Pan, R.-L. Wang, J.-L. Xiao, Y.-J. Chang, J.-Y. Cheng, C.-H. Lee, Using optical profilometry to characterize cell membrane roughness influenced by amyloid-beta 42 aggregates and electric fields, *J. Biomed. Opt.* 19 (1) (2014) 11009.
- [44] C.-W. Lee, L.-L. Jang, H.-J. Pan, Y.-R. Chen, C.-C. Chen, C.-H. Lee, Membrane roughness as a sensitive parameter reflecting the status of neuronal cells in response to chemical and nanoparticle treatments, *J. Nanobiotechnol.* 14 (1) (2016) 9.
- [45] H. Asai, S. Ikezu, S. Tsunoda, M. Medalla, J. Luebke, T. Haydar, B. Wolozin, O. Butovsky, S. Kügler, T. Ikezu, Depletion of microglia and inhibition of exosome synthesis halt tau propagation, *Nat. Neurosci.* 18 (11) (2015) 1584.
- [46] H. Lian, A. Litvinchuk, A.C.A. Chiang, N. Aithmitti, J.J. Jankowsky, H. Zheng, Astrocyte-microglia cross talk through complement activation modulates amyloid pathology in mouse models of Alzheimer's disease, *J. Neurosci.* 36 (2) (2016) 577–589.
- [47] R. Brandt, J. Léger, G. Lee, Interaction of tau with the neural plasma membrane mediated by tau's amino-terminal projection domain, *J. Cell Biol.* 131 (5) (1995) 1327–1340.
- [48] M. Leslie, Annexin keeps tau on a short leash, *J. Cell Biol.* 192 (4) (2011) 542.
- [49] A. Gauthier-Kemper, M.S. Alonso, F. Sündermann, B. Niewidok, M.-P. Fernandez, L. Bakota, J.J. Heinisch, R. Brandt, Annexins A2 and A6 interact with the extreme N terminus of tau and thereby contribute to tau's axonal localization, *J. Biol. Chem.* 293 (21) (2018) 8065–8076.
- [50] A. Yuan, A. Kumar, C. Peterhoff, K. Duff, R.A. Nixon, Axonal transport rates in vivo are unaffected by tau deletion or overexpression in mice, *J. Neurosci.* 28 (7) (2008) 1682–1687.